PERFORMANCE EVALUATION OF SEAWATER COUNTER FLOW COOLING TOWERS

BY

IQBAL HUSAIN

A Thesis Presented to the

DEANSHIP OF GRADUATE STUDIES

KING FAHD UNIVERSITY OF PETROLEUM & MINERALS

DHAHRAN, SAUDI ARABIA

In Partial Fulfillment of the
Requirements for the Degree of

MASTER OF SCIENCE

In

MECHANICAL ENGINEERING

MAY 2011

In the name of Allah, the Most Gracious and the Most Merciful

KING FAHD UNIVERSITY OF PETROLEUM AND MINERALS

DHAHRAN 31261, SAUDI ARABIA

DEANSHIP OF GRADUATE STUDIES

This thesis, written by IQBAL HUSAIN under the direction of his thesis advisor and approved by his thesis committee, has been presented to and accepted by the Dean of Graduate Studies, in partial fulfillment of the requirements for the degree of MASTER OF SCIENCE in MECHANICAL ENGINEERING.

Thesis Committee

Dr. Syed M. Zubair (Advisor)

Dr. Mostafa H. Elsharqawy (Co-Advisor)

Dr. Mohamed A. Antar (Member)

Dr. Amro M. Al-Qutub
(Department Chairman)

Dr. Salam A. Zummo
(Dean of Graduate Studies)

8/6/11

Date

عمادة الدراسات العليا
DEANSHIP OF GRADUATE STUDIES

Dedicated

to

My Beloved Parents and Brothers

ACKNOWLEDGMENTS

All praise and thanks are due to Almighty Allah, Most Gracious and Most Merciful, for his immense beneficence and blessings. He bestowed upon me health, knowledge and patience to complete this work. May peace and blessings be upon prophet Muhammad (PBUH), his family and his companions.

Thereafter, acknowledgement is due to KFUPM for the support extended towards my research through its remarkable facilities and for granting me the opportunity to pursue graduate studies.

I acknowledge, with deep gratitude and appreciation, the inspiration, encouragement, valuable time and continuous guidance given to me by my thesis advisor, Dr. Syed M. Zubair. I am highly grateful to my thesis co-advisor Dr. Mostafa H. Elsharqawy for his valuable guidance, suggestions and motivation. His strong support and co-operation towards this research during experiments was a boon to me. I am also grateful to my Committee member, Dr. Mohammed A. Antar for his constructive guidance and support.

My heartfelt thanks are due to my parents and brothers for their prayers, guidance, and moral support throughout my academic life. My parents' advice, to strive for excellence has made all this work possible.

I am deeply indebted and grateful to Mr. Mohammad S. A. Karam (Heat Engines Lab Engineer) for his help and support during experiments and also thanks are due to all other professors of Mechanical Engineering Department, Mr. Mohammed Nazeeruddin Sayeed (Scientist II) and Lab Engineer Mr. Saeed Al-Baba.

Special thanks are due to my senior colleagues at the university, Bilal, Sarfaraz, Hasan, Ammar, Abdurrahman, Mumtaz, Shahid, Faizan, Abdul Malik, Omeir, Islam, Zahid, Ishaq, Abdurrahman, and many others for their help and prayers. I would also like to thank my friends Awad, Azhar, Umar, Wajahat, Mohsin, Ahmad Eter, Abdullah Bazrah, Ibrahim, Aqeel, Abdul Subhan, Akber, Khaleel, Naeem, Rizwan, Irfan and all others who provided wonderful company and good memories that will last a life time.

TABLE OF CONTENTS

LIST OF TABLES

LIST OF FIGURES

THESIS ABSTRACT (ENGLISH)

NAME: **IQBAL HUSAIN**

TITLE: **PERFORMANCE EVALUATION OF SEAWATER COUNTER FLOW COOLING TOWERS**

MAJOR FIELD: **MECHANICAL ENGINEERING**

DATE OF DEGREE: **JUMADA AL-AKHIRAH 1432 (H) (MAY 2011 G)**

A cooling tower is a heat rejection device. Heat rejection in cooling towers is specified as convection between the fine droplets of water and the surrounding air, and also most importantly as an evaporation which allows a small portion of water to evaporate into the moving air stream. Therefore, the process involves both heat and mass transfer. In this thesis work the study of counterflow cooling tower for fresh water and seawater is investigated experimentally and is validated by simulating the performance by developing a numerical code. The second law (exergy) analysis is also carried out on both fresh water and seawater cooling towers. The thermal performance of the cooling tower for fresh water and seawater is clearly explained in terms of exergy distribution of air and water along the height of the tower. In addition, performance results identifying important cooling tower variables such as air and water effectiveness, second law efficiency are examined as a function of mass ratio ($MR = \dot{m}_W / \dot{m}_a$) for different water salinities both for design and performance evaluation purpose. Furthermore, the performance characteristics of spray (shower) towers are investigated experimentally and compared with the fill packing tower.

MASTER OF SCIENCE DEGREE

KING FAHD UNIVERSITY OF PETROLEUM AND MINERALS

Dhahran, Saudi Arabia

THESIS ABSTRACT (ARABIC)

ملخص الرسالة

الاسم: إقبال حسين

عنوان الرسالة: تقييم أداء أبراج تبريد ذات تدفق معاكس تستخدم مياه البحر

التخصص: الهندسة الميكانيكية

تأريخ التخرج: جمادى الآخرة 1432 هـ - (مايو 2011 م)

برج التبريد هو مبادل حرارى يقوم بتبريد المياة بطرد الحراره الى الهواء المحيط عن طريق تبخر جزء صغير من الماء لتتبخر في تيار الهواء المتحرك. لذلك فأن عملية التبريد تحتوي على انتقال للكتله والحراره فى نفس الوقت. في هذه الرسالة يتم دراسة وتقييم الأداء الحرارى لأبراج التبريد التى تعمل بالمياه العذبة ومياه البحر عن طريق نموذج رياضى يأخذ فى الاعتبار جميع المتغيرات التى تتحكم فى الأداء. ويتم التحقق من صحة نتائج النموذج الرياضى تجريبيا من خلال أداء قياسات عملية لبرج تبريد بأبعاد مصغرة. كما تم ايضا اختبار النتائج بتطبيق القانون الثاني للديناميكا الحرارية على كل من نتائج استخدام المياه العذبة ومياه البحر مع برج التبريد. وفى ذلك تم شرح خصائص الاداء الحراري لبرج التبريد عن طريق توزيع الاكسيرجي لكل من الهواء والماء على طول برج التبريد والذى يحدد المتغيرات الهامه مثل: فعالية الهواء والماء وكفاءة القانون الثانى للديناميكا الحرارية كمتغيرات مع نسبة معدل سريان الماء الى الهواء عند درجات مختلفة من ملوحة المياه. وعلاوة على ذلك ، فقد تم دراسة ابراج التبريد التى تعمل بالرذاذ بدون مادة حشو ووجد ان الاداء الحرارى لها منخفض بنسة تصل الى 50% عن الابراج التى تحتوى على مادة حشو حيث تعمل على زيادة المساحة السطحية لأنتقال الكتلة والحرارة.

شهادة ماجستير علوم

جامعة الملك فهد للبترول والمعادن

الظهران ، المملكة العربية السعودية

CHAPTER 1

INTRODUCTION

A cooling tower is a heat rejection device. Heat is discharged in power generation, refrigeration, petrochemical, steel, processing and many other industrial plants. In many cases, heat is discharged into the atmosphere with the aid of a cooling tower. Main function of cooling tower is to extract waste heat from warm water to the atmosphere. Heat rejection in cooling towers is specified as convection between the fine droplets of water and the surrounding air, and also as evaporation which allows a small portion of water to evaporate into moving air. Therefore, the process involves both heat and mass transfer. Convection depends on the temperature difference, the surface area, air velocity, etc. Evaporation is by far the most important effect. Cooling takes place as the molecules of H_2O diffuse from the surface into the surrounding air. These molecules are then replaced by others from the liquid and the energy required for this is taken from the remaining liquid. The make-up water source is used to replenish water lost to evaporation.

The rate of evaporation from a wet surface into the surrounding air is determined by the difference between the vapor pressure at the water-air interface (i.e. the saturation pressure corresponding to the water-air interface temperature) and the vapor pressure in the surrounding air. The partial pressure of the water vapor in the atmosphere depends on the humidity content in the air.

Figure 1.1 shows the evaporation process of water vapor from water droplets into the surrounding air.

Inside the cooling tower, the two fluids, ambient air and hot water come into direct contact with each other. This device uses evaporative heat and mass transfer to cool warm water. The water to be cooled is commonly distributed over a packing material in the tower.

The packing is the most crucial part of the cooling tower. The purpose of the packing material is to provide a large surface area for contact between air and water by distributing the water flow uniformly to enhance evaporation and heat transfer. The type of packing material used in the cooling tower has an important role in the tower as it provides a very large surface area for evaporative heat and mass transfer to take place from hot water to ambient air. As the water flows down the packing, it contacts air that is forced across the packing by a fan.

A small percentage of the water evaporates with a corresponding extraction of heat from the remaining water, while the air stream is humidified by picking up heat and moisture. The warm, moist air then passes through a drift eliminator that exists at the top of the tower. Drift eliminators capture the water droplets entrapped in the air stream that otherwise would be lost to the atmosphere. A typical closed loop cooling tower system is shown in Fig. 1.2.

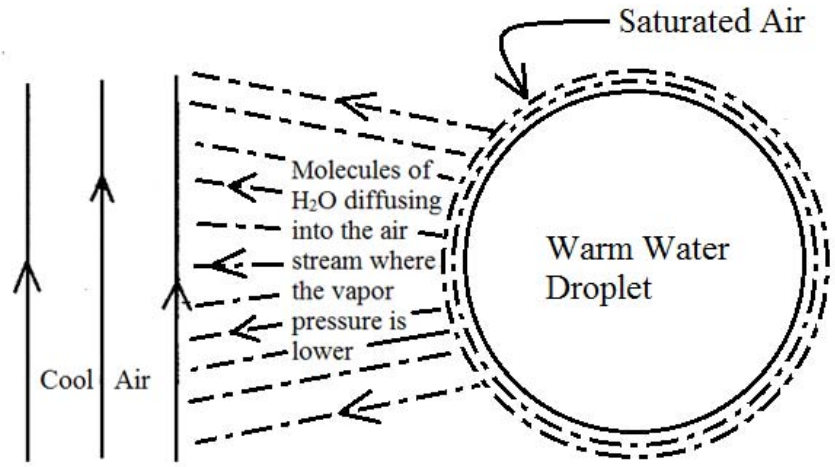

Figure 1.1 Evaporation of water droplet into air stream

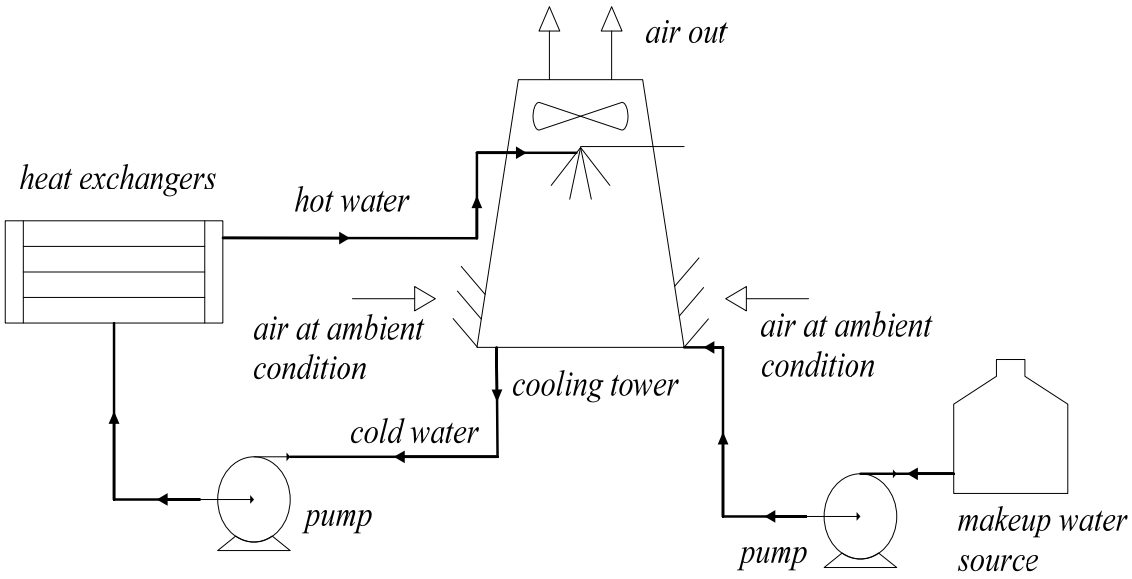

Figure 1.2 A typical closed-loop cooling tower system

1.1 TYPES OF COOLING TOWER

Cooling towers fall into two main categories: Natural draft and Mechanical draft.

1.1.1 Natural Draft Cooling Tower

The natural draft cooling tower is known as hyperbolic cooling tower because of its shape. The natural draft cooling tower makes use of the difference in temperature between the ambient air and the hotter air inside the tower. As hot air moves upwards through the tower, fresh cool air is drawn into the tower through an air inlet at the bottom. Due to the layout of this tower, no fan is required and there is almost no circulation of hot air that could affect the performance of the cooling tower. Concrete is used for the construction of tower shell. The height of natural draft towers may reach to 200 m. They are used mostly for large heat duties for water flow rates above 45,000 m^3/hr. They are mainly used by utility power stations.

There are two main types of natural draft towers:

- **Cross flow tower** (Fig. 1.3)**: -** In cross flow tower air is drawn across the falling water and the fill is located outside the tower.
- **Counter flow tower** (Fig. 1.4)**: -** In counter flow tower air is drawn up through the falling water and the fill is therefore located inside the tower, although design depends on specific site conditions.

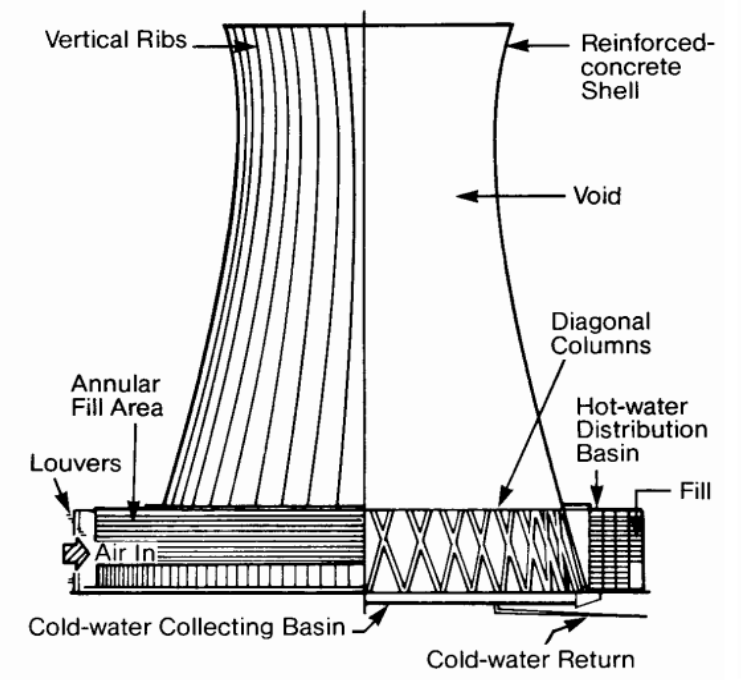

Figure 1.3 Cross flow natural draft cooling tower [40]

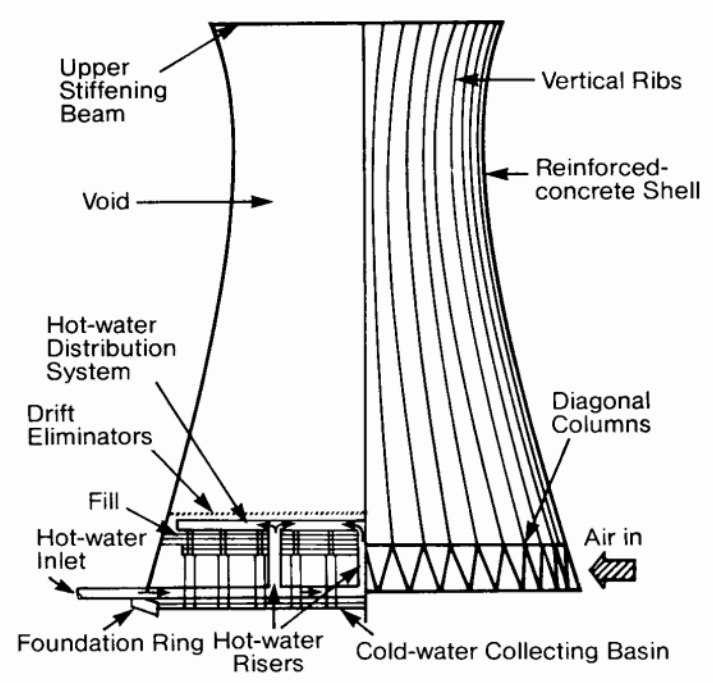

Figure 1.4 Counter flow natural draft cooling tower [40]

1.1.2 Mechanical Draft Cooling Tower

Mechanical draft cooling towers have large fans to force or draw air along the cooling tower. The water falls downwards over the fill surface, to increase the contact time between the water and the air. This maximizes the heat transfer between air and water streams. Cooling rates of mechanical draft towers depend upon various parameters such as fan diameter and speed of operation, fills for system resistance etc.

Mechanical draft towers are available in a large range of capacities. Towers can be either factory built or field erected – for example concrete towers are only field erected.

Many towers are constructed in modular basis so that they can be grouped together to achieve the desired capacity. Thus, many cooling towers are assemblies of two or more individual cooling towers or "cells." The number of cells they have, e.g., an eight-cell tower, often refers to such towers. Multiple-cell towers can be lineal, square, or round depending upon the shape of the individual cell and whether the air inlets are located on the sides or bottoms of the cells.

There are three types of mechanical draft cooling towers:

- **Forced draft cooling tower** (Fig. 1.5)**: -** In this type of tower, air is blown through the tower by a fan located at the air inlet. The fan forces the air to flow through the top of the tower. These towers have high air resistance and therefore centrifugal blower fans are used. The Fans are relatively quiet but air recirculation is due to high air-entry velocity and low air-exit velocity. This can be solved by locating towers in plant rooms combined with discharge ducts.

- **Induced draft cross flow cooling tower: -** In this type of tower hot water enters at top and passes over the fills while air enters on one side in single-cross flow tower (Fig. 1.6a) or opposite sides in double-cross flow tower (Fig. 1.6b). An induced draft fan at top of tower draws air across the fills towards exit of the tower. Here the recirculation of air is less than forced draft towers because the speed of the air at the exit is 3-4 times higher than at the inlet. However fans and the motor drive mechanism require weather-proofing against moisture and corrosion because they are in the path of humid exit air.

- **Induced draft counter flow cooling tower** (Fig. 1.7)**: -** In this type of tower hot water enters at the top and passes over the fills while air enters at the bottom and exits at the top of the tower. An induced draft fan at top of tower draws air across the fills towards exit of the tower. Here the recirculation of air is less than forced draft towers because the speed of exit air is 3-4 times higher than entering air. The fans and the motor drive mechanism require weather-proofing against moisture and corrosion because they are in the path of humid exit air.

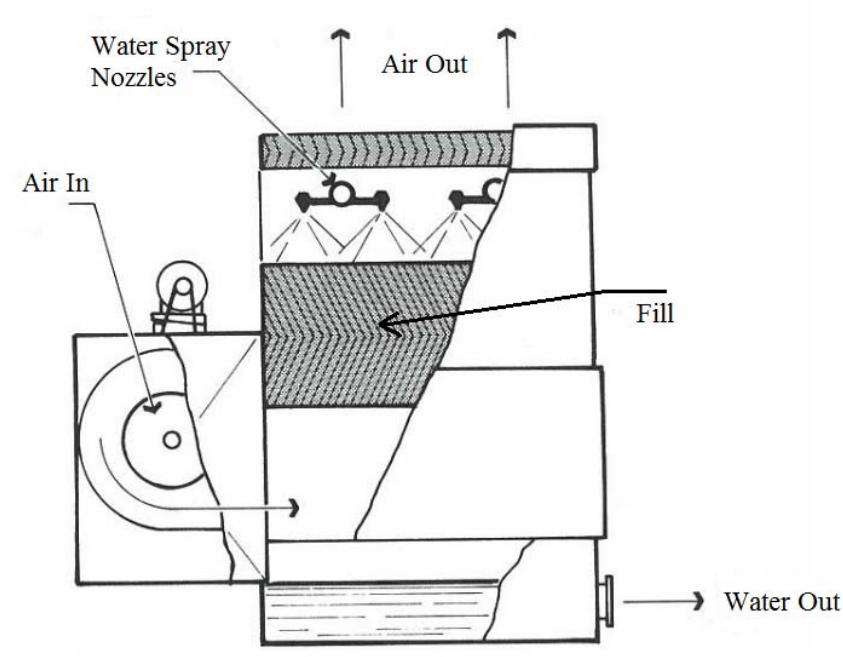

Figure 1.5 Forced draft cooling tower [41]

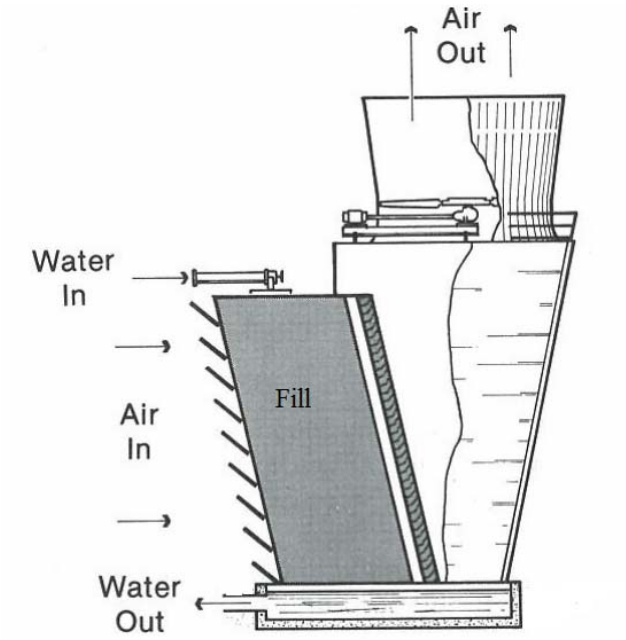

Figure 1.6a Induced draft single-cross flow cooling tower [41]

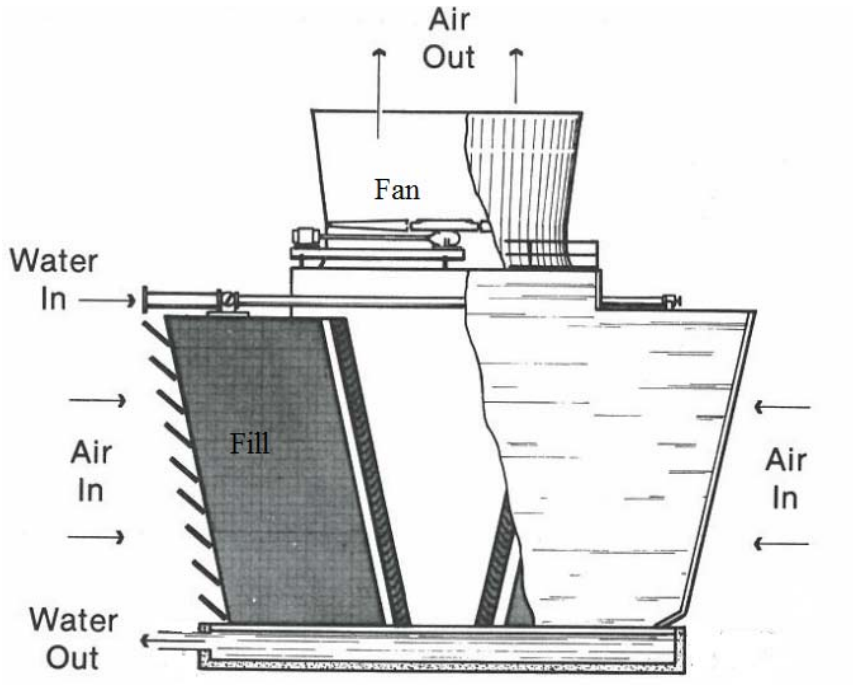

Figure 1.6b Induced draft double-cross flow cooling tower [41]

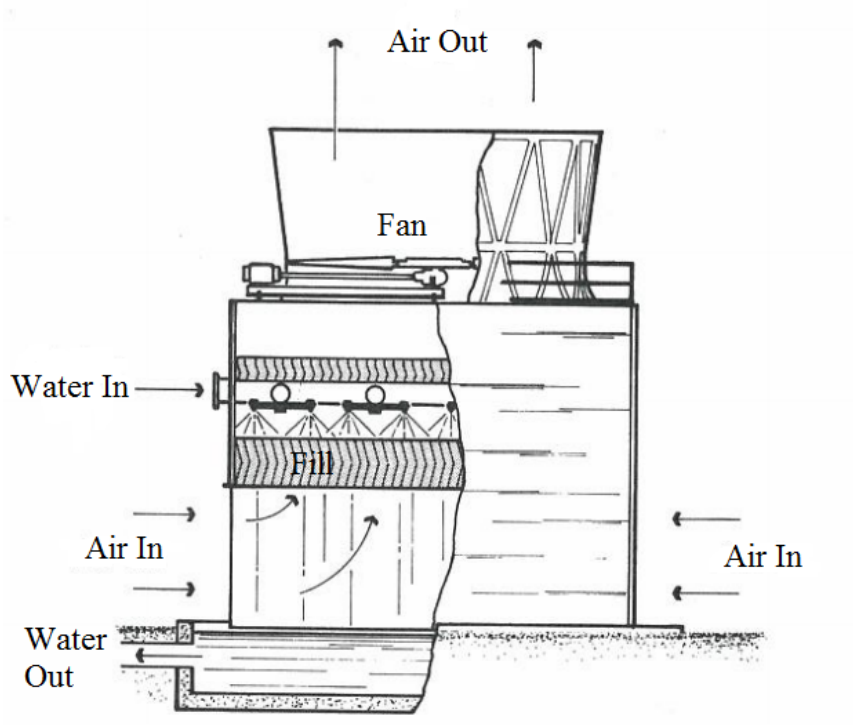

Figure 1.7 Induced draft counter flow cooling tower [41]

1.2 COMPONENTS OF A COOLING TOWER

The basic components of a cooling tower are the frame and casing, fill, water basin, drift eliminators, air inlet louvers, nozzles and fans. These components are described below.

Frame and casing: - Most cooling towers have structural frames that support the exterior enclosures (casings), motors, fans, and other components. With some smaller designs, such as some glass fiber units, the casing may essentially be the frame.

Fill: - Fills are generally made of plastic or wood to facilitate heat transfer by maximizing water and air contact. There are two types of fill:

- **Splash fill: -** In splash fills water droplets fall over successive layers of horizontal splash bars so that it continuously breaks into smaller droplets, while also wetting the fill surface. Plastic splash fills promote better heat transfer than wood splash fills.
- **Film fill: -** It consists of thin, closely spaced plastic surfaces over which the water spreads, forming a thin film in contact with the air. These surfaces have flat, corrugated, honeycombed, or other patterns. The film type of fill is the more efficient and provides same heat transfer in a smaller volume than the splash fill. So these fills are generally used where the circulating water is free of debris that could block the fill passageways.

Water basin: - The cold-water basin is located at or near the bottom of the tower, and it receives the cooled water that flows down through the tower and the fills. The basin usually has a sump or low point for the cold-water discharge connection. In many tower

designs, the cold-water basin is beneath the entire fill. In some forced draft counter flow design, however, the water at the bottom of the fill is channeled to a perimeter trough that functions as the cold-water basin. Propeller fans are mounted beneath the fill to blow the air up through the tower. With this design, the tower is mounted on legs, providing easy access to the fans and their motors.

Drift eliminators: - The function of the drift eliminators is to capture water droplets entrapped in the air stream that otherwise would be lost to the atmosphere.

Air inlet: - This is the point of entry for the air entering a tower. The inlet may take up an entire side of a tower in a cross-flow design or be located low on the side or the bottom of the tower in a counter-flow design of cooling towers.

Louvers: - Generally, cross-flow cooling towers have inlet louvers. The purpose of louvers is to equalize air flow into the fill and retain the water within the tower. Many counter flow tower designs do not require louvers.

Nozzles: - These spray water to wet the fills. Uniform water distribution at the top of the fill is essential to achieve proper wetting of the entire fill surface. Nozzles can either be fixed and spray in a round or square patterns, or they can be part of a rotating assembly as found in some circular cross-section towers.

Fans: - Both axial (propeller type) and centrifugal fans are used in cooling towers. Generally, propeller fans are used in induced draft cooling towers and both propeller and centrifugal fans are used in forced draft towers. Depending upon the size of cooling tower, the type of propeller fans used is either fixed or variable pitch. A fan with non-

automatic adjustable pitch blades can be used over a wide kW range because the fan can be adjusted to deliver the desired air flow at the lowest power consumption. Automatic variable pitch blades can vary air flow in response to changing load conditions.

1.3 COOLING TOWER MATERIALS

Originally, cooling towers were constructed primarily of wood, including the frame, casing, louvers, fill and cold-water basin. Sometimes the cold-water basin was made of concrete. Today, manufacturers use a variety of materials to construct cooling towers. Materials are chosen to enhance corrosion resistance, reduce maintenance, and promote reliability and long service life of cooling towers. Galvanized steel, various grades of stainless steel, glass fiber, and concrete are widely used in tower construction, as well as aluminum and plastics for some components.

Frame and casing: - Frames are generally made of glass fiber. Casings and basins in many towers are constructed of galvanized steel but where a corrosive atmosphere is a problem, they are made of stainless steel. Large cooling towers are made of concrete. Glass fiber is also widely used for cooling tower casings and basins, because they extend the life of the cooling tower and provide protection against harmful chemicals.

Fill: -For fill material, plastics are widely used, including PVC, polypropylene, and other polymers. When water conditions require the use of splash fill, treated wood splash fill is still used in wooden towers, but plastic splash fill is also widely used.

Nozzles: - Plastics are also widely used materials for nozzles. Many nozzles are made of PVC (Polyvinyl chloride), ABS (Acrylonitrile Butadiene Styrene), polypropylene, and glass-filled nylon.

Fans: - Aluminum, glass fiber and hot-dipped galvanized steel are commonly used fan materials. Centrifugal fans are often fabricated from galvanized steel. Propeller fans are made from galvanized steel, aluminum, or molded glass fiber reinforced plastic.

1.4 ASSESMENT OF COOLING TOWERS

This section describes how the performance of cooling towers can be assessed. The performance of cooling towers is evaluated to determine the approach and range against their design values, identify areas of energy wastage and to suggest improvements.

During the performance evaluation, portable monitoring instruments are used to measure the following parameters:

- Inlet air wet bulb temperature
- Inlet air dry bulb temperature
- Inlet water temperature
- Outlet water temperature
- Exit air dry bulb temperature
- Exit air wet bulb temperature
- Electrical power consumption of pumps and fan motors
- Water flow rate
- Air flow rate

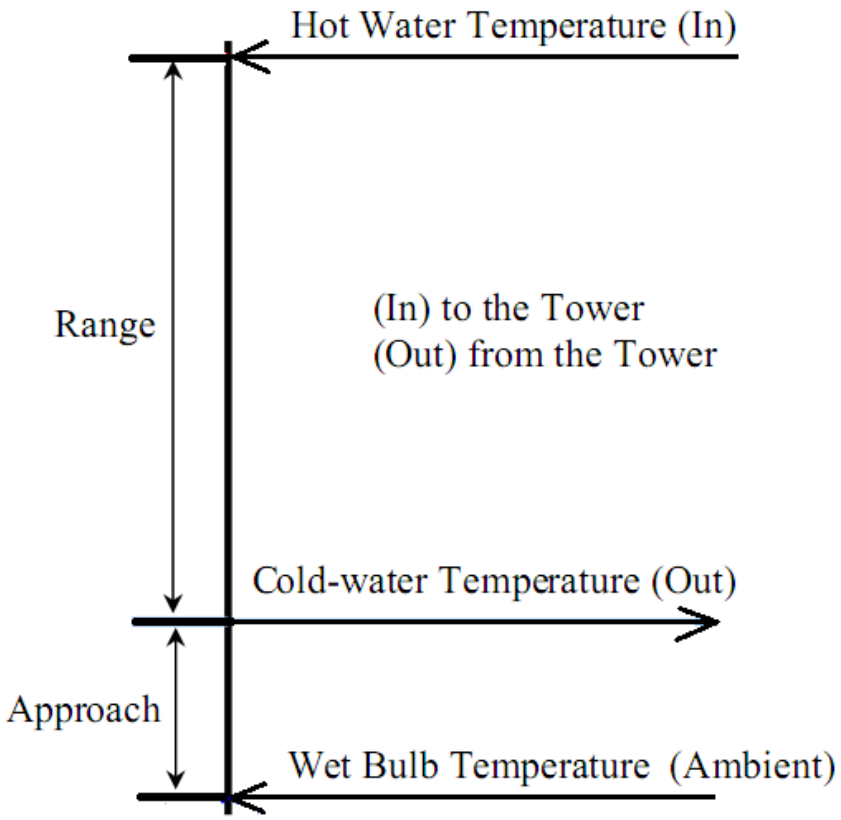

Figure 1.8 Range and approach of cooling tower

These measured parameters are used to determine the cooling tower performance in several ways:

i) Range: - This is the difference between the cooling tower water inlet and outlet temperature. A high CT Range means that the cooling tower has been able to reduce the water temperature effectively, and is thus performing well.

Cooling Tower Range (°C) = Hot Water inlet temp (°C) – Cold Water outlet temp (°C)

ii) Approach: - This is the difference between the cold-water outlet temperature and ambient wet bulb temperature. The lower the approach the better is the cooling tower performance. Although, both range and approach should be monitored, the `Approach' is a better indicator of cooling tower performance.

Cooling Tower Approach (°C) = Cold Water outlet temp (°C) – Air inlet wet bulb temp (°C) (1.1)

iii) Air effectiveness: - This is the ratio of the heat transfer to the air to the maximum heat transfer when the air is saturated at the outlet of cooling tower at the inlet water temperature.

$$\varepsilon_{air} = \frac{h_{air,out} - h_{air,in}}{h_{s,w,in} - h_{air,in}} \tag{1.2}$$

where,

$h_{s,w,in}$ is the enthalpy of saturated air at inlet water temperature

iv) Water effectiveness: - This is the ratio of the heat transfer from the water to the maximum heat transfer when the water outlet temperature is equal to the inlet wet bulb temperature of air.

$$\varepsilon_{water} = \frac{\dot{m}_{SW,in} h_{SW,in} - \dot{m}_{w,out} h_{SW,out}}{\dot{m}_{SW,in} h_{SW,in} - \dot{m}_{w,out} h_{SW,ideal}} \quad (1.3)$$

where,

$h_{SW,ideal}$ is the enthalpy of seawater at inlet wet bulb temperature of air

v) Cooling capacity: - This is the rate of heat rejected in kW or TR, given as product of mass flow rate of water, its specific heat and its temperature difference.

vi) Evaporation loss: - This is the water quantity evaporated for cooling duty. As a rule of thumb, the evaporation quantity works out to 1.8 m^3 for every 4186800 kJ heat rejected.

vii) Cycles of concentration (C.O.C): - This is the ratio of dissolved solids in circulating water to the dissolved solids in makeup water.

viii) Blow down loss: - Blow down loss depends upon cycles of concentration (C.O.C.) and the evaporation loss and is given by formula:

Blow down = Evaporation loss / (C.O.C. – 1) (1.4)

ix) Liquid Gas Ratio: - The Liquid to Gas ratio of a cooling tower is the ratio between the water and the air mass flow rates. Cooling towers have certain design values, but seasonal variations require adjustment and tuning of water and air flow rates to get the

best cooling tower effectiveness. Adjustments can be made by water box loading changes or blade angle adjustments.

1.5 FACTORS AFFECTING COOLING TOWER PERFORMANCE

A number of factors influence the cooling towers performance and should be considered when choosing a cooling tower. These are capacity, range, approach, heat load, wet bulb temperature, and the relationship between these factors. Some of predominant factors are discussed below;

i) Heat load: - The heat load imposed on a cooling tower is determined by the process being served. It is the amount of heat to be removed from the circulating water within the tower. The degree of cooling required is controlled by the desired operating temperature of the process. In most cases, a low operating temperature is desirable to increase process efficiency or to improve the quality or quantity of the product, e.g. condensers of the power plant. However, in some applications high operating temperatures are desirable, e.g. internal combustion engines. The size and the cost of the cooling towers increase with increasing the heat load.

ii) Wet bulb temperature: - The temperature of the air measured by the thermometer when it is covered by wet wick is called as wet bulb temperature (WBT). Inlet air wet bulb temperature is a significant factor in the performance of the cooling tower, because it is the lowest possible temperature to which water can be cooled. For this reason, the wet bulb temperature of the air entering the cooling tower determines the minimum operating temperature level of the process. Theoretically, a cooling tower will cool water to the entering wet bulb temperature. In practice, however, water is cooled to a

temperature higher than the wet bulb temperature of the entering air stream. In general, the design temperature selected for the cooling tower shall be close to the average maximum wet bulb temperature in summer of the site of the cooling tower.

iii) Relationship between range, flow and heat load: - The range of the cooling tower increases when the quantity of circulated water or heat load increases. This means that increasing the range as a result of added heat load requires a larger tower.

iv) Relationship between approach and wet bulb temperature: - The design wet bulb temperature is determined by the geographical location of the site of the cooling tower. For a certain approach value (and at a constant range and flow range), the higher the wet bulb temperature, the smaller the tower required.

CHAPTER 2

LITERATURE REVIEW

2.1 WET COOLING TOWERS

Several researchers have studied and investigated cooling tower performance analytically and numerically since a long time. Walker et al. [1] were the first to propose a basic theory of cooling tower operation. They used the ambient air humidity as a sole driving force for the cooling process in cooling towers. The practical use of basic differential equations, however, was first presented by Merkel [2] in which he combined the equations for heat and water vapor transfer. He showed the utility of total heat or enthalpy difference as a driving force to allow for both sensible and latent heats. The basic postulations and approximations that are inherent in Merkel's theory are:

- The resistance for heat transfer in the liquid film is negligible.
- The mass flow rate of water per unit cross sectional area of the tower is constant, i.e. there is no loss of water due to evaporation.
- The specific heat of the air stream mixture at constant pressure is the same as that of dry air.
- The Lewis number for humid air is unity.

Merkel's theory in cooling tower design and rating is presented and discussed in detail throughout most unit operations and process heat transfer text books.

London et al. [3] used the enthalpy of the humid air-water vapor mixture as the actual driving force without explaining the derivation. They also recognized for the first time that water evaporation must be taken into consideration for the true heat balance. Simpson and Sherwood [4] studied and experimented small mechanical draft cooling towers to evaluate its performance.

Sutherland [5] developed a computer program to compare the accurate analysis of mechanical draught counter flow cooling towers, including water loss by evaporation, with the approximate Merkel method. He found that counter-flow cooling towers could be undersized between 5 to 15% with the average value around 8%, through the use of the Merkel method if "true" mass transfer coefficients are used. He also studied the effect of variation of atmospheric pressure on cooling towers to a certain extent and showed that the NTU increases with increasing pressure.

Webb [6] performed a unified theoretical treatment for thermal analysis of cooling towers, evaporative condensers, and evaporative fluid coolers. He explained specific calculation procedures for sizing and rating of each type of evaporative exchanger. Webb and Villacres [7] described three computer algorithms that have been developed to perform rating calculations of three evaporatively cooled heat exchangers. The algorithms are particularly useful for rating commercially available heat exchangers at part load conditions. The heat and mass transfer ''characteristic equation'' of one of the heat exchangers is derived from the manufacturers rating data at the design point.

Jaber and Webb [8] presented an analysis that shows how the theory of heat exchanger design may be applied to cooling towers. They demonstrated that the effectiveness (ε) and NTUs definitions are in very good agreement with those used for heat exchanger design and are applicable to all cooling tower operating conditions. It is important to note that they did not consider heat transfer resistance in the air-water interface and the effect of water evaporation in the cooling tower. The results are only applicable for Lewis number equal to one.

Braun et al. [9] presented effectiveness models for cooling towers and cooling coils. The models utilize existing thermal effectiveness relationships developed for sensible heat exchangers with modified definitions of the number of transfer units and the fluid capacitance rate ratio. The results of the models were compared with those of more detailed numerical solutions to the basic heat and mass transfer equations and experimental data. They also did not consider the effect of air–water interface temperature; however, they did consider the effect of water along the vertical length of the tower. The results are only presented for a Lewis number equal to unity.

Mohiuddin and Kant [10, 11] described a detailed procedure for the thermal design of wet, counter-flow and cross-flow mechanical and natural draught cooling towers.

El-Dessouky et al. [12] presented a solution for the steady state counter flow wet cooling tower with new definitions of tower effectiveness and number of transfer units. They did consider the effect of interface temperature and nonunity of the Lewis number, however, the effect of water evaporation on the air process states along the vertical length is not considered. Furthermore, they used an approximate equation for calculating the moist air

enthalpy, which was obtained by curve fitting the tabulated thermodynamic properties of saturated air–water vapor mixtures. The data obtained from the application of the model showed that a substantial error can be obtained when the resistance to heat transfer in water film is neglected and the Lewis number is considered to be unity. However, the amount of error depends very strongly on the ratio between the heat and mass transfer coefficients used in the calculations.

Jorge and Armando [13] tested a new closed wet cooling tower for use in chilled ceilings in buildings. They also obtained experimental correlations for the heat and mass transfer coefficients and concluded that existing thermal models were found to predict reliably the thermal performance of cooling towers. Bernier [14, 15] explained the performance of a cooling tower by examining the heat and mass transfer mechanism from a single water droplet to the ambient air. He did not consider the effect of air temperature as it moved from the bottom to the top of the tower. Nimr [16] presented a mathematical model to describe the thermal behavior of cooling towers that contain packing material. The model takes into account both sensible and latent heat cooling effects on the cooling tower performance. A closed form solution was obtained for both the transient and steady temperature distribution in a cooling tower.

Khan et al. [17] described a more realistic detail model for the steady-state operation of a counter flow wet cooling tower with respect to example problems. In this model, they considered the effect of water evaporation on the air process states, the resistance of heat transfer in the water film and the non-unity of the Lewis number. The data obtained from the application of the model showed that a substantial error can be made when the resistance to heat transfer in the water film is neglected and the Lewis number is

considered to be unity. However, the magnitude of errors in calculating tower thermal parameters is a strong function of the ratio between the heat and mass transfer coefficients that are used in the calculations.

Jose [18] defined a new parameter called ‘‘thermo fluid dynamic efficiency’’, to quantify the performance of cooling tower fills. Thermo-fluid dynamic efficiency means the maximum heat transfer in the cooling tower with the minimum pressure drop. To show this, he evaluated the heat transfer related to the pressure drop in isolated fills with different types of water cooling towers. He showed thermo-fluid dynamic efficiency values obtained with available experimental results acquired from commercial fills, concluded that this efficiency is not a function of the height of the fill.

Zubair et al. [19] investigated the performance characteristics of the counter flow wet cooling towers by using a detailed model. The thermal performance of the cooling towers is explained with different air and water temperatures. The result showed that a majority mode of heat transfer rate is evaporation, where it was 62.5% of the total heat transfer rate at the bottom and about 90% of that at the top of the tower. The variation of air and water temperatures along the height of the tower (process line) is explained on psychometric charts. Since evaporation is by far the most effective factor in cooling towers, the accuracy of the predicted conditions are directly dependent on it.

Kloppers and Kröger [20] studied a detailed derivation of the heat and mass transfer equations of evaporative cooling in wet cooling towers. They presented the equations of the ε-NTU method applied to wet cooling towers. They gave a more detailed representation of the Merkel number by extending the governing equations the Poppe

method. They described the differences in the heat and mass transfer analyses and solution techniques of the Merkel and Poppe methods with the aid of enthalpy diagrams and psychometric charts.

Kloppers and Kröger [21] published a summary of some of the methods that attempt to evaluate wet cooling towers performance. They compared cooling tower performance obtained by Merkel, Poppe and ε-NTU methods. They investigated the effects of the temperature inversion profile on the performance of cooling towers.

Kloppers and Kröger [22] investigated the effect of the Lewis factor, or Lewis relation, on the performance prediction of natural draft and mechanical draft wet-cooling towers. The Lewis factor relates the relative rates of heat and mass transfer in wet-cooling towers. In this study, they discussed the history and development of the Lewis factor and its application in wet-cooling tower heat and mass transfer analyses. They also investigated the relation of the Lewis factor to Lewis number. The influence of the Lewis factor on the prediction of wet cooling tower performance is subsequently investigated. If the inlet ambient air temperature is relatively high, the influence of the Lewis factor, on tower performance diminishes.

Kaiser et al. [23] developed a numerical model for studying the evaporative cooling processes that take place in a new type of cooling tower. In contrast to conventional cooling towers, they used a new device called Hydrosolar Roof which presents lower droplet fall and uses renewable energy instead of fans to generate the air mass flow within the tower. The numerical model developed to analyze its performance is based on computational flow dynamics for the two-phase flow of humid air and water droplets. The

Eulerian approach is used for the gas flow phase and the Lagrangian approach for the water droplet flow phase, with two- way coupling between both phases. The main results of this study showed the strong influence of the average water drop size on efficiency of the system and revealed the effect of other variables like wet bulb temperature, water mass flow to air mass flow ratio and temperature gap between water inlet temperature and wet bulb temperature.

Papaefthimiou et al. [24] developed an analytical model to describe thermodynamically the water evaporation process inside a counter flow wet cooling tower, where the air stream is in direct contact with the falling water, based on the implementation of the energy and mass balance between air and water stream. They described the rate of change of air temperature, humidity ratio, and water temperature and evaporated water mass along the cooling tower height. According to their results, the thermal performance of the cooling tower is sensitive to the degree of saturation of inlet air. They showed that the cooling capacity of the cooling tower increases with decreasing inlet air wet bulb temperature whereas the overall water temperature fall is curtailed with increasing water to air mass ratio.

Muangnoi et al. [25] have used the exergy analysis to investigate the performance characteristics of counter flow wet cooling tower. They developed a mathematical model based on heat and mass transfer principle. They validated the model by experimental data analysis. They showed that the lowest exergy destruction is located at the top of the tower.

Nunez et al. [26] investigated temperature disturbances in a cooling system in various ways, namely: changes in the wet bulb temperature, changes in the heat load and by the deterioration of the coolers performance due to fouling. The response of cooling systems to temperature disturbances is shown to be a function of the overall system thermal effectiveness which in turn is a function of the cooling tower thermal effectiveness and of the network over all thermal effectiveness.

Gharagheizi et al. [27] did an experimental and a comparative study on terms of tower characteristic ratio ($h_D A_V V/\dot{m}_w$), water to air flow ratio ($\dot{m}_w/\dot{m}_a$) and efficiency for two film type packings are presented for a wide range of ($\dot{m}_w/\dot{m}_a$) ratio from 0.2 to 4. The packings used in this work are vertical corrugated packing (VCP) and horizontal corrugated packing (HCP). The obtained results showed that the performance of the cooling tower is affected by the type and arrangement of the packings. Also, the tower performance showed a decrease with an increase in the mass ratio ($\dot{m}_w/\dot{m}_a$) as is also observed in other types of cooling towers. The results showed the tower with vertical corrugated packing (VCP) has higher efficiency than the one with horizontal corrugated packing (HCP).

Ataei et al. [28] investigated the influence of the environmental conditions on the thermal efficiency of the cooling tower. They studied thermal behavior of counter-flow wet cooling tower through a simulation model by varying air and water temperatures and of the ambient conditions. They also performed exergetic analysis in the cooling tower and validated the model against the experimental data.

Lemouari et al. [29] studied an experimental analysis of simultaneous heat and mass transfer phenomena between water and air by direct contact in a packed cooling tower. They used the tower filled with a "VGA" (Vertical Grid Apparatus) type packing which having 0.42 m height and containing four galvanized sheets in a zigzag form, between which three metallic vertical grids are disposed in parallel with a cross-sectional test area of 0.15 m x 0.148 m. They investigated the effect of the air and water flow rates on the heat and mass transfer coefficient as well as the evaporation rate of water into the air stream, for different inlet water temperatures.

Lemouari et al. [30] studied the performance characteristics of a counter flow wet cooling tower by the heat rejected from the tower and its thermal effectiveness. They showed the effect of the air, water flow rates and the inlet water temperatures on the thermal effectiveness of the cooling tower as well as the heat rejected by the tower from water to be cooled to the air stream discharged into the atmosphere. They concluded that the water to air mass flow rate ratio, as well as the inlet water temperature are the parameters of great importance in determining the performance of wet cooling towers.

2.2 SEAWATER COOLING TOWERS

There is increasing interest in using high-salinity water for power plant cooling towers. The growing demands for electricity and water have created pressure to consider using non-fresh water for power plant cooling at new and existing plants designed for closed-cycle cooling. Seawater cooling towers have been used since the 1970's in power generation and other industries, so as to reduce the consumption of freshwater. Sources of high salinity water that could be used in cooling towers include naturally occurring

brackish ground water sources, produced water (ground water that is produced with oil and gas pumping), seawater etc.

Sharqawy et al. [31] investigated the thermal performance of seawater cooling towers using a detailed model of a counter flow wet cooling tower. They considered the coupled heat and mass transfer processes in the study of model. The salts in seawater are known to create a number of operational problems including salt deposition, packing blockage, corrosion, and certain environmental impacts from salt drift and blow down return. In addition, the salinity of seawater affects the thermo physical properties [32] including vapor pressure, density, specific heat, viscosity, thermal conductivity and surface tension, which in turn change the thermal performance of cooling towers. Based on the results of the model, they obtained a correction factor correlation, which relates the effectiveness of the seawater cooling tower with that of fresh water cooling tower for the same tower size and operating conditions. This correction factor equation is valid up to salinity of 120 g/kg. It characterizes the degradation of the cooling tower effectiveness when seawater is used. They showed that an increase in salinity decreases the air effectiveness by 5 to 20% relative to fresh water cooling tower.

The corrosion problems in seawater cooling towers can be avoided by appropriate selection of construction material and equipment. The use of plastic and asbestos for packing, pipes and water distribution system provides a practical and predictable solution for most of the corrosion problems. The use of exposed ferrous material must be avoided and for specific requirements monel or stainless steel should be used. Coatings such as epoxy may also be used to cover special metal construction joints or galvanized rubber

can also be used in critical areas. More details and material selection for seawater cooling towers can be found in Walston [33].

The thermal performance data of seawater cooling towers are mostly in technical reports, feasibility studies, or design guidance reports. A detailed study was done by Bing Yuan and David M. Suptic [34]. They showed economic comparisons of cooling towers. Salt has three basic effects upon the water which in turn affect the thermal performance of the cooling towers. It lowers the vapor pressure, increases the density of the seawater and reduces the specific heat. The lower vapor pressure reduces the rate of evaporation, which in turn changes the thermal performance of cooling tower. As the density of seawater increases, specific heat of seawater decreases more rapidly than it. Consequently the heat absorbing capacity of seawater is less than that of an equivalent volume of fresh water. A saltwater tower, then, must have either the greater water flow or more range in order to handle the same heat load. The environmental issues related to the discharge or treatment of blowdown from salt or brackish water cooling towers app ears to differ little from those for freshwater towers due to high salinity. Elevated salinity in the circulating water could affect drift emissions the drift droplets have a higher salinity, so the mass emission of salt increases while the emission of the drift itself remains unchanged. This introduces the concerns that the mass deposition of salt on neighboring soils, vegetation, buildings, vehicles, and equipment will be higher than for freshwater towers.

CHAPTER 3

MATHEMATICAL MODEL

In this chapter, the mathematical formulation of the seawater wet counter flow cooling towers is discussed. A schematic of the wet counter flow cooling tower process is shown in Fig. 3.1.

The incremental control volume of the basic model of the seawater wet counter flow cooling tower is shown in Fig. 3.2. The major assumptions that are used to derive the basic modeling equations may be summarized as below [35, 36];

- Negligible heat and mass transfer through the tower walls to the environment.
- Water lost by drift is negligible.
- Constant mass transfer coefficient for the cooling tower.
- The Lewis factor that relates the heat and mass transfer coefficients is not unity.
- Water mass flow lost by evaporation is not neglected.
- Uniform temperature throughout the water stream at any cross section.
- Uniform cross-sectional area of the tower.
- The atmospheric pressure is constant along the tower and equal to 101.325 kPa.

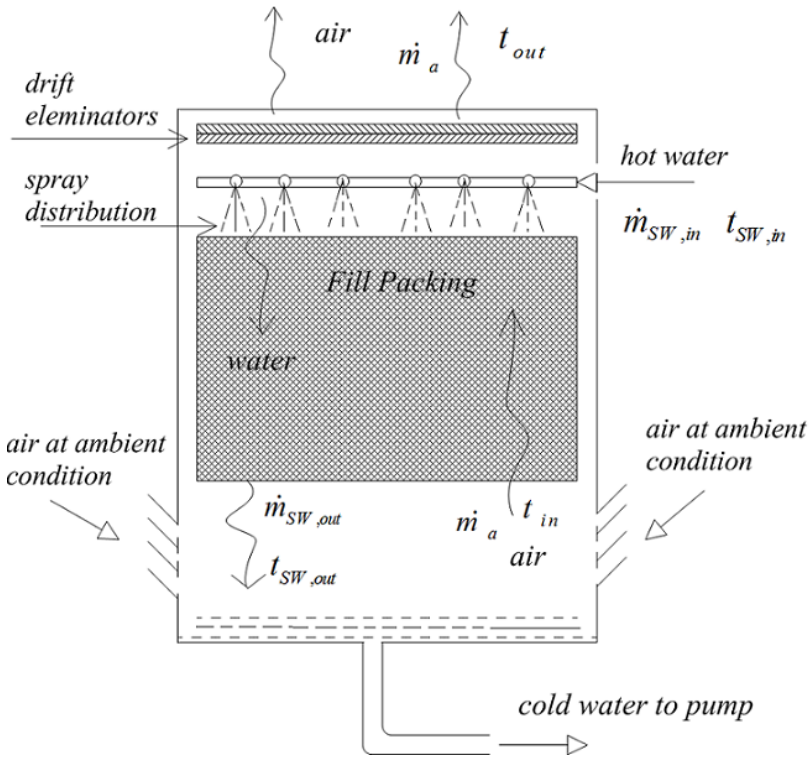

Figure 3.1 Schematic view of a wet counter flow cooling tower

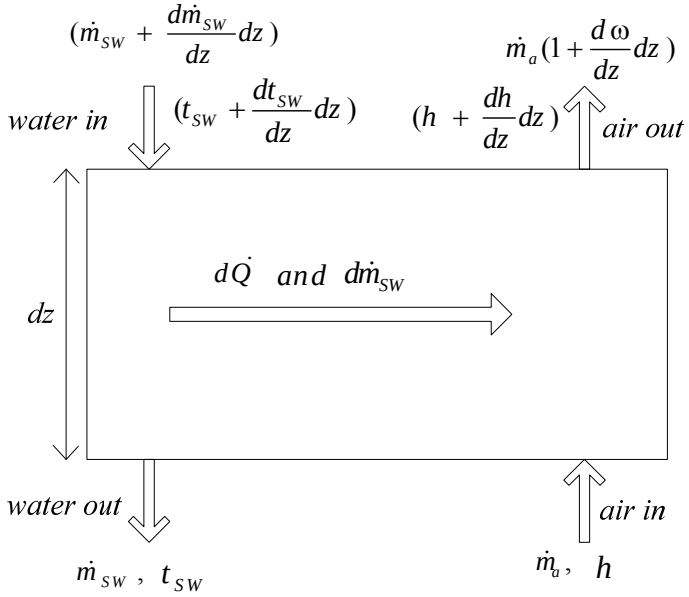

Figure 3.2 Mass and energy balance on an incremental control volume of the seawater counter flow cooling tower

From the steady state energy and mass balances on an incremental control volume (refer to Fig. 3.2) the following differential equations model of cooling tower may be deduced;

3.1 MASS BALANCE ON WATER

total mass in = total mass out

$$\dot{m}_a + (\dot{m}_{SW} + \frac{d\dot{m}_{SW}}{dz}dz) = \dot{m}_{SW} + \dot{m}_a(1 + \frac{d\,\omega}{dz}dz) \tag{3.1}$$

On simplifying, we get;

$$d\dot{m}_{SW} = \dot{m}_a d\,\omega \tag{3.2}$$

The air side water vapor mass balance is defined as follows;

$$d\dot{m}_{SW} = h_D A_V dV\ (\omega_{s,SW} - \omega) \tag{3.3}$$

$$\dot{m}_a d\,\omega = h_D A_V dV\ (\omega_{s,SW} - \omega) \tag{3.4}$$

3.2 MASS BALANCE ON SALTS

The salinity (S) of seawater is defined as,

$$S = \frac{\dot{m}_S}{\dot{m}_S + \dot{m}_w} = \frac{\dot{m}_S}{\dot{m}_{SW}} \tag{3.5}$$

$$\therefore \dot{m}_S = \frac{S}{1-S}\dot{m}_w \tag{3.6}$$

The differential form of this equation is written as;

$$d\dot{m}_S = \frac{S}{1-S} d\dot{m}_w + \frac{dS}{(1-S)^2} \dot{m}_w \tag{3.7}$$

Since the mass of salt will not be changed in the seawater while going from top to bottom inside the cooling tower, so the $d\dot{m}_S$ will be zero.

$$0 = \frac{S}{1-S} d\dot{m}_w + \frac{dS}{(1-S)^2} \dot{m}_w \tag{3.8}$$

After solving this equation and putting $d\dot{m}_w = \dot{m}_a d\,\omega$

We get;

$$\frac{dS}{d\,\omega} = -S \frac{\dot{m}_a}{\dot{m}_{SW}} \tag{3.9}$$

The salinity of seawater inside the cooling tower is calculated by integrating equation (3.9) between the specified limit from $V_1 = 0$ to $V_2 = V$.

3.3 ENERGY BALANCE ON AN INCREMENTAL VOLUME

$$\dot{m}_a.h + (\dot{m}_{SW} + \frac{d\dot{m}_{SW}}{dz} dz).(h_{SW} + \frac{dh_{SW}}{dz} dz) = \dot{m}_{SW}.h_{SW} + \dot{m}_a(h + \frac{dh}{dz} dz) \tag{3.10}$$

On simplifying the above equation, we get;

$$\dot{m}_{SW}\, dh_{SW} + \dot{m}_a d\,\omega h_{SW} = \dot{m}_a dh \tag{3.11}$$

$$d\,\omega = \frac{1}{h_{SW}} \left[dh - \frac{\dot{m}_{SW}}{\dot{m}_a} dh_{SW} \right] \tag{3.12}$$

We may also write the seawater energy balance in terms of the heat and mass transfer coefficients, h_c and h_D, respectively i.e in terms of heat transfer due to convection and evaporation;

$$\dot{m}_{SW}\, dh_{SW} + d\dot{m}_{SW}\, h_{SW} = h_c A_V\, dV\, (t_{SW} - t) + h_D A_V\, dV\, (\omega_{s,SW} - \omega) h_{g,SW} \qquad (3.13)$$

Simplifying the above equation, results in

$$\dot{m}_{SW}\, dh_{SW} = h_c A_V\, dV\, (t_{SW} - t) + h_D A_V\, dV\, (\omega_{s,SW} - \omega) h_{fg,SW} \qquad (3.14)$$

Where,

A_V is contact surface area of water droplets per unit volume of fill, (m^2/m^3)

h_c is convective heat transfer coefficient of air, ($kW/m^2\,K$)

h_D is convective mass transfer coefficient, ($kg/m^2\,s$)

$h_{fg,SW}$ is the latent heat of vaporization, (kJ/kg)

$\omega_{s,SW}$ is the humidity ratio of saturated moist air at evaluated at t_{SW}

In above equations the term $(t_{SW} - t)$ is representing the potential for the convection and the term $(\omega_{s,SW} - \omega)$ is the potential for the evaporation inside the cooling tower.

The Lewis Factor (Le_f) relates the rates of heat and mass transfer in cooling towers as follows;

$$Le_f = \frac{h_c}{c_{p,a} h_D} \qquad (3.15)$$

The Lewis Number (Le) is defined as the ratio of thermal diffusivity (α) to mass diffusivity (D);

$$Le = \frac{\alpha}{D} = \frac{k_a}{\rho_a c_{p,a} D} \tag{3.16}$$

where,

$c_{p,a}$ is heat capacity of air, (kJ/kg K)

D is the mass diffusivity of water in air, (m^2/s)

k_a is the thermal conductivity of air (kW/m K)

ρ_a is the density of air, (kg/m^3)

Lewis factor is provided by Bosnjakovic as a function of Lewis number as follows [22];

$$Le_f = Le^{2/3} \frac{\left(\frac{\omega_{s,w} + d_r}{\omega + d_r}\right) - 1}{\ln\left(\frac{\omega_{s,w} + d_r}{\omega + d_r}\right)} \tag{3.17}$$

d_r = molecular weight ratio of water and air = 0.622

Substituting the Lewis factor in equation (3.14), we get;

$$\dot{m}_{SW} dh_{f,SW} = Le_f h_D c_{p,a} A_V dV (t_{SW} - t) + h_D A_V dV (\omega_{s,SW} - \omega) h_{fg,SW} \tag{3.18}$$

The mass variation of seawater, temperature change, humidity ratio, enthalpy of moist air inside the cooling tower is calculated by integrating the differential equations between the specified limit from $V_1 = 0$ to $V_2 = V$.

The Number of transfer units of the cooling tower is calculated by;

$$NTU = \frac{h_D A_V V}{\dot{m}_a} \tag{3.19}$$

The mass ratio is defined as,

$$MR = \frac{\dot{m}_{SW,in}}{\dot{m}_a} \tag{3.20}$$

The convection heat transfer inside the cooling tower is calculated by;

$$\dot{Q}_{conv} = h_c A_V (t_{SW} - t) V \tag{3.21}$$

The evaporation heat transfer inside the cooling tower is calculated by;

$$\dot{Q}_{evap} = h_D A_V (\omega_{s,SW} - \omega) h_{fg,SW} V \tag{3.22}$$

Range of the cooling tower = $\left(t_{SW,in} - t_{SW,out}\right)$ (3.23)

Approach of the cooling tower = $\left(t_{SW,out} - t_{wb,in}\right)$ (3.24)

3.4 AIR EFFECTIVENESS

This is the ratio of the heat transfer to the air to the maximum possible heat transfer when the outlet air is saturated at the inlet water temperature.

$$\varepsilon_{air} = \frac{h_{air,out} - h_{air,in}}{h_{s,w,in} - h_{air,in}} \tag{3.25}$$

where,

$h_{s,w,in}$ is the enthalpy of saturated air at inlet water temperature

3.5 WATER EFFECTIVENESS

This is the ratio of the heat transfer from the water to the maximum possible heat transfer when the water outlet temperature is equal to the inlet wet bulb temperature of air.

$$\varepsilon_{water} = \frac{\dot{m}_{SW,in} h_{SW,in} - \dot{m}_{w,out} h_{SW,out}}{\dot{m}_{SW,in} h_{SW,in} - \dot{m}_{w,out} h_{SW,ideal}} \tag{3.26}$$

where,

$h_{SW,ideal}$ is the enthalpy of seawater at inlet wet bulb temperature of air

3.6 MERKEL NUMBER CALCULATION

The Merkel number is a non-dimensional coefficient of performance of cooling tower and it is given by equation 3.27.

$$Me = \frac{h_D A_V V}{\dot{m}_{SW,in}} \tag{3.27}$$

The effective value of Merkel number is found by the iterative method from the experimental results by numerical analysis. The inlet experimental values are taken for the numerical analysis and the outlet values are calculated by iteration of Merkel number to get these outlet values similar to experimental values. Once the Merkel Number is calculated the average mass transfer coefficient ($h_D A_V$) for given operating conditions can also be calculated from equation 3.27.

3.7 EXERGY ANALYSIS OF COOLING TOWER

In the wet type cooling tower, seawater and air are the only two kinds of working fluids in operation. Considering dry air and water vapor as an ideal gas, an alternative formula presented by Wepfer et al. [37], gives the convection and evaporation flow exergy of humid air per kilogram of dry air. They used approximate formulations to calculate

exergies for pure components, as is also referred to, in many advanced thermodynamics text books [38, 39].

Conditions at dead states are defined as;

T_o = 298 [K], dead state temperature;

P_o = 101.325, [kPa] dead state pressure;

θ_o = 50 % , dead state relative humidity;

w_o = 0.009923, [kg_w/kg_a] dead state humidity ratio;

$h_{SW,o}$ [kJ/kg] is the specific enthalpy of water at dead state;

$s_{SW,0}$ [kJ/kg K] is the specific entropy of water at dead state;

Exergy of humid air by convective heat transfer;

$$\dot{X}_{air,conv} = \dot{m}_a.(c_{p,a} + \omega.c_{p,v}).T_0.\left(\frac{T}{T_0} - 1 - \ln\left(\frac{T}{T_0}\right)\right) \tag{3.28}$$

Exergy of humid air by evaporation heat transfer;

$$\dot{X}_{air,evap} = \dot{m}_a.R_a.T_0.\left((1+1.608\omega).\ln\left(\frac{1+1.608\omega_0}{1+1.608\omega}\right) + 1.608\omega.\ln\left(\frac{\omega}{\omega_0}\right)\right) \tag{3.29}$$

Total Flow Exergy of humid air is;

$$\dot{X}_{air,total} = \left(\dot{X}_{air,conv} + \dot{X}_{air,evap}\right) \tag{3.30}$$

Total Flow Exergy of seawater is;

$$\dot{X}_{SW} = \dot{m}_{SW}.\left(h_{SW} - h_{SW,0} - R_v T_0.\ln(\theta_0)\right) - \left(T_0.\left(S_{SW} - \dot{m}_{SW}.s_{SW,0}\right)\right) \tag{3.31}$$

Exergy Loss or Destruction in cooling tower;

$$\dot{X}_D = \left(\dot{X}_{SW,in} - \dot{X}_{SW,out}\right) + \left(\dot{X}_{air,in} - \dot{X}_{air,out}\right) \tag{3.32}$$

$$\dot{X}_D = \left(\dot{X}_{SW,2} - \dot{X}_{SW,1}\right) + \left(\dot{X}_{air,1} - \dot{X}_{air,2}\right) \tag{3.33}$$

3.8 SECOND LAW EFFECIENCY

The second law efficiency is a measure of irreversible losses in a given process and for the cooling tower analysis; it is defined as follows;

$$\eta_{II} = 1 - \frac{\dot{X}_D}{\dot{X}_{SW,in} + \dot{X}_{air,in}} \tag{3.34}$$

The Engineering Equation Solver (EES) program is used to solve the differential equations model of seawater cooling tower as discussed in above sections by integration method. The program uses an automatic step size adjustment algorithm for the integration variable while numerically evaluating the integral between the specified limits. A $IntegralTable directive is used to automatically generate an Integral Table holding intermediate values of specified integrated quantities. The software has built-in moist air, water, seawater, water-vapor properties that are needed at each step of numerical calculation. The input variables to the program are given from the inlet conditions of the experimental readings and thus the numerical analysis is carried out to find outlet conditions. Since the integration is taking place from the bottom to the top of the tower. The input variables given to the program are inlet mass flow rate of air, inlet air dry-bulb and wet-bulb temperatures, outlet mass flow rate of water, water outlet temperature, salinity of water at outlet, average mass transfer coefficient ($h_D A_V$) of the tower, heat loss or energy loss in cooling process, cross-sectional area, and the volume of the tower.

The outlet mass flow rate of water and water outlet temperature is given to program by iterative method to find the exact inlet water flow rate and its temperature value. The code of the program used in the numerical analysis is presented in Appendix E.

CHAPTER 4

EXPERIMENTAL APPARATUS

The experimental study is carried out in the heat transfer laboratory of Mechanical Engineering department at King Fahd University of petroleum & Minerals, Saudi Arabia. The apparatus used for the experiments is a bench-top cooling tower H892 model from Hilton. The bench-top cooling tower is a forced draft counter flow wet cooling tower. A schematic of the bench-top cooling tower is shown in Fig. 4.1 and a photograph of the apparatus is shown in Fig. 4.2.

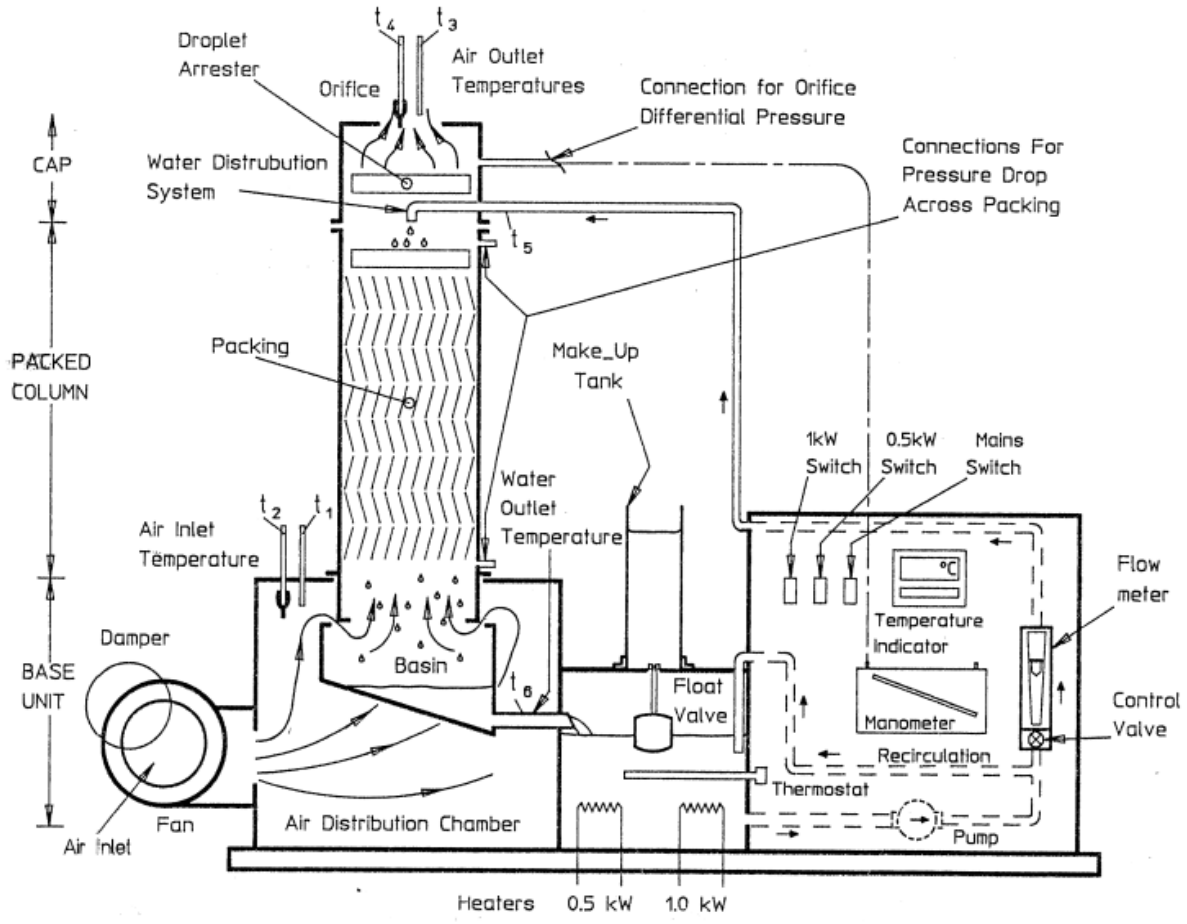

Figure 4.1 Schematic of the bench-top cooling tower Hilton, model H892 [42]

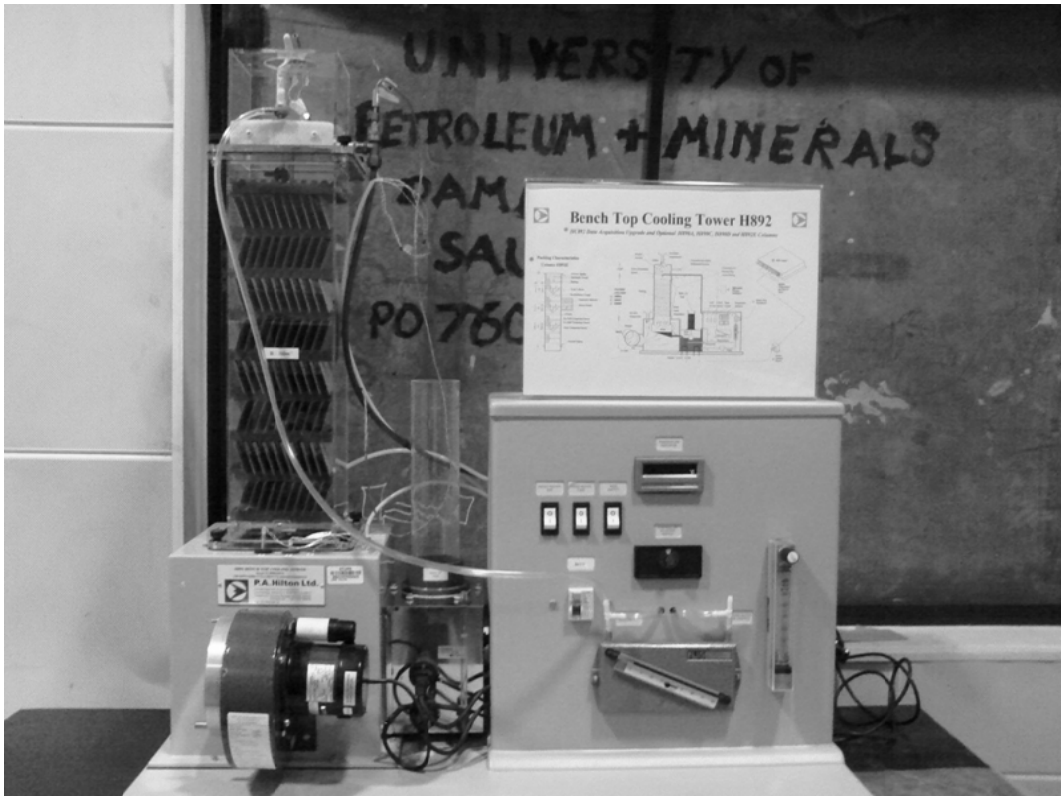

Figure 4.2 Photograph of bench-top cooling tower Hilton, model H892 [42]

4.1 BENCH-TOP COOLING TOWER PROCESS DESCRIPTION

The description of the bench-top cooling tower used in this study is as follows;

Water Circuit

Water is pumped from a storage tank and passes through a control valve (to control the flow rate) then through a rotameter to measure the flow rate of water. Temperature indicators show the inlet and outlet temperatures of water to and from the tower. The water is uniformly distributed over the top of the packing and it spreads over the plates thus a large thin film of water is exposed to the air stream. During its downward passage through the packing, the water is cooled, largely by the evaporation of a small portion of the total flow.

The cooled water falls from the lowest packing deck into the basin where it passes to the storage tank where it is heated by electric heaters before pumping it to again to the tower. Due to evaporation, the level of the water in the tank decreases. This causes a float operated needle valve to open and transfer water from the make-up tank into the storage tank. Under steady conditions, the rate at which the water leaves the make-up tank is equal to the rate of evaporation and the small water droplets drift in the air discharge. The water capacity of the system is 3 liters excluding make-up tank and the energy transferred to water by pump is about 0.1 kW. In addition, two electric heaters (0.5 kW and 1 kW) are inserted in the storage tank to heat water.

Air Circuit

Air at ambient condition enters the blower at a rate which is controlled by an intake damper installed at the inlet. The fan discharges air into the distribution chamber and air passes through the wet and dry bulb sensors before entering the packed column. The wet bulb and dry bulb temperatures of the inlet air are monitored by the temperature indicator. As the air flows through the packing, its moisture content increases due to evaporation of water. On leaving top of the column, air passes through the droplet arrester (drift eliminator), which traps most of the entrained droplets in air stream and returns them to the packings. The air is then discharged to the atmosphere via an orifice and further wet and dry bulb temperatures sensors. The orifice differential pressure reading is measured by an inclined manometer. The pressure drop across the packings is also measured by the same inclined manometer. The wet bulb and dry bulb temperatures of the air discharged from the column are monitored by the temperature indicator. Flow through the column may be observed through the transparent casing.

4.2 SPECIFICATION

The specification of the bench-top cooling tower is as follows;

Base Unit: - All components are mounted on a robust G.R.P. (**Glass-reinforced plastic**) base plate with integral instrument panel. The components include:

i) Air distribution chamber

ii) A tank with heaters to simulate cooling loads of 0.5. 1.0 and 1.5 kW

iii) A make-up tank with gauge mark and float operated control valve

iv) A centrifugal fan with intake damper to give 0.06 kg/s maximum air flow

v) A bronze and stainless steel glandless pump

vi) A water collecting basin

vii) An electrical control panel

Packed Column: - There are four columns available each of 150 mm x 150 mm x 600 mm high and fabricated from P.V.C. Three of them have pressure tapping points and contain eight decks of inclined, wettable, laminated plastic plates, retained by water distribution troughs while the fourth column has no packings. The packing data for the columns is summarized in Table 4.1.

Table 4.1 Packing specification of the columns

	1st Column	2nd Column	3rd Column
Number of decks	8	8	8
Number of plates per deck	7	10	18
Total surface area of packing, m^2	0.83	1.19	2.16
Height of packing, m	0.48	0.48	0.48
Packing specific area, m^2/m^3	77	110	200

Column cap: - This fits on the top of the column and includes:

i) An 80 mm diameter sharp edged orifice and pressure tapping

ii) A droplet arrester (drift eliminator)

iii) Water distributor

4.3 INSTRUMENTATION

Temperature indicator: - There are 6 points of digital temperature indicator with type K thermocouple sensors to measure terminal water temperatures, and wet and dry bulb temperatures at the inlet and outlet of the column.

Inclined U-tube manometer: - One inclined U-tube manometer is used to measure the differential pressure across the orifice or packing. Its range is 0 to 40 mm H_2O. Inclined U-tube manometers provide greater readability by stretching a vertical differential along an inclined indicating column, giving more graduations per unit of vertical height and increasing the instrument's sensitivity and accuracy.

Variable area flow meter (rotameter): - It is used to measure the water flow rate to packings with control valve. Its range is 0 to 50 g/s.

4.4 SAFETY DEVICES

Water level: - A sight glass fitted to the load tank indicates the water level within the tank. During operation, this level must not be allowed to fall below the electric heater surface to avoid burn out of heaters.

Water temperature: - The water temperature should not exceed 50 ^{o}C because of some PVC components in the test rig. Therefore, a thermostat is fitted in the load tank to switch off the heaters if the temperature exceeds 50 ^{o}C.

Heating elements: - All heating elements are provided with automatically reset thermal protection devices, which will operate in the unlikely event of the element overheating.

4.5 CALIBRATION METHODS AND PROCEDURES FOR THERMOCOUPLES, MANOMETER, FLOW METER AND ORIFICE CONSTANT "C"

Calibration is the comparison of an instrument's actual measurement performance to a standard of known readings. Accuracy and reliability of all such measurements would be doubtful if the instruments used were not calibrated. Calibration ensures that a measuring instrument displays an accurate and reliable value of the quantity being measured. Thus, calibration is an essential activity in any measurement process.

4.5.1 Thermocouples Calibration

For accurate temperature measurements, the thermocouples used are calibrated. In this experimental setup the K-type thermocouples are used to measure the temperatures at six points. These six points are dry bulb inlet, wet bulb inlet, dry bulb outlet, wet bulb outlet, water inlet and water outlet temperatures.

The calibration of the thermocouples is carried out by placing all the thermocouples in temperature controllable bath and setting the temperature controllable bath at different constant water temperatures of 10, 20, 30, 35, 40, 45, and 50 ^{o}C at atmospheric pressure. The true temperature readings are recorded from the thermometer in the temperature controllable bath and the measured value of temperature readings are recorded by the

data acquisition system in the computer. The data of the thermocouples calibration are given in Table [4.2].The best fit correlations are given by the equations (4.1) to (4.7)

The equation of temperature correction for thermocouple # 1 (dry bulb inlet) is given by Eq. (4.1) and the calibration curve is plotted in Fig. 4.3;

$$T_{true1} = 0.0001\,T1^3 - 0.0095\,T1^2 + 1.2157\,T1 - 5.238 \quad (4.1)$$

Table 4.2 Thermocouples calibration data

T_{true} (^oC)	T1 (^oC)	T2 (^oC)	T3 (^oC)	T4 (^oC)	T5 (^oC)	T6 (^oC)
10	13.82	14.32	13.74	14.44	14.39	14.42
20	23.67	24.17	23.59	24.29	24.37	24.28
30	34.54	35.82	34.82	35.4	35.72	35.39
35	39.29	40.28	39.82	40.52	40.73	40.15
40	43.92	45.28	44.59	45.29	45.73	45.14
45	48.43	49.9	49.33	49.91	50.47	50.25
50	52.99	54.82	54.12	57.98	55.27	55.05

The equation of temperature correction for thermocouple # 2 (wet bulb inlet) is given by Eq. (4.2) and calibration curve is plotted in Fig. 4.4;

$$T_{true2} = 0.0001\,T2^3 - 0.0094\,T2^2 + 1.2078\,T2 - 5.5831 \quad (4.2)$$

The equation of temperature correction for thermocouple # 3 (dry bulb outlet) is given by Eq. (4.3) and calibration curve is plotted in Fig. 4.5;

$$T_{true3} = 0.0001\,T3^3 - 0.0111\,T3^2 + 1.2657\,T3 - 5.5421 \quad (4.3)$$

The equation of temperature correction for thermocouple # 4 (wet bulb outlet) is given by Eq. (4.4) and calibration curve is plotted in Fig. 4.6;

$$T_{true4} = -0.0002\,T4^3 + 0.0151\,T4^2 + 0.5258\,T4 - 0.0679 \quad (4.4)$$

The equation of temperature correction for thermocouple # 5 (water inlet) is given by Eq. (4.5) and calibration curve is plotted in Fig. 4.7;

$$T_{true5} = 0.0001\,T5^3 - 0.0119\,T5^2 + 1.2889\,T5 - 6.4036 \quad (4.5)$$

The equation of temperature correction for thermocouple # 6 (water outlet) is given by Eq. (4.6) and calibration curve is plotted in Fig. 4.8;

$$T_{true6} = 8\times10^{-05}\,T6^3 - 0.0076\,T6^2 + 1.1898\,T6 - 5.7542 \quad (4.6)$$

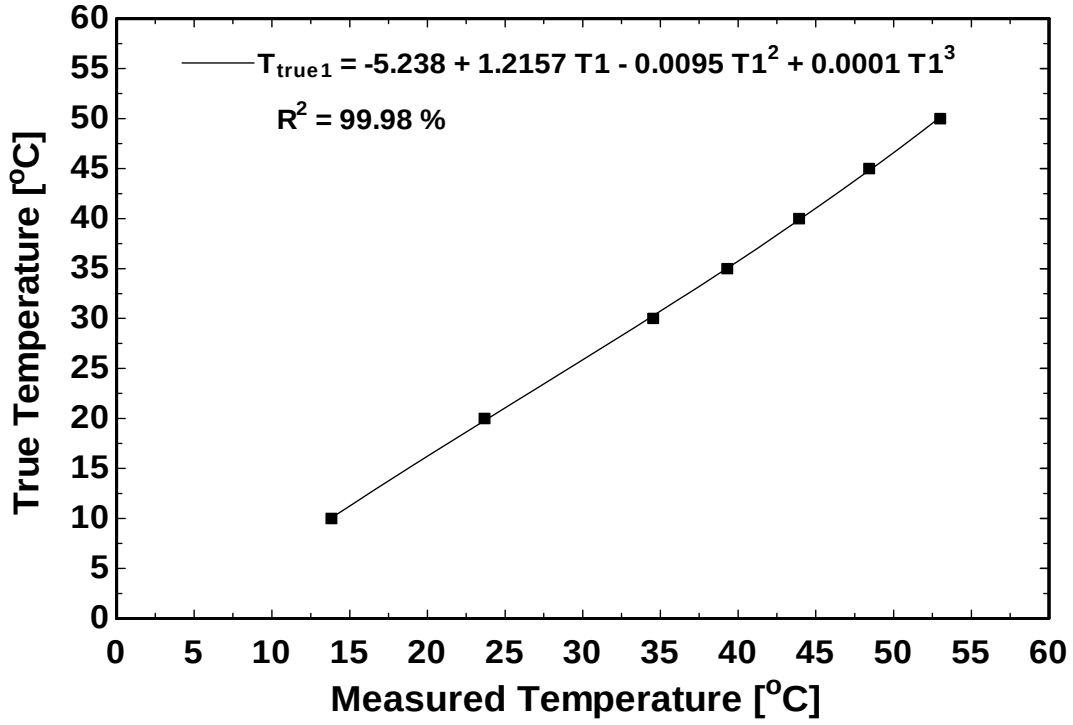

Figure 4.3 Calibration of thermocouple # 1

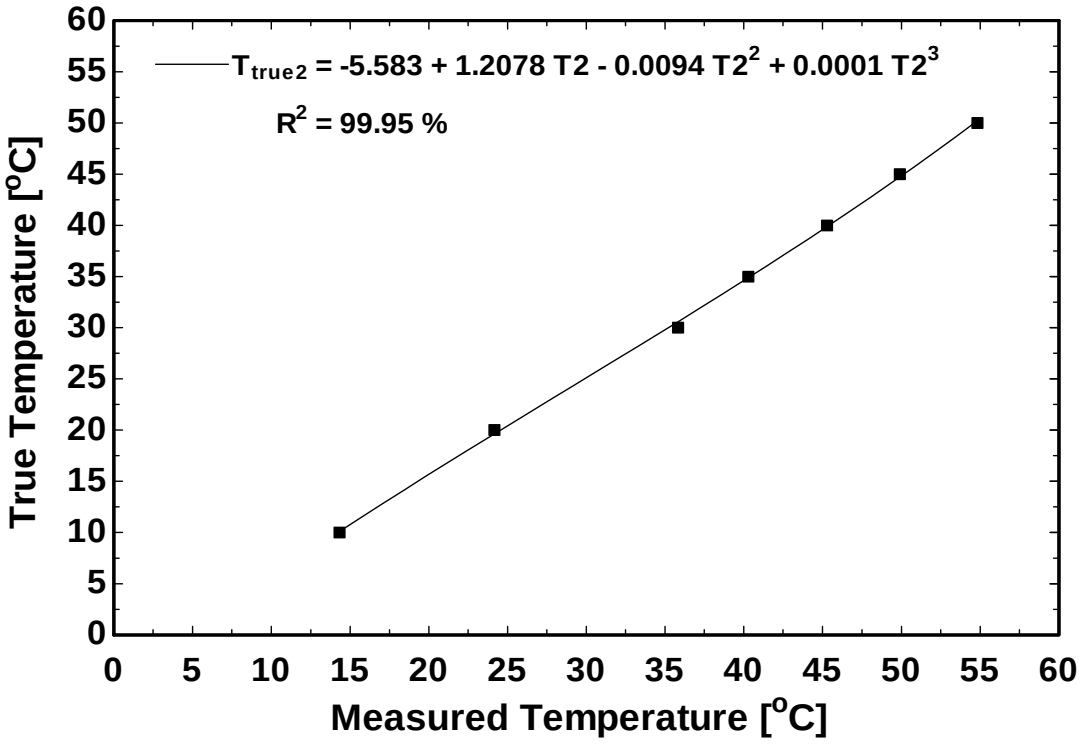

Figure 4.4 Calibration of thermocouple # 2

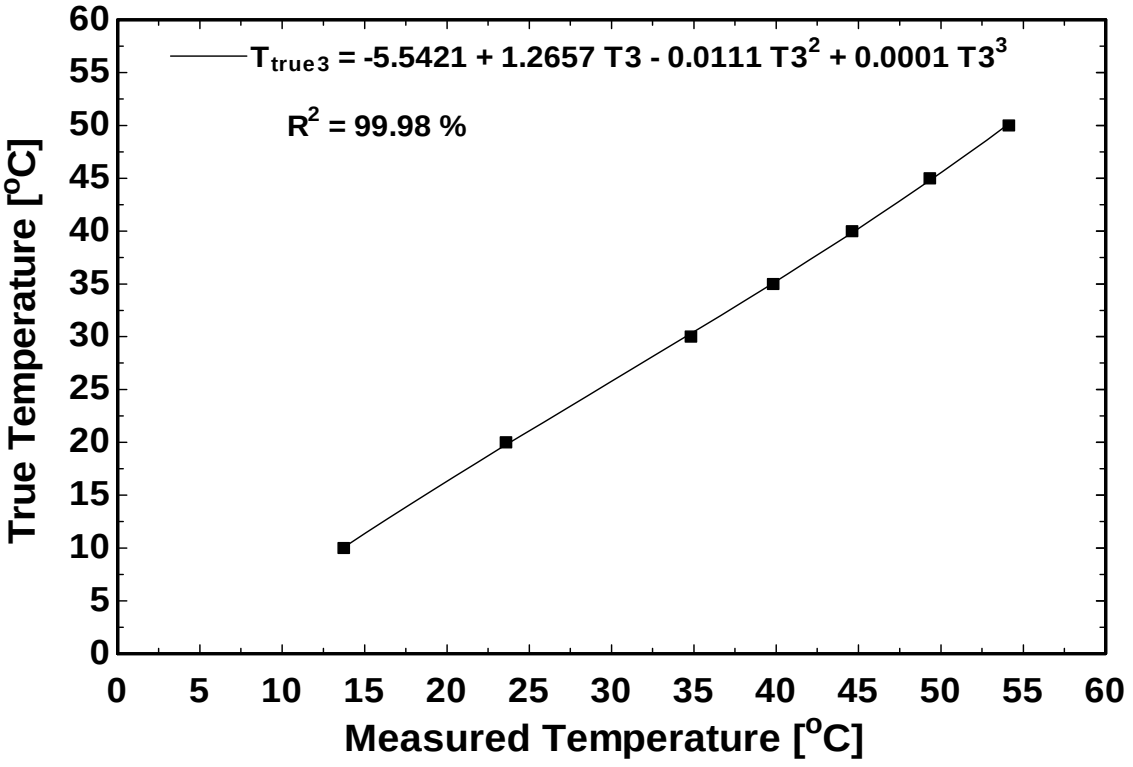

Figure 4.5 Calibration of thermocouple # 3

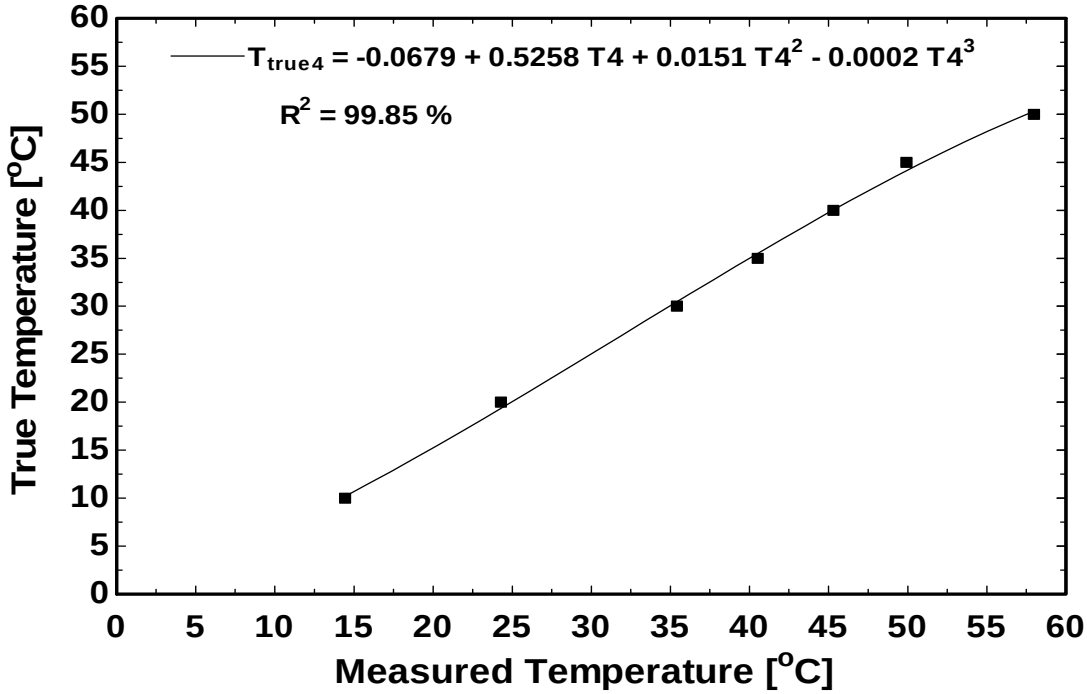

Figure 4.6 Calibration of thermocouple # 4

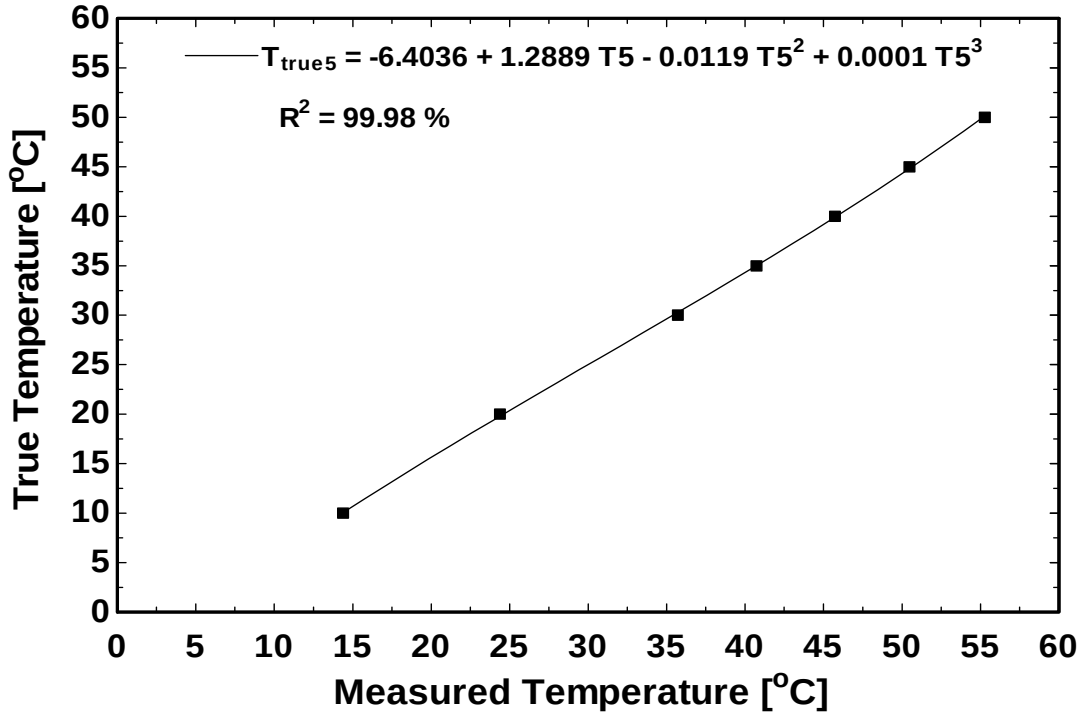

Figure 4.7 Calibration of thermocouple # 5

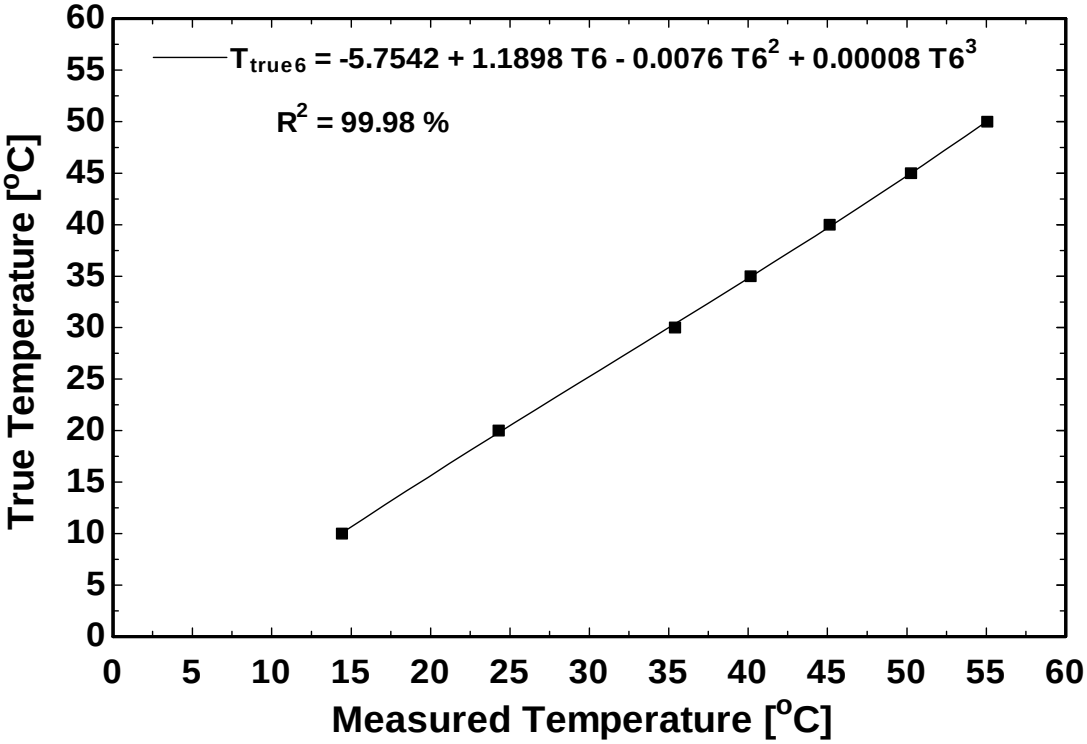

Figure 4.8 Calibration of thermocouple # 6

The thermocouple # 6 is fitted outside the water outlet pipe which contains an error due to temperature difference through pipe thickness. Therefore to reduce the error in the measurement of the exit water temperature (T6), another thermocouple is inserted in the exit water flow stream, so that the exit water temperature is more accurate. This thermocouple is named T7 and it is calibrated also similar to the other thermocouples. The equation of temperature correction for thermocouple #7 (water outlet) is given by Eq. (4.7) and calibration curve is plotted in Fig. 4.9.

$$T_{true7} = 9\times10^{-05}\, T7^3 - 0.0078\, T7^2 + 1.143\, T7 - 1.812 \qquad (4.7)$$

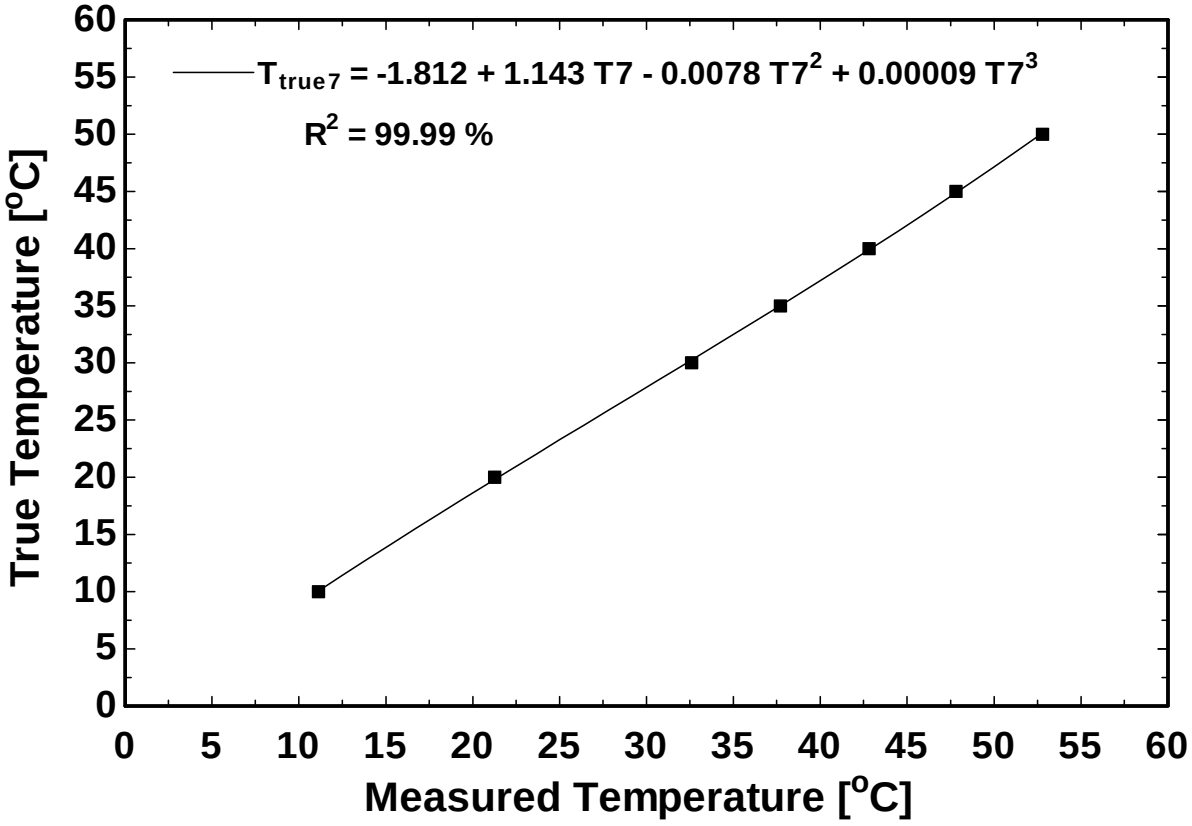

Figure 4.9 Calibration of thermocouple # 7

4.5.2 Manometer Calibration

Manometer readings at different air flow rates are recorded by data acquisition system and simultaneously the true readings are recorded by the manometer. The results from the manometer calibration are shown in Fig. 4.10. The equation of differential pressure correction for manometer is obtained from the plot of measured differential pressure and true differential pressure using recorded data with the help of Microsoft Office Excel. The data of differential pressure recorded by the data acquisition system of values greater than 20 mm H_2O is suddenly changing from the trend line of data up to 20 mm H_2O values. So for precision and accuracy two equations are fitted for the pressure of range up to 20 mm H_2O and another for the pressure of range greater than 20 mm H_2O. The best fit is observed by the visual observation of behavior of data.

The equation of differential pressure correction for manometer is as follows;

$$x_{true} = 0.965\, x_{measured} + 0.533;\ \text{for } x_{measured} < 20 \text{ mm } H_2O \tag{4.8}$$

$$x_{true} = 0.7165\, (x_{measured})^2 - 27.025\, x_{measured} + 274.2;\ \text{for } x_{measured} \geq 20 \text{ mm } H_2O \tag{4.9}$$

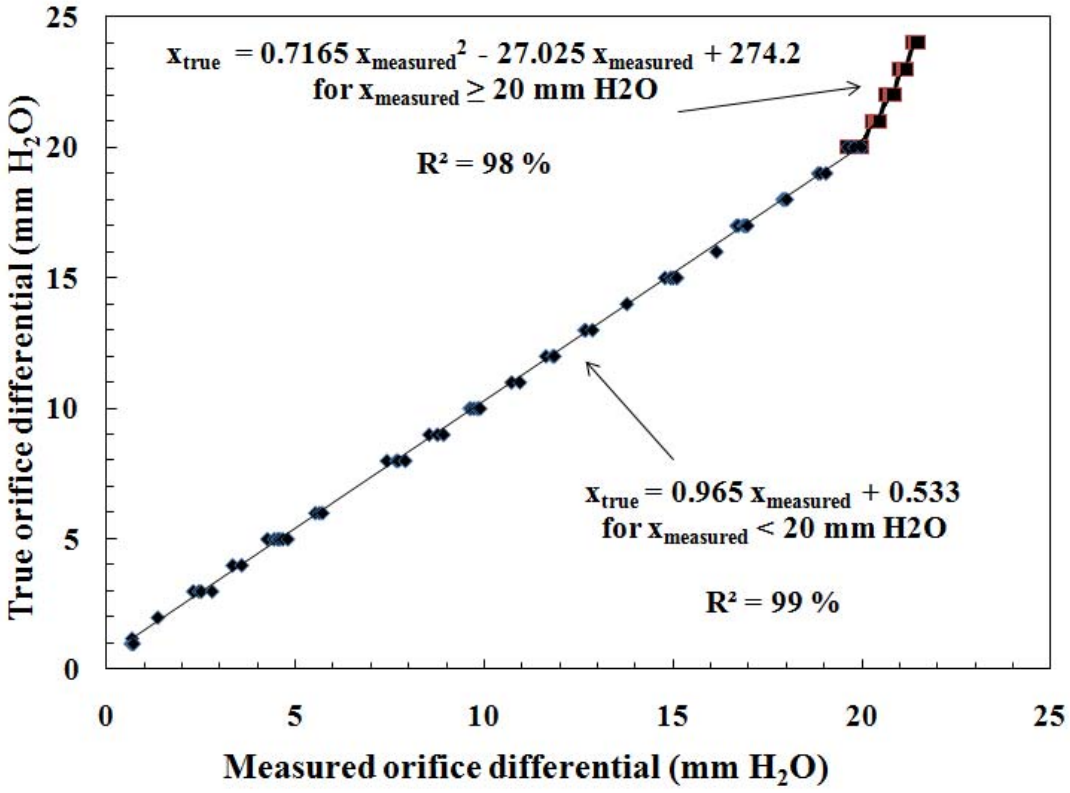

Figure 4.10 Calibration of manometer

4.5.3 Flowmeter Calibration

Flowmeter readings at different water flow rates are recorded by data acquisition system and simultaneously the true readings are recorded by the flow meter. The results from the flow meter calibration are shown in Fig. 4.11. The equation of water flow rate correction for flow meter is obtained from the plot of measured water flow rate and true water flow rate using recorded data. The best fit correlation is given by the equation (4.10).

The equation of water flow rate (g/sec) correction for flow meter is as below;

$$m_{true} = 1.1382\, m_{measured} - 8.9059 \tag{4.10}$$

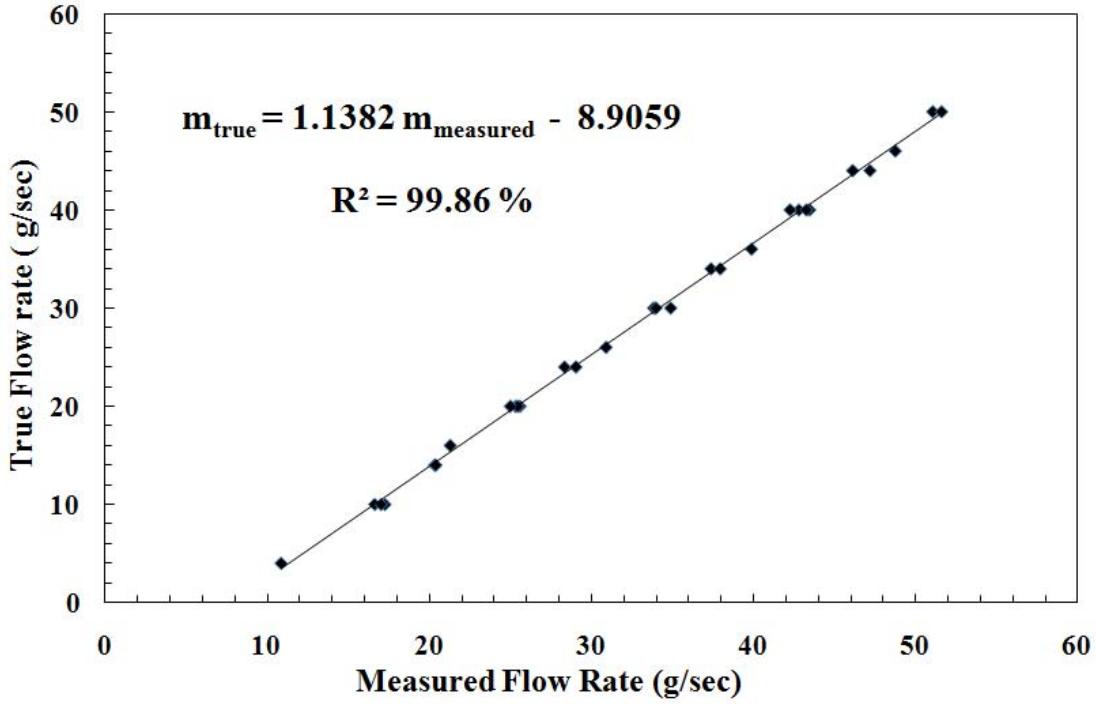

Figure 4.11 Calibration of flowmeter

4.5.4 Air Flow Orifice Calibration

The orifice discharge coefficient is a very significant factor to calculate the air flow rate. The mass flow rate of moist air from the orifice can be calculated by the following equation;

$$\dot{m}_a = \frac{1}{v_a} A_c v = \frac{(1+\omega_o) A_c v}{v_{da}} \tag{4.11}$$

Where, $\dot{m}_a$ = moist air mass flow rate (kg/s)

v_a = specific volume of moist air leaving from the orifice (m^3/kg)

v_{da} = specific volume of dry air leaving from the orifice (m^3/kg)

A_c = cross-sectional area of the orifice (m^2) = 0.005027

v = velocity of air leaving from the orifice (m/s)

ω_o = humidity ratio of moist air at outlet of tower

And mass flow rate of air in terms of orifice differential pressure is given by;

$$\dot{m}_a = C\sqrt{\frac{x}{v_a}} = C\sqrt{\frac{x}{v_{da}/(1+\omega_o)}} \tag{4.12}$$

So from equations 4.11 and 4.12, it is deduced;

$$\frac{(1+\omega_o) A_c v}{v_{da}} = C\sqrt{\frac{x}{v_{da}/(1+\omega_o)}} \tag{4.13}$$

The value of "C" can be calculated by plotting the Eq. (4.13) for the data at different orifice differential pressures.

The velocity of air at the orifice exit is measured by a hot wire anemometer. Hot wire anemometer can measure air velocity with a single probe. At the end of the rod there is a thermal hot wire or hot bead which is cooled by the air flow and the cooling effect has a direct relationship with the velocity of the air it is measuring.

The correct values of different orifice differential pressures and the corresponding air velocity, specific volumes of dry air and humidity ratios are shown in Table 4.3 and the data is shown by Fig. 4.12.

Table 4.3 Air flow orifice calibration data

x	V	v_{da}	ω_o
(mm H_2O)	**(m/s)**	**(m^3/kg)**	**(kg_w/kg_a)**
4.82	4.9	0.8646	0.0167
9.66	8.2	0.8617	0.0161
14.61	9.6	0.8555	0.0143
19.66	11.7	0.8532	0.0136

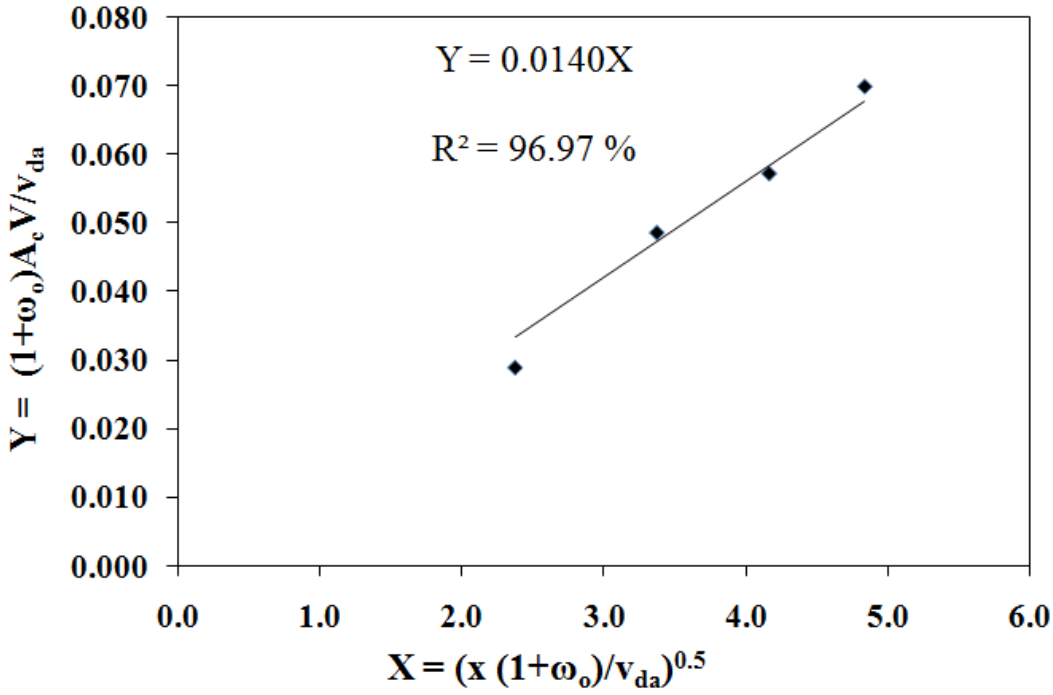

Figure 4.12 Calibration of Orifice discharge coefficient "C"

A best fit line is obtained for the relationship between measured data. The discharge coefficient is obtained from the slope of this line to be “C” = 0.014.

4.6 MODIFICATION OF THE EXPERIMENTAL TEST RIG

The bench-top cooling tower Hilton, model H892 [42] is modified to achieve higher mass flow ratio by increasing the mass flow rate of water. A higher capacity pump 0.5 HP is added to the experimental test rig to spray water at the top of cooling tower. The water is sucked from the water tank by the pump and delivered to the cooling tower. A water tank of 30 liter capacity of PVC material is made. Three heaters each of 1.5 kW are placed in the water tank. A rotameter of max capacity 6 liter/min is placed to measure the water flow rate. For the accuracy of air inlet dry bulb and inlet wet bulb temperature, dry bulb and wet bulb temperature sensors are fitted in a PVC pipe of diameter 16 mm at the air suction inlet of blower and the damper is placed at the inlet of pipe to control the air flow rate. The heaters are connected to the variacs to supply the required amount of energy to heat the water. The schematic diagram of the modified experimental test rig of the cooling tower is shown in Fig. 4.13. The photograph of the modified experimental test rig of the cooling tower is shown in Fig. 4.14 (a). The piping, valves, tank of the experimental test rig are shown in Fig. 4.14 (b).

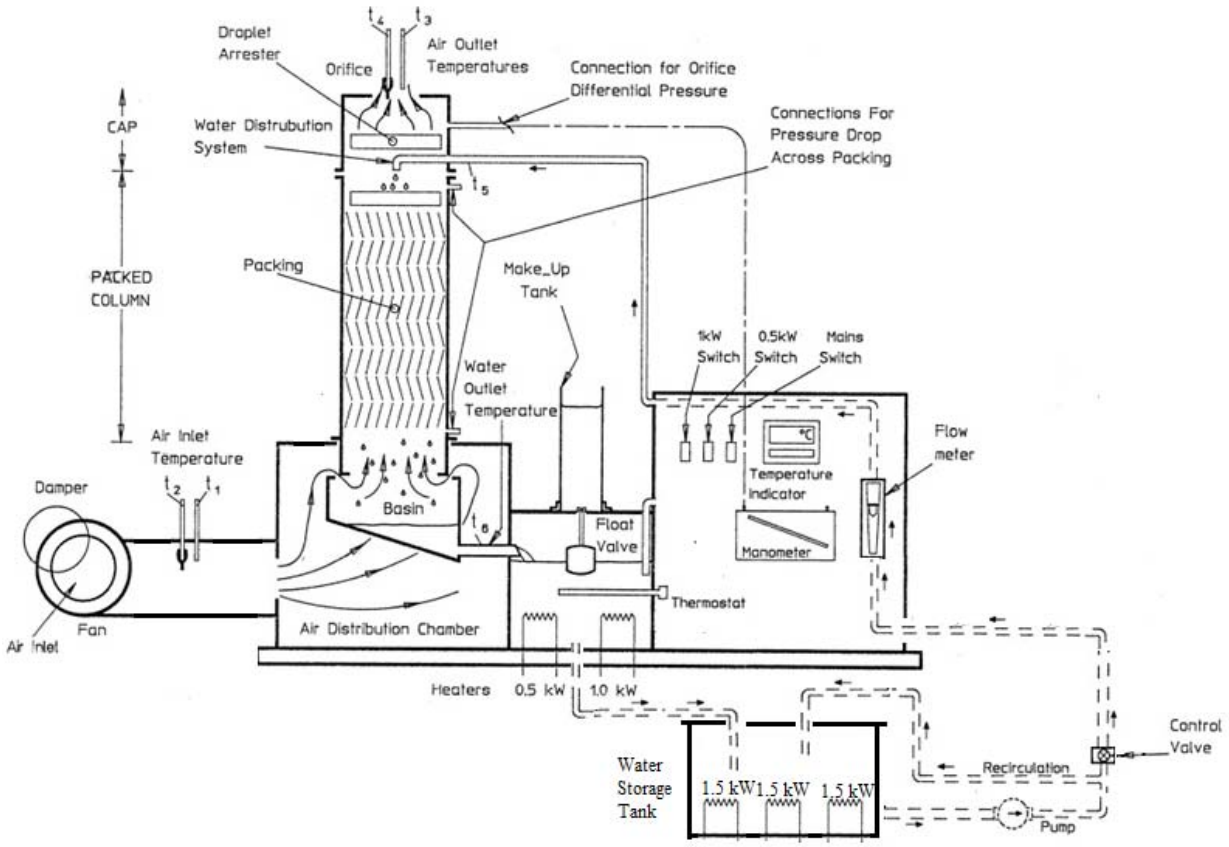

Figure 4.13 Schematic diagram of the modified experimental test rig

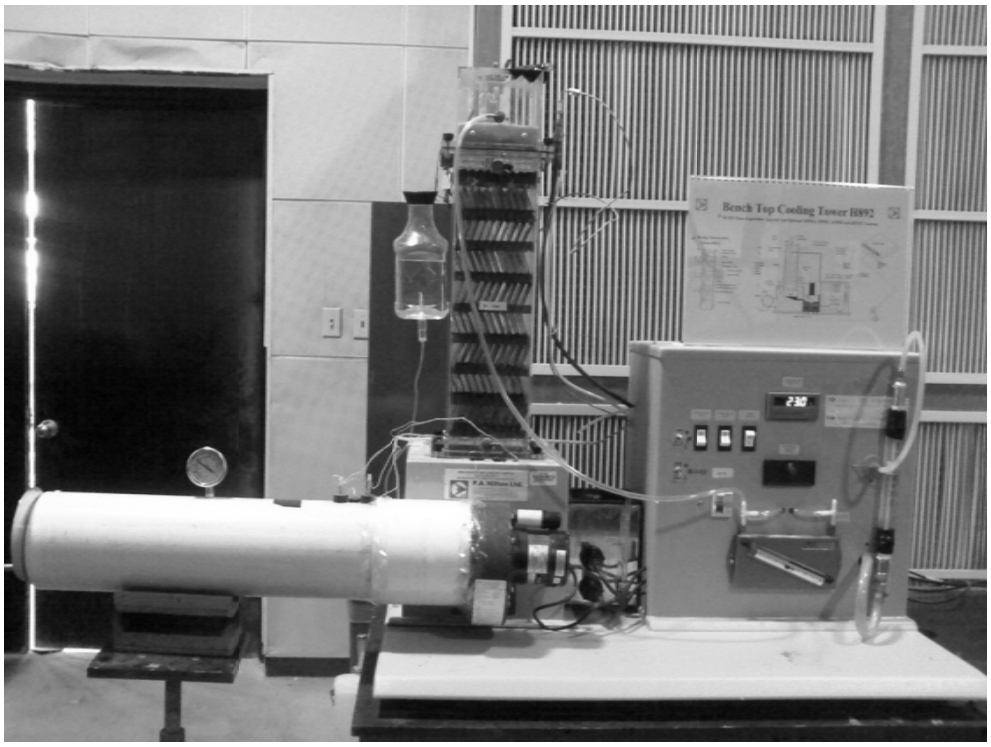

Figure 4.14 (a) Front view of the modified experimental test rig

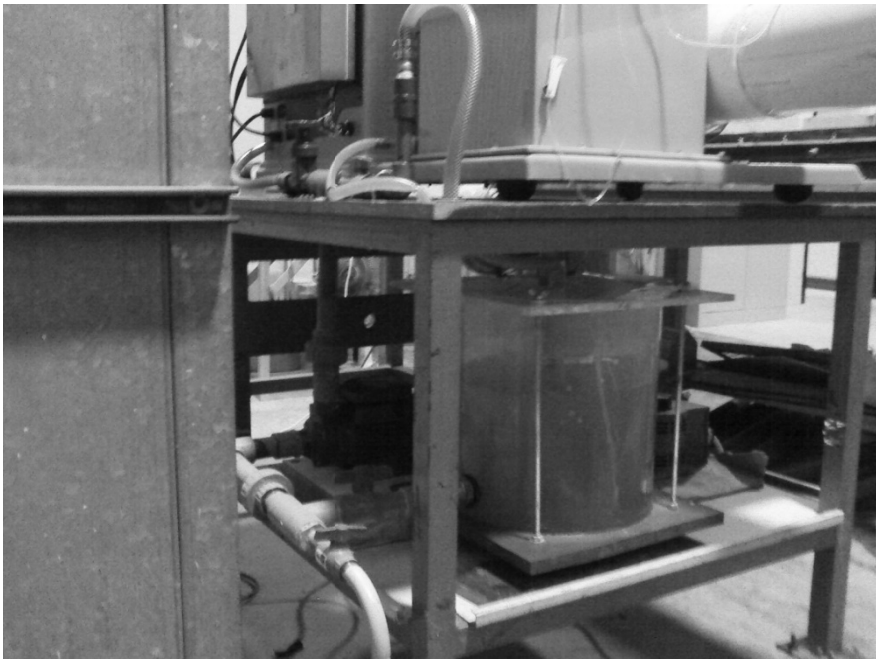

Figure 4.14 (b) Side view of the modified experimental test rig

4.7 EXPERIMENTAL TEST RIG OF SHOWER TOWER

The modified bench-top cooling tower Hilton, model H892 [42] is used for shower cooling tower experiment. The tower used for this case is the one without fill packing. A spray nozzle is fitted at the top of the tower to atomize water inside the tower. Other settings are kept same as for the experimental test rig of the cooling tower. A photograph of the shower cooling tower is shown in Fig. 4.15.

Figure 4.15 Shower tower without Fill Packing

CHAPTER 5

RESULTS AND DISCUSSIONS

5.1 FRESH WATER AND SEAWATER EXPERIMENTAL RESULTS FOR COOLING TOWER

Experiments are carried out on the bench-top cooling tower (refer to Fig. 4.13) with packing of specific area 110 m^{-1} as described earlier in Table 4.1. The dimension of the tower is 150 mm x 150 mm x 600 mm high and fabricated from P.V.C. The experimental data is obtained for fresh water of salinity equal to 0.5 g/kg and seawater of salinity equal to 44 g/kg and 85 g/kg. The seawater used was brought from the Arabian gulf having salinity 44 g/kg. A concentrated salinity solution (S= 85 g/kg) was prepared by circulating the seawater in cooling tower experimental test rig for about 4 to 5 hours. The details of seawater salinity measurement are given in Appendix D. The inlet air dry bulb temperature is 22.4 ± 1.1 ^{o}C, the air wet-bulb temperature is 16.8 ± 1.5 ^{o}C and water inlet temperature is 31.5 ± 0.2 ^{o}C for all test runs. The mass ratios (mass flow rate of water to air) for these readings are varied from 0.5 to 4.8. The thermal performance of the cooling tower is determined by calculating enthalpy, exergy, exergy loss, energy loss, percentage energy loss, Merkel number and effectiveness values by the program that is

written in Engineering Equation Solver (EES) for all the data of fresh water and seawater. All the experimental data obtained from the experimental test rig are summarized in Table B.1; however, the calculated numerical results including uncertainty calculations are presented in Table B.2.

The numerical analysis is carried out in Engineering Equation Solver (EES) by taking all the experimental inlet values such as mass flow rate of air and water, temperature values of water inlet, air dry-bulb inlet and air wet-bulb inlet as shown in Table B.1. The numerical analysis results thus obtained through the program developed in this work are summarized in Table B.3.

The experimental data is collected for all the mass ratios of fresh water and seawater from an initial state; that is at t = 0 to a steady state condition at which the variation of temperature is ± 0.1 ^{o}C. The temperature variation versus time plots are shown in figures (5.1), (5.2) and (5.3) for fresh water of mass ratio 1.0, seawater (S = 44 g/kg) of mass ratio 1.0 and seawater (S = 85 g/kg) of mass ratio 1.1 respectively. For seawater (S = 85 g/kg), the mass ratio obtained is 1.1 that is more than that of the fresh water and the seawater (S = 44 g/kg) because in experimental test rig we fixed the volume flow of the water and since the density of seawater (S = 85 g/kg) and higher compare to fresh water and the seawater (S = 44 g/kg) so the mass flow rate of water is higher and that's why mass ratio is increased. The temperature variation versus time plots for other operating conditions at different mass ratios are presented in Appendix B. It is important to note that the steady state temperatures of water inlet and outlet, air dry-bulb inlet and outlet, and air wet-bulb inlet and outlet are found by taking the average values at the last 10 minutes of the steady state conditions. As shown in figures (5.1), (5.2) and (5.3) all the

temperatures reach steady-state value after about 20-30 minutes from the starting of the experiment. It is noticed that inlet dry-bulb and wet-bulb temperatures of air remains almost constant during the experiment, but the water inlet temperature due to the heat input to achieve the desired water inlet temperature takes about 30 minutes to reach the target value.

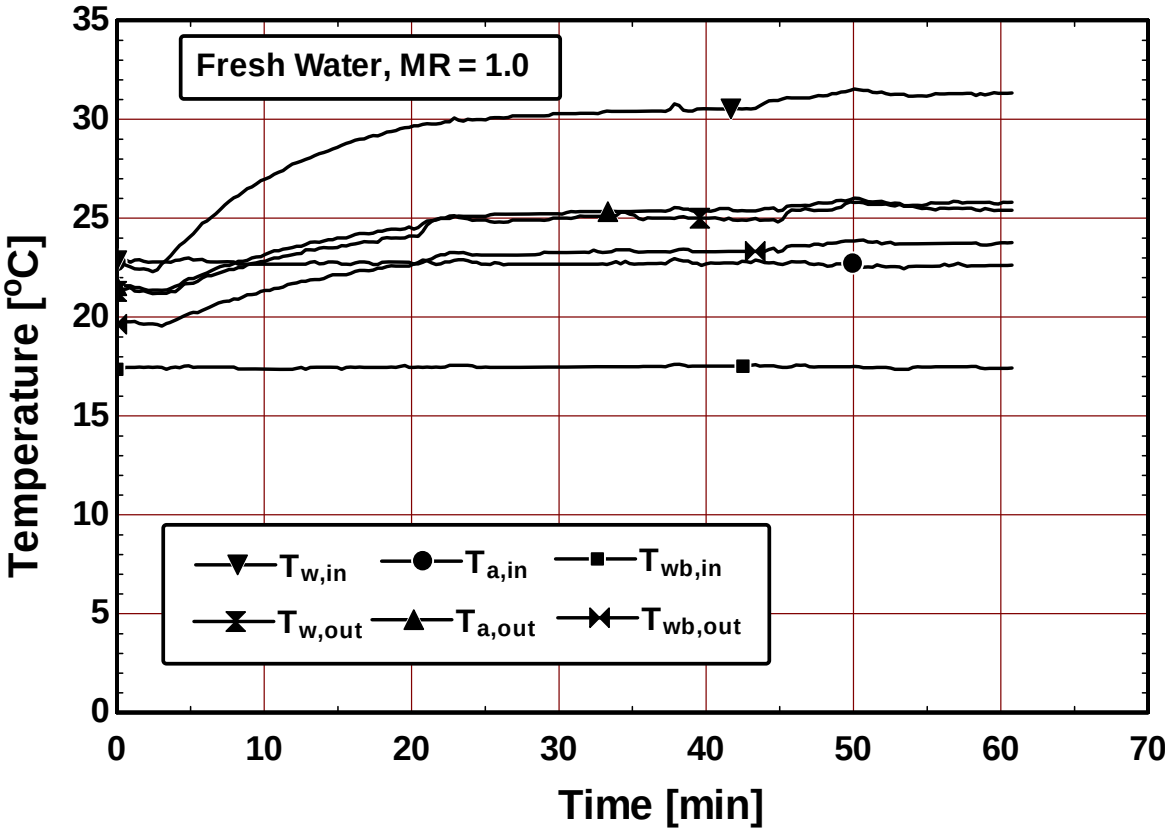

Figure 5.1 Temperature variations versus time for fresh water at mass ratio of 1.0 for cooling tower

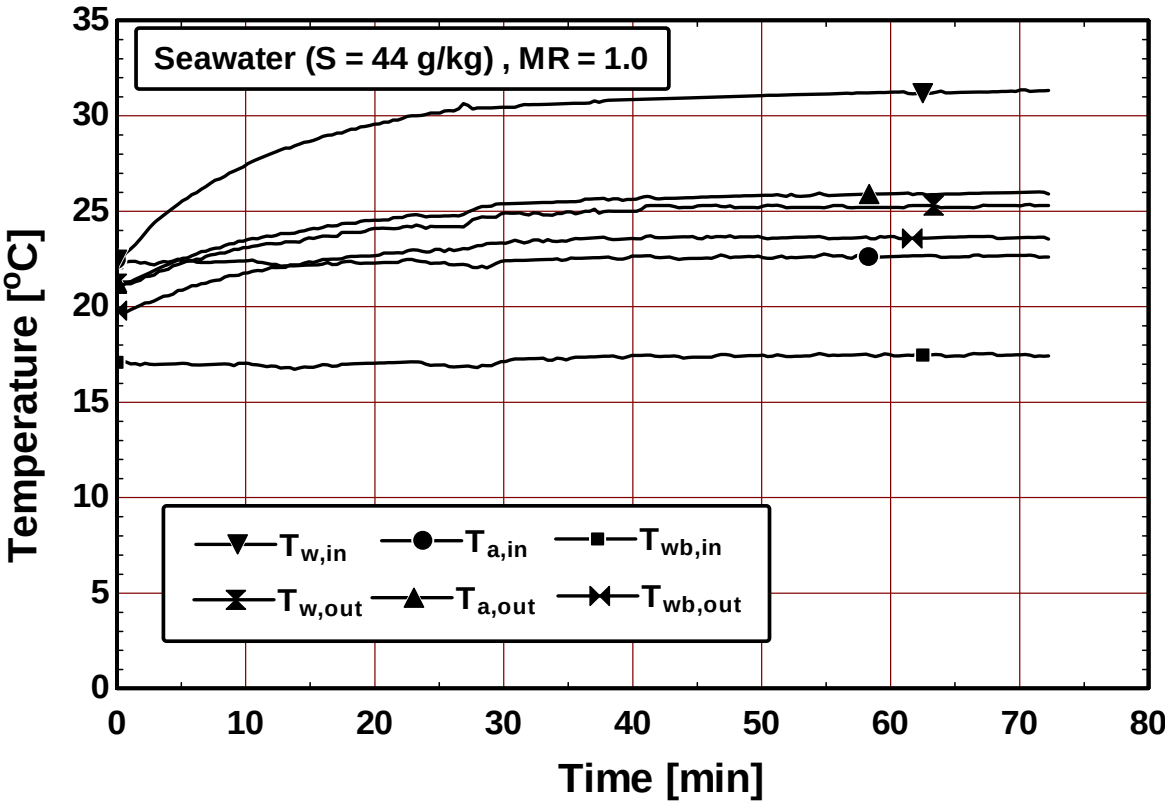

Figure 5.2 Temperature variations versus time for seawater (Salinity = 44 g/kg) at mass ratio of 1.0 for cooling tower

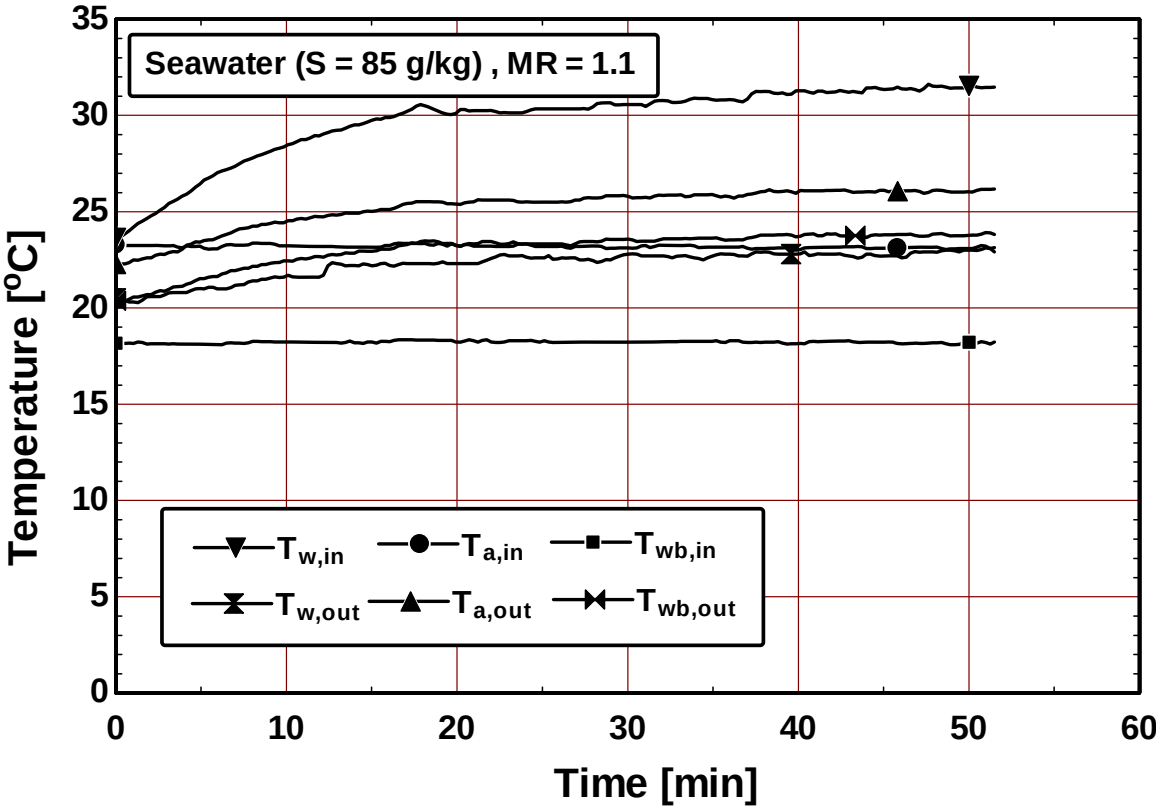

Figure 5.3 Temperature variations versus time for seawater (Salinity = 85 g/kg) at mass ratio of 1.1 for cooling tower

Air effectiveness and water effectiveness versus mass ratios for fresh water, seawater (S = 44 g/kg) and seawater (S = 85 g/kg) of cooling tower are plotted in Figures (5.4) and (5.5). As shown in Fig. (5.4), air effectiveness increases with the increase of the mass ratio because as mass ratio increases air at the outlet of tower gets more saturated and thus it's enthalpy at the outlet increases and thus the air effectiveness; and air effectiveness decreases with increasing the salinity of the seawater. Regression correlations, representing the best fitted curves through the experimental data of air effectiveness are shown in Fig. (5.4). The relation between air effectiveness and mass ratio for the experimental results of fresh water is $\varepsilon_{air,exp} = 0.363MR^{0.361}$ with correlation coefficient $R^2 = 98.14$ %. For seawater (S = 44 g/kg), a relation between air effectiveness and mass ratio is obtained as $\varepsilon_{air,exp} = 0.345MR^{0.354}$ with correlation coefficient $R^2 = 95.26$ %. For seawater (S = 85 g/kg) the fitted relation between air effectiveness and mass ratio is $\varepsilon_{air,exp} = 0.333MR^{0.346}$ with $R^2 = 97.37$ %.

Figure (5.5) shows water effectiveness of fresh water, seawater (S = 44 g/kg) and seawater (S = 85 g/kg) versus mass ratio. As shown the water effectiveness decreases with the increase in the mass ratio; however, it increases with increasing the salinity of the seawater. Regression correlations, representing the best fitted curves through the experimental data of air effectiveness are shown in Fig. (5.5). The relation between water effectiveness and mass ratio for the experimental results of fresh water is $\varepsilon_{water,exp} = 0.811\exp(-0.63MR)$ with correlation coefficient $R^2 = 99.37$ %. For seawater (S = 44 g/kg), a relation between water effectiveness and mass ratio is obtained as $\varepsilon_{water,exp} = 0.902\exp(-0.605MR)$ with correlation coefficient $R^2 = 99.56$ %. For seawater (S = 85

g/kg) the fitted relation between water effectiveness and mass ratio is $\varepsilon_{water,exp}$= 0.975exp(-0.537MR) with correlation coefficient R^2 = 99.16 %.

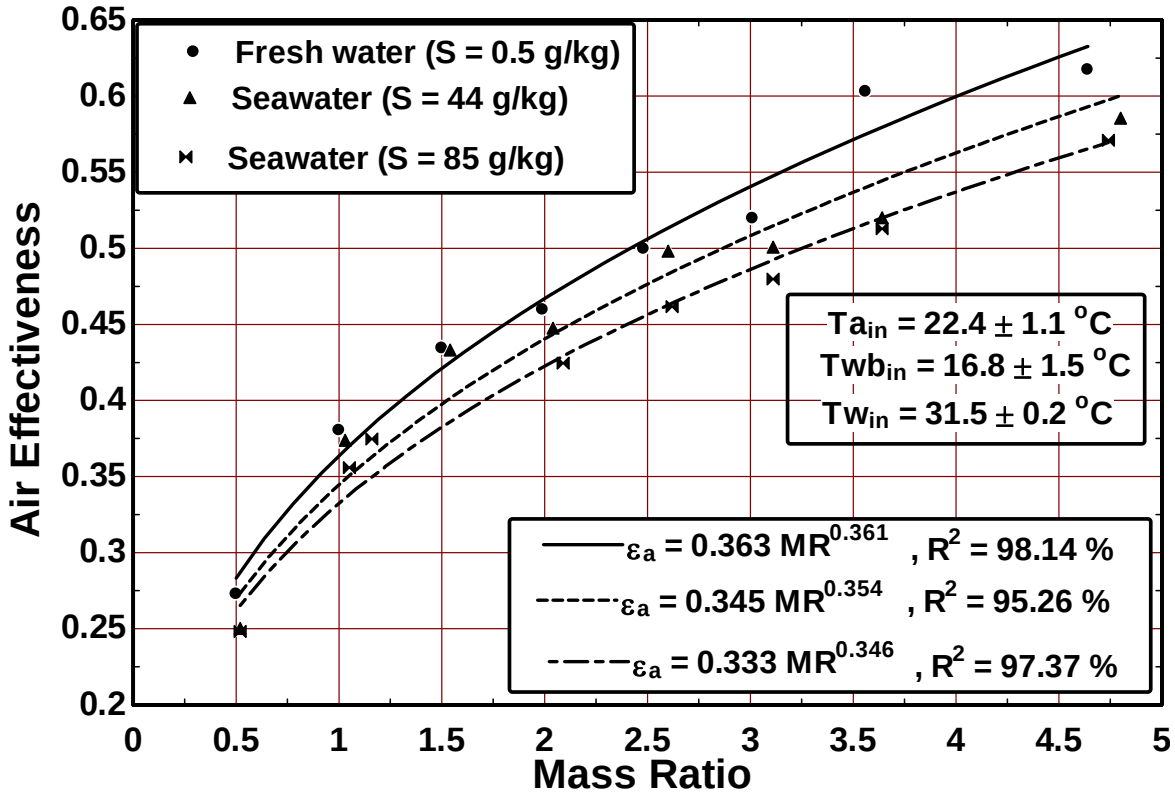

Figure 5.4 Air effectiveness versus mass ratio for the experimental results of fresh water and seawater for Cooling Tower

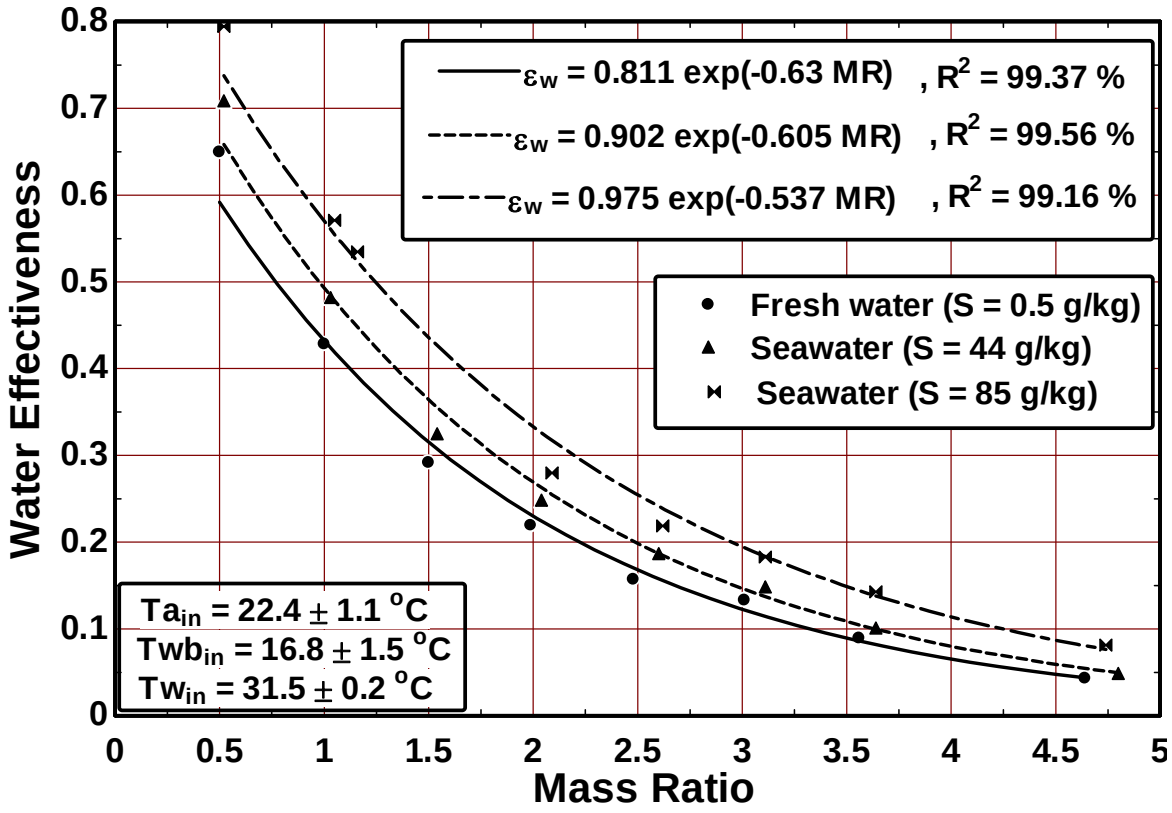

Figure 5.5 Water effectiveness versus mass ratio for the experimental results of fresh water and seawater for Cooling Tower

The experimental values of air effectiveness at each mass ratio for fresh water presented in Table B.2 are compared with that obtained from the numerical results presented in Table B.3 and is plotted in Fig. 5.6. The regression equations, representing the best curves through the experimental data of air effectiveness for fresh water are shown in Fig. 5.6 as well. The relation between air effectiveness and mass ratio for the experimental results of fresh water is $\varepsilon_{air,exp} = 0.363MR^{0.361}$ with $R^2 = 98.14$ %.

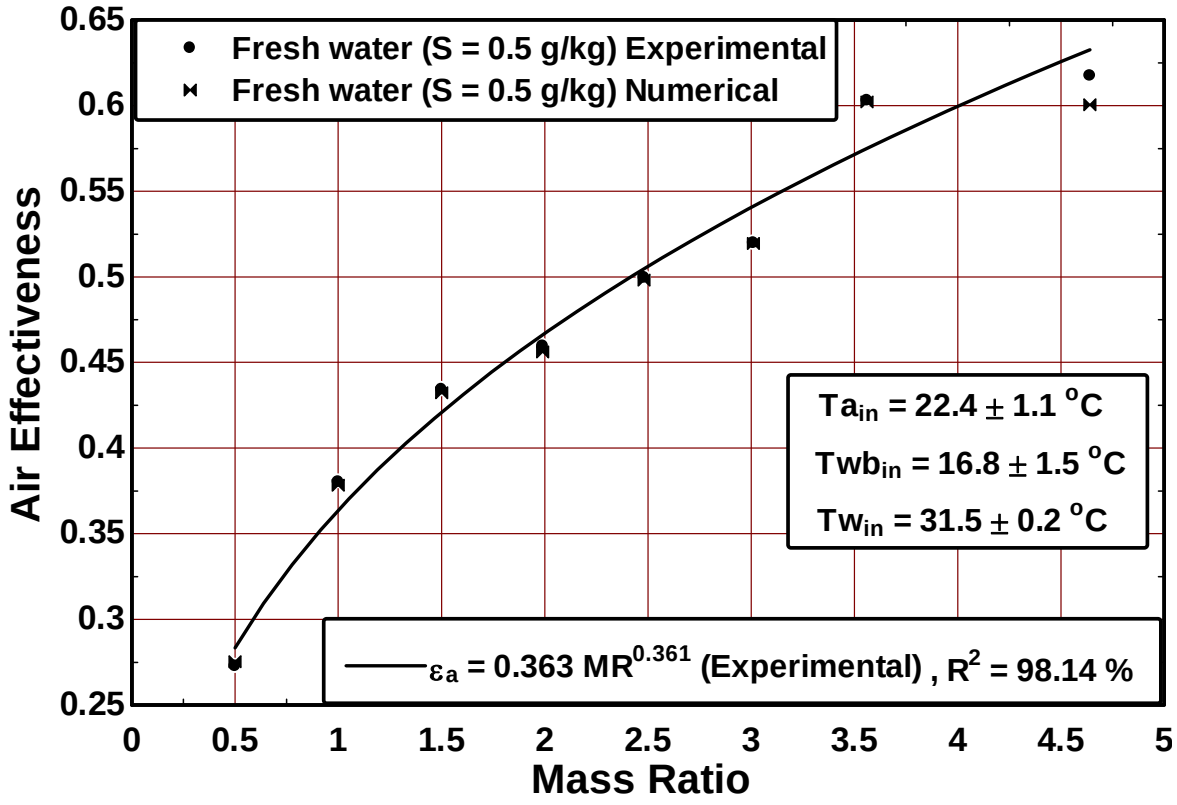

Figure 5.6 Air effectiveness of fresh water versus mass ratio of the experimental results compared with numerical results for cooling tower

The experimental values of water effectiveness values at each mass ratio for fresh water presented in Table B.2 are compared with that obtained from the numerical results presented in Table B.3 and is plotted in Fig. 5.7. The regression equations, representing the best curves through the experimental data of water effectiveness for fresh water are shown in Fig. 5.7 as well. The relation between water effectiveness and mass ratio for the experimental results of fresh water is $\varepsilon_{water,exp} = 0.811\exp(-0.63MR)$ with correlation coefficient $R^2 = 99.37$ %.

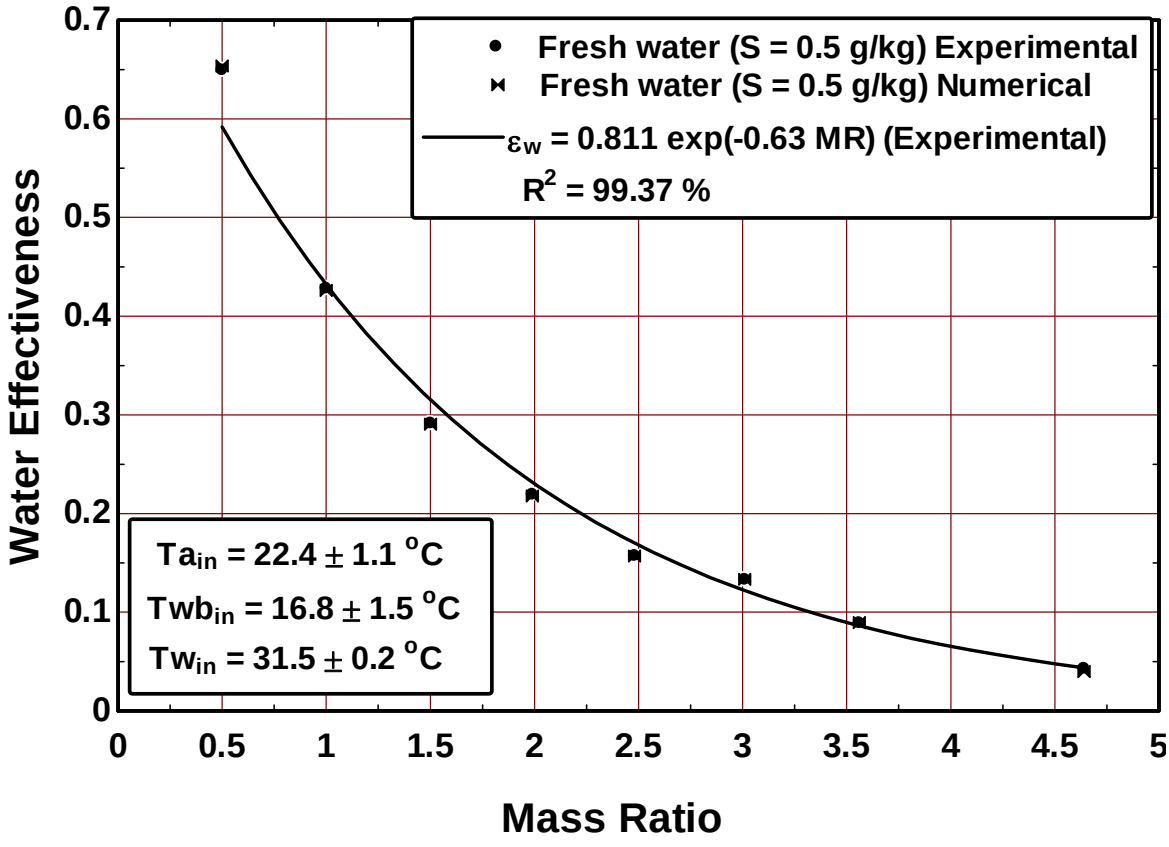

Figure 5.7 Water effectiveness of fresh water versus mass ratio of the experimental results compared with numerical results for cooling tower

The experimental values of air effectiveness for seawater (S = 44 g/kg) presented in Table B.2 are compared with that obtained from the numerical results presented in Table B.3 and is plotted in Fig. 5.8. The regression equation, representing the best curve through the experimental data of air effectiveness for seawater (S = 44 g/kg) are shown in Fig. 5.8 as well. The relation between air effectiveness and mass ratio for the experimental results of seawater (S = 44 g/kg) is $\varepsilon_{air,exp} = 0.345MR^{0.354}$ with correlation coefficient $R^2 = 95.26$ %.

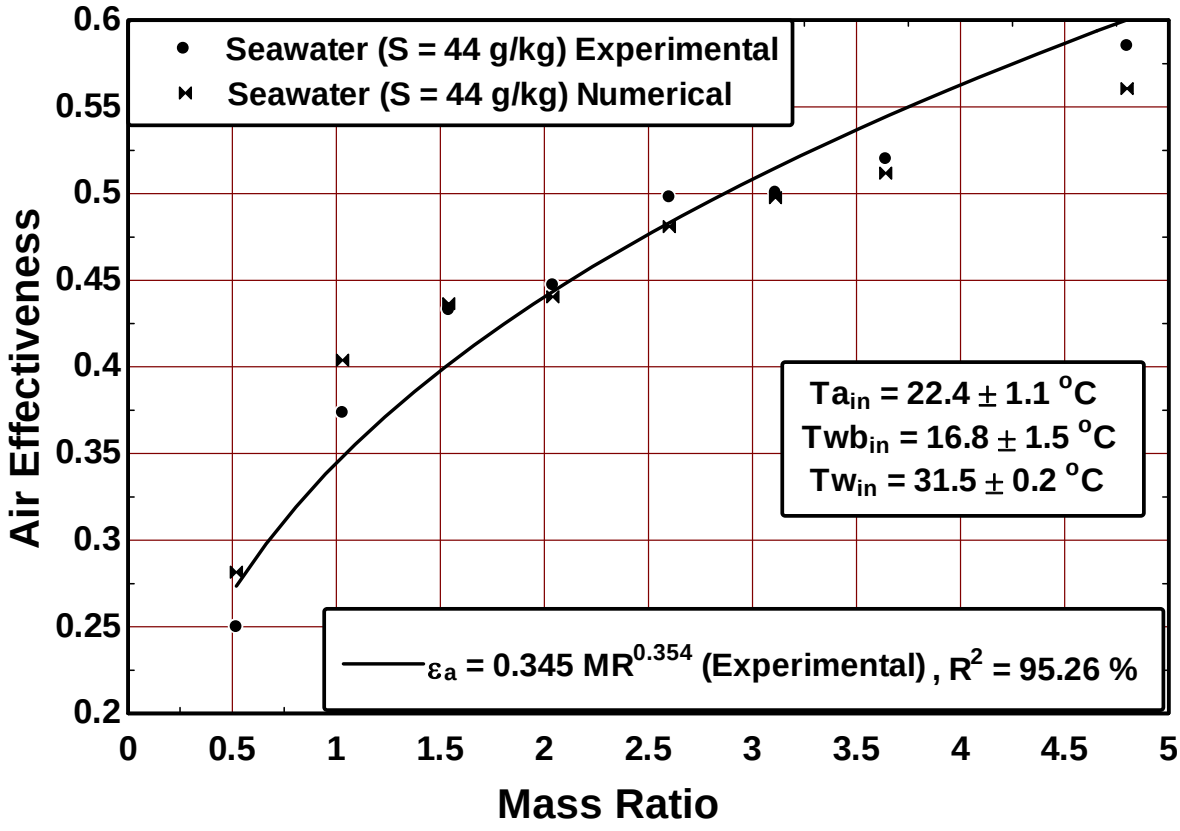

Figure 5.8 Air effectiveness of seawater (salinity = 44 g/kg) versus mass ratio of the experimental results compared with numerical results for cooling tower

The experimental values of water effectiveness for seawater (S = 44 g/kg) presented in Table B.2 are compared with that obtained from the numerical results presented in Table B.3 and is plotted in Fig. 5.9. The regression equations, representing the best curves through the experimental data and of water effectiveness for seawater (S = 44 g/kg) are shown in Fig. 5.9 as well. The relation between water effectiveness and mass ratio for the experimental results of seawater (salinity = 44 g/kg) $\varepsilon_{water,exp} = 0.902\exp(-0.605MR)$ with correlation coefficient $R^2 = 99.56$ %.

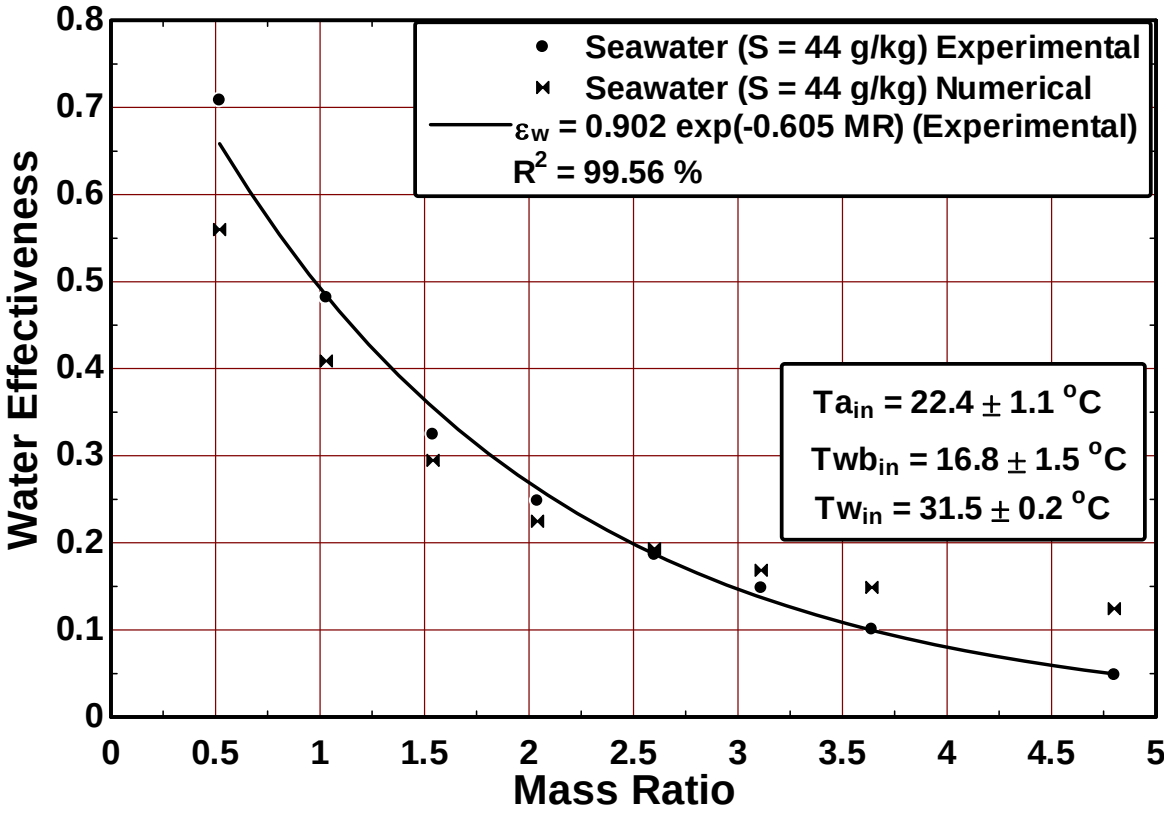

Figure 5.9 Water effectiveness of seawater (salinity = 44 g/kg) versus mass ratio of the experimental results compared with numerical results for cooling tower

The experimental values of air effectiveness for seawater (S = 85 g/kg) presented in Table B.2 are compared with that obtained from the numerical analysis results presented in Table B.3 and is plotted in Fig. 5.10. The regression equations, representing the best curves through the experimental data and of air effectiveness for seawater (S = 85 g/kg) are also shown in Fig. 5.10 as well. The relation between air effectiveness and mass ratio for the experimental results of seawater (salinity = 85 g/kg) is $\varepsilon_{air,exp} = 0.333MR^{0.346}$ with correlation coefficient R^2 is 97.37 %.

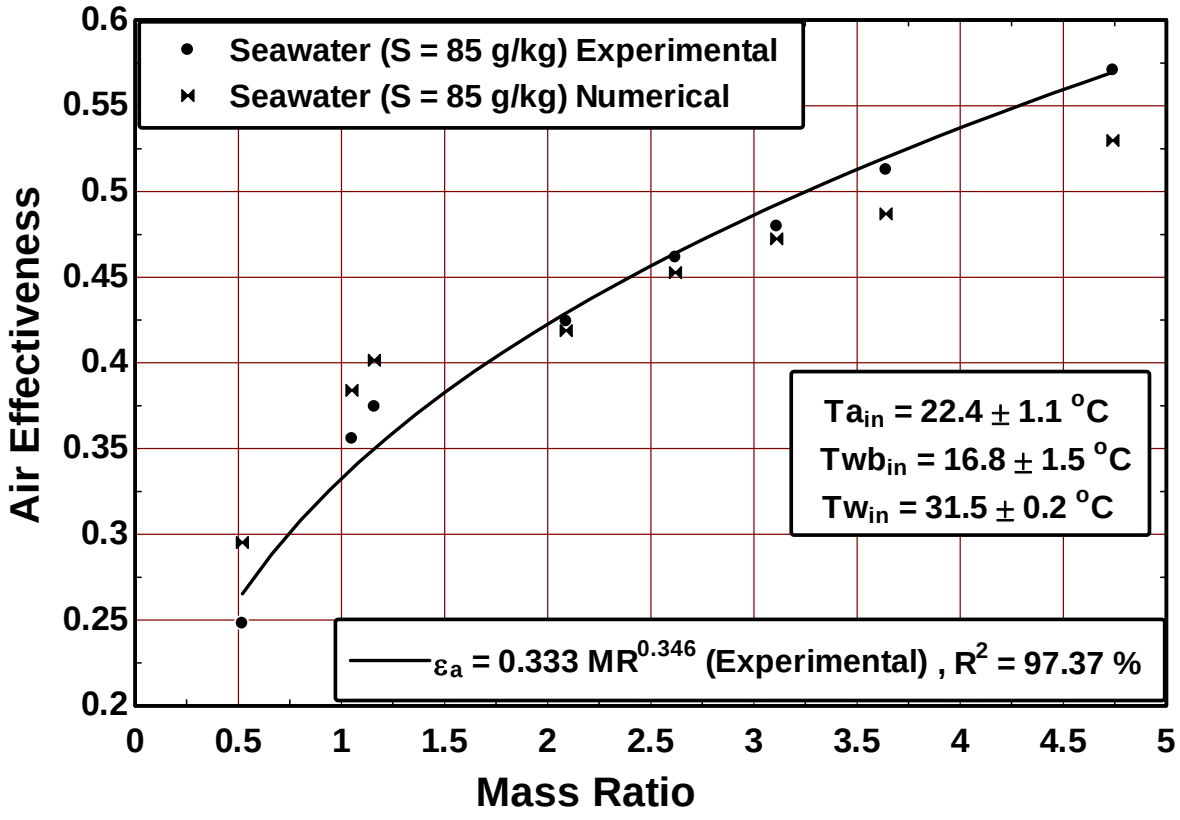

Figure 5.10 Air effectiveness of seawater (salinity = 85 g/kg) versus mass ratio of the experimental results compared with numerical results for cooling tower

The experimental values of water effectiveness for the seawater (salinity = 85 g/kg) presented in Table B.2 are compared with that obtained from the numerical results from Table B.3 and is plotted in Fig. 5.11. The curve fit line equation is obtained for the experimental data of water effectiveness. The relation between water effectiveness and mass ratio for the experimental results of seawater (salinity = 85 g/kg) is $\varepsilon_{water,exp}$= 0.975exp(-0.537MR) and the correlation coefficient R^2 is 99.16 %.

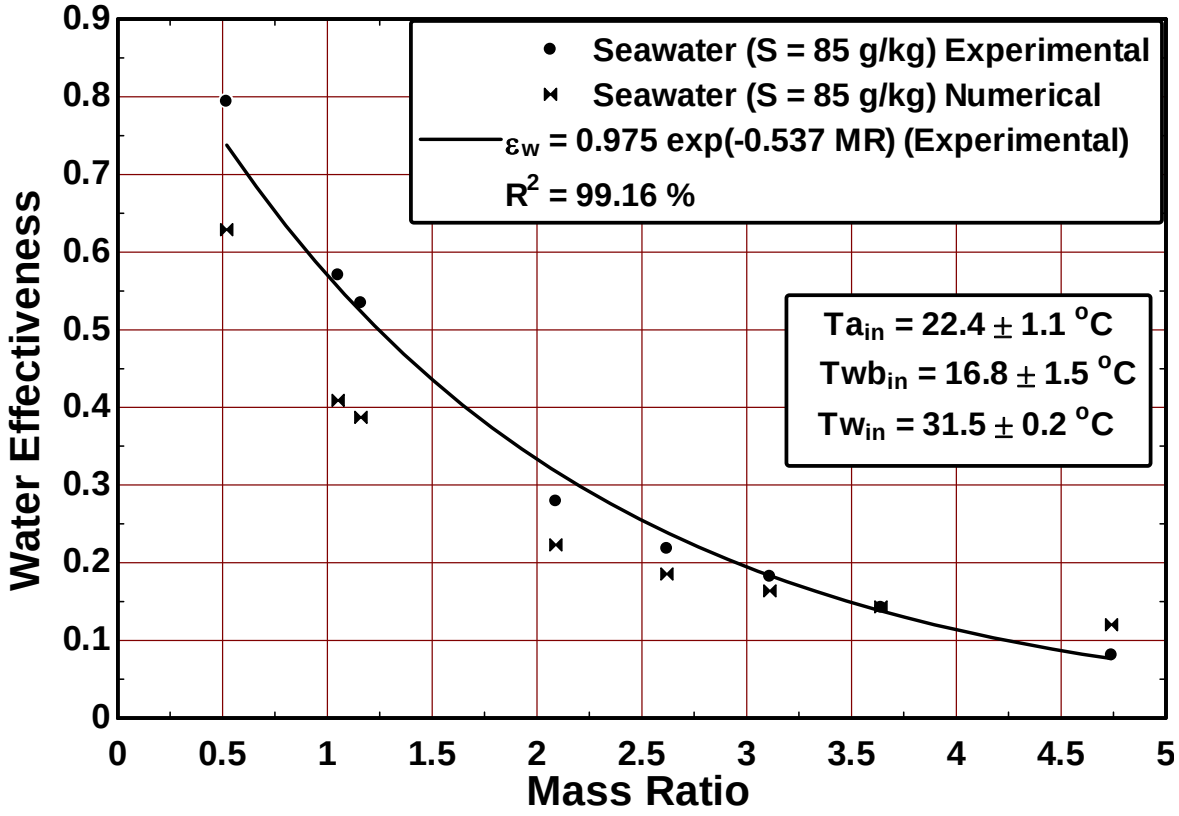

Figure 5.11 Water effectiveness of seawater (salinity = 85 g/kg) versus mass ratio of the experimental results compared with numerical results for cooling tower

The effective value of Merkel number is found by the iterative method of the experimental results by numerical analysis. The inlet water and air experimental values are taken for the numerical analysis and the outlet values are calculated by iteration of Merkel number to get outlet values similar to the outlet values in experiments. Merkel number versus mass ratio plot for fresh water, seawater (S = 44 g/kg) and seawater (S = 85 g/kg) for cooling tower is shown in Fig. 5.12. This figure shows that as mass ratio increases Merkel number decreases for all salinities. However at higher mass ratios (> 2), it is shown that Merkel number decreases with higher rate for lower salinities. This means that Merkel number increases with the salinity at higher mass ratios. Therefore larger packing volume is required for higher salinity water to get the same cooling tower performance compared to the tower working with lower salinity water at the same operating conditions. Best fit correlations are obtained for Merkel number varying with mass ratio. For mass ratio ≤ 2 the relation between Merkel number and mass ratio for fresh water, seawater (salinity = 44 g/kg) and seawater (salinity = 85 g/kg) is $Me = 1.94\exp(-0.854MR)$. For mass ratio > 2 the Merkel number for fresh water and both seawater (salinity = 44 g/kg and 85 g/kg) is deviating from the trend line so the relation between Merkel number and mass ratio (for mass ratio > 2), for fresh water is $Me = 1.38\exp(-0.66MR)$, for seawater (salinity = 44 g/kg) is $Me = 0.54\exp(-0.214MR)$ and for seawater (salinity = 85 g/kg) is $Me = 0.52\exp(-0.215MR)$.

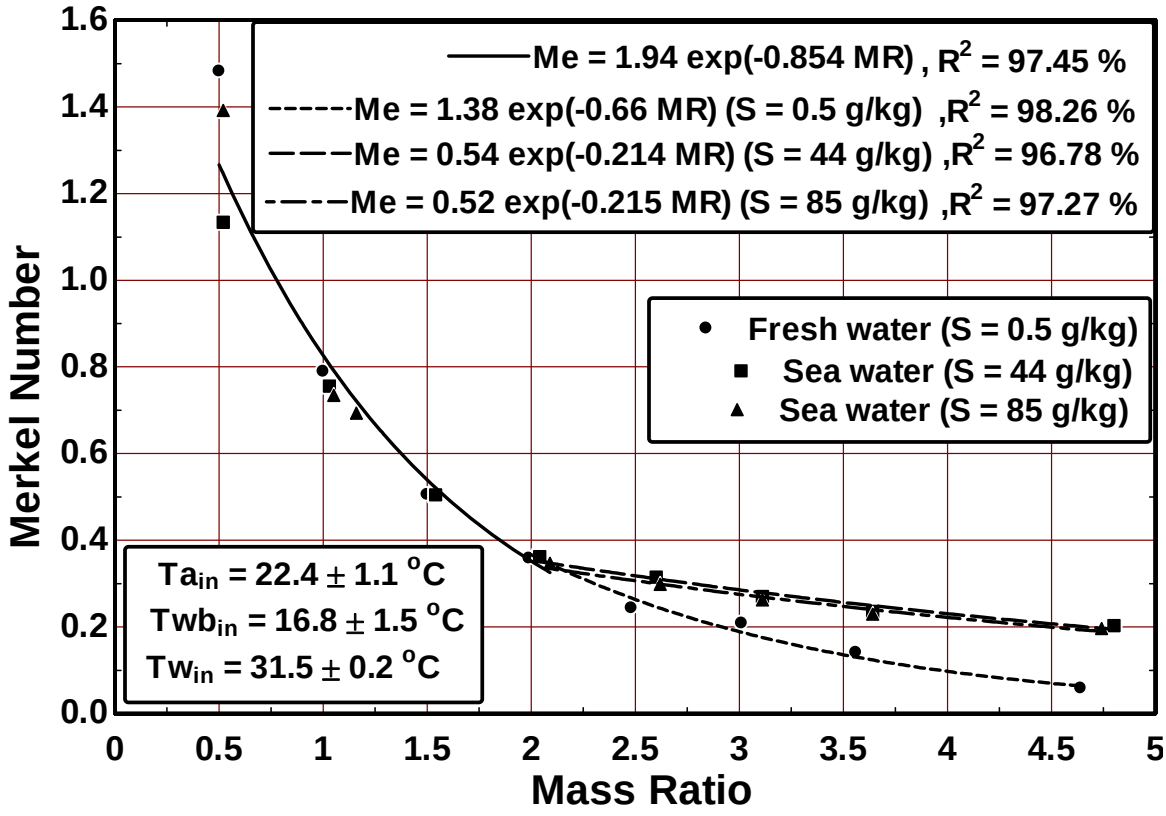

Figure 5.12 Merkel number versus mass ratio for cooling tower

5.2 FRESH WATER AND SEAWATER EXPERIMENTAL RESULTS FOR SHOWER TOWER

Experiment readings for shower tower are carried out with the bench-top cooling tower shown in Fig. 4.15 without fill packing. Experimental data is taken for fresh water salinity 0.5 g/kg and seawater of salinity 44 g/kg. The inlet conditions as follows, air dry-bulb temperature 21.8 ± 0.5 ^{o}C, air wet-bulb temperature 15.4 ± 0.4 ^{o}C and water inlet temperature 31.4 ± 0.1 ^{o}C. The mass flow rate ratios are varied from 0.5 to 2.0. Experimental readings are summarized in Table C.1. The enthalpy, exergy, exergy loss, energy loss, percentage energy loss, Merkel number, effectiveness values are calculated by the program that is written in Engineering Equation Solver (EES) for all the data of fresh water and seawater and results are summarized in Table C.2.

Experimental data is collected for all the mass ratios of fresh water and seawater from an initial state; that is at t = 0 to a steady state condition at which the variation of temperature is ± 0.1 ^{o}C. The temperature variations versus time plots are shown in Fig. (5.13a) and (5.13b) for fresh water of mass ratio 1.0 and seawater (S = 44 g/kg) of mass ratio 1.0 respectively. The temperature variation versus time plots for other operating conditions at different mass ratios are shown in Appendix C. It is important to note that the steady state temperatures of water inlet and outlet, air dry-bulb inlet and outlet, and air wet-bulb inlet and outlet are found by taking the average values at the last 10 minutes of the steady state conditions. As shown in Fig. 5.13a and Fig. 5.13b all temperatures reach steady-state value after about 20 - 30 minutes from the starting of the experiment. It is noticed that inlet dry-bulb and wet-bulb temperatures of air remains almost constant

during the experiment, but the water inlet temperature due to the heat input to achieve the desired water inlet temperature takes about 20 minutes to reach the target value.

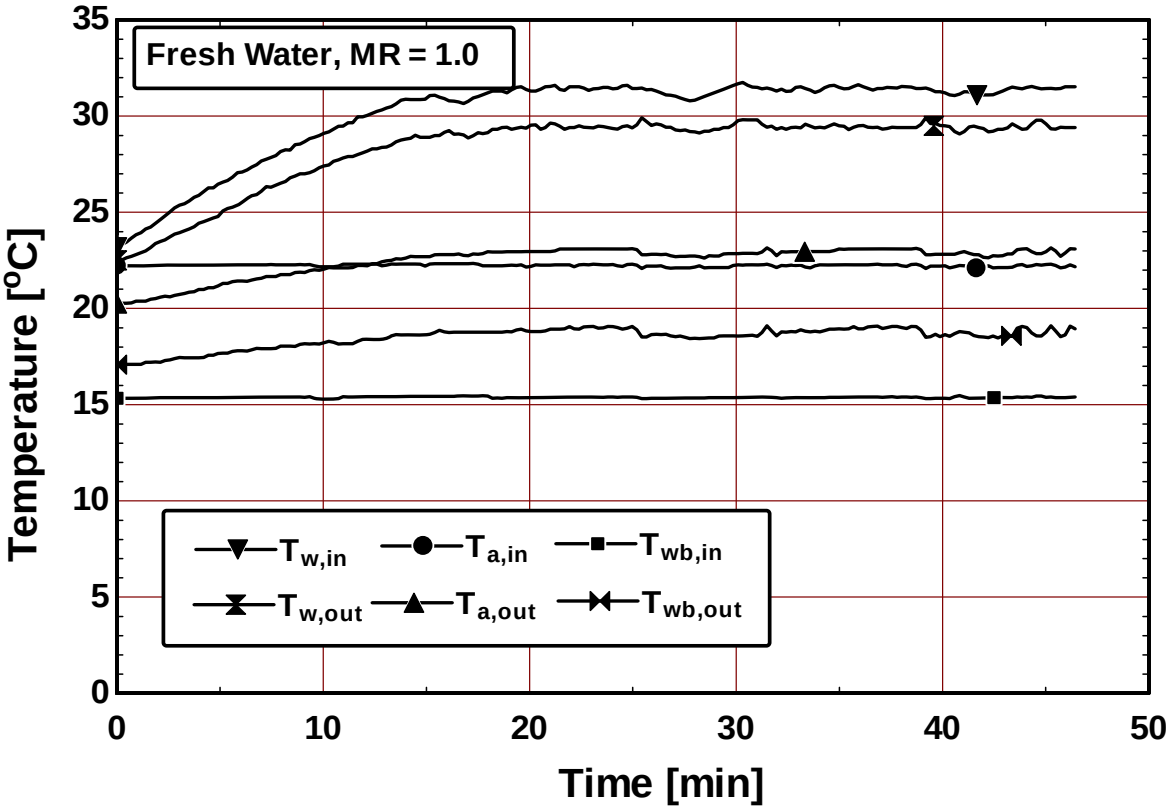

Figure 5.13a Temperature variation versus time for fresh water at mass ratio of 1.0 for shower cooling tower

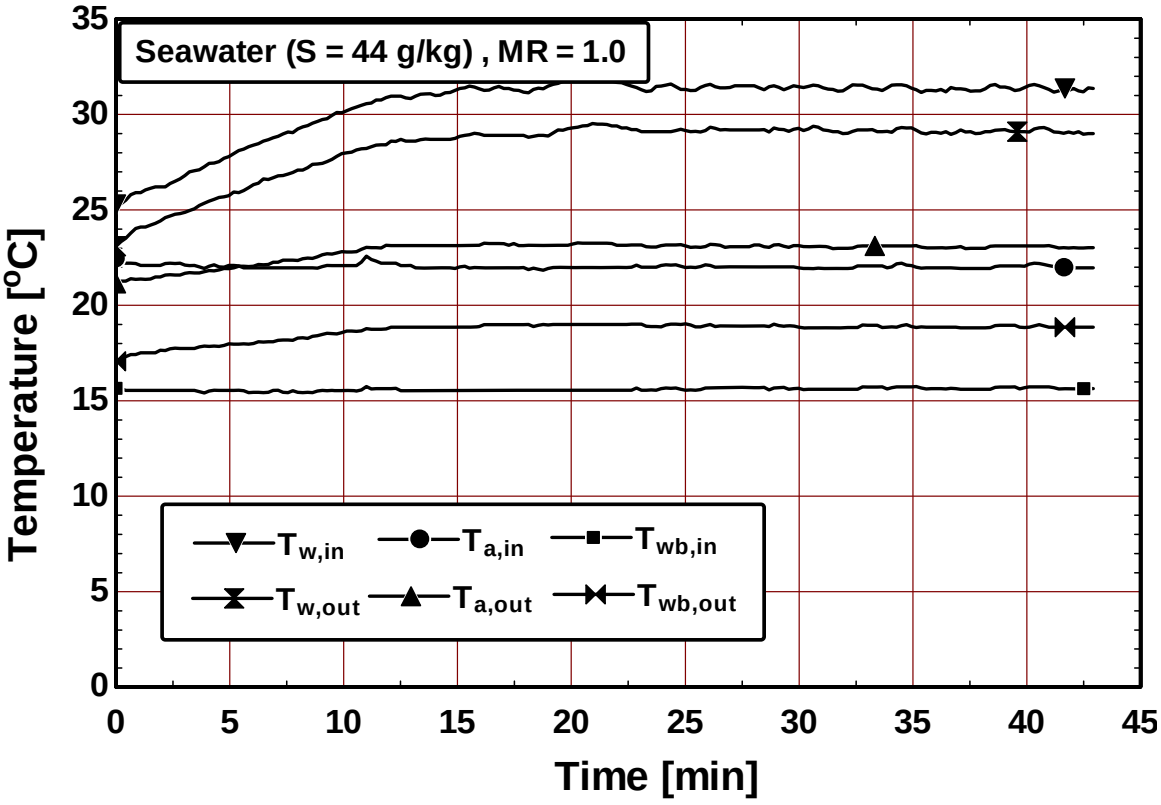

Figure 5.13b Temperature variation versus time for seawater (salinity = 44 g/kg) at mass ratio of 1.0 for shower cooling tower

Air effectiveness and water effectiveness versus mass ratio for fresh water and seawater (S = 44 g/kg) of shower cooling tower are plotted in Fig. 5.14 and Fig. 5.15. As shown in Fig. (5.14), air effectiveness increases with the increase of the mass ratio. Regression correlations, representing the best fitted curves through the experimental data of air effectiveness are shown in Fig. 5.14. The relation between air effectiveness and mass ratio for the experimental results of fresh water is $\varepsilon_{air,exp} = 0.11\exp(-0.356MR)$ with $R^2 = 98.48$ %. For seawater (S = 44 g/kg), relation between air effectiveness and mass ratio is $\varepsilon_{air,exp} = 0.1\exp(-0.45MR)$ with correlation coefficient $R^2 = 98.95$ %.

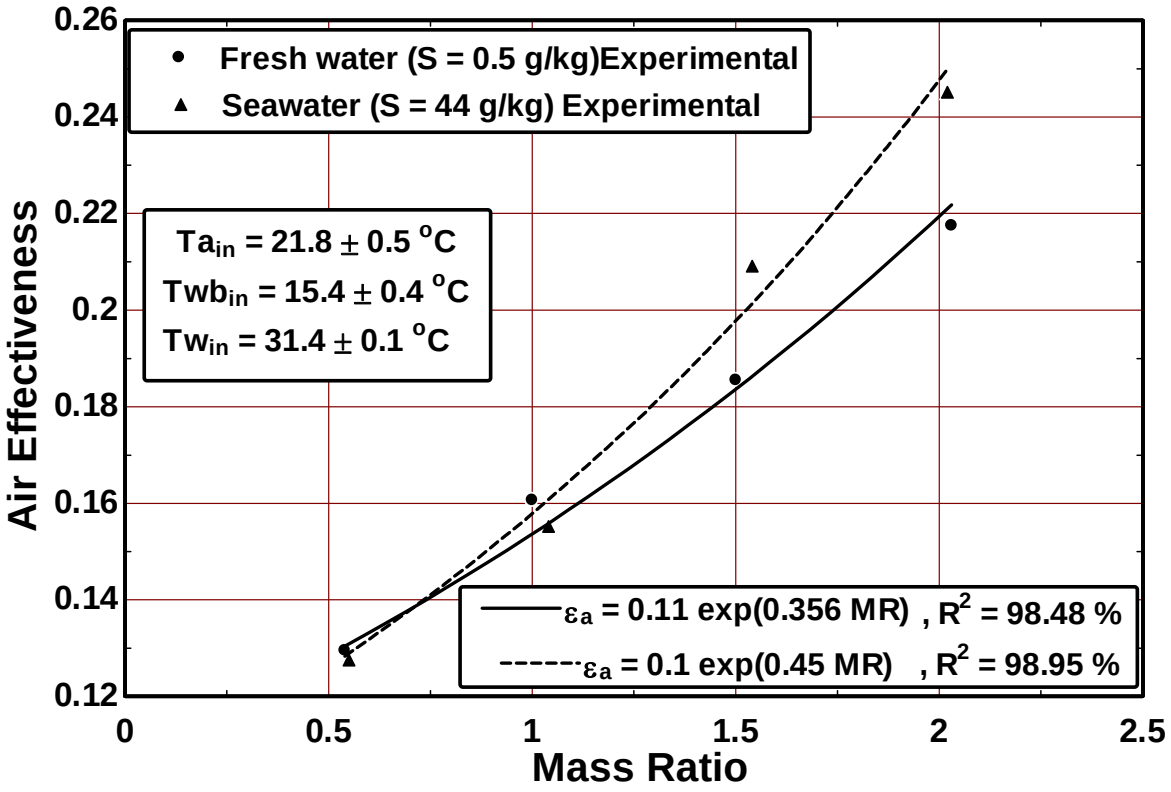

Figure 5.14 Air effectiveness versus mass ratio for the experimental results of fresh water and seawater shower cooling tower

Figure 5.15 shows water effectiveness of fresh water and seawater (S = 44 g/kg) versus mass ratio. As shown water effectiveness decreases with the increase in the mass ratio; however it increases with increasing the salinity of the seawater. Regression correlations, representing the best fitted curves through the experimental data of water effectiveness are shown in Fig. 5.15. The relation between water effectiveness and mass ratio for the experimental results of fresh water is $\varepsilon_{water,exp} = 0.385\exp(-1.05MR)$ with $R^2 = 99.55$ %. For seawater (S = 44 g/kg), relation between water effectiveness and mass ratio is $\varepsilon_{water,exp} = 0.475\exp(-0.886MR)$ with correlation coefficient $R^2 = 93.5$ %.

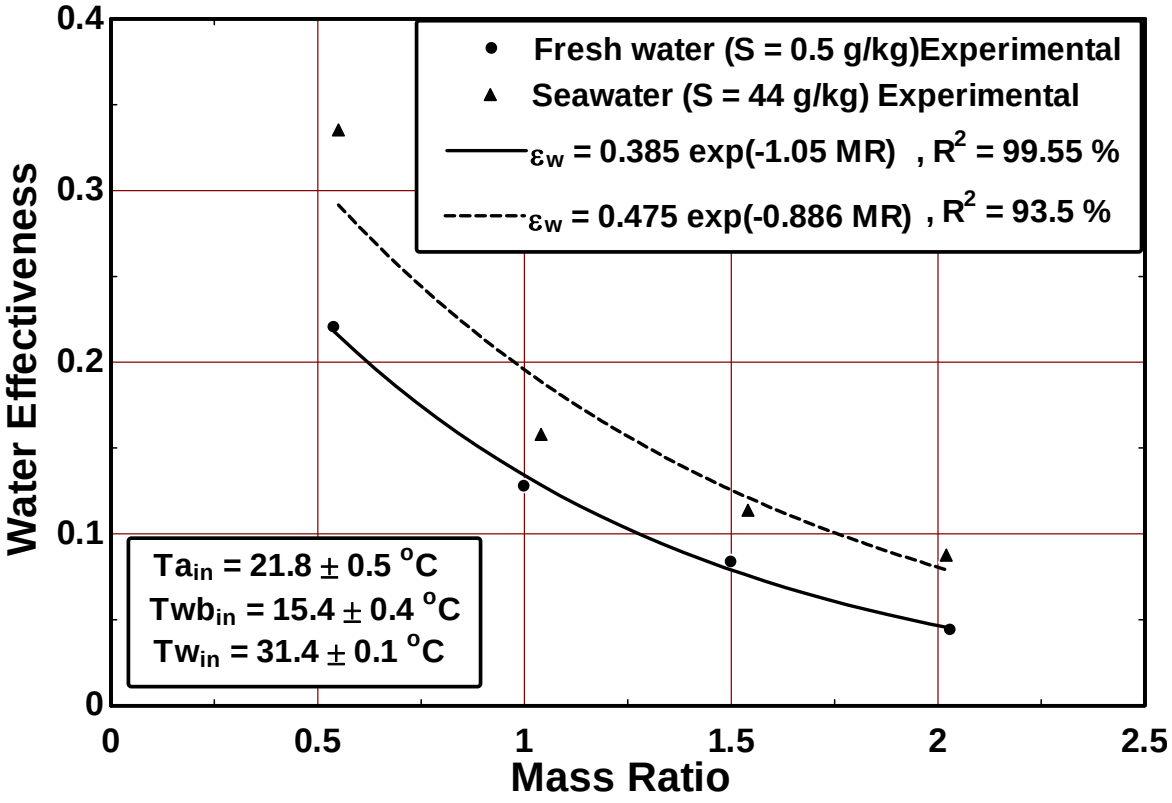

Figure 5.15 Water effectiveness versus mass ratio for the experimental results of fresh water and seawater shower cooling tower

Air effectiveness of the fresh water of the cooling tower is compared with that of the shower cooling tower in Fig. 5.16. Figure 5.16 shows that air effectiveness decreases by about (52 % to 58 %) when operating without packing (shower cooling tower). This decrease in effectiveness is due to less wet surface area available for heat and mass transfer process. Regression correlations, representing the best curves through the experimental data of air effectiveness for both fresh water of cooling tower and shower cooling tower are also shown on the plots. Relation between air effectiveness and mass ratio for the experimental results of fresh water for cooling tower is $\varepsilon_{air,ct} = 0.365MR^{0.385}$ with correlation coefficient $R^2 = 97.68$ % and relation between air effectiveness and mass ratio for the fresh water for shower cooling tower is $\varepsilon_{air,sct} = 0.162MR^{0.383}$ with correlation coefficient $R^2 = 99.21$ %.

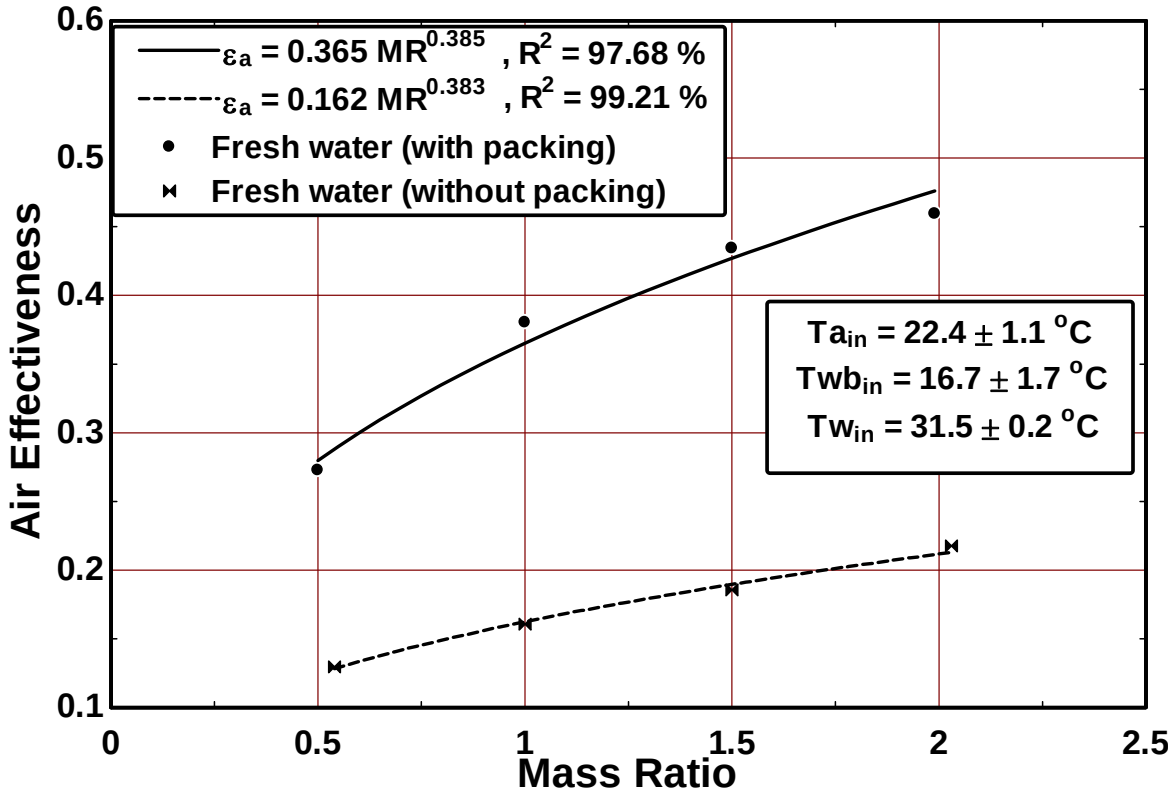

Figure 5.16 Comparison of air effectiveness of cooling tower and shower cooling tower with mass ratio for the experimental results of fresh water

Water effectiveness of the fresh water of the cooling tower is compared with that of the shower cooling tower in Fig. 5.17. Figure 5.17 shows that water effectiveness decreases by about (66 % to 80 %) when operating without packing (shower cooling tower). This decrease in effectiveness is due to less wet surface area available for heat and mass transfer process. Regression correlations, representing the best curves through the experimental data of water effectiveness for both fresh water cooling tower and shower cooling tower are also shown on the plots. Relation between water effectiveness and mass ratio for the experimental results of fresh water for cooling tower is $\varepsilon_{water,ct}$ = 0.911exp(-0.732MR) with correlation coefficient R^2 = 99.39 % and relation between water effectiveness and mass ratio for the fresh water for shower cooling tower is $\varepsilon_{water,sct}$ = 0.385exp(-1.056MR) with correlation coefficient R^2 = 99.55 %.

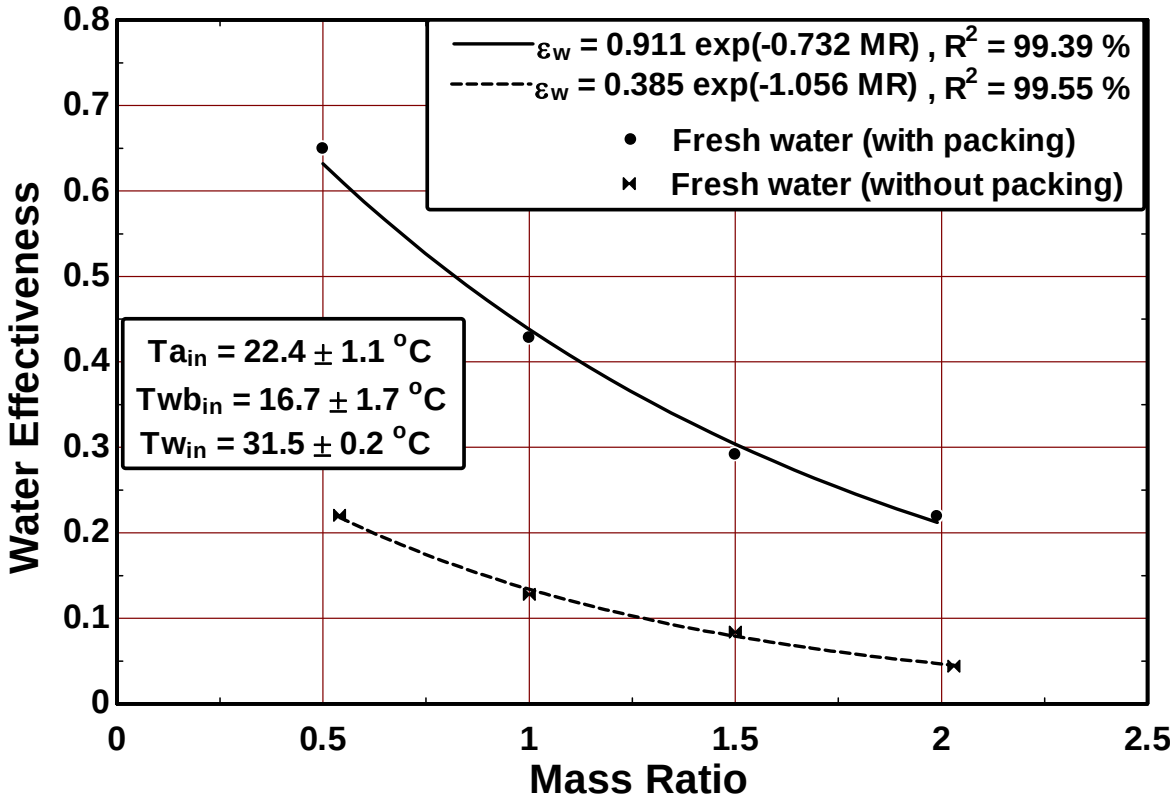

Figure 5.17 Comparison of water effectiveness cooling tower and shower cooling tower with mass ratio for the experimental results of fresh water

Air effectiveness of the seawater (S = 44 g/kg) of the cooling tower is compared with that of the shower cooling tower in Fig. 5.18. Figure 5.18 shows that the air effectiveness of the seawater (S = 44 g/kg) of the shower cooling tower decreases by about (45 % to 59 %) when operating without packing (shower cooling tower). This decrease in effectiveness is due to less wet surface area available for heat and mass transfer process. Regression correlations, representing the best curves through the experimental data of air effectiveness for both seawater (S = 44 g/kg) of cooling tower and shower cooling tower are also shown on the plots. Relation between air effectiveness and mass ratio for the experimental results of seawater (S = 44 g/kg) for cooling tower is $\varepsilon_{air,ct} = 0.346MR^{0.44}$ with correlation coefficient $R^2 = 95.4$ % and relation between air effectiveness and mass ratio for the seawater (S = 44 g/kg) for shower cooling tower is $\varepsilon_{air,sct} = 0.166MR^{0.509}$ with correlation coefficient $R^2 = 95.98$ %.

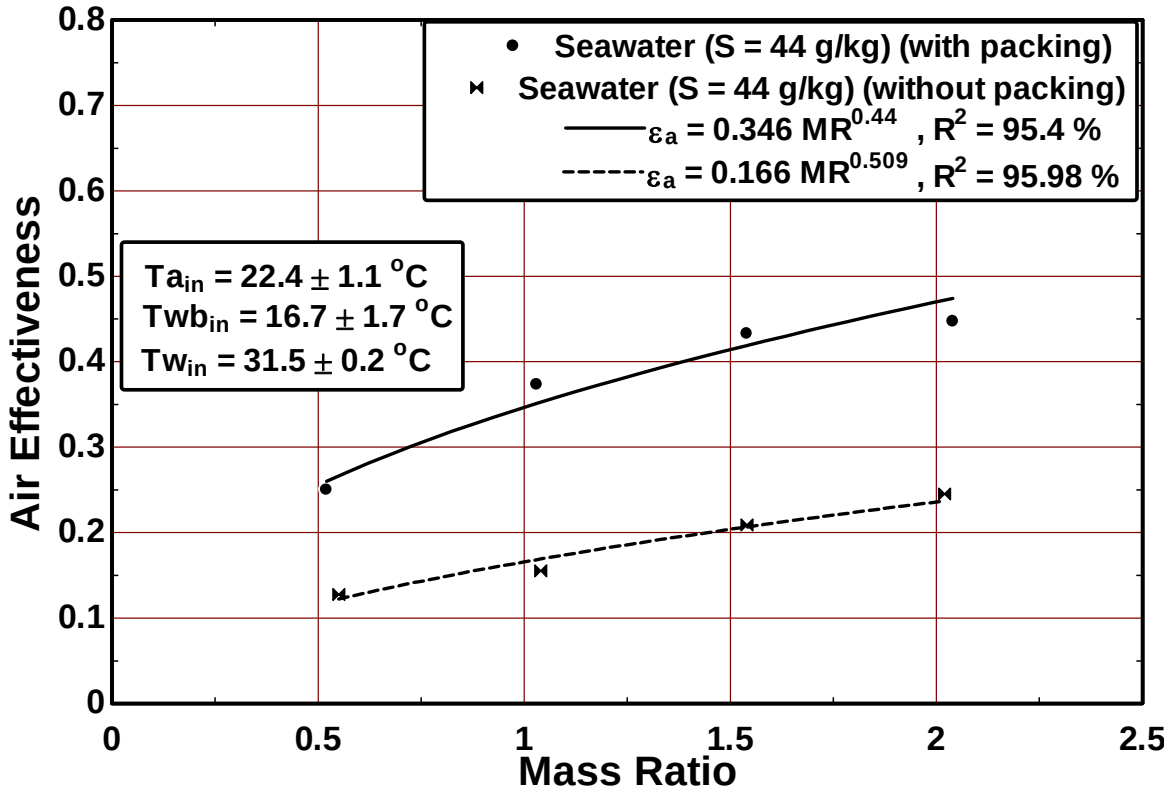

Figure 5.18 Comparison of air Effectiveness of cooling tower and shower cooling tower with mass ratio for the experimental results of seawater (Salinity = 44 g/kg)

Water effectiveness of the seawater (S = 44 g/kg) of the cooling tower is compared with that of the shower cooling tower in Fig. 5.19. Figure 5.19 shows that the water effectiveness of the seawater (S = 44 g/kg) of the shower cooling tower decreases by about (52 % to 67 %) when operating without packing (shower cooling tower). This decrease in effectiveness is due to less wet surface area available for heat and mass transfer process. Regression correlations, representing the best curves through the experimental data of water effectiveness for both seawater (S = 44 g/kg) of cooling tower and shower cooling tower are also shown on the plots. Relation between water effectiveness and mass ratio for the experimental results of seawater (S = 44 g/kg) for cooling tower is $\varepsilon_{water,ct} = 0.997\exp(-0.698MR)$ with correlation coefficient $R^2 = 99.38$ % and relation between water effectiveness and mass ratio for the fresh water for shower cooling tower is $\varepsilon_{water,sct} = 0.474\exp(-0.886MR)$ with correlation coefficient $R^2 = 93.5$ %.

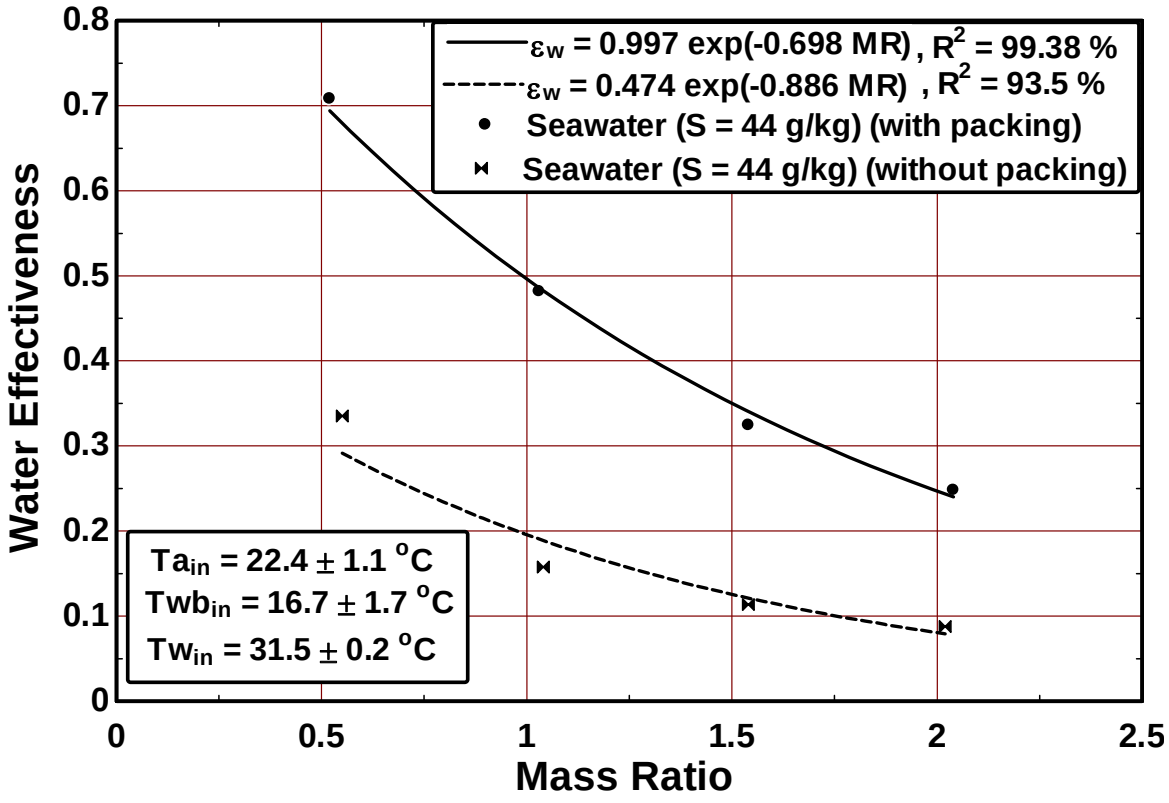

Figure 5.19 Comparison of water effectiveness of cooling tower and shower cooling tower with mass ratio for the experimental results of seawater (Salinity = 44 g/kg)

5.3 EXERGY ANALYSIS OF COOLING TOWER

Exergy analysis of cooling tower is carried out to find the optimum performance of the cooling tower under different operating conditions. The detailed mathematical procedure to calculate exergy due to various components of air and water inside the cooling tower is presented in section 3.7.

5.3.1 Exergy Analysis of Fresh Water Cooling Tower

Air and water flow exergy are calculated at the inlet and outlet using the experimental data presented in Table B.1. The calculated flow exergy values of air and water as well as exergy loss at different mass ratios of fresh water are given in Table B.2. Exergy distribution along the cooling tower at mass ratios 0.5, 1.0, 1.5 and 2.0 of fresh water are plotted in Figures (5.20), (5.21) and (5.22).

Figures (5.20a) ,(5.20b), (5.20c) and (5.20d) show flow exergy of air due to convective ($\dot{X}_{air,conv}$) and evaporative ($\dot{X}_{air,evap}$) heat transfer rates along the tower height for mass ratio 0.5, 1.0, 1.5 and 2.0 respectively of the fresh water cooling tower. The total exergy due to convective and evaporative heat transfer rate ($\dot{X}_{air} = \dot{X}_{air,conv} + \dot{X}_{air,evap}$) is also shown on these figures. Figure 5.20 (a - d) show that the flow exergy of air due to evaporation is much higher than that of the convection component of heat transfer. The evaporation component of exergy increases exponentially with the tower height, while the convective component is more-or-less remains constant throughout the height of the tower. This clearly shows that evaporation is the dominant mode of transfer energy from water to air in a cooling tower.

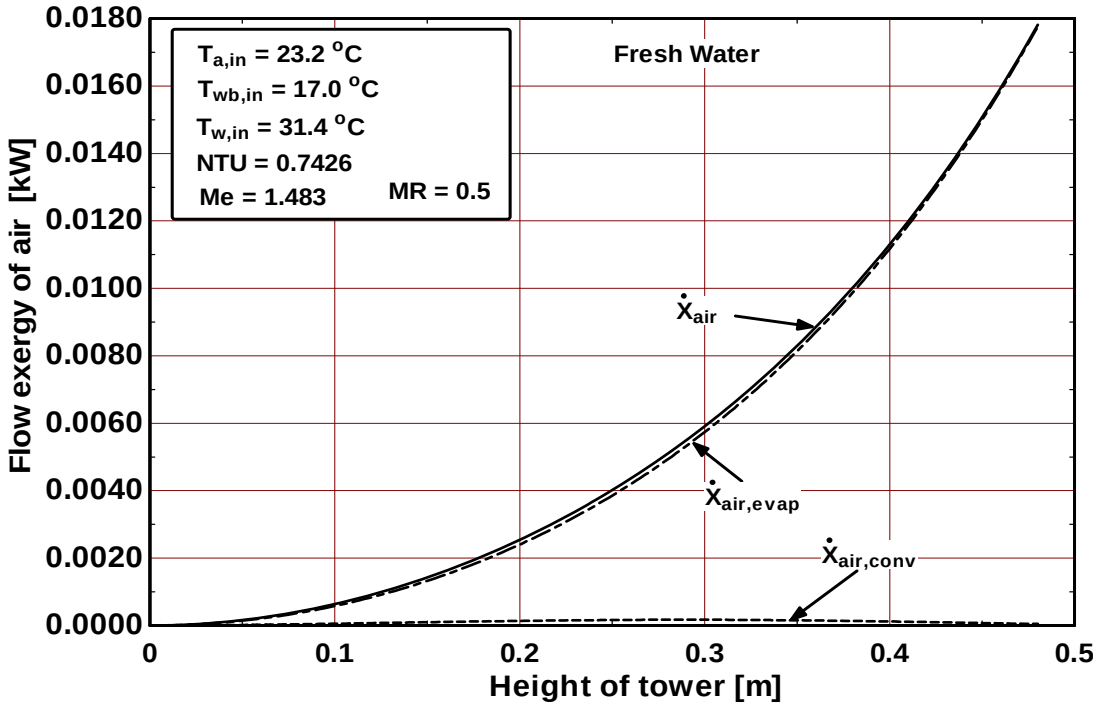

Figure 5.20a Flow exergy of air along the height of tower for fresh water at mass ratio = 0.5

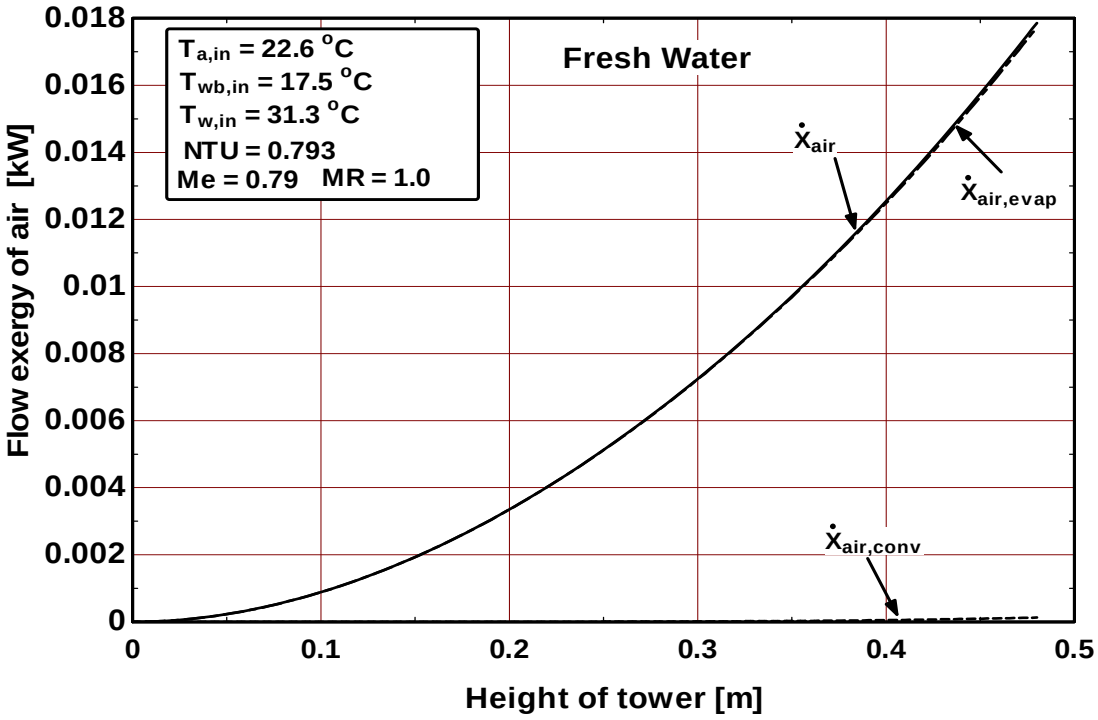

Figure 5.20b Flow exergy of air along the height of tower for fresh water at mass ratio = 1.0

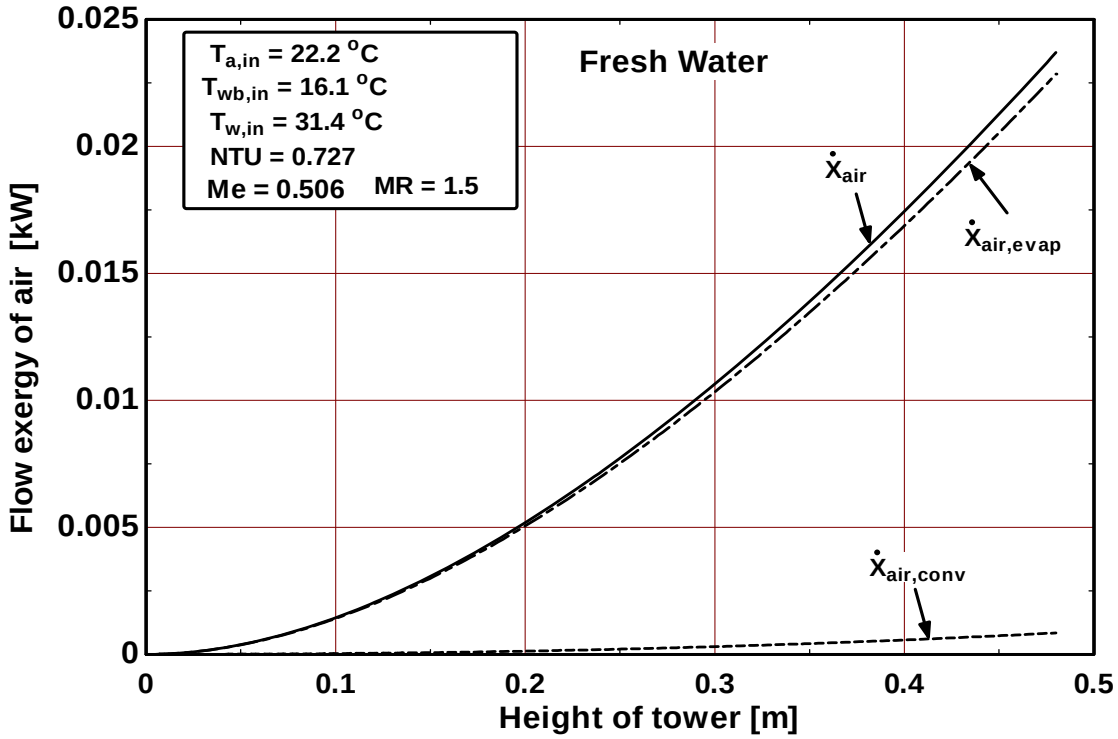

Figure 5.20c Flow exergy of air along the height of tower for fresh water at mass ratio = 1.5

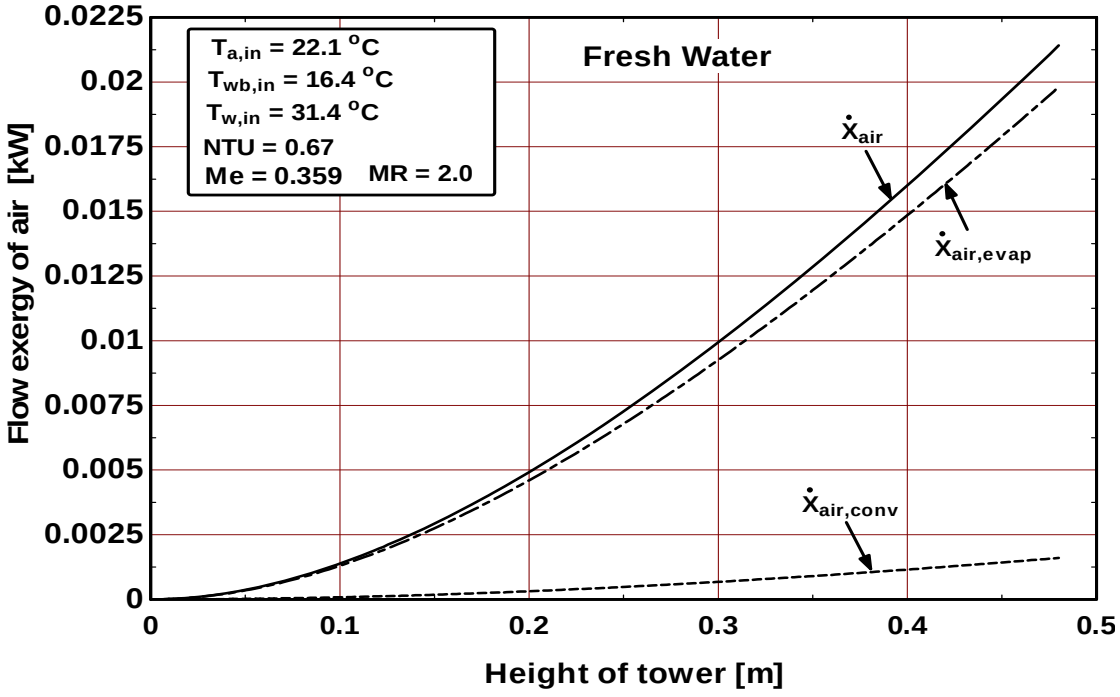

Figure 5.20d Flow exergy of air along the height of tower for fresh water at mass ratio = 2.0

Figures (5.21a), (5.21b), (5.21c) and (5.21d) show flow exergy of water ($\dot{X}_{water}$) at mass ratios 0.5, 1.0, 1.5 and 2.0 respectively of the fresh water cooling tower. It is shown that water exergy decreases continuously from the top to bottom of the tower due to exergy transfer from the water to the air stream. When comparing with exergy of air that is discussed earlier in Fig.5.20 (a - d), it is noted that the values of $\dot{X}_{water}$ are comparatively more than those of $\dot{X}_{air}$ throughout the tower height. This means that exergy contained in the water is transferred to the surrounding air stream with some losses, which is typically defined as exergy losses. This exergy loss is due to the irreversibilities in the system associated with temperature difference and concentration difference. It is also defined as exergy destruction, given by

$$\dot{X}_D = \left(\dot{X}_{w,in} - \dot{X}_{w,out}\right) + \left(\dot{X}_{air,in} - \dot{X}_{air,out}\right) \tag{5.1}$$

Figure (5.22a), (5.22b), (5.22c) and (5.22d) shows the exergy destruction along the height of the cooling tower at mass ratios 0.5, 1.0, 1.5 and 2.0 respectively of the fresh water cooling tower. Fig. 5.22a shows that the exergy destruction is low at the bottom and increases at the top of the tower. Fig. 5.22b shows that the exergy destruction is low at the middle of the tower. Fig. 5.22c and Fig. 5.22d shows that the exergy destruction is high at the bottom and decreases at the top of the tower. The total exergy destruction for mass ratio 0.5 is 0.085 kW, for mass ratio 1.0 is 0.0812 kW, for mass ratio 1.5 is 0.089 kW and for mass ratio 2.0 is 0.0814 kW.

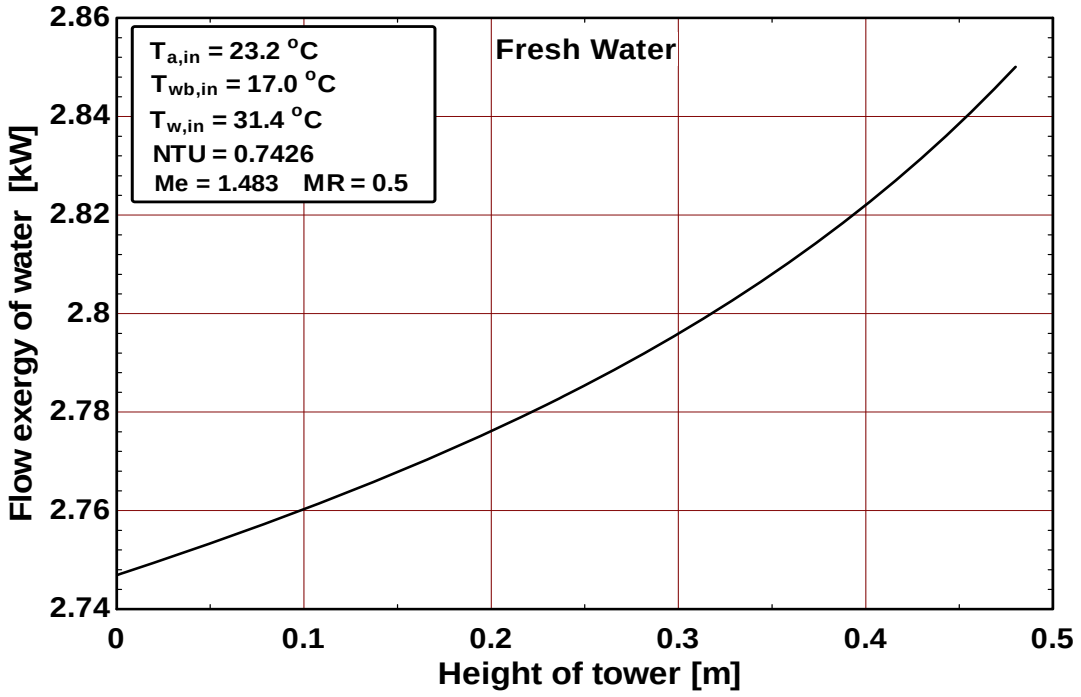

Figure 5.21a Flow exergy of water along the height of tower for fresh water at mass ratio = 0.5

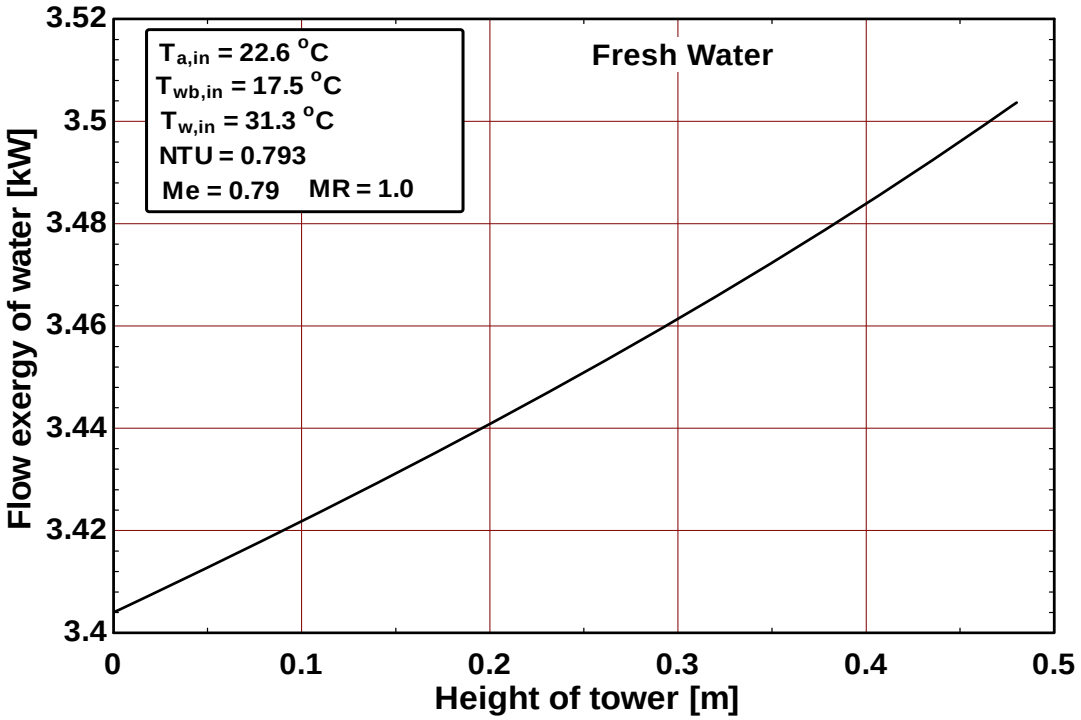

Figure 5.21b Flow exergy of water along the height of tower for fresh water at mass ratio = 1.0

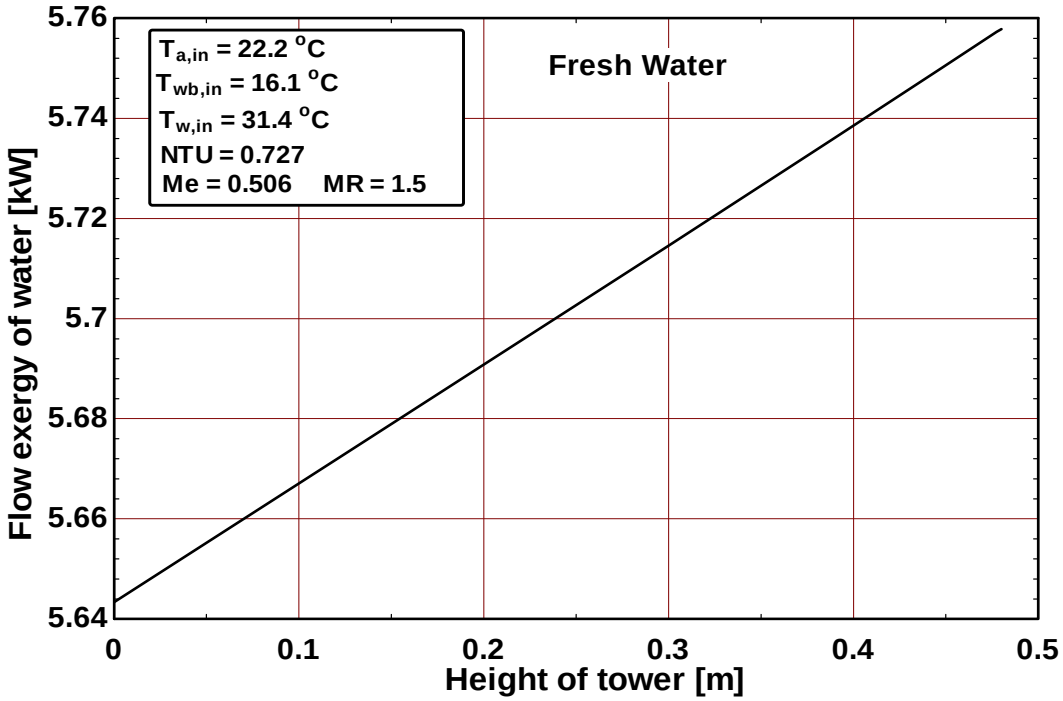

Figure 5.21c Flow exergy of water along the height of tower for fresh water at mass ratio = 1.5

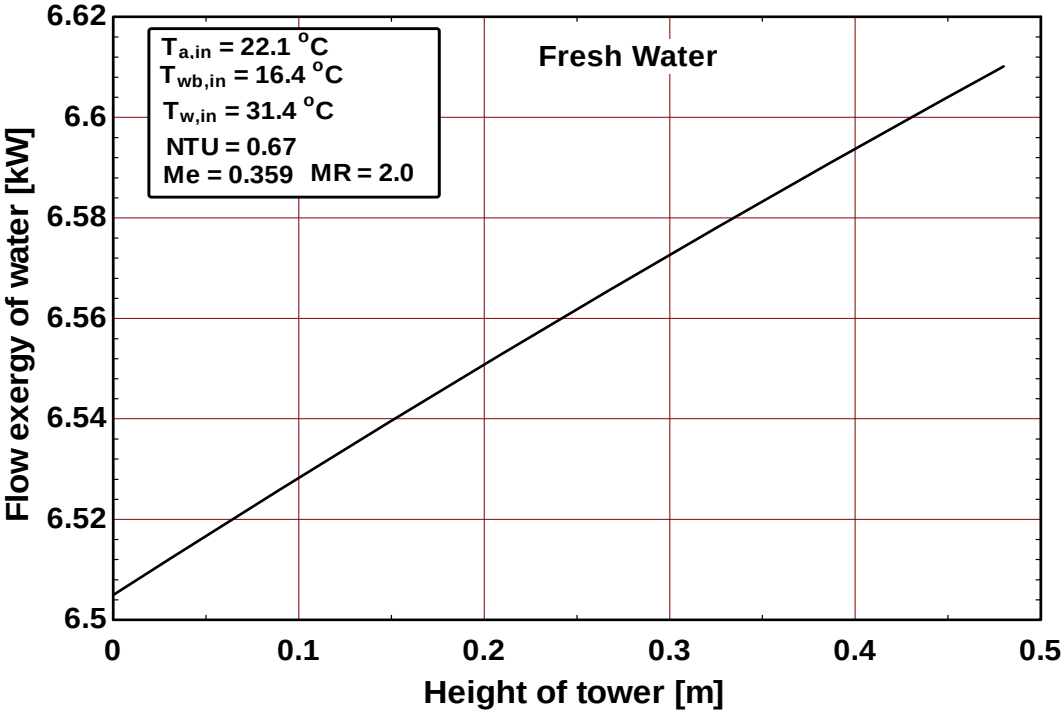

Figure 5.21d Flow exergy of water along the height of tower for fresh water at mass ratio = 2.0

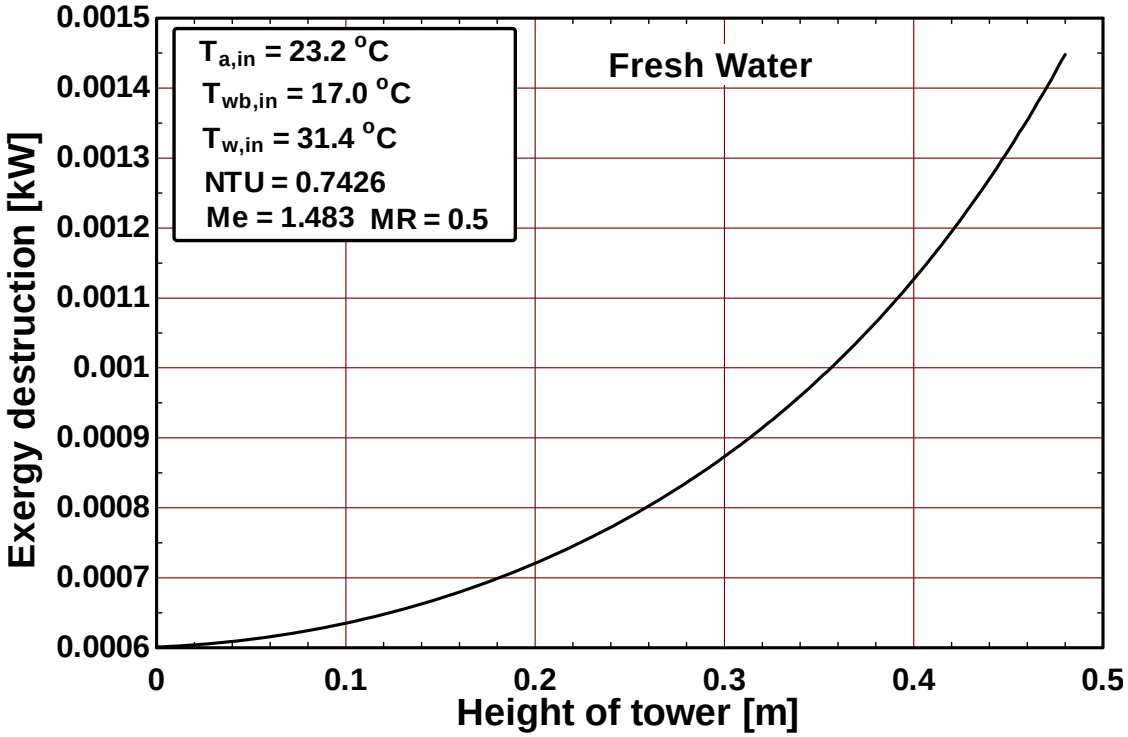

Figure 5.22a Exergy destruction along the height of tower for fresh water at mass ratio = 0.5

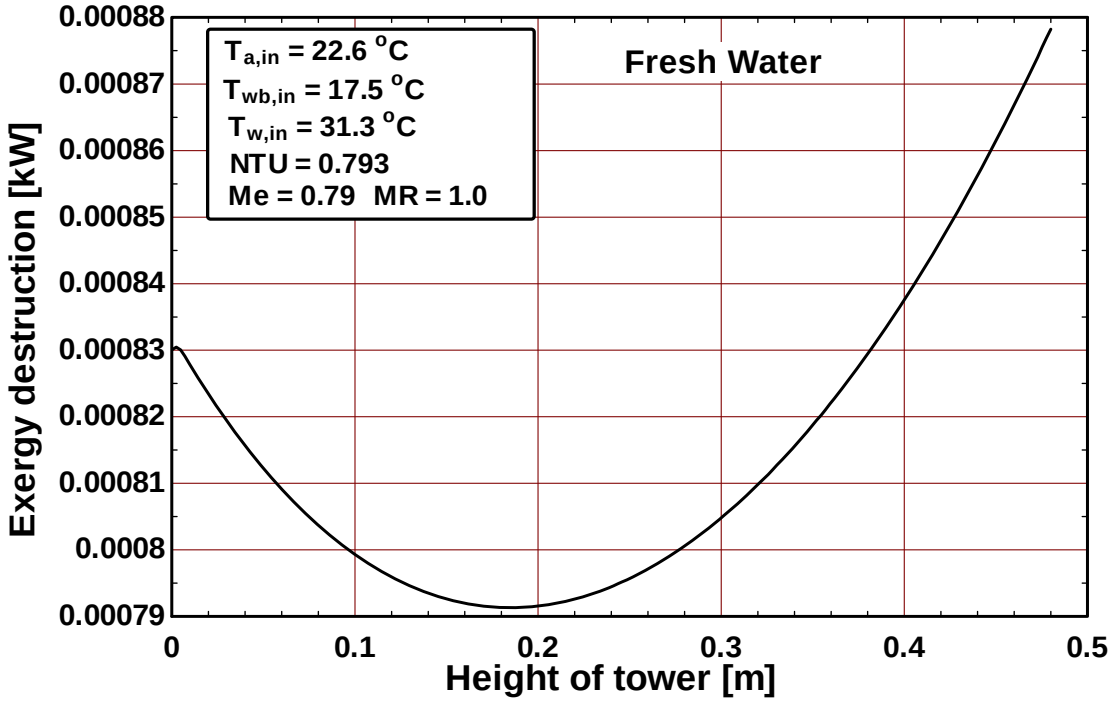

Figure 5.22b Exergy destruction along the height of tower for fresh water at mass ratio = 1.0

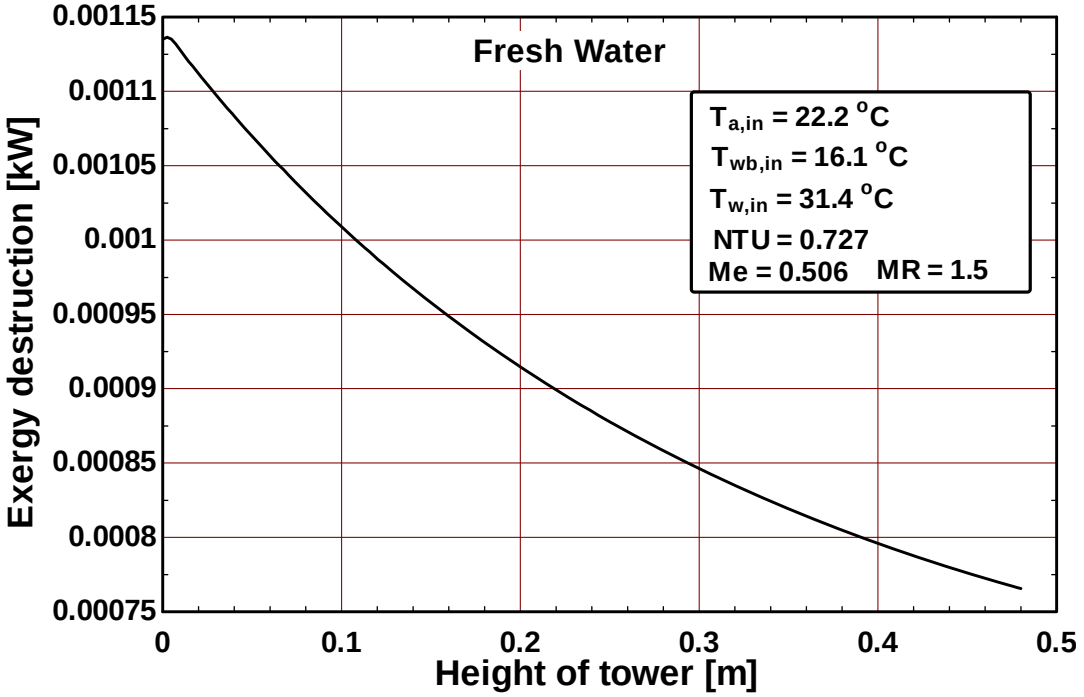

Figure 5.22c Exergy destruction along the height of tower for fresh water at mass ratio = 1.5

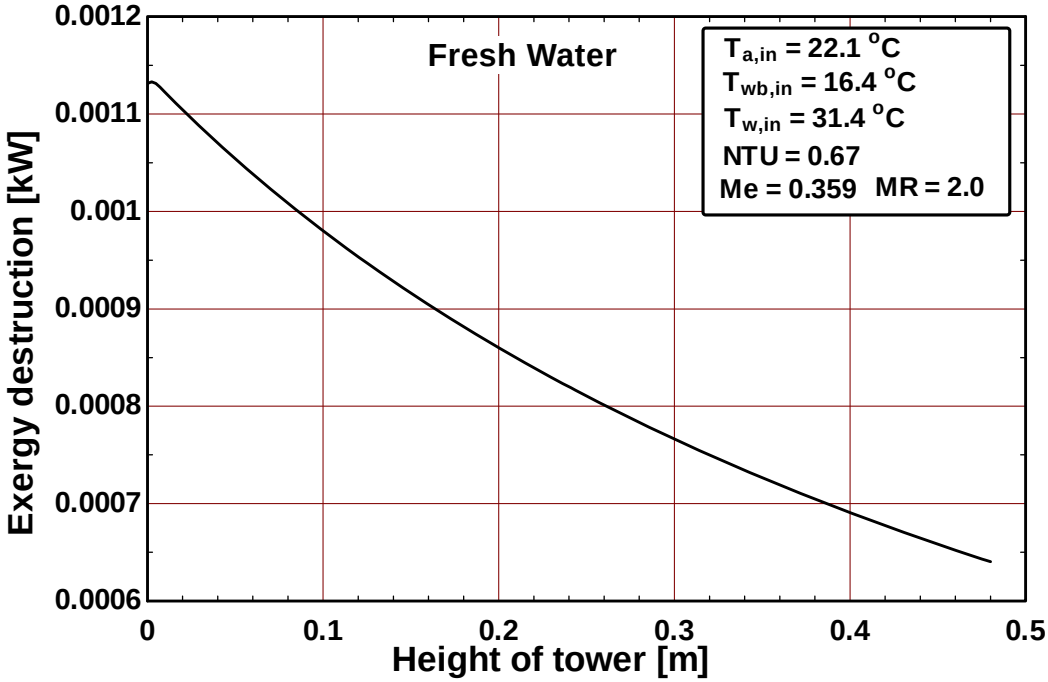

Figure 5.22d Exergy destruction along the height of tower for fresh water at mass ratio = 2.0

5.3.2 Exergy Analysis of Seawater (salinity = 44 g/kg) Cooling Tower

Air and water flow exergy are calculated at the inlet and outlet using the experimental data presented in Table B.1. The calculated flow exergy values of air and water as well as exergy loss at different mass ratios of seawater (S = 44 g/kg) are given in Table B.2. Exergy distribution along the cooling tower at mass ratios 0.5, 1.0, 1.5 and 2.0 of seawater (S = 44 g/kg) are plotted in Figures (5.23), (5.24) and (5.25).

Figures (5.23a), (5.23b), (5.23c) and (5.23d) show flow exergy of air due to convective ($\dot{X}_{air,conv}$) and evaporative ($\dot{X}_{air,evap}$) heat transfer rates along the tower height for mass ratio 0.5, 1.0, 1.5 and 2.0 respectively of the seawater (S = 44 g/kg) cooling tower. The total exergy due to convective and evaporative heat transfer rate ($\dot{X}_{air} = \dot{X}_{air,conv} + \dot{X}_{air,evap}$) is also shown on these figures. Figure 5.23 (a - d) show that the flow exergy of air due to evaporation is much higher than that of the convection component of heat transfer. The evaporation component of exergy increases exponentially with the tower height, while the convective component is more-or-less remains constant throughout the height of the tower. This clearly shows that evaporation is the dominant mode of transfer energy from water to air in a cooling tower.

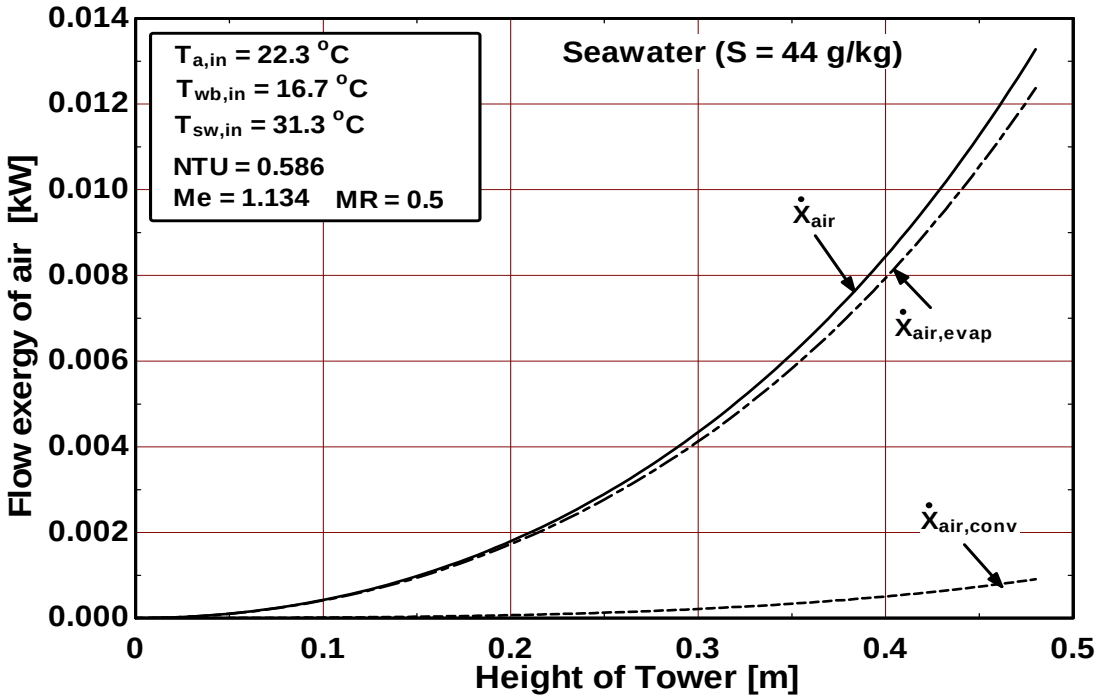

Figure 5.23a Flow exergy of air along the height of tower for seawater (salinity = 44 g/kg) at mass ratio = 0.5

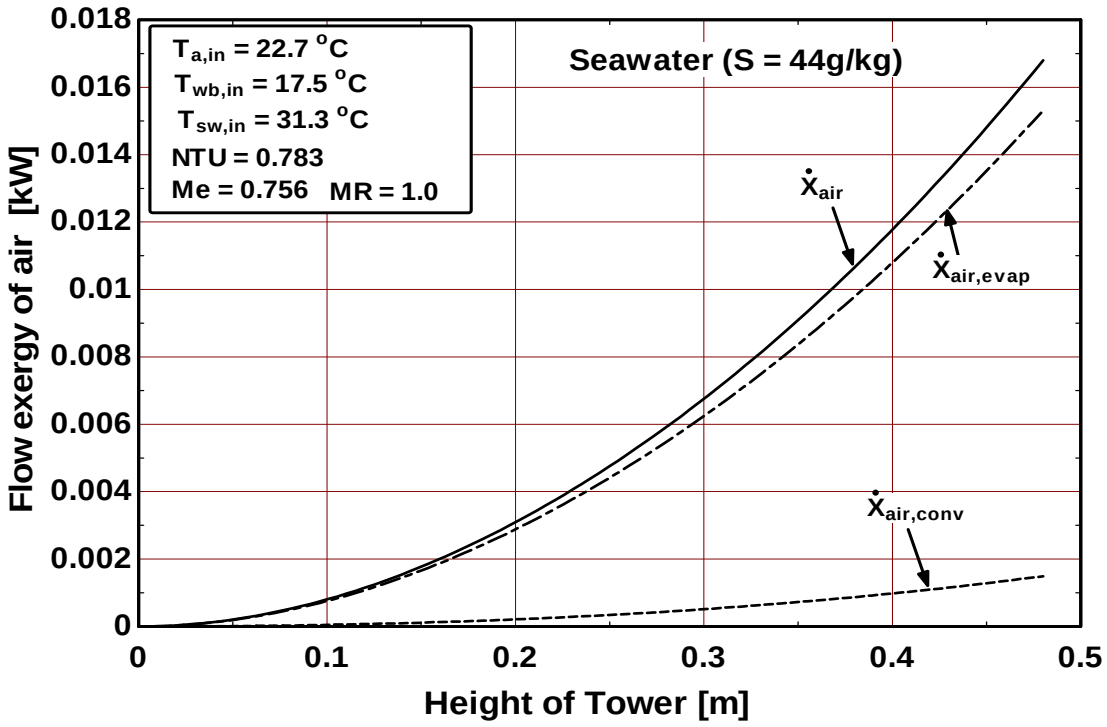

Figure 5.23b Flow exergy of air along the height of tower for seawater (salinity = 44 g/kg) at mass ratio = 1.0

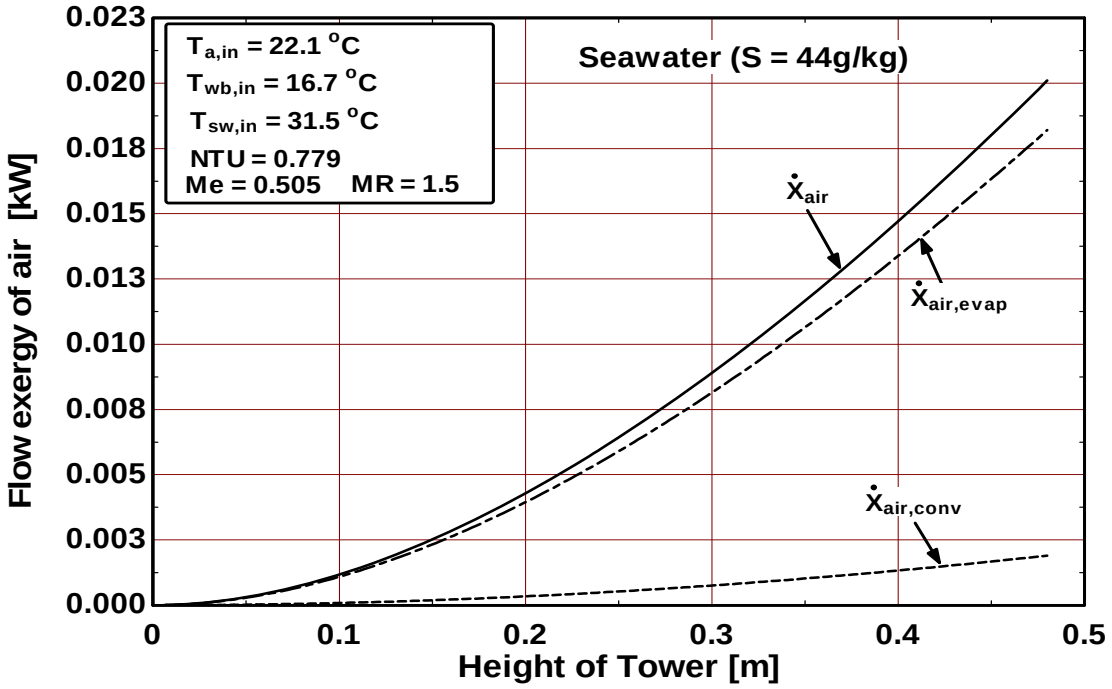

Figure 5.23c Flow exergy of air along the height of tower for seawater (salinity = 44 g/kg) at mass ratio = 1.5

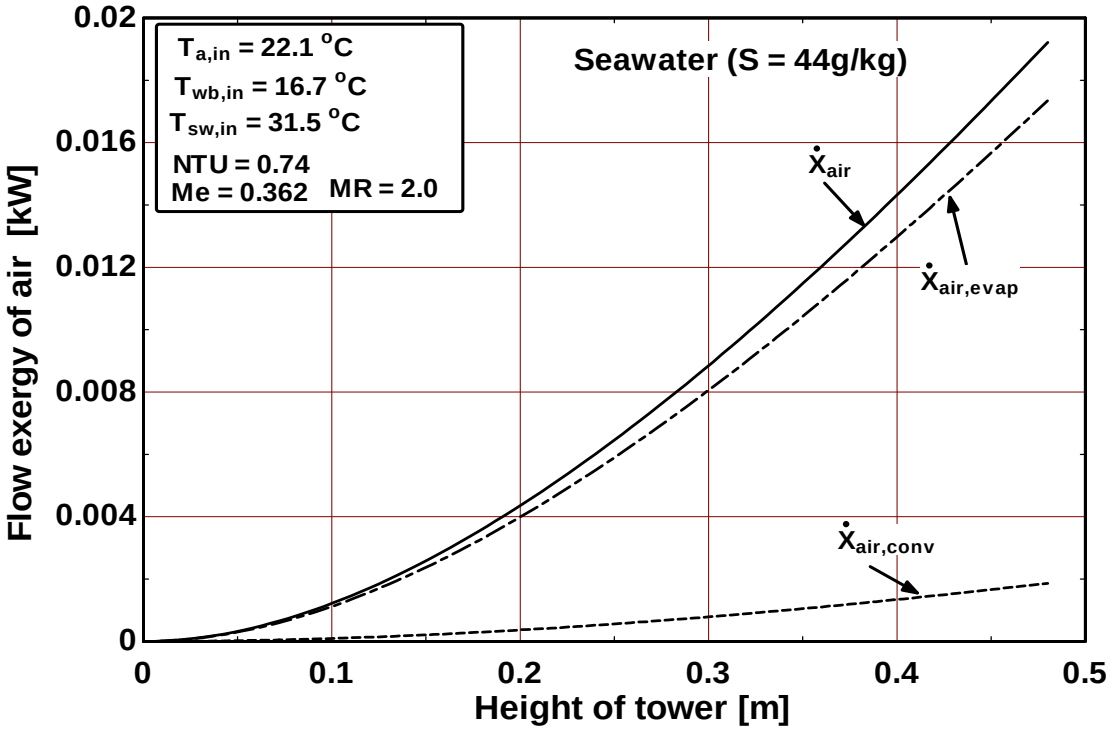

Figure 5.23d Flow exergy of air along the height of tower for seawater (salinity = 44 g/kg) at mass ratio = 2.0

Figures (5.24a), (5.24b), (5.24c) and (5.24d) show flow exergy of water ($\dot{X}_{seawater}$) at mass ratios 0.5, 1.0, 1.5 and 2.0 respectively of the seawater (S = 44 g/kg) cooling tower. It is shown that seawater exergy decreases continuously from the top to bottom of the tower due to exergy transfer from the water to the air stream. When comparing with exergy of air that is discussed earlier in Fig.5.23 (a - d), it is noted that the values of $\dot{X}_{seawater}$ are comparatively more than those of $\dot{X}_{air}$ throughout the tower height. This means that exergy contained in the seawater is transferred to the surrounding air stream with some losses, which is typically defined as exergy losses. This exergy loss is due to the irreversibilities in the system associated with temperature difference and concentration difference. It is also defined as exergy destruction, given by

$$\dot{X}_D = \left(\dot{X}_{SW,in} - \dot{X}_{SW,out}\right) + \left(\dot{X}_{air,in} - \dot{X}_{air,out}\right) \tag{5.2}$$

Figure (5.25a), (5.25b), (5.25c) and (5.25d) shows the exergy destruction along the height of the cooling tower at mass ratios 0.5, 1.0, 1.5 and 2.0 respectively of the seawater (S = 44 g/kg) cooling tower. Fig. 5.25a shows that the exergy destruction is low at the bottom and increases at the top of the tower. Fig. 5.25b, Fig. 5.25c and Fig. 5.25d show that the exergy destruction is high at the bottom and decreases at the top of the tower. The total exergy destruction for mass ratio 0.5 is 0.0309 kW, for mass ratio 1.0 is 0.0291 kW, for mass ratio 1.5 is 0.0337 kW and for mass ratio 2.0 is 0.0337 kW.

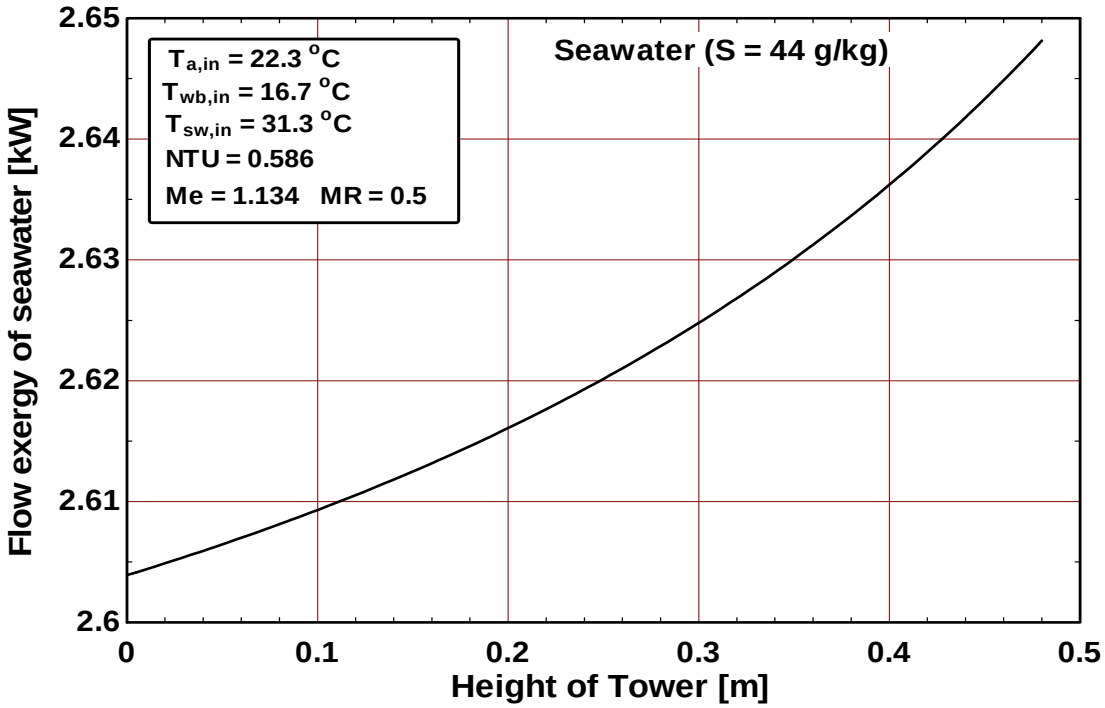

Figure 5.24a Flow exergy of seawater along the height of tower for seawater (salinity = 44 g/kg) at mass ratio = 0.5

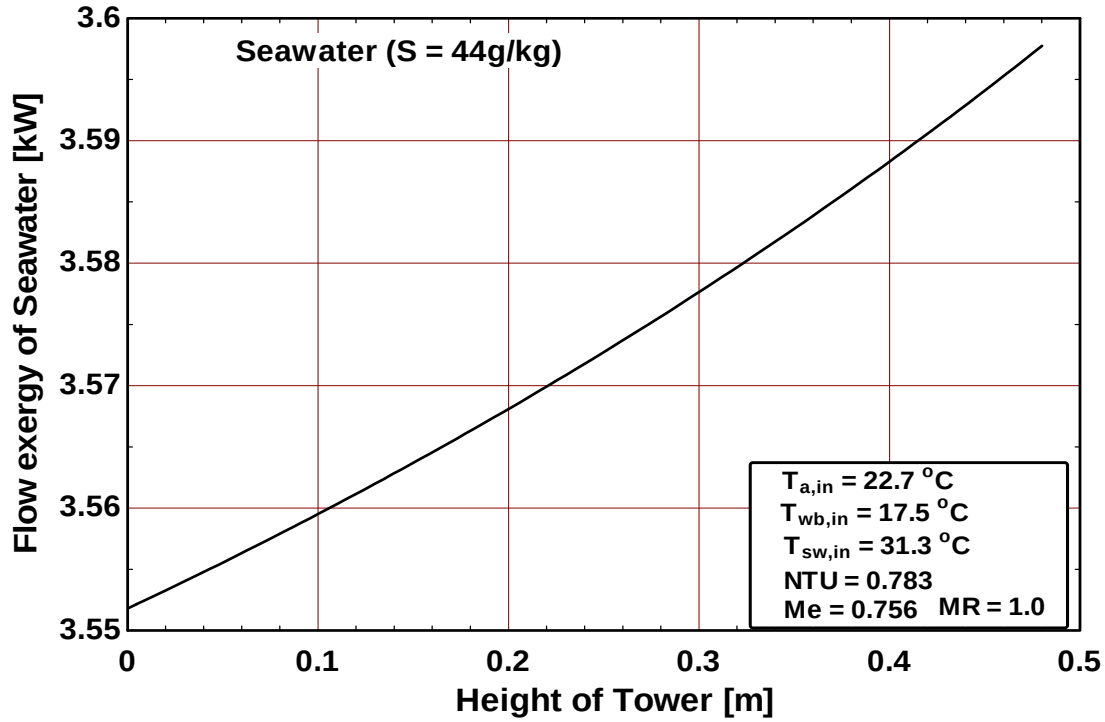

Figure 5.24b Flow exergy of water along the height of tower for seawater (salinity = 44 g/kg) at mass ratio = 1.0

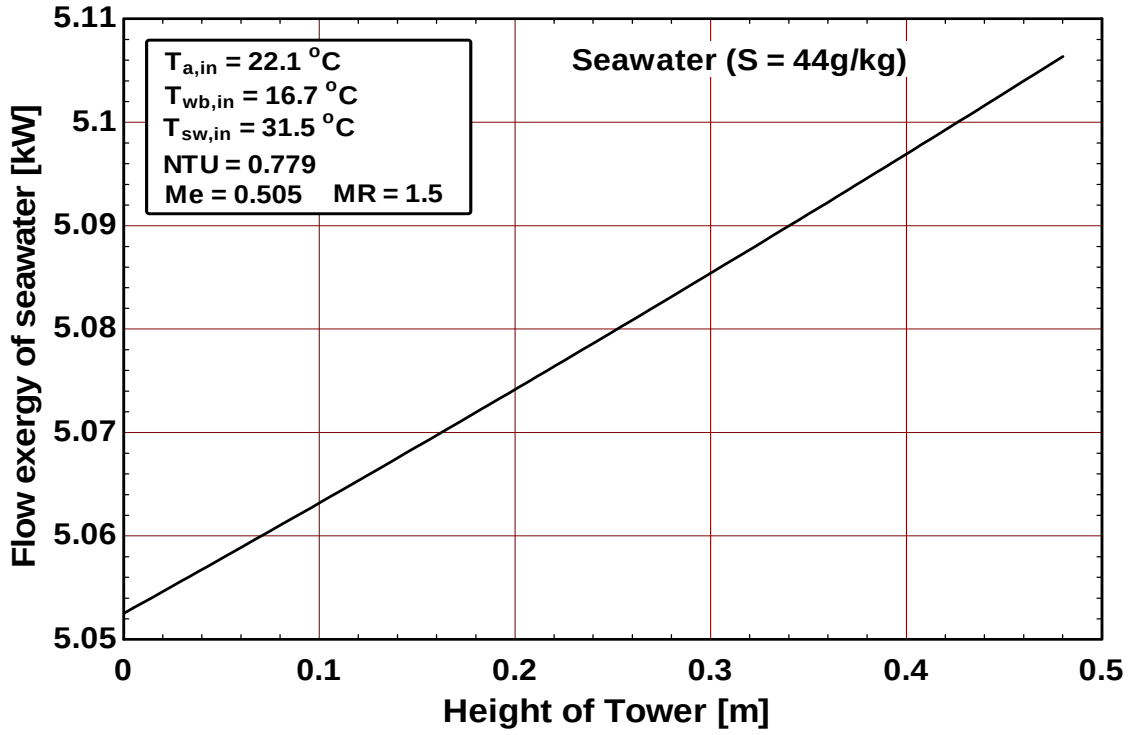

Figure 5.24c Flow exergy of water along the height of tower for seawater (salinity = 44 g/kg) at mass ratio = 1.5

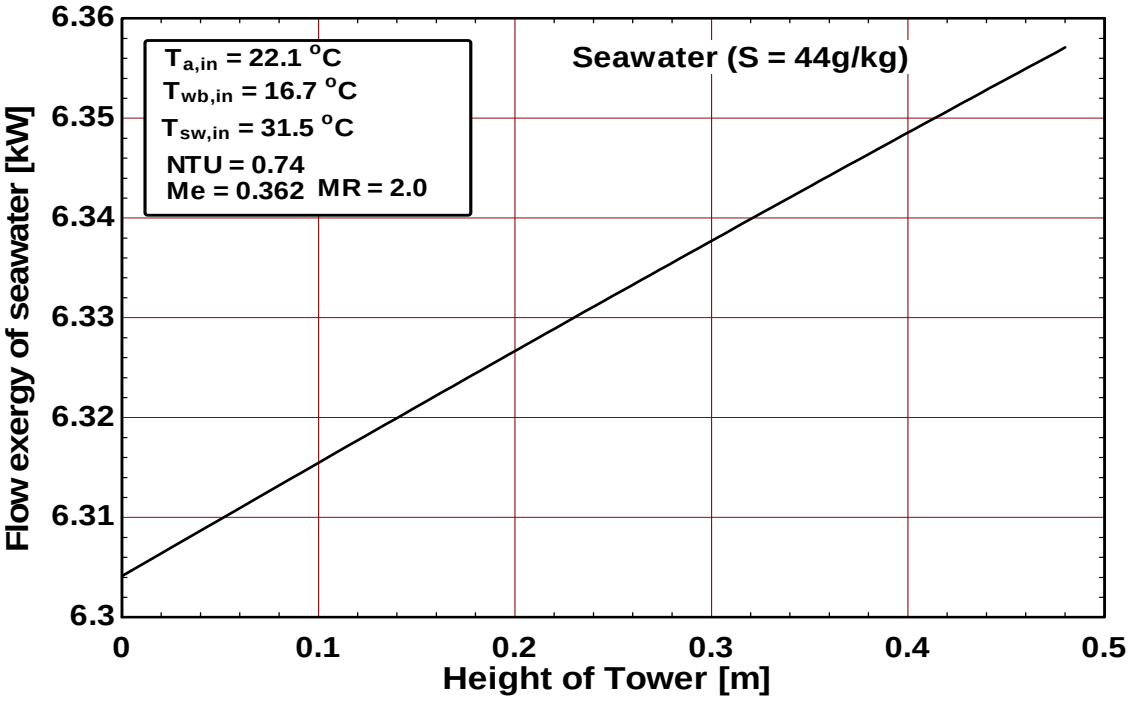

Figure 5.24d Flow exergy of water along the height of tower for seawater (salinity = 44 g/kg) at mass ratio = 2.0

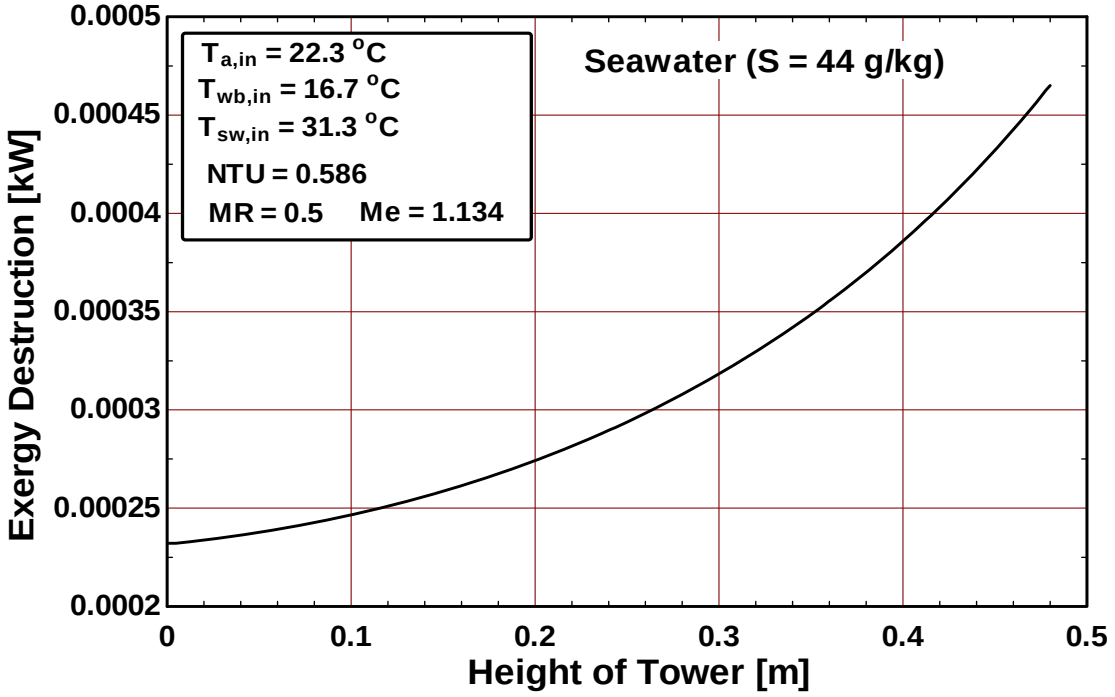

Figure 5.25a Exergy destruction along the height of tower for seawater (salinity = 44 g/kg) at mass ratio = 0.5

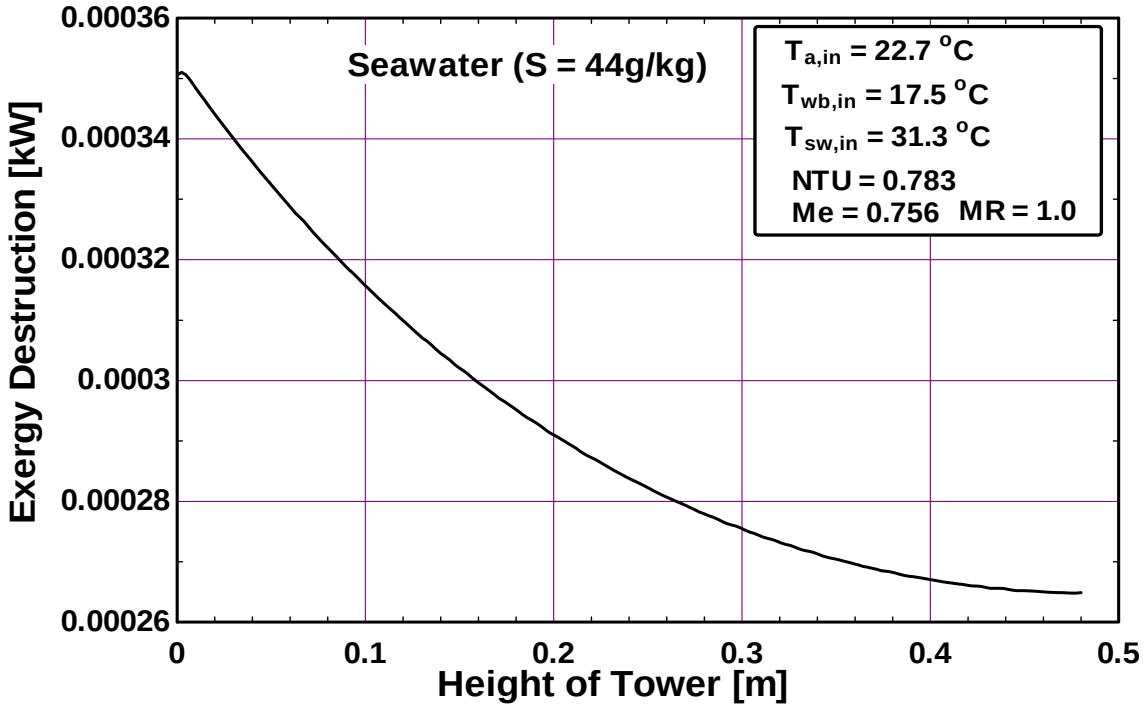

Figure 5.25b Exergy destruction along the height of tower for seawater (salinity = 44 g/kg) at mass ratio = 1.0

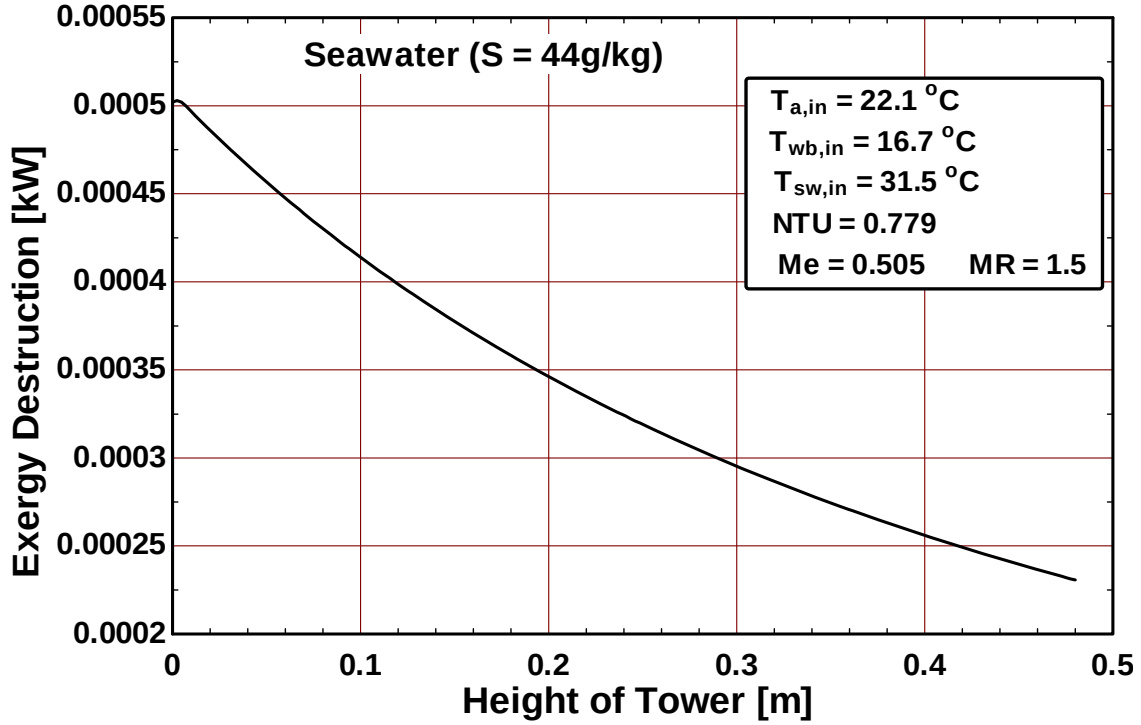

Figure 5.25c Exergy destruction along the height of tower for seawater (salinity = 44 g/kg) at mass ratio = 1.5

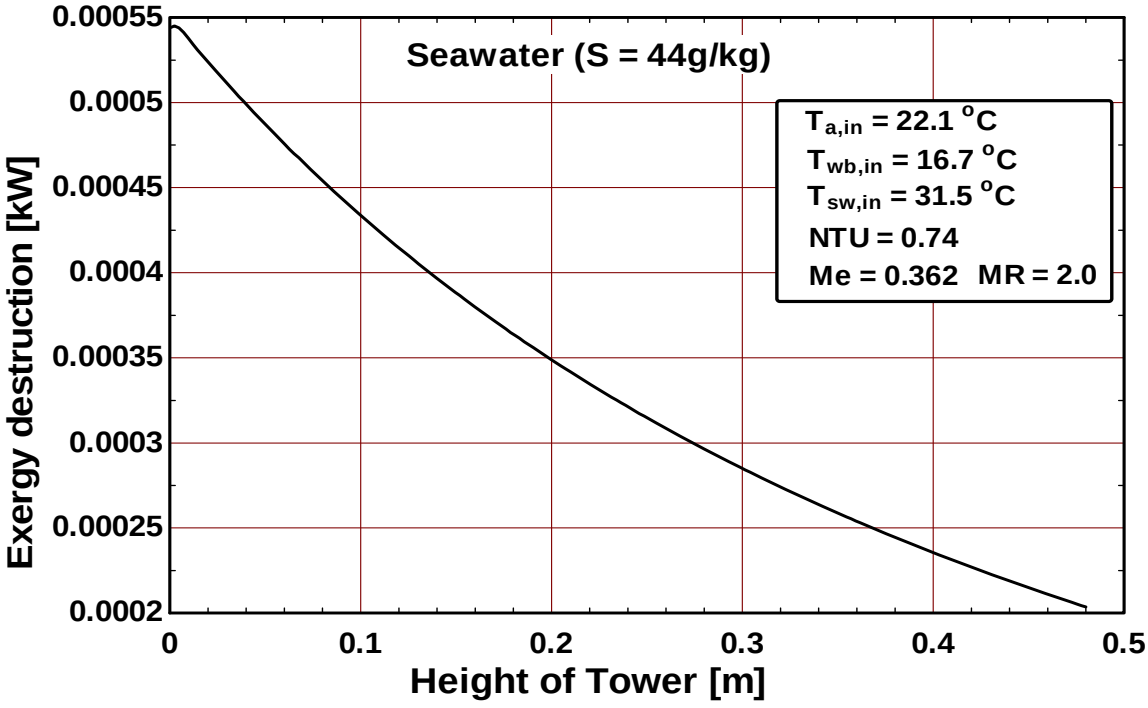

Figure 5.25d Exergy destruction along the height of tower for seawater (salinity = 44 g/kg) at mass ratio = 2.0

5.3.3 Exergy Analysis of Seawater (salinity = 85 g/kg) Cooling Tower

Air and water flow exergy are calculated at the inlet and outlet using the experimental data presented in Table B.1. The calculated flow exergy values of air and water as well as exergy loss at different mass ratios of seawater (S = 85 g/kg) are given in Table B.2. Exergy distribution along the cooling tower at mass ratios 0.5, 1.0, 1.5 and 2.0 of seawater (S = 44 g/kg) are plotted in Figures (5.26), (5.27) and (5.28).

Figures (5.26a), (5.26b), (5.26c) and (5.26d) show flow exergy of air due to convective ($\dot{X}_{air,conv}$) and evaporative ($\dot{X}_{air,evap}$) heat transfer rates along the tower height for mass ratio 0.5, 1.0, 1.5 and 2.0 respectively of the seawater (S = 85 g/kg) cooling tower. The total exergy due to convective and evaporative heat transfer rate ($\dot{X}_{air} = \dot{X}_{air,conv} + \dot{X}_{air,evap}$) is also shown on these figures. Figure 5.26 (a - d) show that the flow exergy of air due to evaporation is much higher than that of the convection component of heat transfer. The evaporation component of exergy increases exponentially with the tower height, while the convective component is more-or-less remains constant throughout the height of the tower. This clearly shows that evaporation is the dominant mode of transfer energy from water to air in a cooling tower.

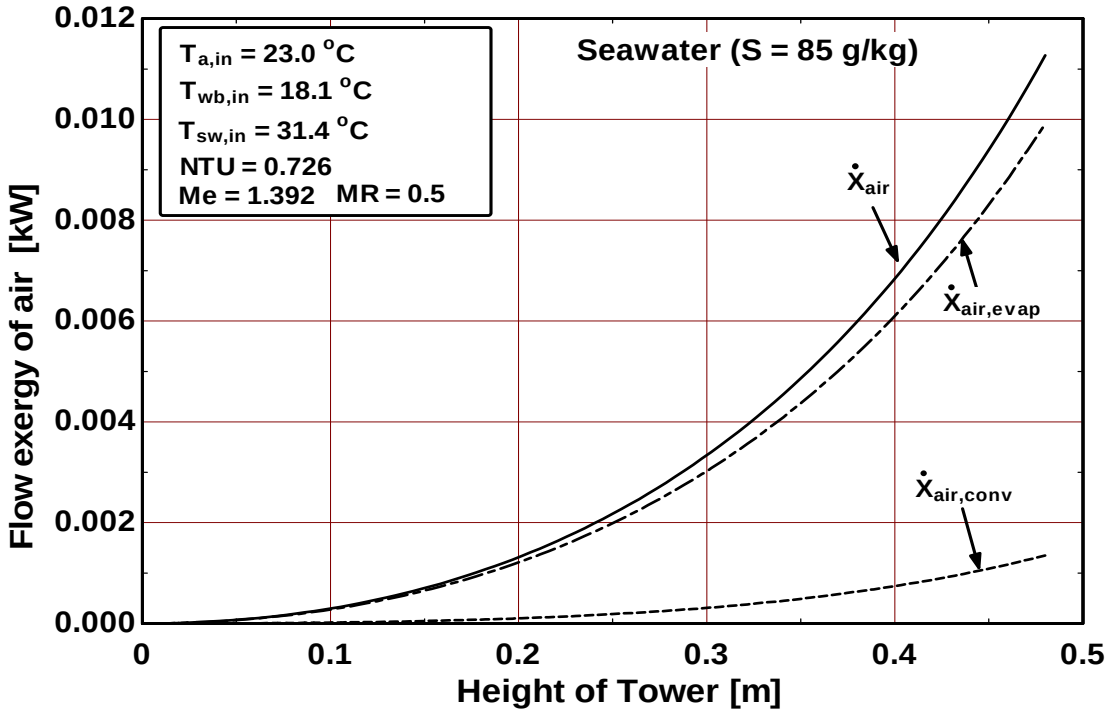

Figure 5.26a Flow exergy of air along the height of tower for seawater (salinity = 85 g/kg) at mass ratio = 0.5

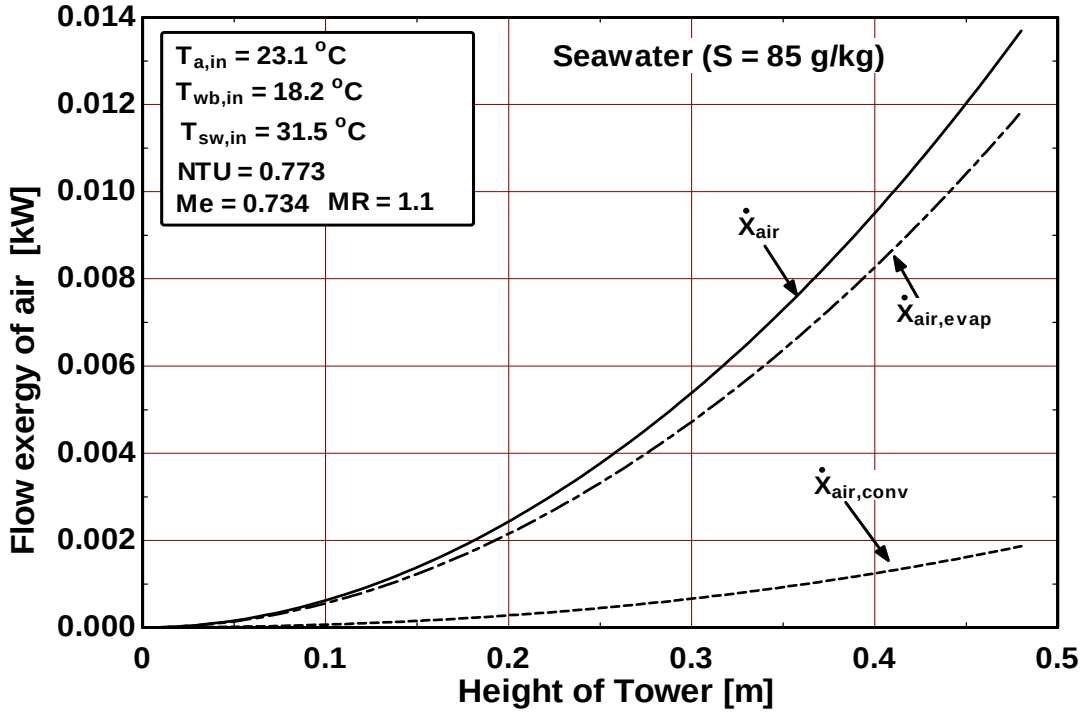

Figure 5.26b Flow exergy of air along the height of tower for seawater (salinity = 85 g/kg) at mass ratio = 1.1

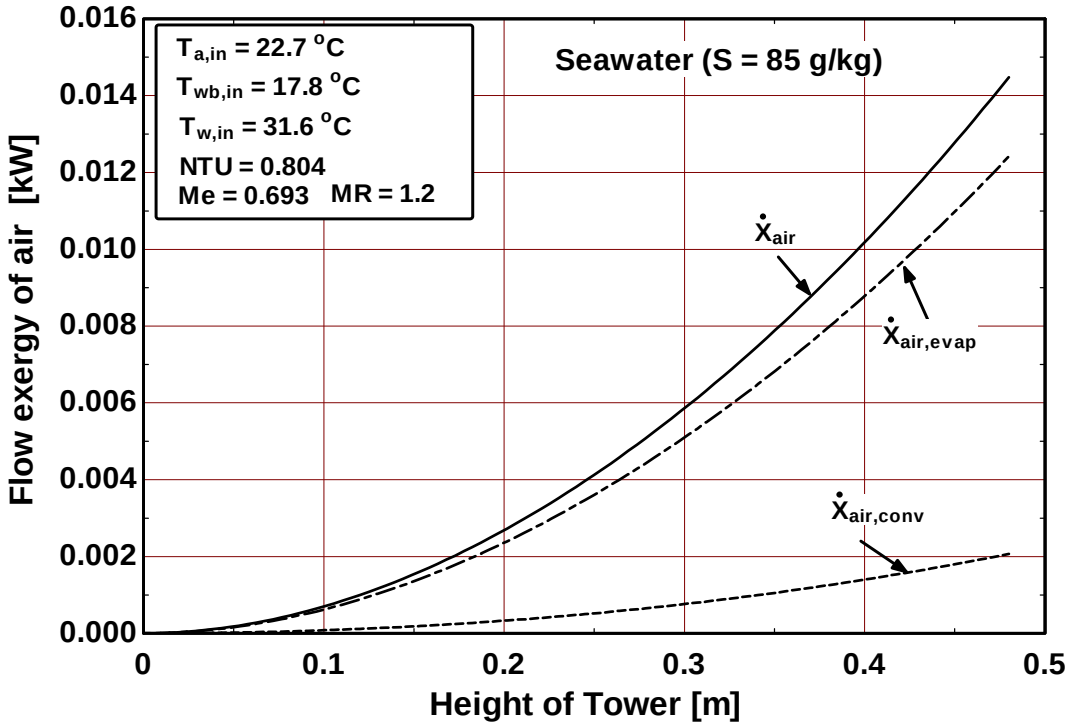

Figure 5.26c Flow exergy of air along the height of tower for seawater (salinity = 85 g/kg) at mass ratio = 1.2

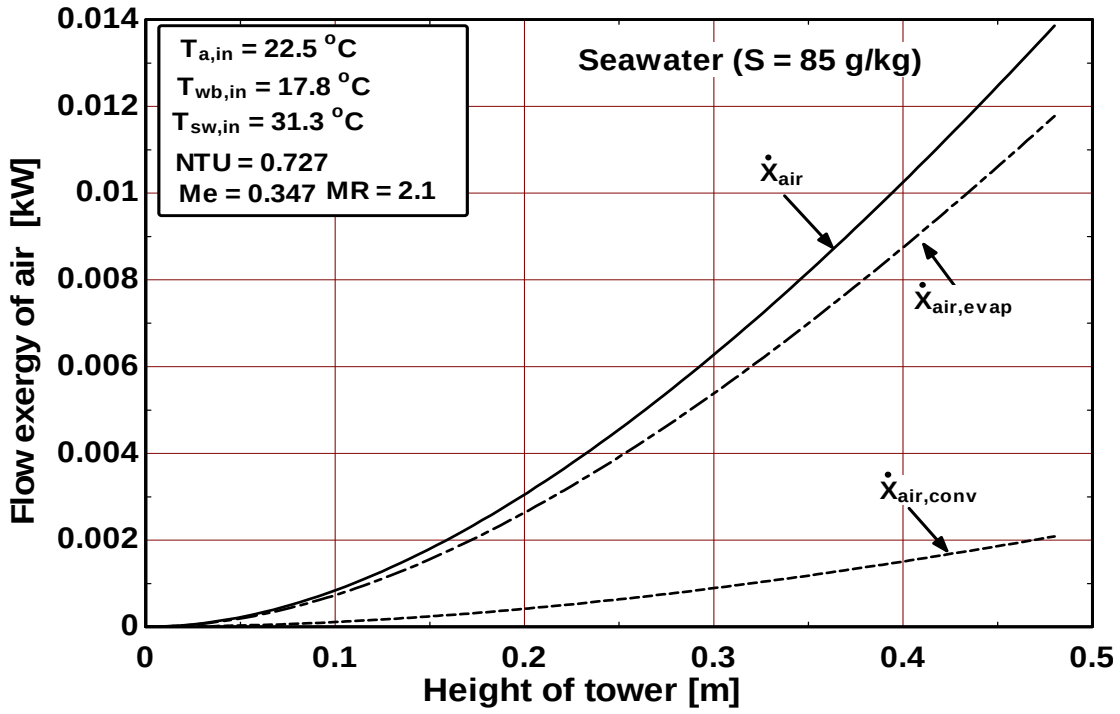

Figure 5.26d Flow exergy of air along the height of tower for seawater (salinity = 85 g/kg) at mass ratio = 2.1

Figures (5.27a), (5.27b), (5.27c) and (5.27d) show flow exergy of water ($\dot{X}_{seawater}$) at mass ratios 0.5, 1.0, 1.5 and 2.0 respectively of the seawater (S = 85 g/kg) cooling tower. It is shown that seawater exergy decreases continuously from the top to bottom of the tower due to exergy transfer from the water to the air stream. When comparing with exergy of air that is discussed earlier in Fig.5.26 (a - d), it is noted that the values of $\dot{X}_{seawater}$ are comparatively more than those of $\dot{X}_{air}$ throughout the tower height. This means that exergy contained in the seawater is transferred to the surrounding air stream with some losses, which is typically defined as exergy losses. This exergy loss is due to the irreversibilities in the system associated with temperature difference and concentration difference.

Figure (5.28a), (5.28b), (5.28c) and (5.28d) shows the exergy destruction along the height of the cooling tower at mass ratios 0.5, 1.0, 1.5 and 2.0 respectively of the seawater (S = 85 g/kg) cooling tower. Fig. 5.28a shows that the exergy destruction is low at the bottom and increases at the top of the tower. Fig. 5.28b, Fig. 5.28c and Fig. 5.28d show that the exergy destruction is high at the bottom and decreases at the top of the tower. The total exergy destruction for mass ratio 0.5 is 0.0232 kW, for mass ratio 1.1 is 0.0249 kW, for mass ratio 1.2 is 0.0251 kW and for mass ratio 2.1 is 0.0265 kW.

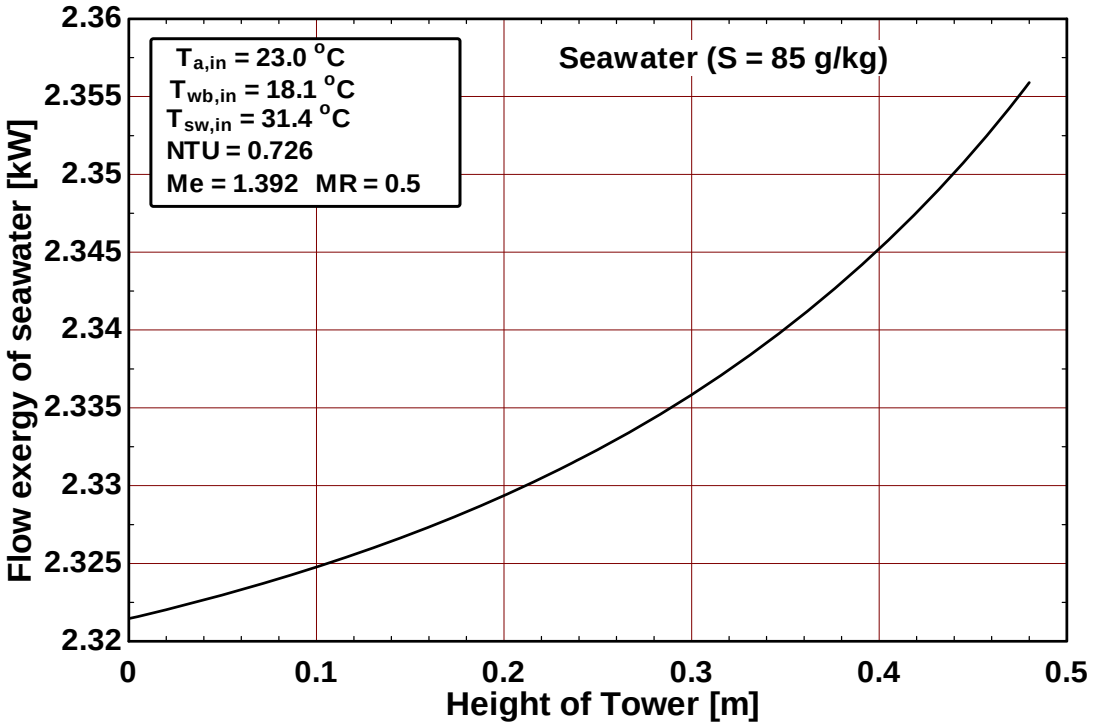

Figure 5.27a Flow exergy of seawater along the height of tower for seawater (salinity = 85 g/kg) at mass ratio = 0.5

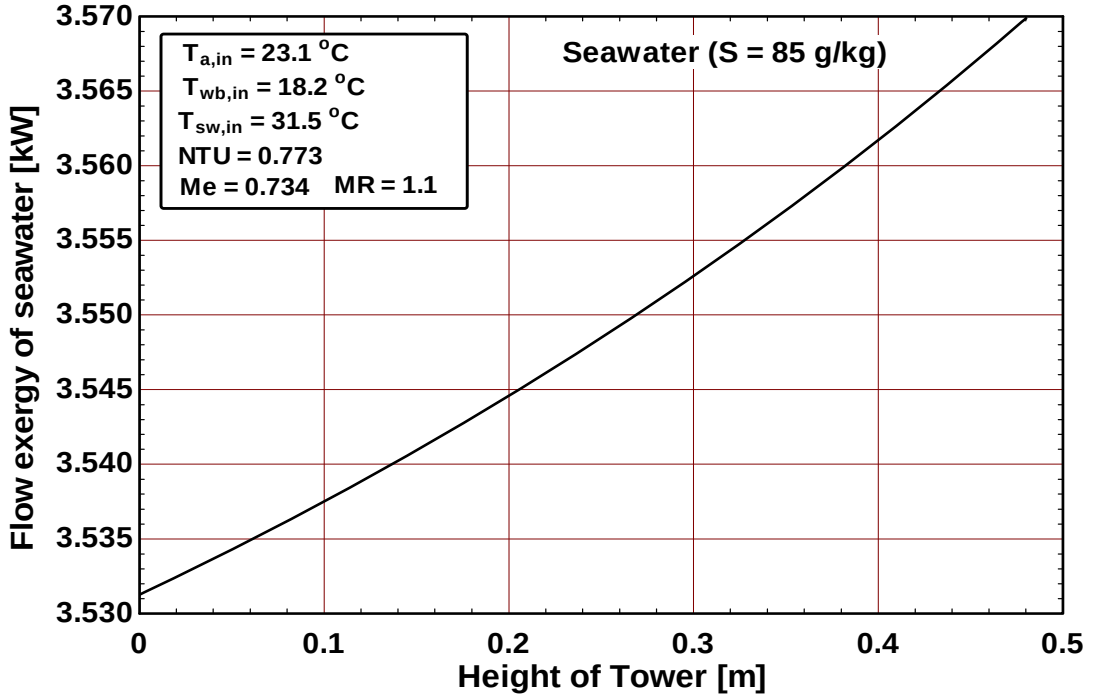

Figure 5.27b Flow exergy of water along the height of tower for seawater (salinity = 85 g/kg) at mass ratio = 1.1

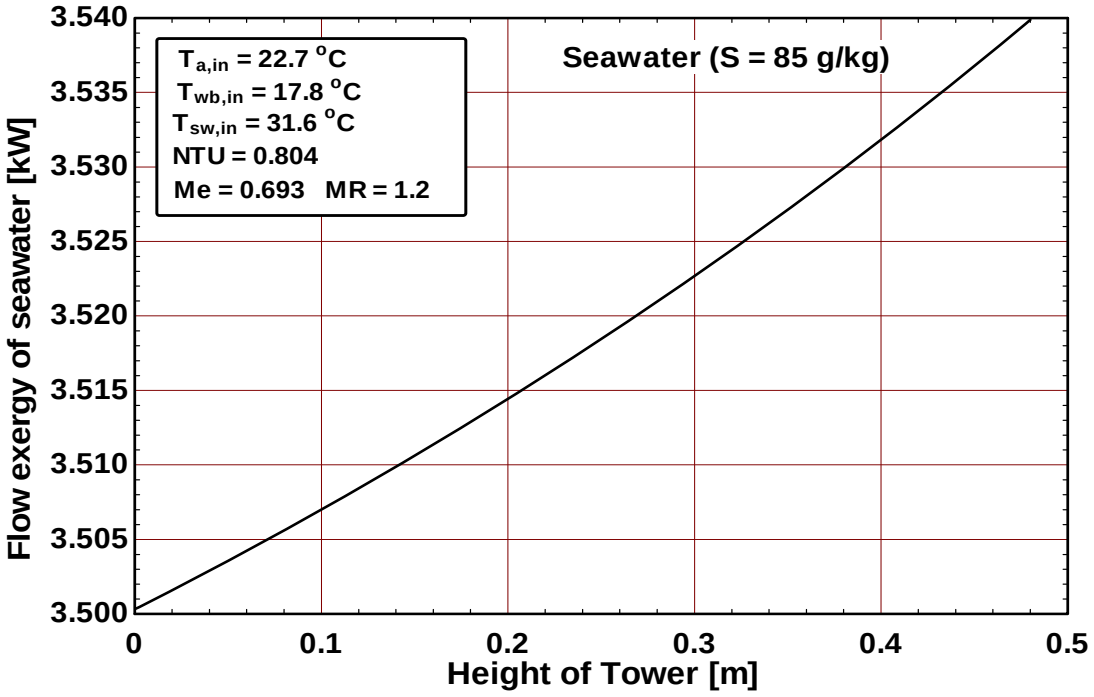

Figure 5.27c Flow exergy of water along the height of tower for seawater (salinity = 85 g/kg) at mass ratio = 1.2

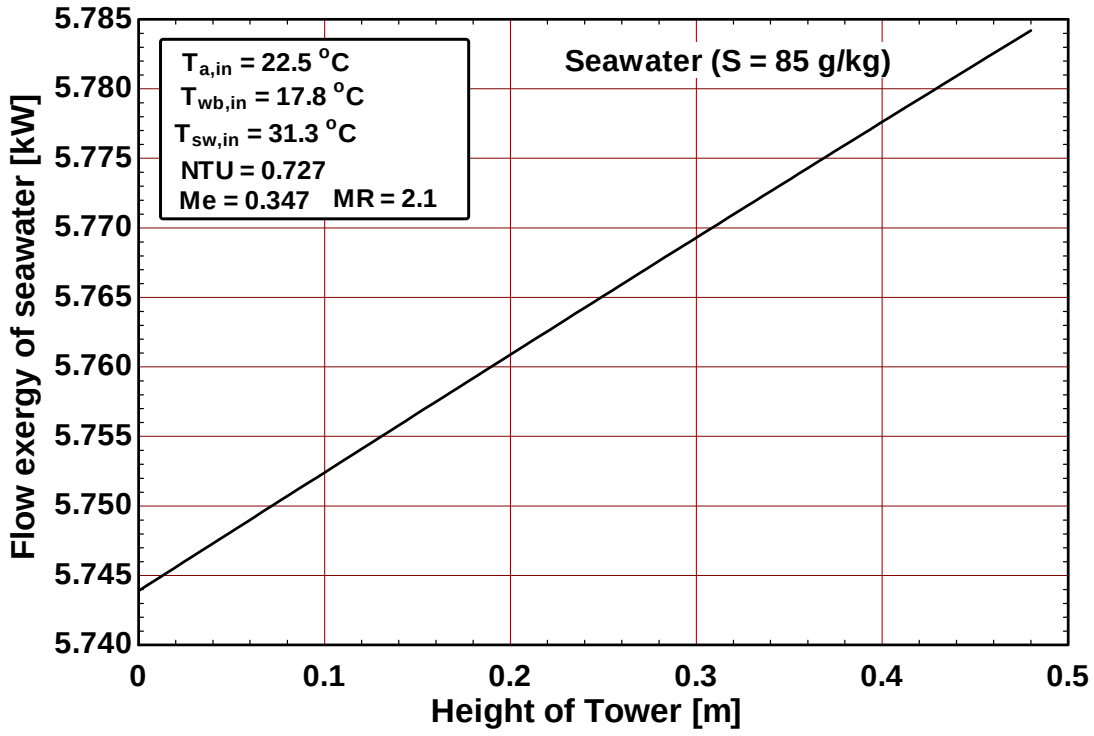

Figure 5.27d Flow exergy of water along the height of tower for seawater (salinity = 85 g/kg) at mass ratio = 2.1

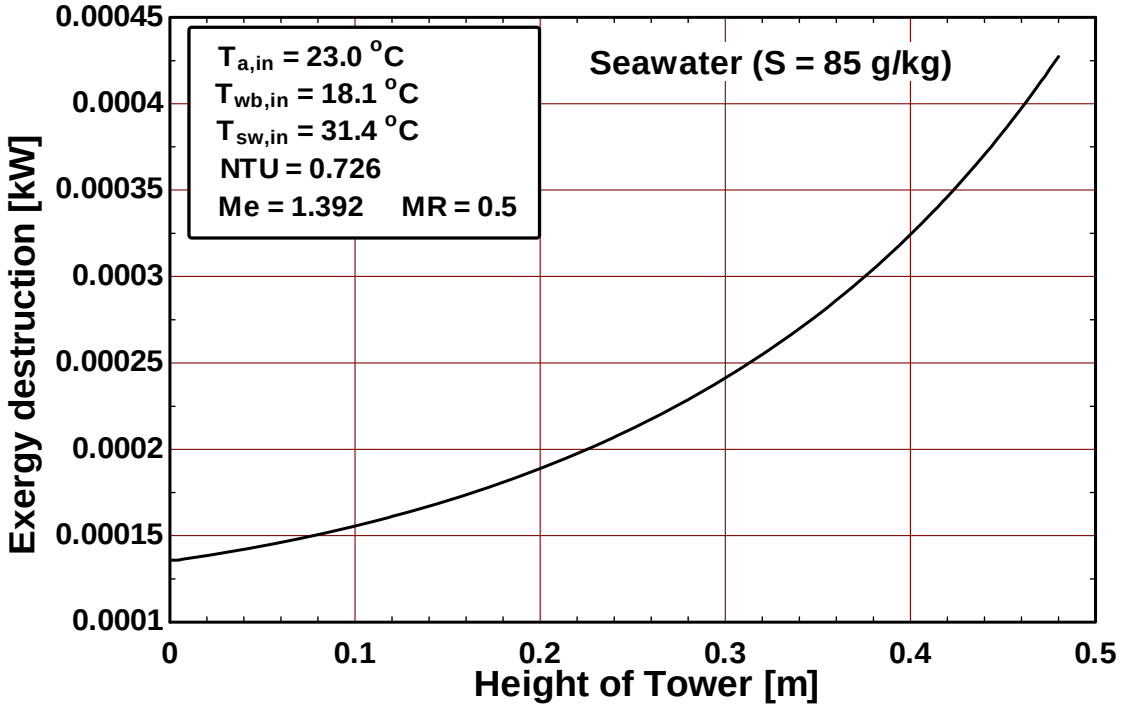

Figure 5.28a Exergy destruction along the height of tower for seawater (salinity = 85 g/kg) at mass ratio = 0.5

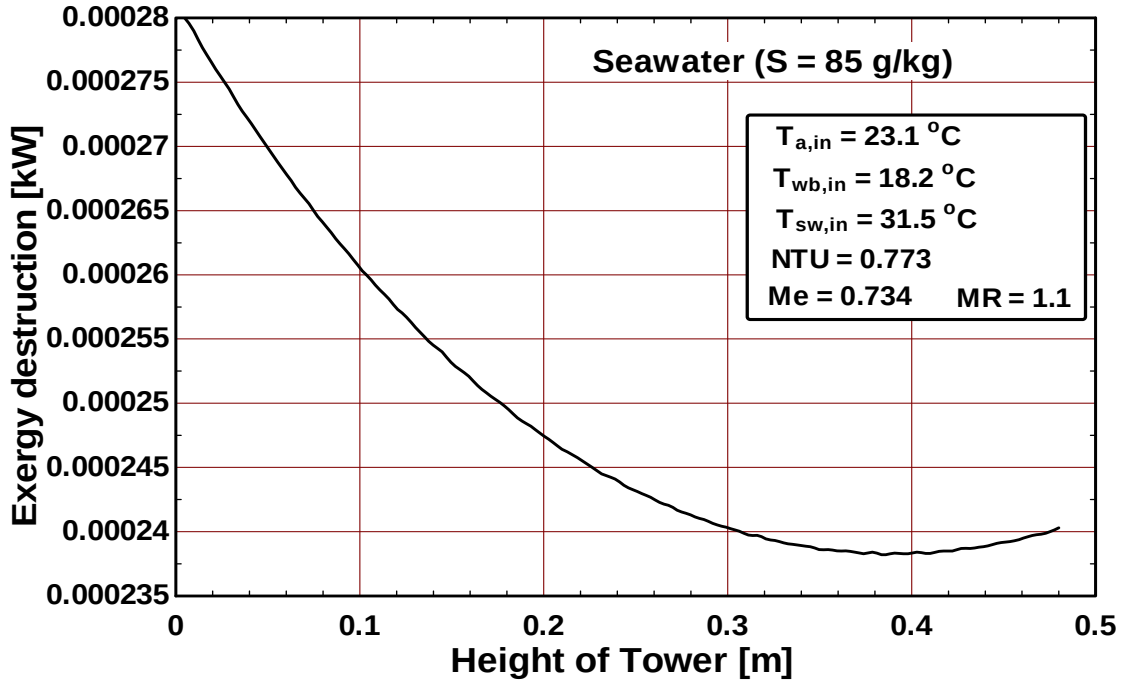

Figure 5.28b Exergy destruction along the height of tower for seawater (salinity = 85 g/kg) at mass ratio = 1.1

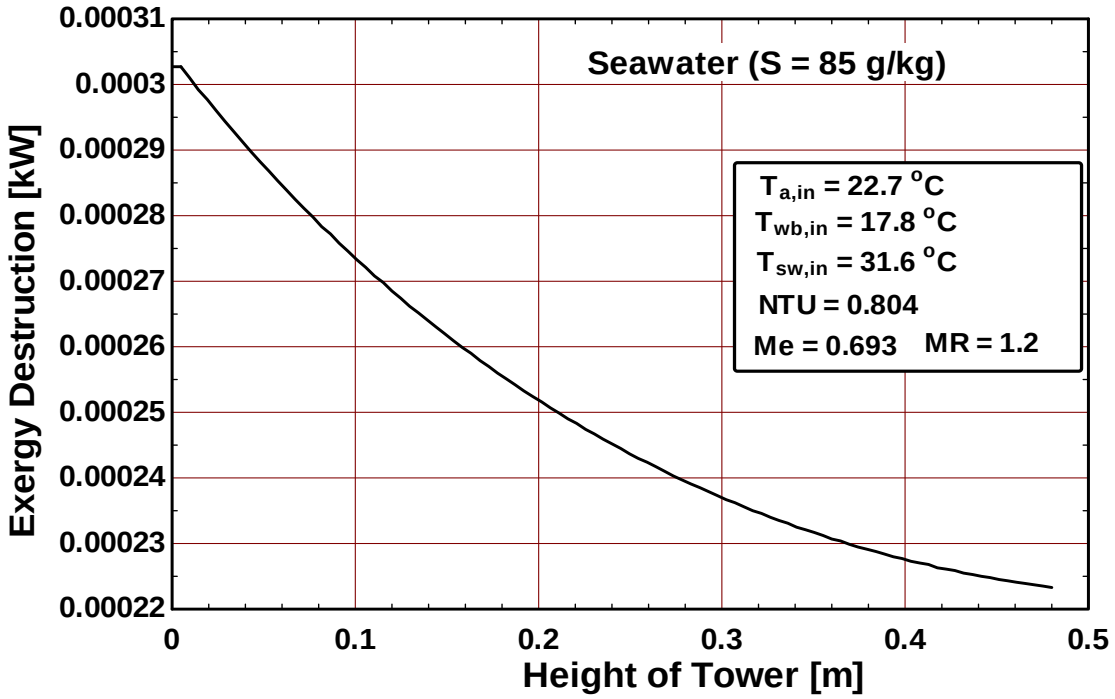

Figure 5.28c Exergy destruction along the height of tower for seawater (salinity = 85 g/kg) at mass ratio = 1.2

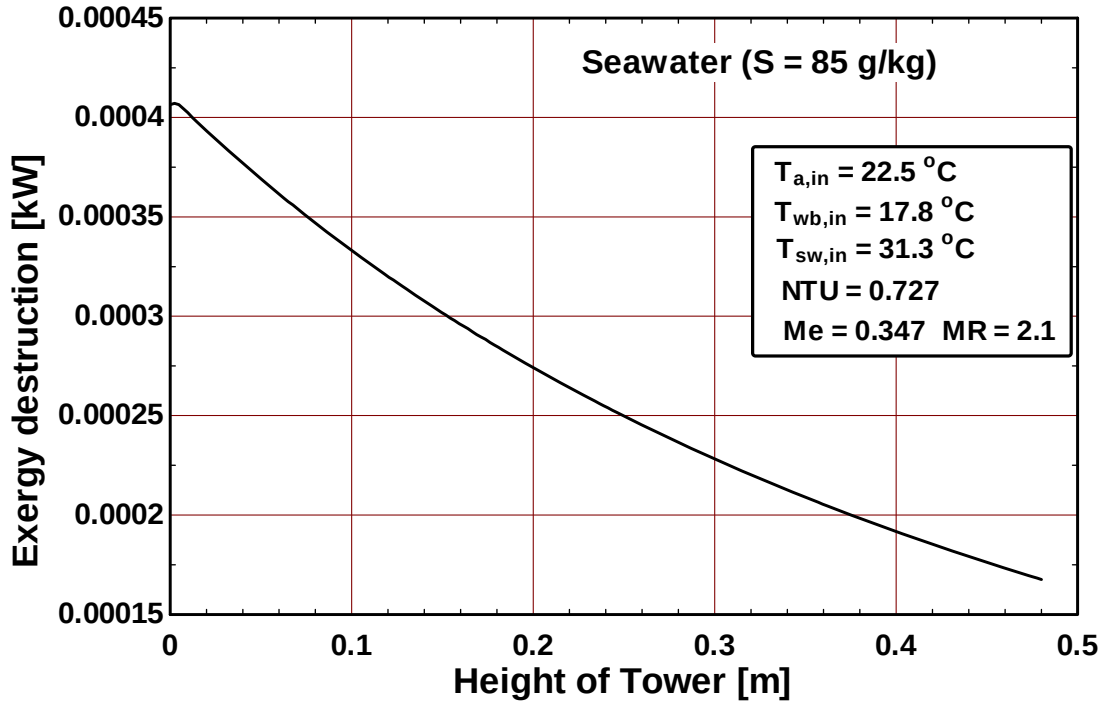

Figure 5.28d Exergy destruction along the height of tower for seawater (salinity = 85 g/kg) at mass ratio = 2.1

Moreover the exergy analysis of fresh water and seawater shows that the exergy destruction decreases as the salinity increases. This can also be verified by the second law efficiency because as the salinity increases, the second law efficiency also increases. The second law efficiency is given by the Eq. (3.34). The calculated values of second law efficiency are given in Table B.3, and are also plotted in Fig. 5.29. It is observed that as mass ratio increases, the second law efficiency also increases and it also increases with the salinity of water. The regression equations, representing the best curves through the second law efficiency of fresh water, seawater (S = 44 g/kg) and seawater (S = 85 g/kg) with different mass ratios are also shown in Fig. 5.29. The best fit correlation between second law efficiency and mass ratio for the fresh water is $\eta_{II} = 0.978MR^{0.013}$ with R^2 = 99.18 %. For seawater (S = 44 g/kg), the best fit correlation is $\eta_{II} = 0.991MR^{0.004}$ with R^2 = 98.92 %. For seawater (S = 85 g/kg) the best fit correlation is $\eta_{II} = 0.992MR^{0.003}$ with R^2 = 99.29 %.

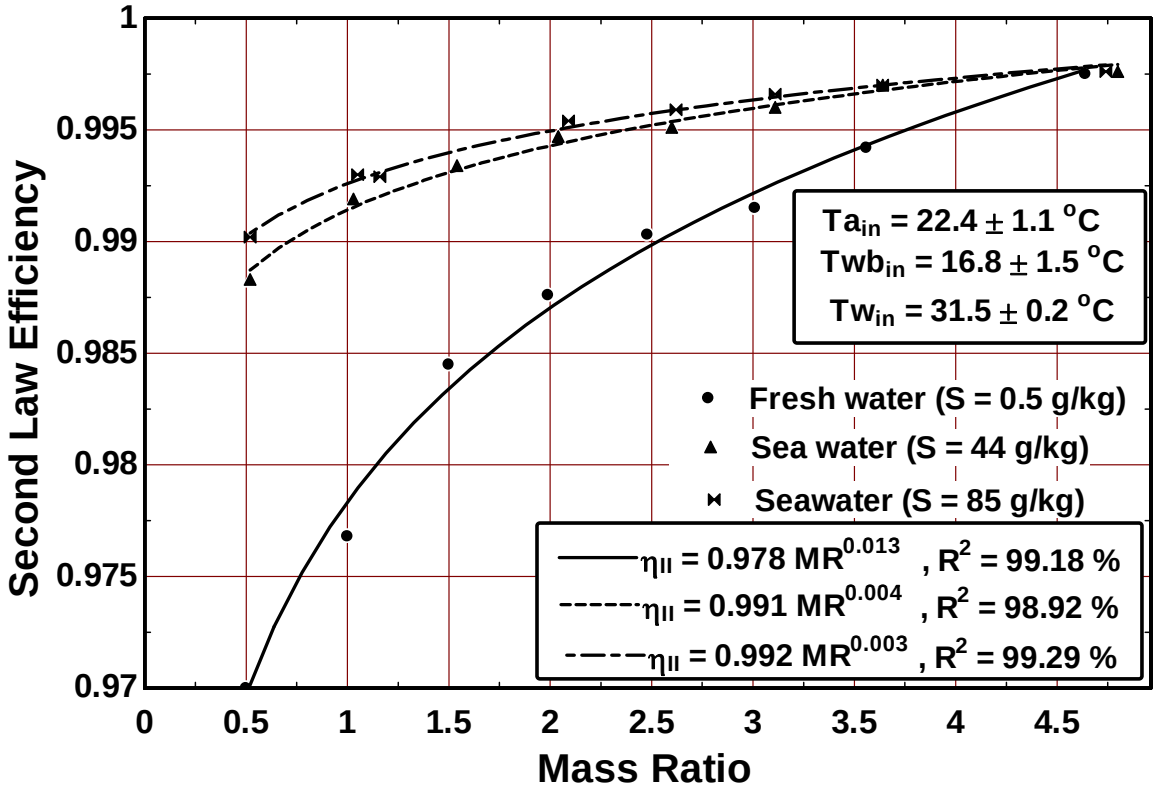

Figure 5.29 Second law efficiency at different mass ratios for fresh water and seawater

CHAPTER 6

CONCLUSIONS AND RECOMMENDATIONS

In this work, counterflow cooling tower for fresh water and seawater is investigated both experimentally and numerically. The numerical model developed takes into consideration the coupled heat and mass transfer processes and does not make any of the conventional cooling tower approximations. The temperature variation versus time plots for all the runs show that the water outlet temperature is always greater than the air wet-bulb inlet temperature, indicating that approach for the tower varied from 4.9 ^{o}C to 15.0 ^{o}C in the experiments. The water outlet temperature is always less than the inlet water temperature because of the transfer of energy from water to air, indicating that the range of the tower varied from maximum 9.5 ^{o}C to minimum 0.5 ^{o}C.

Air effectiveness plots for fresh water, seawater (S = 44 g/kg) and seawater (S = 85 g/kg) show that the air effectiveness increases with the increase of mass ratio because as the mass ratios increases, evaporation rate increases and the air at the outlet becomes more saturated. The air effectiveness value at each mass ratio decreases with increasing the salinity of the seawater because as the salinity increases the vapor pressure of seawater decreases and it reduces the rate of evaporation and thus the air effectiveness. This demonstrates that the seawater cooling tower has less air effectiveness value

compared to fresh water cooling tower at the same operating conditions. The maximum decrease in air effectiveness was found to be 15% for seawater having salinity 85 g/kg at mass ratio 3.6. Regression equations, representing the best curves through the experimental data and numerical data of air effectiveness as a function of mass ratio for fresh water, and both salinities of seawater are also obtained. These fitted equations are the best fit correlations between air effectiveness and the mass ratio with correlation coefficient R^2 = 99 % around. These fitted models can be used for prediction of air effectiveness as a function of mass ratio for the tested tower fill under the tested operating conditions.

Water effectiveness plots for fresh water, and seawater (S = 44 and 85 g/kg) show that the water effectiveness (in contrast to air effectiveness) decreases with the increase in the mass ratio because as the mass ratio increases the enthalpy of water at the outlet increases due to slight increase in water outlet temperature; however, the water effectiveness value at each mass ratio increases with increasing the salinity of the seawater because of the decrease in enthalpy of water at the outlet due to slight decrease in water outlet temperature. This demonstrates that the seawater cooling tower has a higher water effectiveness value compared to the fresh water cooling tower at the same operating conditions. The maximum increase in water effectiveness was found to be 87.9 % for seawater having salinity 85 g/kg at mass ratio 4.7. The regression equations, representing the best curves through the experimental data of water effectiveness for fresh water and seawater salinities are also shown on these plots. Theses fitted equations as described earlier can be very useful information for estimation and prediction of water effectiveness of the tower.

Exergy analysis of cooling tower is carried out on fresh water and seawater to find location of lower exergy destruction (losses) of the cooling tower under different operating conditions. The flow exergy of air along the tower shows that the evaporation component of exergy increases significantly along the tower height, while the convective component was more-or-less remains constant throughout the height of tower. This clearly explains that evaporation is dominant in transferring energy from water to the surrounding air stream in a cooling tower. Water flow exergy distribution shows that it decreases continuously from the top to bottom of the tower due to transfer of energy from water to the stream with exergy losses. The lower exergy destruction region through the analysis of exergy destruction plots showed that there is an optimum performance region inside the cooling tower. These exergy analyses of fresh water and seawater show that the exergy loss (or exergy destruction) decreases as the mass ratio increases and also exergy destruction decreases as the salinity of the water used in cooling tower increases. This was also explained by the second law efficiency data, which clearly demonstrated that as mass ratio increases second law efficiency of the system increases exponentially and also second law efficiency of the system increases as the salinity of water used in cooling tower increases. This fact demonstrated that the high salinity cooling tower has higher value of second law efficiency compared to the fresh water tower for the same operating conditions. The shower cooling tower (i.e. without fill packing) was also investigated in this study and compared with the cooling tower with fill packing. Air effectiveness of the fresh water of the experimental readings of the cooling tower is compared with that of the shower tower. It was found that the air effectiveness of the fresh water of the shower tower decreased by about 50 % when compared to the fill packing for the tested mass

ratios that varied from 0.5 to 2.0. Similarly water effectiveness of the fresh water of the shower cooling tower was found to be decreased by as much as 79 % for a mass ratio 2 when compared to the fill packing tower under the similar operating conditions. This clearly showed that the shower tower has less performance compared to the fill packing tower. Similar analysis was also carried out for seawater having salinity = 44 g/kg, it showed that the air effectiveness of shower tower decreased by around 50 % to that of the fill packing tower, whereas water effectiveness of the shower tower decreased as much as 67 % at a mass ratio of 1 when compared to the fill packing tower.

Since seawater cooling tower research is the vital topic and need of the future so it is recommended to carry out similar experimental analysis for different fill packings having different packing density to calculate the effectiveness of fresh water cooling tower and seawater cooling tower, and validate the experimental results by the numerical code that was developed in this work. The shower cooling tower can also be experimented by using more efficient atomizing nozzle system that can help to improve both the air and water effectiveness under different operating conditions for both the fresh- and sea-water applications. In addition exergy analysis of the towers indicate that there is a possibility to minimize overall exergy destruction in the tower by provided variable mass ratio of water–to-air as a function of tower height.

APPENDICES

APPENDIX A: THERMOPHYSICAL PROPERTIES OF SEAWATER

Thermophysical properties of seawater are comprehensively reviewed recently by Sharqawy et al. [32]. Some of the relevant properties that are needed for the present work are reproduced below:

Vapor Pressure

The vapor pressure of seawater is less than that of fresh water which reduces the potential for water evaporation. The vapor pressure can be calculated using Raoult's law. The equation for seawater vapor pressure based on Raoult's law is;

$$\frac{p_{v,w}}{p_{v,SW}} = 1 + 0.57357 \times \left(\frac{S}{1000 - S} \right) \tag{A.1}$$

Where, S is the seawater salinity in g/kg.

Specific Heat

The specific heat of seawater is less than that of freshwater which reduces the amount of sensible heat that can be transferred at the same temperature difference. The equation for seawater specific heat is;

$$c_{p,SW} = A + Bt_{SW} + Ct_{SW}^2 + Dt_{SW}^3 \tag{A.2}$$

Where, $c_{p,SW}$ is in kJ/kg.K and t_{SW} is in ^{o}C and S is in g/kg.

$$A = 5.328 - 9.76\times10^{-2}S + 4.04\times10^{-4}S^2$$

$$B = -6.913\times10^{-3} + 7.351\times10^{-4}S - 3.15\times10^{-6}S^2$$

$$C = 9.6\times10^{-6} - 1.927\times10^{-6}S + 8.23\times10^{-9}S^2$$

$$D = 2.5\times10^{-9} + 1.666\times10^{-9}S - 7.125\times10^{-12}S^2$$

Equation (A.2) is valid for temperatures of 0 - 180 ^{o}C and salinities of 0 - 180 g/kg.

Specific volume

The specific volume is the inverse of the density. Both are intensive properties however in thermodynamics literature it is preferred to use the specific volume instead of the density because it is directly related to the flow work. The density of seawater is higher than that of pure water due to the salts; consequently the specific volume is lower. The density is given by Eq. (A.4).

$$v_{SW} = \frac{1}{\rho_{SW}} \tag{A.3}$$

$$\rho_{SW} = \rho_W + S(b_1 + b_2 t_{SW} + b_3 t_{SW}^2 + b_4 t_{SW}^3 + b_5 S t_{SW}^2) \tag{A.4}$$

$$\rho_W = (a_1 + a_2 t_{SW} + a_3 t_{SW}^2 + a_4 t_{SW}^3 + a_5 t_{SW}^4) \tag{A.5}$$

Where,

v_{SW} is the specific volume of seawater in m^3/kg, ρ_{SW} and ρ_W are the density of seawater and pure water respectively in kg/m^3, t_{SW} is in ^{o}C and S is in g/kg.

$a_1 = 9.999\times10^{2}, a_2 = 2.034\times10^{-2}, a_3 = -6.162\times10^{-3},$

$a_4 = 2.261\times10^{-5}, a_5 = -4.657\times10^{-8}, b_1 = 0.8020,$

$b_2 = -2.001\times10^{-3}, b_3 = 1.677\times10^{-5}, b_4 = -3.060\times10^{-8},$

$b_5 = -1.613\times10^{-11}$

Equation (A.4) has an accuracy of ±0.1% and valid for temperatures of 0 – 180 ^{o}C and salinities of 0 – 160 g/kg.

Specific enthalpy

The specific enthalpy of seawater is lower than that of pure water since the heat capacity of seawater is less than that of pure water. It can be calculated using Eq. (A.6).

$$h_{SW} = h_W - S(b_1 + b_2 S + b_3 S^2 + b_4 S^3 + b_5 t_{SW} + b_6 t_{SW}^2 + b_7 t_{SW}^3 + b_8 S t_{SW} + b_9 S^2 t_{SW} + b_{10} S t_{SW}^2) \quad \text{(A.6)}$$

$$h_W = 141.355 + 4202.07\times t_{SW} - 0.535\times t_{SW}^2 + 0.004\times t_{SW}^3 \quad \text{(A.7)}$$

Where,

h_{SW} and h_W are the specific enthalpy of seawater and pure water respectively in (J/kg), S is in g/kg and t_{SW} is in ^{o}C.

$b_1 = -2.348\times10^{1}, b_2 = 3.152\times10^{-1}, b_3 = 2.803\times10^{-3}, b_4 = -1.446\times10^{-5}, b_5 = 7.826$

$b_6 = -4.417\times10^{-2}, b_7 = 2.139\times10^{-4}, b_8 = -1.991\times10^{-2}, b_9 = 2.778\times10^{-5}, b_{10} = 9.728\times10^{-5}$

Equation (A.6) is valid for a temperature range of 10 – 120 ^{o}C and salinity range of 0 – 120 g/kg and has an accuracy of ±0.5 %.

Specific entropy

The specific entropy of seawater is lower than that of pure water. It can be calculated using Eq. (A.8)

$$s_{SW} = s_W - S(c_1 + c_2 S + c_3 S^2 + c_4 S^3 + c_5 t_{SW} + c_6 t_{SW}^2 + c_7 t_{SW}^3 + c_8 S t_{SW} + c_9 S^2 t_{SW} + c_{10} S t_{SW}^2) \quad \text{(A.8)}$$

$$s_W = 0.1543 + 15.383 \times t_{SW} - 2.996 \times 10^{-2} \times t_{SW}^2 + 8.193 \times 10^{-5} \times t_{SW}^3 - 1.370 \times 10^{-7} \times t_{SW}^4 \quad \text{(A.9)}$$

Where, s_{SW} and s_W are the specific entropy of seawater and pure water respectively in (J/kg K), S is in g/kg and t_{SW} is in ^{o}C.

$$c_1 = -4.231 \times 10^{-1}, c_2 = 1.463 \times 10^{-2}, c_3 = -9.880 \times 10^{-5}, c_4 = 3.095 \times 10^{-7}, c_5 = 2.562 \times 10^{-2}$$

$$c_6 = -1.443 \times 10^{-4}, c_7 = 5.879 \times 10^{-7}, c_8 = -6.111 \times 10^{-5}, c_9 = 8.041 \times 10^{-8}, c_{10} = 3.035 \times 10^{-7}$$

Equation (A.8) is valid for a temperature range of 10 – 120 ^{o}C and salinity range of 0 – 120 g/kg and has an accuracy of ±0.5 %.

Chemical potential

The chemical potentials of water in seawater and salts in seawater are determined by differentiating the total Gibbs energy function with respect to the composition:

$$\mu_w = \frac{\partial G_{SW}}{\partial m_w} = g_{SW} - S\,\frac{\partial g_{SW}}{\partial S} \tag{A.10}$$

$$\mu_s = \frac{\partial G_{SW}}{\partial m_s} = g_{SW} + (1-S)\frac{\partial g_{SW}}{\partial S} \tag{A.11}$$

Where, g_{SW} is the specific Gibbs energy of seawater defined as;

$$g_{SW} = h_{SW} - (t_{SW} + 273.15)s_{SW} \tag{A.12}$$

The specific Gibbs energy function can be calculated using the enthalpy and entropy correlations given by Eq. (A.6) and (A.8) above. The differentiation of the specific Gibbs energy with respect to salinity is carried out using the enthalpy and entropy correlations as follows,

$$\frac{\partial g_{SW}}{\partial S} = \frac{\partial h_{SW}}{\partial S} - (t_{SW} + 273.15)\frac{\partial s_{SW}}{\partial S} \tag{A.13}$$

Note that the differentiation of the pure water part in Eq. (A.7) and (A.9) with respect to the salt concentration is zero, the differentiation of the enthalpy Eq. (A.6) and entropy Eq. (A.8) with respect to the salt concentration will be

$$\begin{aligned} -\frac{\partial h_{SW}}{\partial S} = {} & b_1 + 2b_2 S + 3b_3 S^2 + 4b_4 S^3 + b_5 t_{SW} + b_6 t_{SW}^2 + b_7 t_{SW}^3 \\ & + 2b_8 S t_{SW} + 3b_9 S^2 t_{SW} + 2b_{10} S t_{SW}^2 \end{aligned} \tag{A.14}$$

$$\begin{aligned} -\frac{\partial s_{SW}}{\partial S} = {} & c_1 + 2c_2 S + 3c_3 S^2 + 4c_4 S^3 + c_5 t_{SW} + c_6 t_{SW}^2 + c_7 t_{SW}^3 \\ & + 2c_8 S t_{SW} + 3c_9 S^2 t_{SW} + 2c_{10} S t_{SW}^2 \end{aligned} \tag{A.15}$$

APPENDIX B: COOLING TOWER

Table B.1 Experimental data for fresh water and seawater for cooling tower

Run	Mass Ratio	ma (kg/s)	mw_{in} (kg/s)	$Salinity_{in}$ (g/kg)	Ta_{in} (^oC)	Twb_{in} (^oC)	Tw_{in} (^oC)	Ta_o (^oC)	Twb_o (^oC)	Tw_o (^oC)
(1)	**0.5**	0.066	0.033	0.0	23.2	17.0	31.4	23.6	21.9	22.2
(2)	**0.5**	0.066	0.034	44.0	22.3	16.7	31.3	23.3	21.3	21.8
(3)	**0.5**	0.068	0.035	85.0	23.0	18.1	31.4	24.1	22.2	23.0
(4)	**1.0**	0.050	0.050	0.0	22.6	17.5	31.3	25.8	23.7	25.5
(5)	**1.0**	0.050	0.051	44.0	22.7	17.5	31.3	26.0	23.6	25.3
(6)	**1.1**	0.050	0.053	85.0	23.1	18.2	31.5	26.1	23.8	25.5
(7)	**1.5**	0.044	0.066	0.0	22.2	16.1	31.4	26.9	24.0	27.1
(8)	**1.5**	0.044	0.069	44.0	22.1	16.7	31.5	27.1	24.3	27.2
(9)	**1.2**	0.046	0.053	85.0	22.7	17.8	31.6	26.3	23.9	25.7
(10)	**2.0**	0.042	0.083	0.0	22.1	16.4	31.4	27.6	24.5	28.2
(11)	**2.0**	0.042	0.086	44.0	22.1	16.7	31.5	27.7	24.5	28.2
(12)	**2.1**	0.042	0.088	85.0	22.5	17.8	31.3	27.8	24.5	28.4
(13)	**2.5**	0.037	0.093	0.0	22.7	17.8	31.5	28.6	25.7	29.5
(14)	**2.6**	0.037	0.096	44.0	21.6	16.8	31.4	27.9	25.2	29.0
(15)	**2.6**	0.038	0.099	85.0	21.3	15.5	31.3	27.6	24.2	28.5
(16)	**3.0**	0.031	0.093	0.0	22.2	17.4	31.5	28.5	25.8	29.7
(17)	**3.1**	0.031	0.096	44.0	22.2	17.2	31.5	28.3	25.5	29.6
(18)	**3.1**	0.032	0.099	85.0	21.7	15.7	31.4	28.2	24.5	29.0
(19)	**3.6**	0.026	0.093	0.0	22.3	17.7	31.4	28.9	26.9	30.3
(20)	**3.6**	0.026	0.096	44.0	23.2	17.6	31.4	28.8	25.8	30.2
(21)	**3.6**	0.027	0.099	85.0	21.6	15.3	31.4	28.6	24.9	29.5
(22)	**4.6**	0.020	0.093	0.0	23.3	17.8	31.4	29.5	27.1	30.8

(23)	**4.8**	0.020	0.096	44.0	23.5	17.9	31.4	29.4	26.7	30.9
(24)	**4.7**	0.021	0.099	85.0	21.6	15.4	31.5	29.2	25.9	30.4

Uncertainty Analysis of Experimental Results

Uncertainty analysis deals with assessing the uncertainty in a measurement. It is well known that errors and uncertainties in any experiments can arise from instrument selection, instrument condition, instrument calibration, environmental conditions, observation and reading and test planning. Uncertainty analysis is needed to prove the accuracy of the experiments. In these experiments, temperatures, water flow rates and differential pressures are measured from thermocouples, rotameter and manometer respectively and results are calculated from these measured parameters such as mass ratios, air and water effectiveness. The uncertainty analysis is carried out in Engineering Equation Solver (EES) software. The uncertainty of thermocouples is ± 0.1 ^{o}C, rotameter is ± 0.1 lit/min, and the manometer is ± 1 mm H_2O. The uncertainty of air effectiveness and water effectiveness versus mass ratios for the fresh water experimental readings are plotted in Fig. B.22 and Fig. B.23 respectively. The uncertainty of air effectiveness and water effectiveness versus mass ratios for the seawater (S = 44 g/kg) experimental readings are plotted in Fig. B.24 and Fig. B.25 respectively. The uncertainty of air effectiveness and water effectiveness versus mass ratios for the seawater (S = 85 g/kg) experimental readings are plotted in Fig. B.26 and Fig. B.27 respectively.

Table B.2 Calculated results of the experimental data for fresh water and seawater for cooling tower

Run	Mass Ratio	Merkel Number	$Energyl_{oss}$ (kW)	$Energyl_{oss}$ (%)	ε_{air}	ε_{water}	Xa_{in} (kW)	Xa_{o} (kW)	Xw_{in} (kW)	Xw_{o} (kW)	$Exergy_{loss}$ (kW)
(1)	0.50 ± 0.06	1.483	0.238	5.45	0.273 ± 0.008	0.650 ± 0.008	0.00	0.015	2.85	2.80	0.035
(2)	0.52 ± 0.07	1.134	0.316	7.47	0.250 ± 0.007	0.709 ± 0.009	0.00	0.012	2.65	2.60	0.033
(3)	0.52 ± 0.07	1.392	0.197	4.81	0.248 ± 0.008	0.794 ± 0.012	0.00	0.009	2.35	2.32	0.027
(4)	1.00 ± 0.09	0.790	0.158	2.42	0.381 ± 0.009	0.428 ± 0.009	0.00	0.015	3.56	3.51	0.034
(5)	1.03 ± 0.10	0.756	0.179	2.83	0.374 ± 0.008	0.482 ± 0.010	0.00	0.014	3.60	3.55	0.032
(6)	1.05 ± 0.10	0.734	0.213	3.47	0.356 ± 0.009	0.571 ± 0.012	0.00	0.012	3.57	3.53	0.030
(7)	1.50 ± 0.12	0.506	0.048	0.55	0.435 ± 0.008	0.292 ± 0.008	0.00	0.021	5.84	5.78	0.041
(8)	1.54 ± 0.13	0.505	0.033	0.39	0.433 ± 0.008	0.325 ± 0.009	0.00	0.019	5.11	5.05	0.035
(9)	1.16 ± 0.11	0.693	0.205	3.32	0.375 ± 0.009	0.534 ± 0.011	0.00	0.013	3.54	3.50	0.031
(10)	1.99 ± 0.16	0.359	-0.030	-0.27	0.460 ± 0.008	0.219 ± 0.009	0.00	0.020	6.73	6.68	0.037
(11)	2.04 ± 0.16	0.362	0.007	0.07	0.447 ± 0.008	0.249 ± 0.009	0.00	0.019	6.36	6.31	0.035
(12)	2.09 ± 0.16	0.347	0.003	0.03	0.425 ± 0.009	0.280 ± 0.012	0.00	0.014	5.78	5.73	0.029
(13)	2.48 ± 0.22	0.244	-0.237	-1.93	0.500 ± 0.009	0.157 ± 0.010	0.00	0.017	6.22	6.18	0.023
(14)	2.60 ± 0.23	0.315	-0.153	-1.29	0.498 ± 0.009	0.187 ± 0.010	0.00	0.019	6.29	6.24	0.027
(15)	2.62 ± 0.23	0.298	-0.012	-0.11	0.462 ± 0.008	0.218 ± 0.010	0.00	0.021	8.30	8.25	0.036
(16)	3.02 ± 0.36	0.209	-0.210	-1.71	0.520 ± 0.009	0.133 ± 0.009	0.00	0.016	6.27	6.23	0.020
(17)	3.11 ± 0.37	0.270	-0.178	-1.50	0.501 ± 0.009	0.148 ± 0.010	0.00	0.015	6.51	6.47	0.021
(18)	3.10 ± 0.35	0.262	-0.061	-0.53	0.480 ± 0.008	0.183 ± 0.010	0.00	0.019	8.70	8.65	0.030
(19)	3.56 ± 0.57	0.142	-0.429	-3.51	0.603 ± 0.010	0.089 ± 0.010	0.00	0.017	5.91	5.88	0.009
(20)	3.64 ± 0.58	0.236	-0.308	-2.59	0.520 ± 0.009	0.101 ± 0.011	0.00	0.014	7.21	7.18	0.013
(21)	3.64 ± 0.55	0.229	-0.168	-1.46	0.513 ± 0.008	0.143 ± 0.010	0.00	0.019	9.26	9.21	0.024
(22)	4.64 ± 1.22	0.059	-0.476	-3.90	0.618 ± 0.010	0.043 ± 0.010	0.00	0.014	7.00	7.03	0.004

(23)	4.80 ± 1.27	0.203	-0.440	-3.70	0.585 ± 0.010	0.048 ± 0.011	0.00	0.012	7.20	7.18	0.004
(24)	4.74 ± 1.16	0.197	-0.354	-3.08	0.571 ± 0.009	0.081 ± 0.010	0.00	0.018	9.04	9.01	0.011

Table B.3 Numerical analysis of the inlet experimental data for fresh water and seawater for cooling tower

Run	Ta_o (^oC)	Twb_o (^oC)	Tw_o (^oC)	Merkel Number	$Energyl_{oss}$ (kW)	$Energyl_{oss}$ (%)	ε_{air}	ε_{water}	Xa_{in} (kW)	Xa_o (kW)	Xw_{in} (kW)	Xw_o (kW)	$Exergy_{loss}$ (kW)	η_{II}
(1)	22.6	21.9	22.2	1.483	0.238	5.45	0.275	0.654	0.0	0.01	2.85	2.80	0.035	0.97
(2)	25.0	21.8	23.3	1.134	0.316	7.47	0.282	0.560	0.0	0.01	2.65	2.60	0.033	0.98
(3)	26.3	22.9	23.2	1.392	0.197	4.81	0.295	0.629	0.0	0.01	2.35	2.32	0.027	0.99
(4)	23.8	23.7	25.6	0.790	0.158	2.42	0.378	0.426	0.0	0.02	3.56	3.51	0.034	0.97
(5)	26.8	24.1	25.8	0.756	0.179	2.83	0.404	0.409	0.0	0.01	3.60	3.55	0.032	0.99
(6)	27.7	24.2	26.2	0.734	0.213	3.47	0.384	0.409	0.0	0.01	3.57	3.53	0.030	0.99
(7)	25.4	23.9	27.1	0.506	0.048	0.55	0.432	0.290	0.0	0.02	5.84	5.78	0.041	0.98
(8)	27.0	24.3	27.3	0.505	0.033	0.39	0.437	0.295	0.0	0.02	5.11	5.05	0.035	0.99
(9)	27.7	24.3	26.4	0.693	0.205	3.32	0.402	0.387	0.0	0.01	3.54	3.50	0.031	0.99
(10)	26.7	24.4	28.2	0.359	-0.03	-0.27	0.456	0.218	0.0	0.02	6.73	6.68	0.037	0.98
(11)	27.1	24.4	28.3	0.362	0.007	0.07	0.441	0.225	0.0	0.02	6.36	6.31	0.035	0.99
(12)	27.8	24.4	28.4	0.347	0.003	0.03	0.419	0.223	0.0	0.01	5.78	5.73	0.029	0.99
(13)	31.1	25.7	29.5	0.244	-0.24	-1.93	0.498	0.157	0.0	0.02	6.22	6.18	0.023	0.99
(14)	27.3	25.0	28.7	0.315	-0.15	-1.29	0.481	0.193	0.0	0.02	6.29	6.24	0.027	0.99
(15)	27.5	24.0	28.5	0.298	-0.01	-0.11	0.453	0.186	0.0	0.02	8.30	8.25	0.036	0.99
(16)	31.3	25.8	29.7	0.209	-0.21	-1.71	0.520	0.133	0.0	0.02	6.27	6.23	0.020	0.99
(17)	27.8	25.4	29.2	0.270	-0.18	-1.50	0.498	0.168	0.0	0.02	6.51	6.47	0.021	0.99
(18)	28.1	24.4	28.9	0.262	-0.06	-0.53	0.472	0.164	0.0	0.02	8.70	8.65	0.030	0.99
(19)	38.4	27.0	30.3	0.142	-0.43	-3.51	0.602	0.089	0.0	0.02	5.91	5.88	0.009	0.99

(20)	28.4	25.7	29.4	0.236	-0.31	-2.59	0.512	0.149	0.0	0.01	7.21	7.18	0.013	0.99
(21)	28.2	24.5	29.2	0.229	-0.17	-1.46	0.487	0.143	0.0	0.02	9.26	9.21	0.024	0.99
(22)	45.6	27.0	30.8	0.059	-0.47	-3.90	0.601	0.040	0.0	0.01	7.00	7.03	0.004	0.99
(23)	29.0	26.4	29.8	0.203	-0.44	-3.70	0.561	0.124	0.0	0.01	7.20	7.18	0.004	0.99
(24)	28.9	25.3	29.6	0.197	-0.35	-3.08	0.530	0.120	0.0	0.02	9.04	9.01	0.011	0.99

The temperature variation versus time plots of the all the Experimental Data (Table B.1) of Fresh water and Seawater for Cooling Tower at different mass ratios

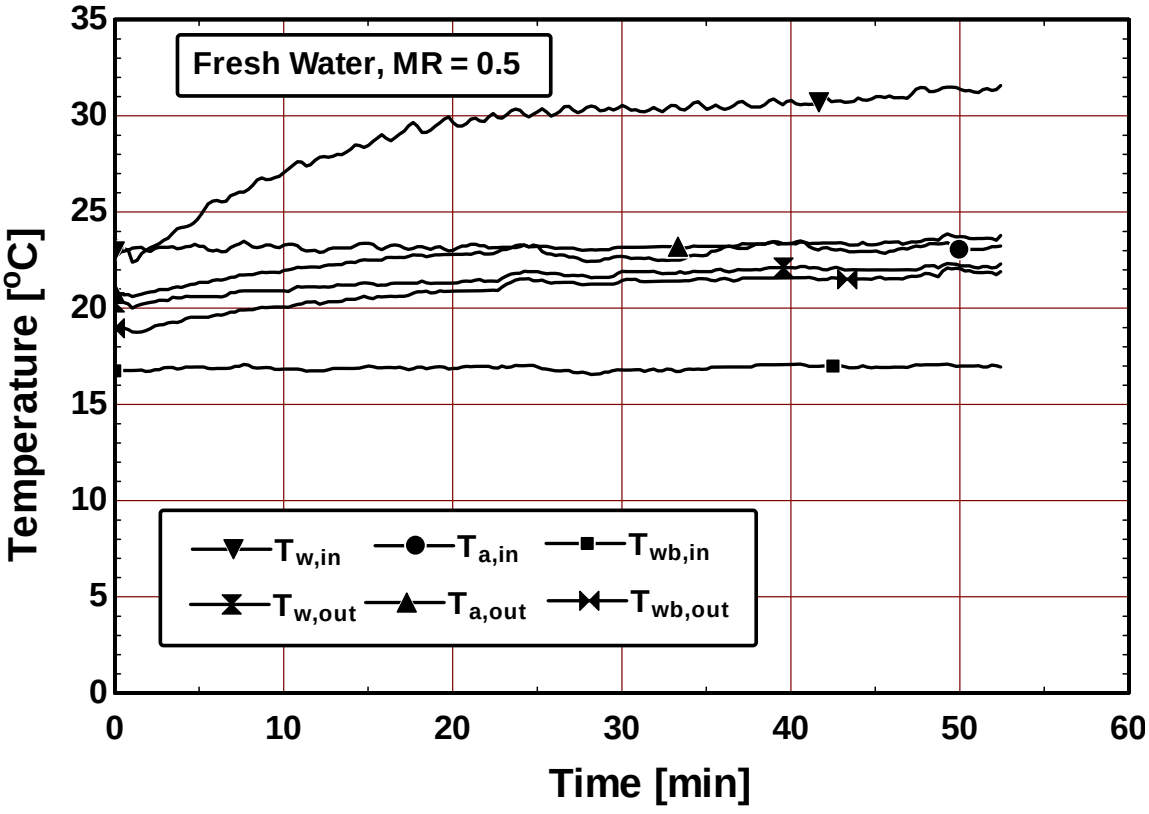

Figure B.1 Temperature variation versus time for fresh water at mass ratio of 0.5 for Cooling Tower

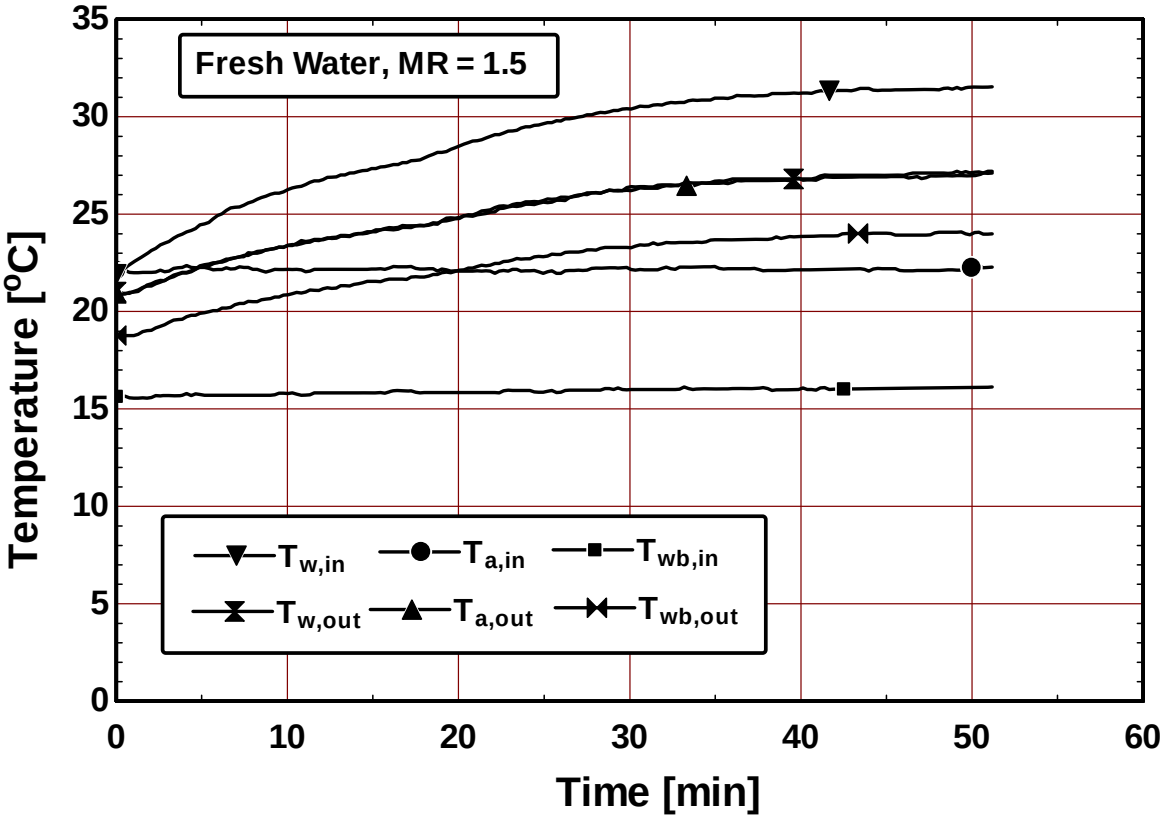

Figure B.2 Temperature variation versus time for fresh water at mass ratio of 1.5 for Cooling Tower

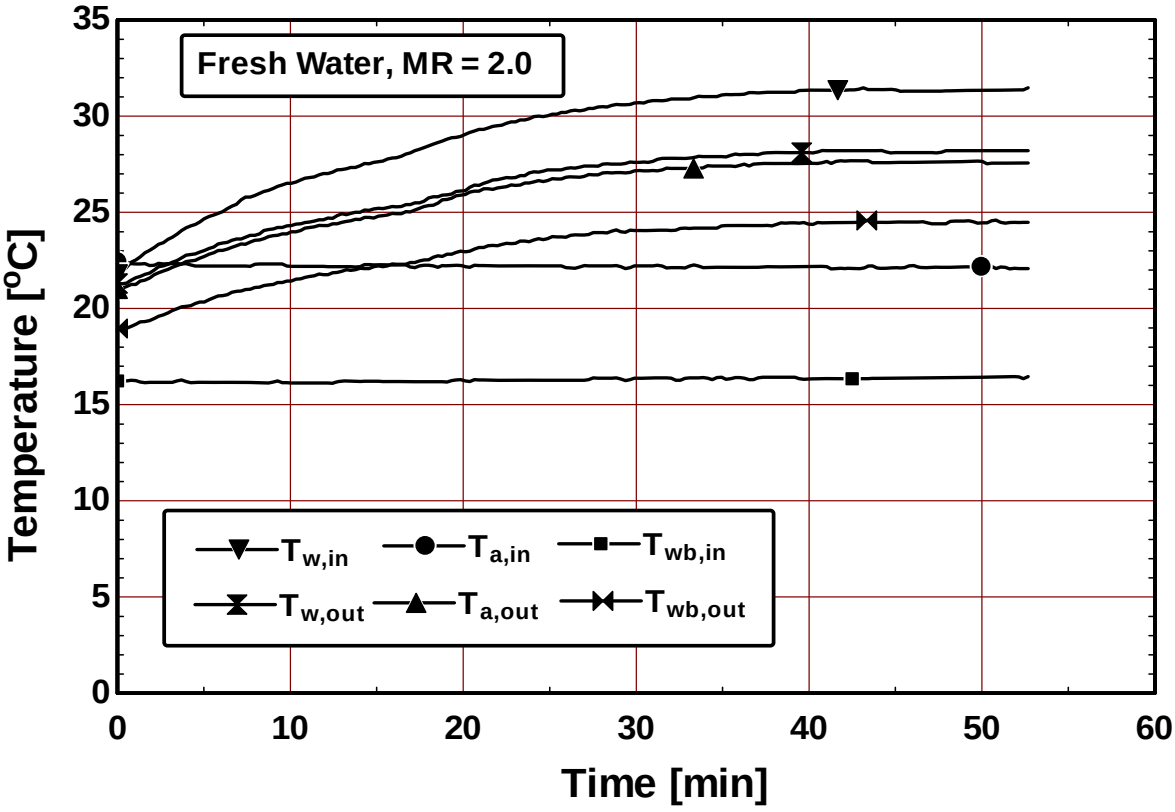

Figure B.3 Temperature variation versus time for fresh water at mass ratio of 2.0 for Cooling Tower

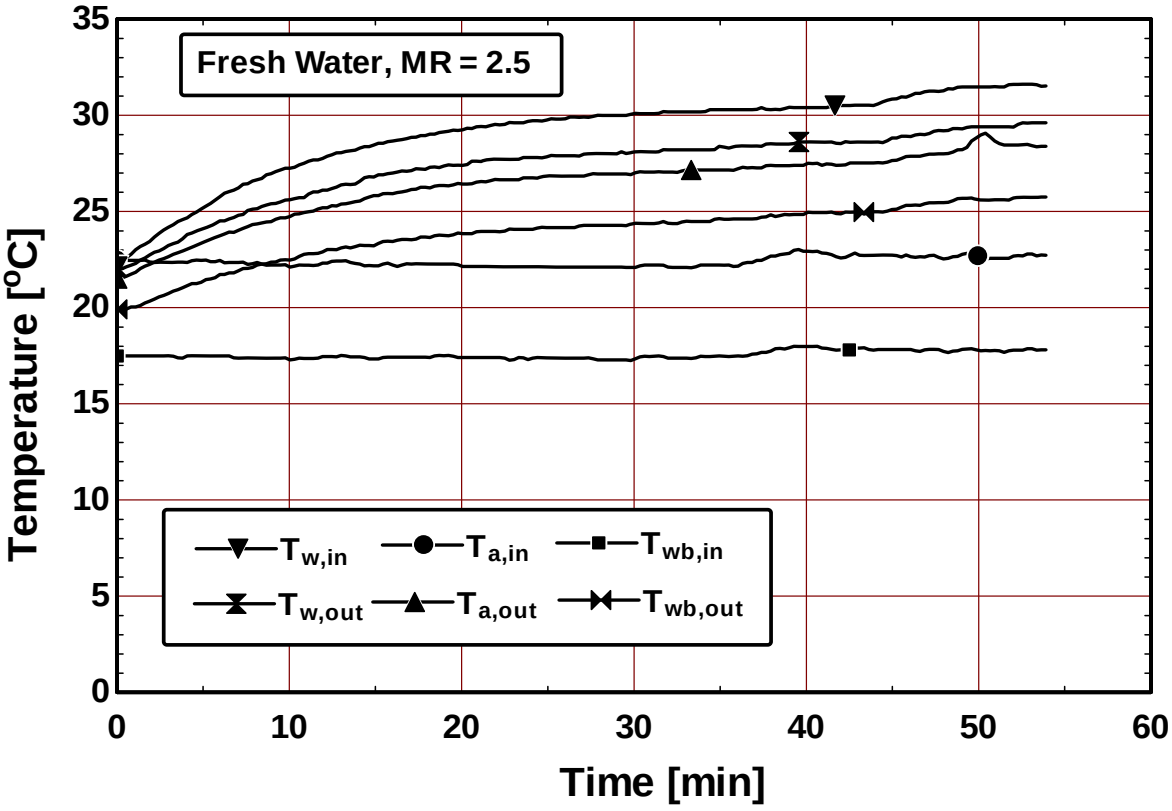

Figure B.4 Temperature variation versus time for fresh water at mass ratio of 2.5 for Cooling Tower

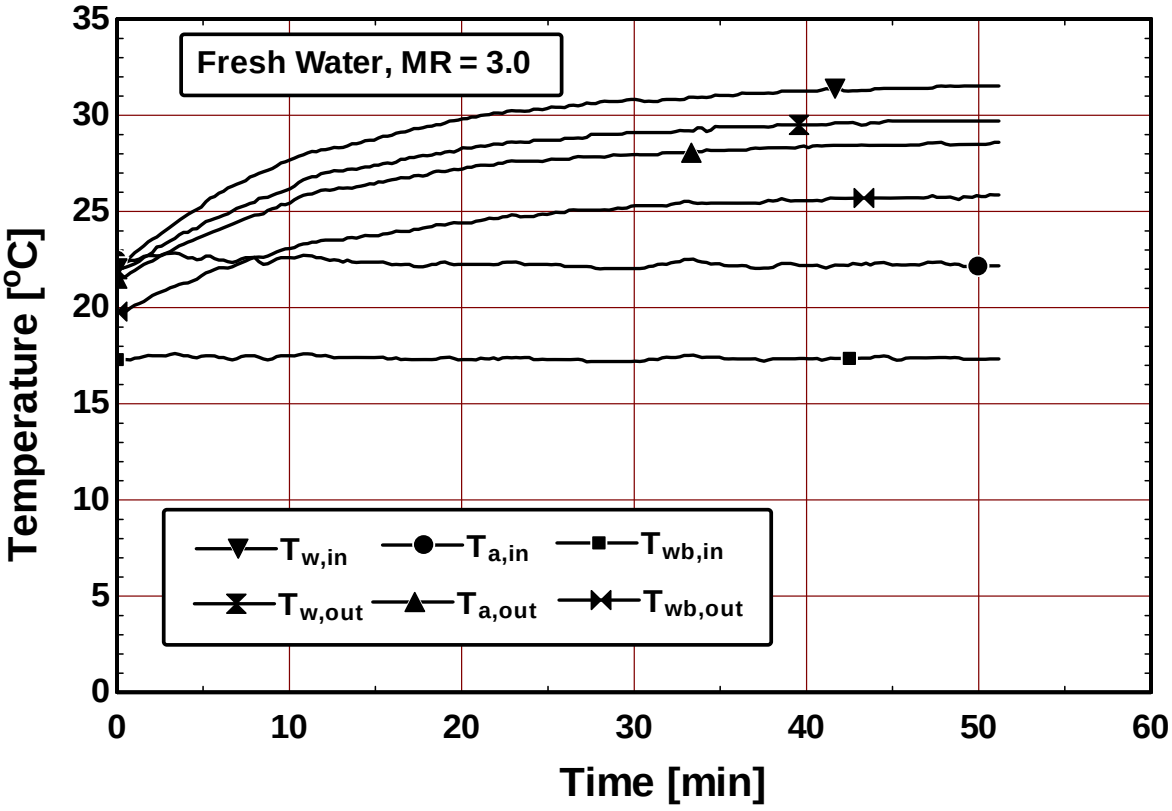

Figure B.5 Temperature variation versus time for fresh water at mass ratio of 3.0 for Cooling Tower

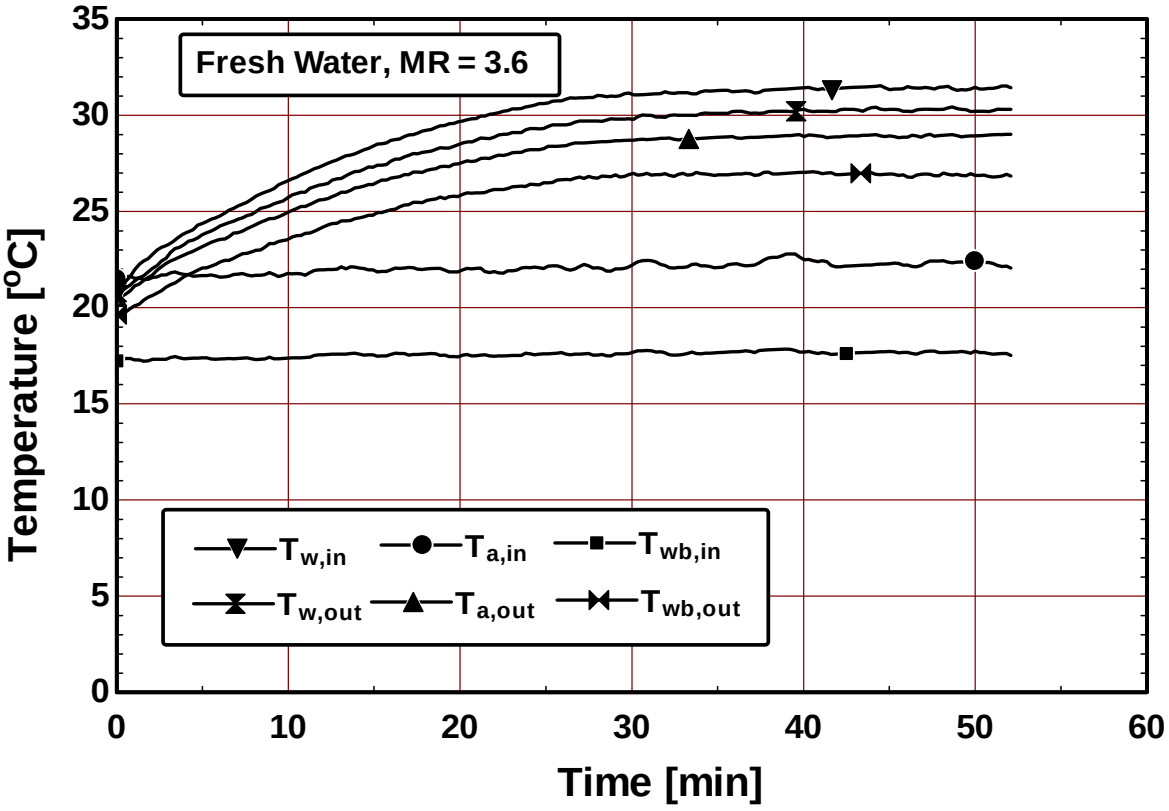

Figure B.6 Temperature variation versus time for fresh water at mass ratio of 3.6 for Cooling Tower

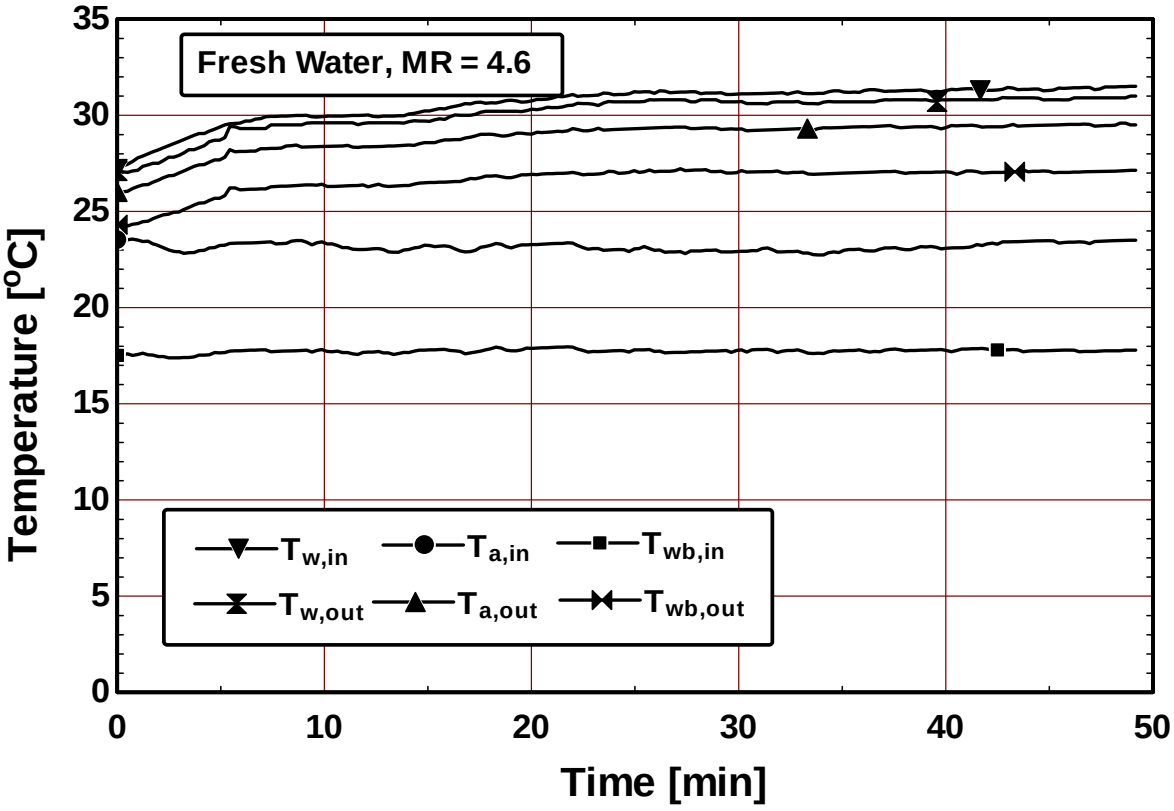

Figure B.7 Temperature variation versus time for fresh water at mass ratio of 4.6 for Cooling Tower

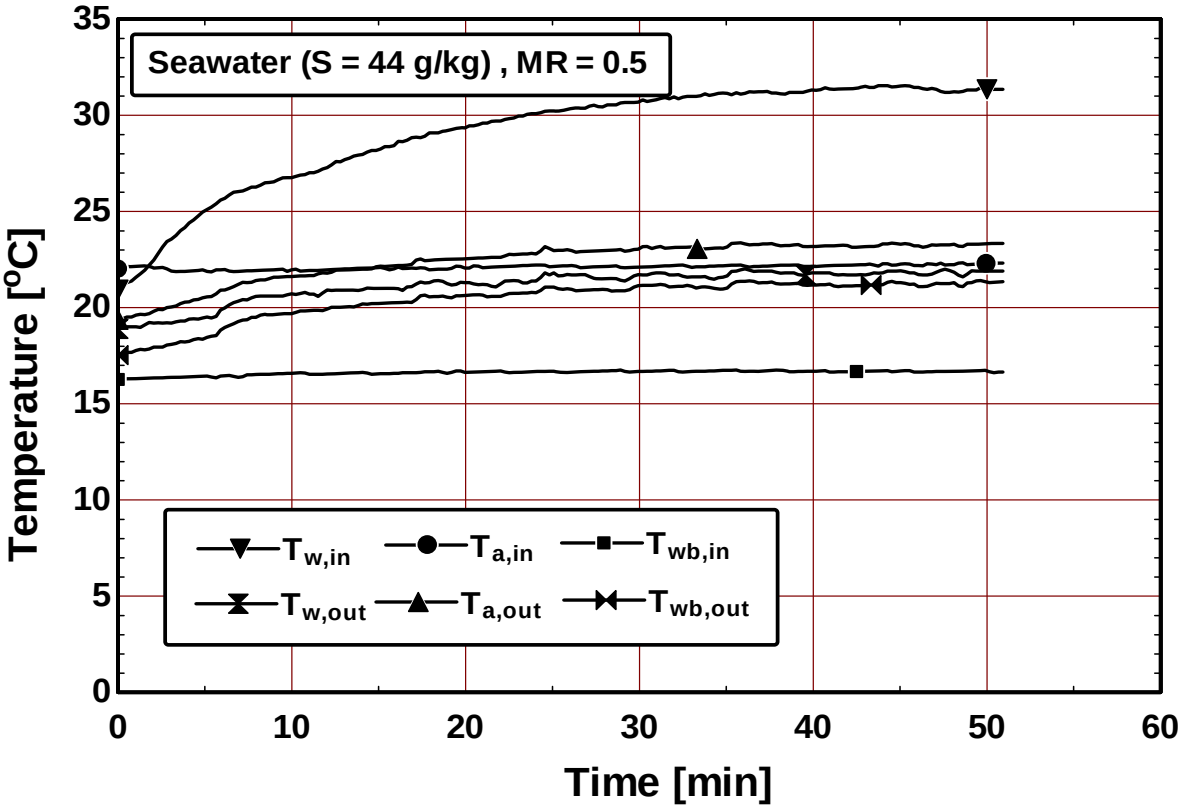

Figure B.8 Temperature variation versus time for seawater (salinity = 44 g/kg) at mass ratio of 0.5 for cooling tower

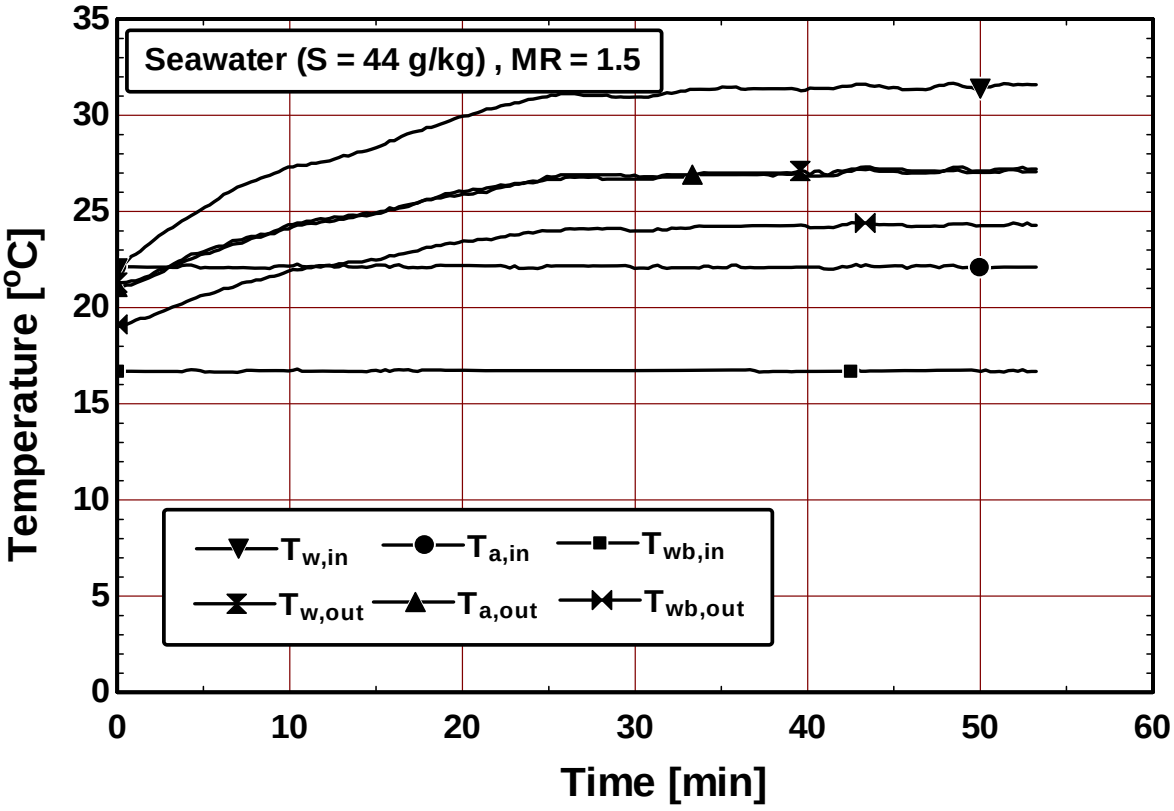

Figure B.9 Temperature variation versus time for seawater (salinity = 44 g/kg) at mass ratio of 1.5 for cooling tower

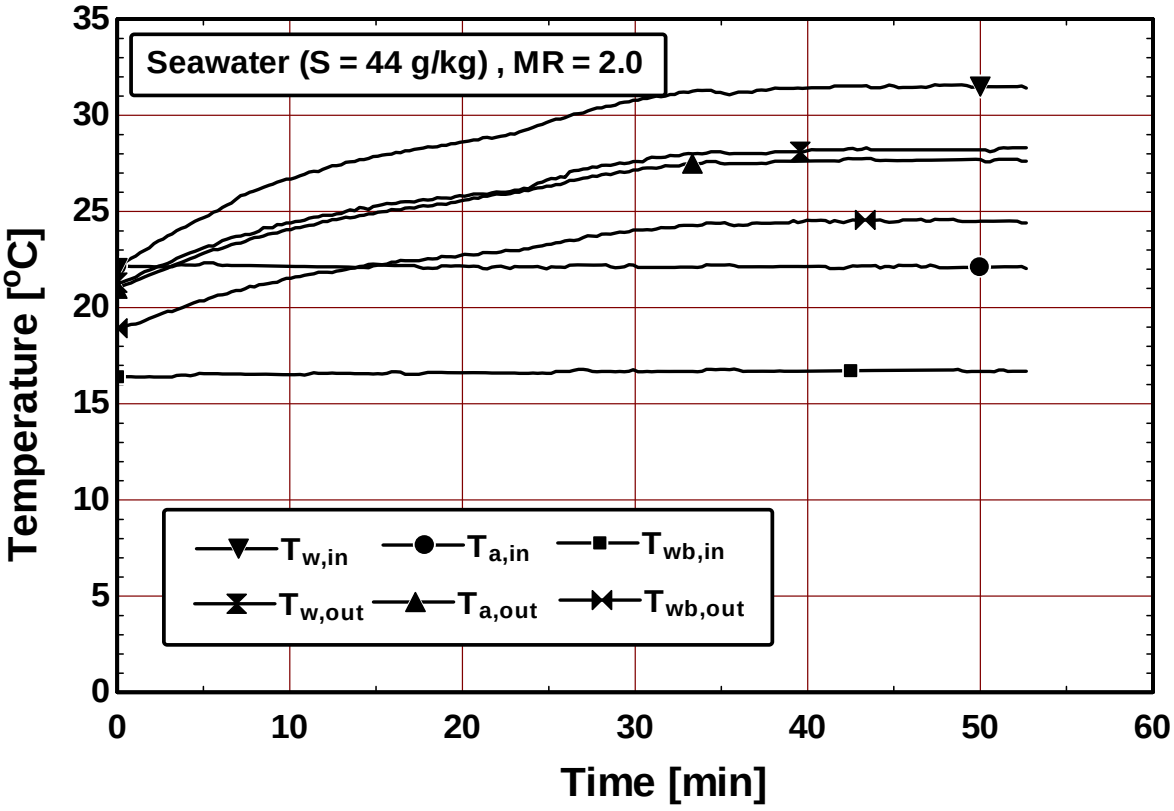

Figure B.10 Temperature variation versus time for seawater (salinity = 44 g/kg) at mass ratio of 2.0 for cooling tower

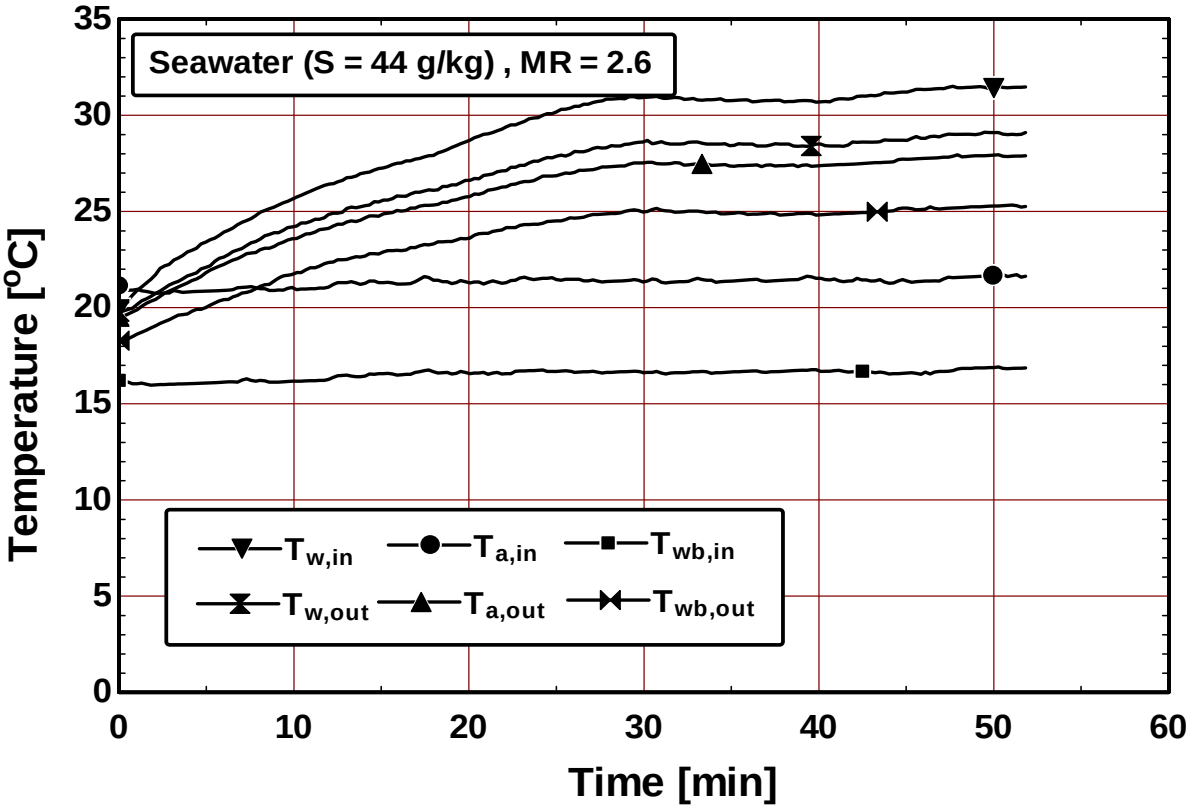

Figure B.11 Temperature variation versus time for seawater (salinity = 44 g/kg) at mass ratio of 2.6 for cooling tower

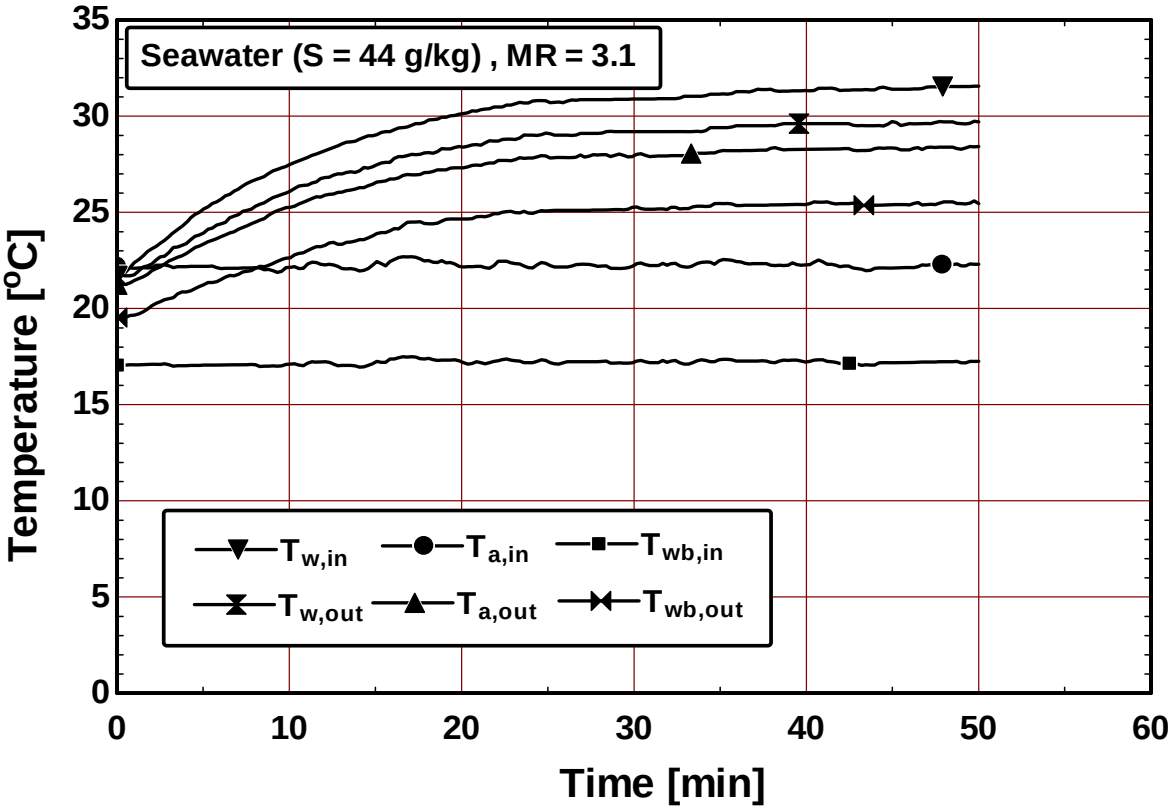

Figure B.12 Temperature variation versus time for seawater (salinity = 44 g/kg) at mass ratio of 3.1 for cooling tower

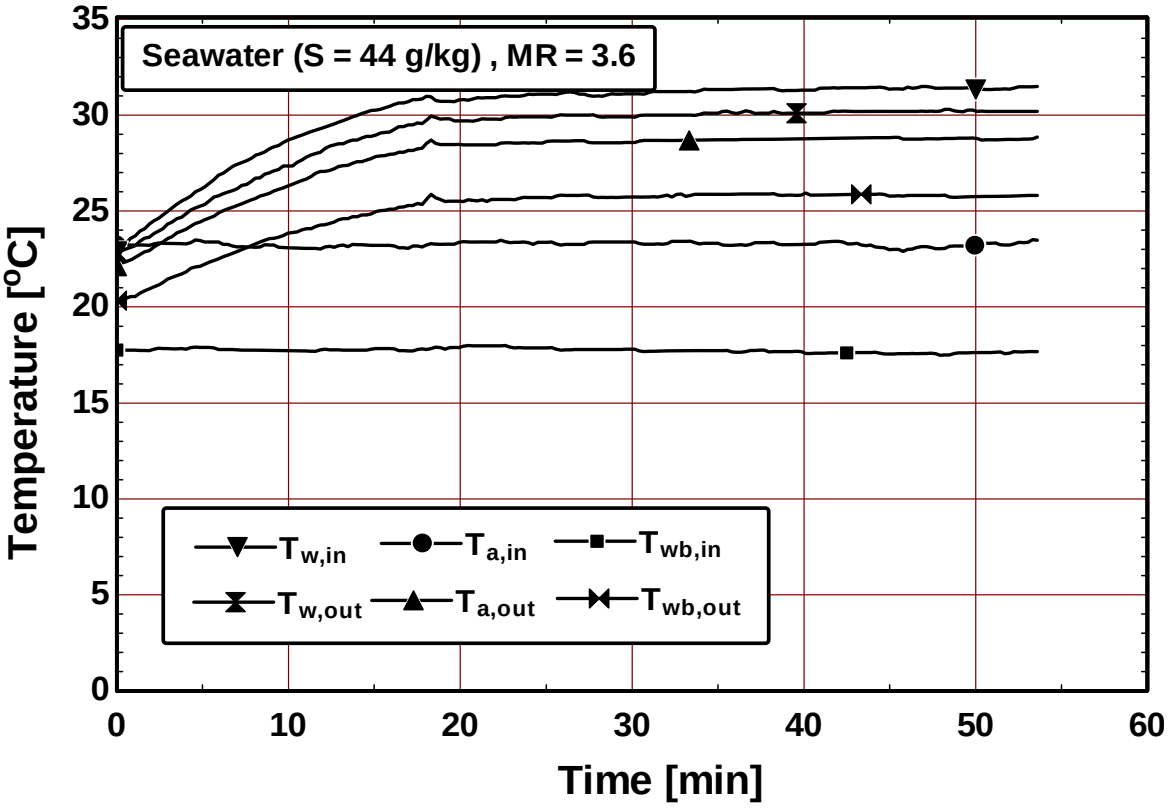

Figure B.13 Temperature variation versus time for seawater (salinity = 44 g/kg) at mass ratio of 3.6 for cooling tower

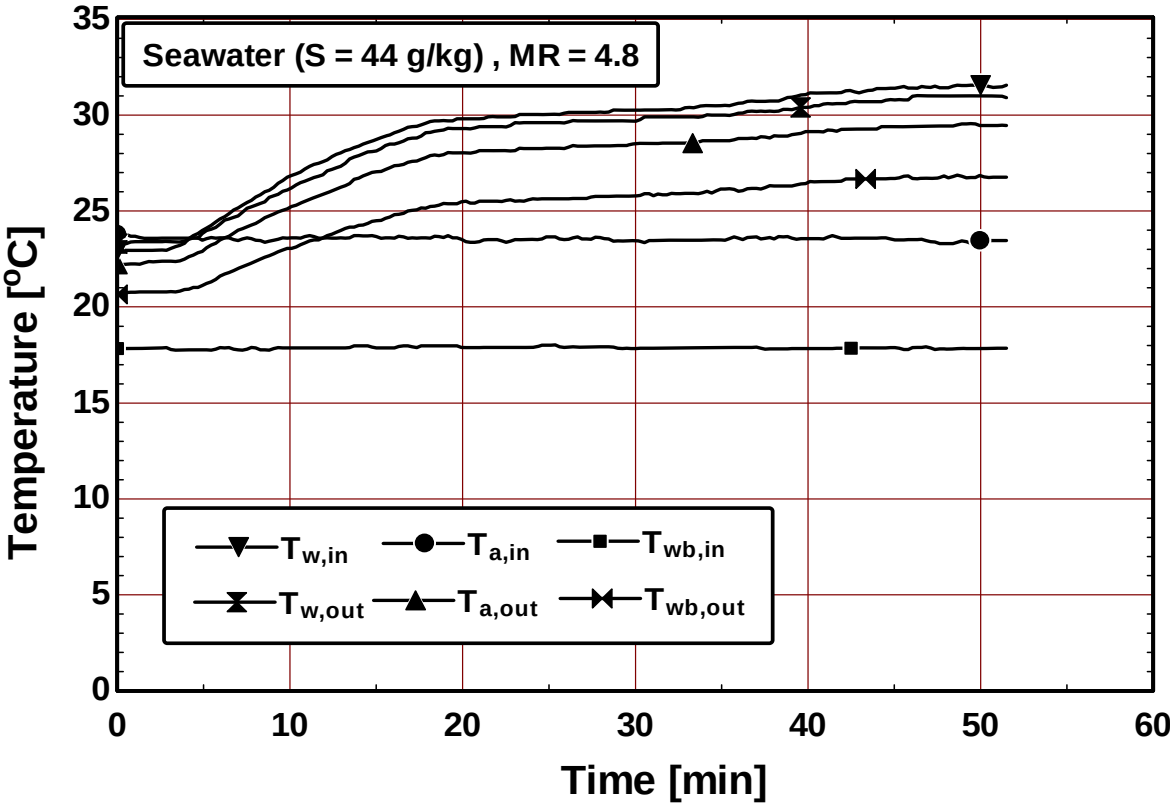

Figure B.14 Temperature variation versus time for seawater (salinity = 44 g/kg) at mass ratio of 4.8 for cooling tower

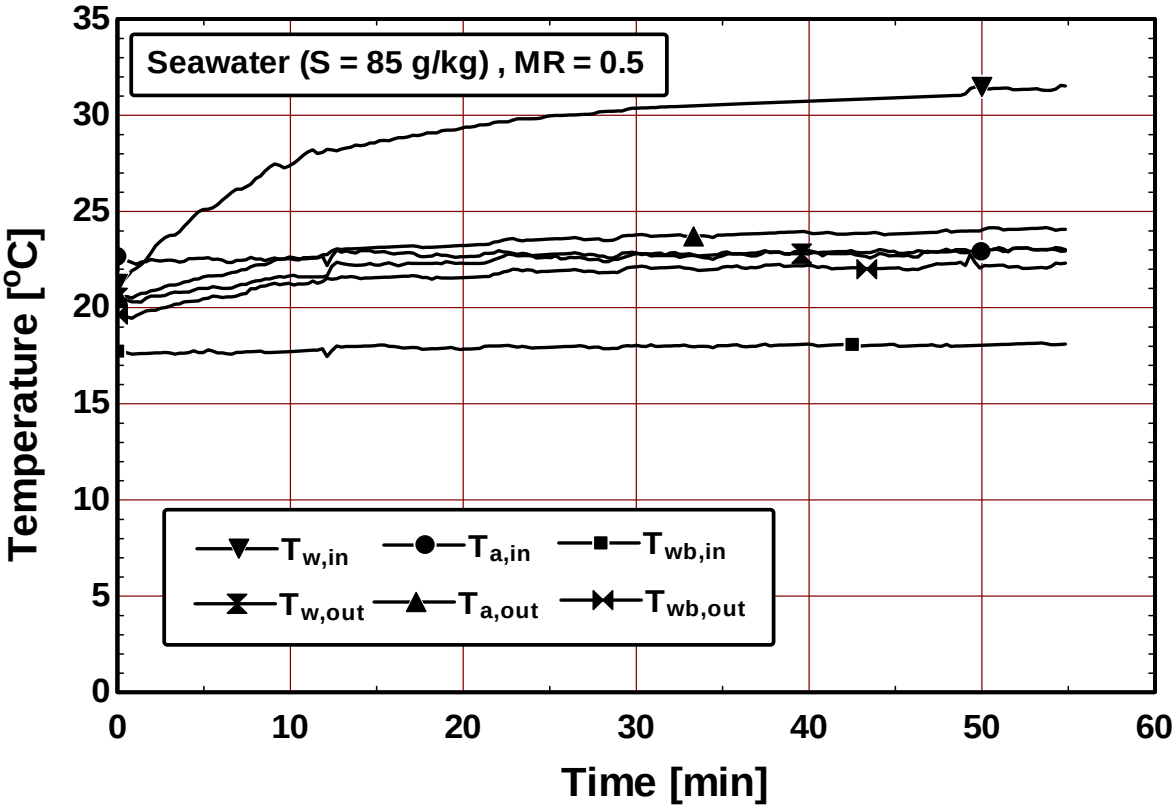

Figure B.15 Temperature variation versus time for seawater (salinity = 85 g/kg) at mass ratio of 0.5 for cooling tower

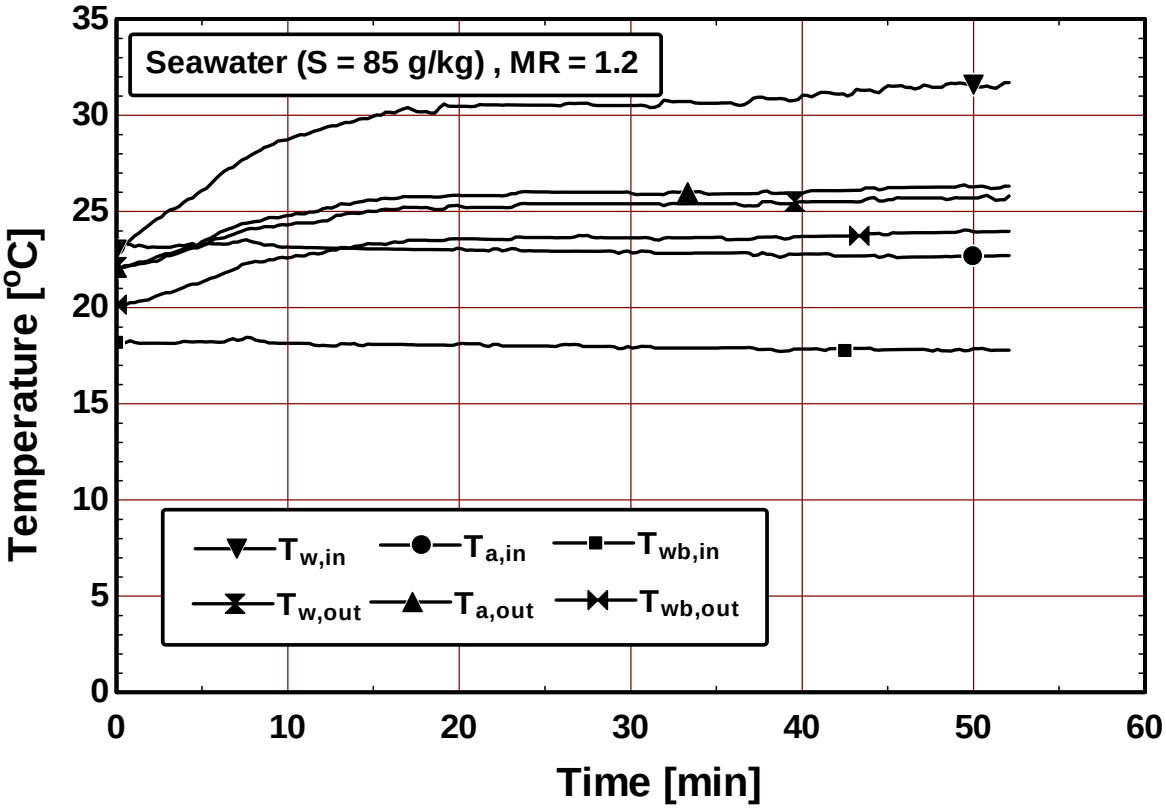

Figure B.16 Temperature variation versus time for seawater (salinity = 85 g/kg) at mass ratio of 1.2 for cooling tower

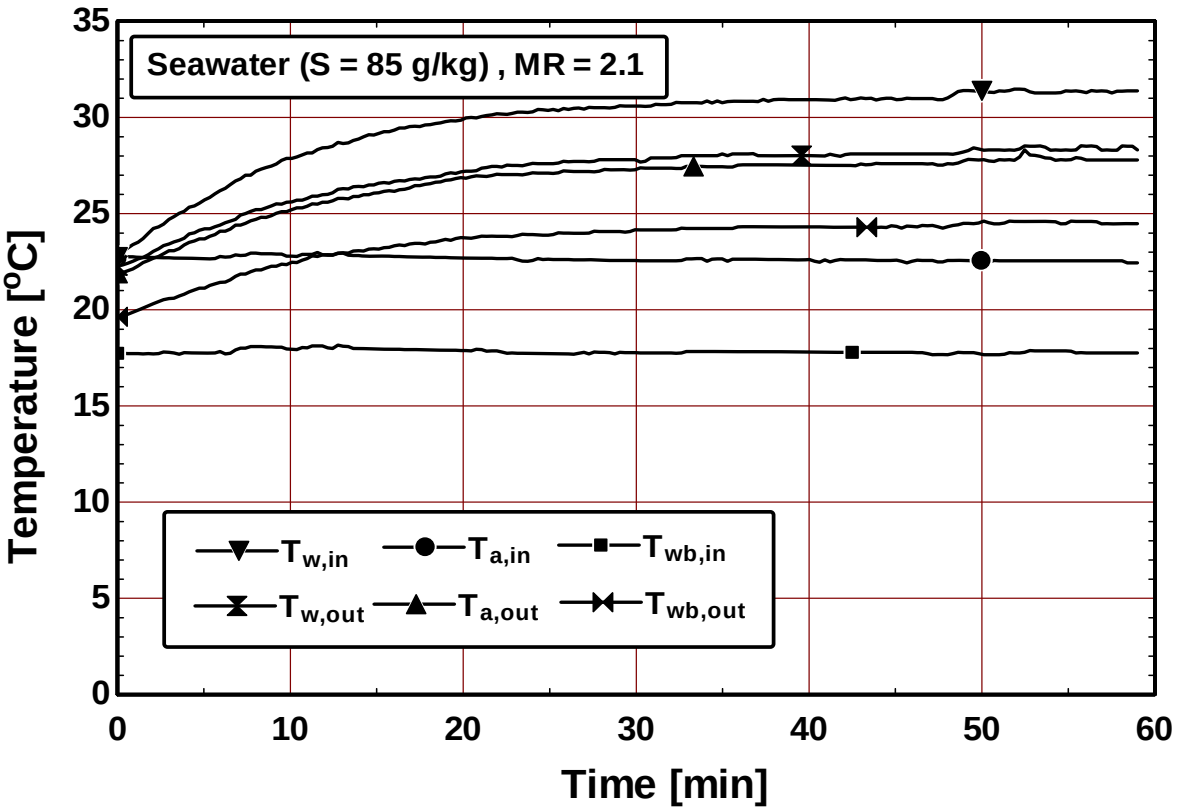

Figure B.17 Temperature variation versus time for seawater (salinity = 85 g/kg) at mass ratio of 2.1 for cooling tower

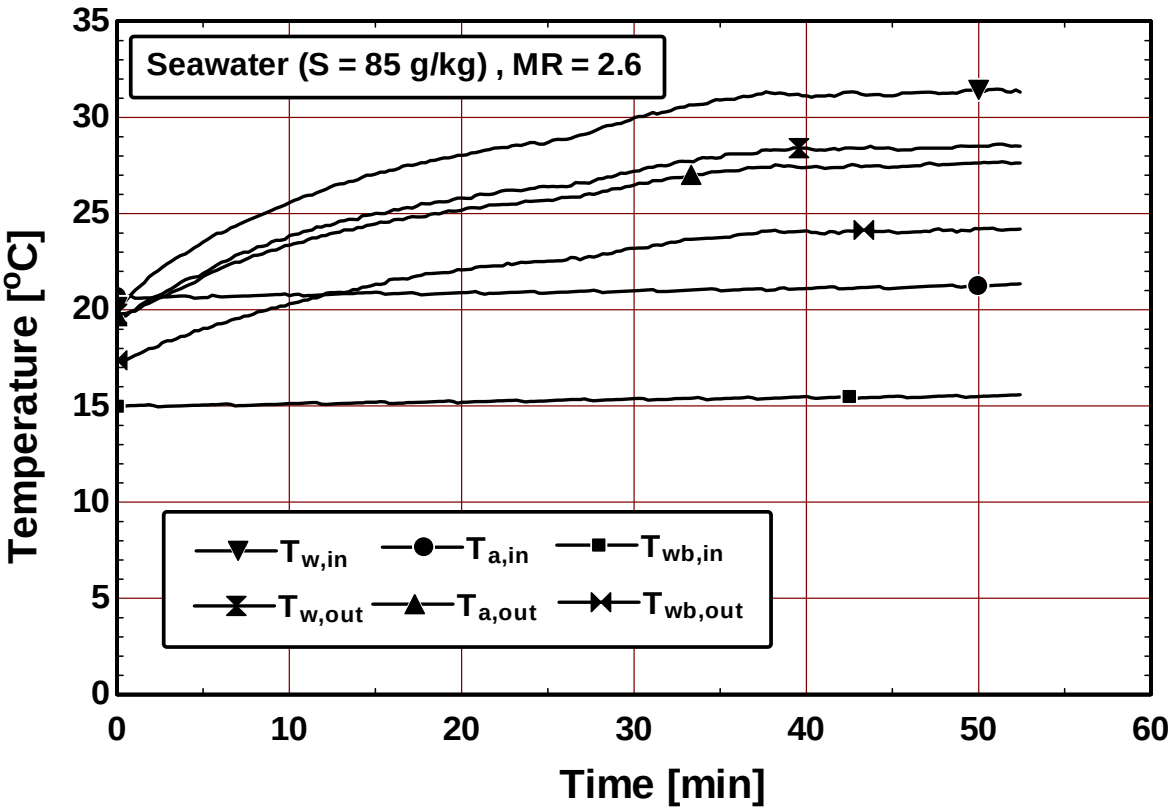

Figure B.18 Temperature variation versus time for seawater (salinity = 85 g/kg) at mass ratio of 2.6 for cooling tower

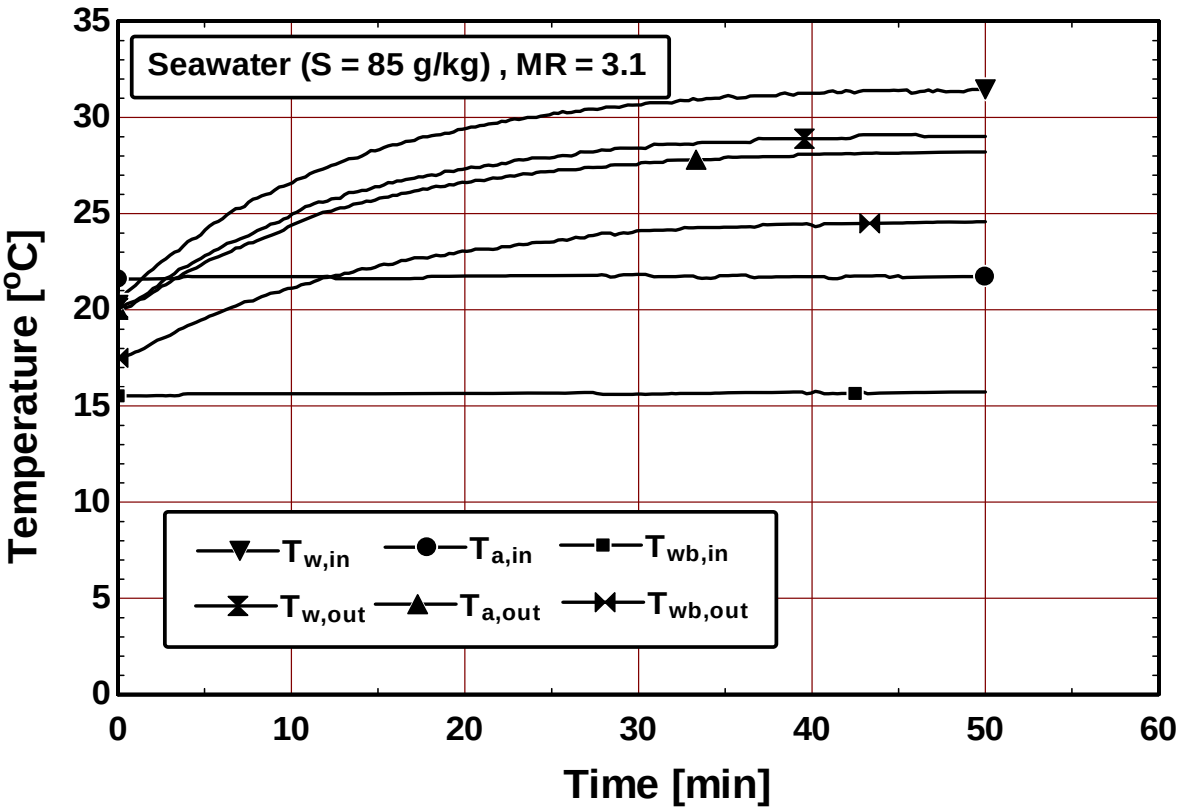

Figure B.19 Temperature variation versus time for Seawater (Salinity = 85 g/kg) at mass ratio of 3.1 for Cooling Tower

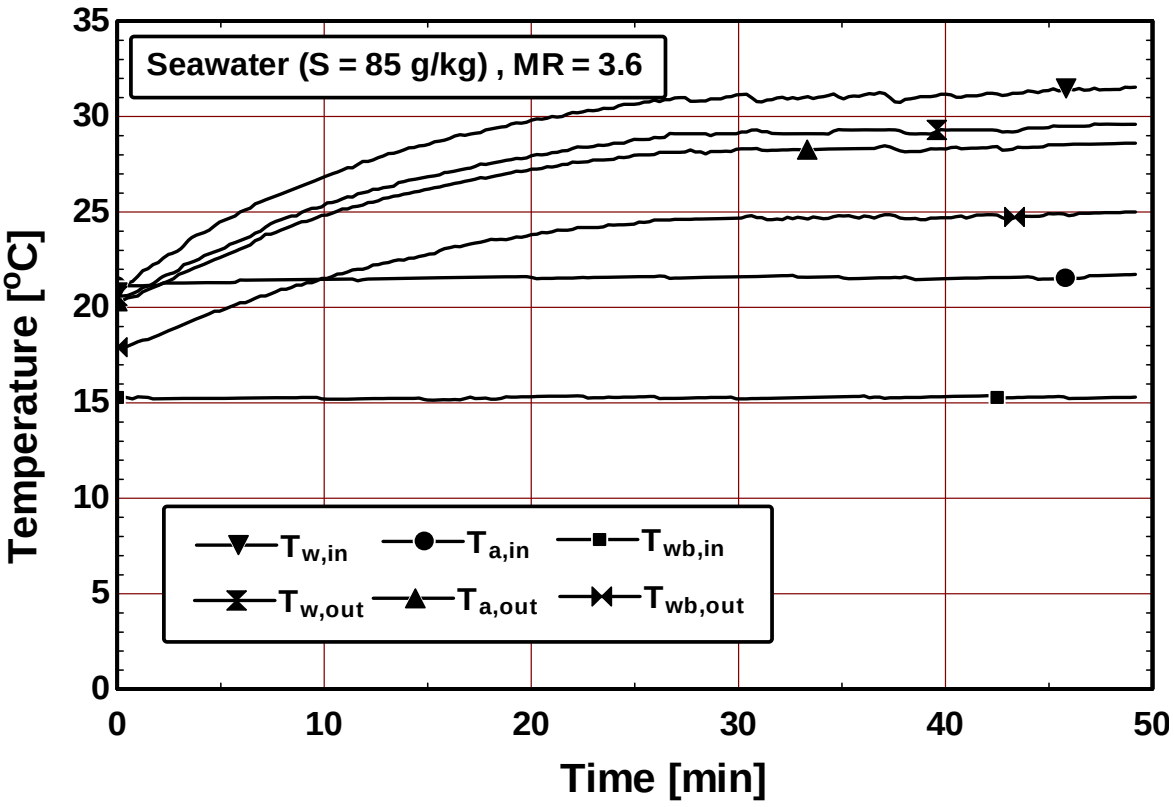

Figure B.20 Temperature variation versus time for seawater (salinity = 85 g/kg) at mass ratio of 3.6 for cooling tower

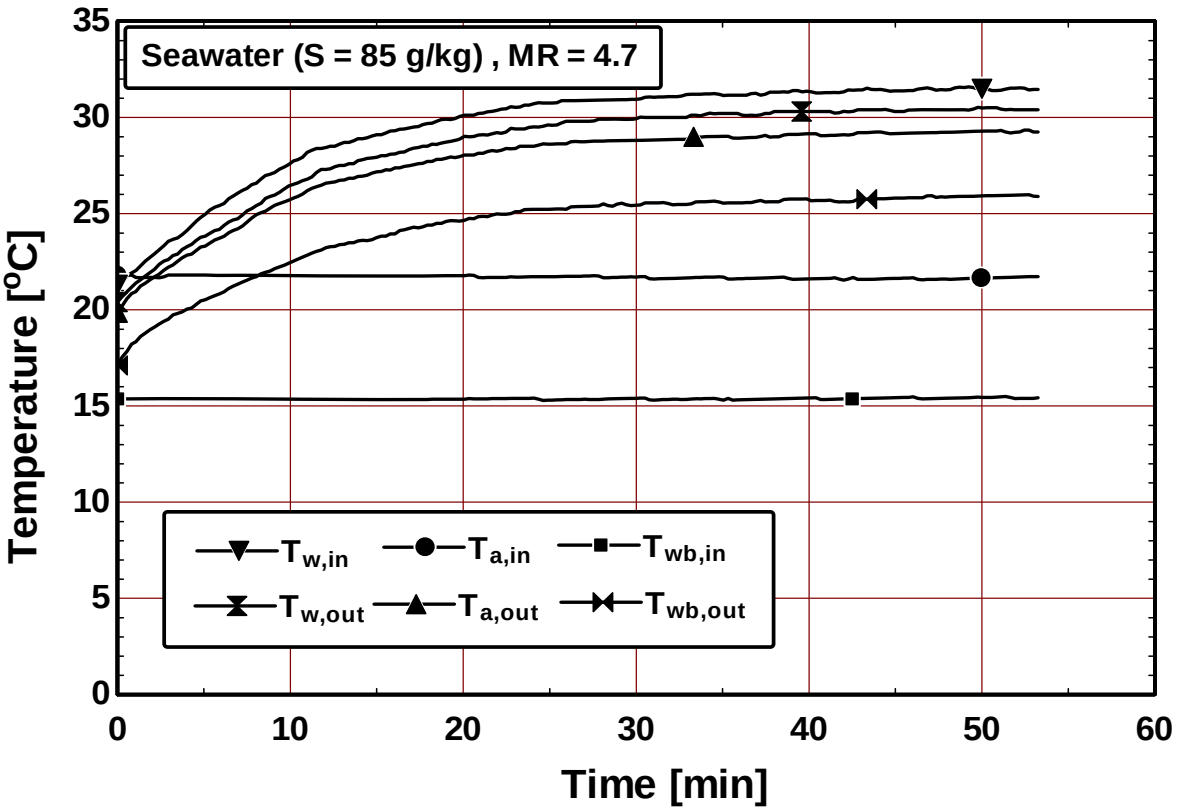

Figure B.21 Temperature variation versus time for seawater (salinity = 85 g/kg) at mass ratio of 4.7 for cooling tower

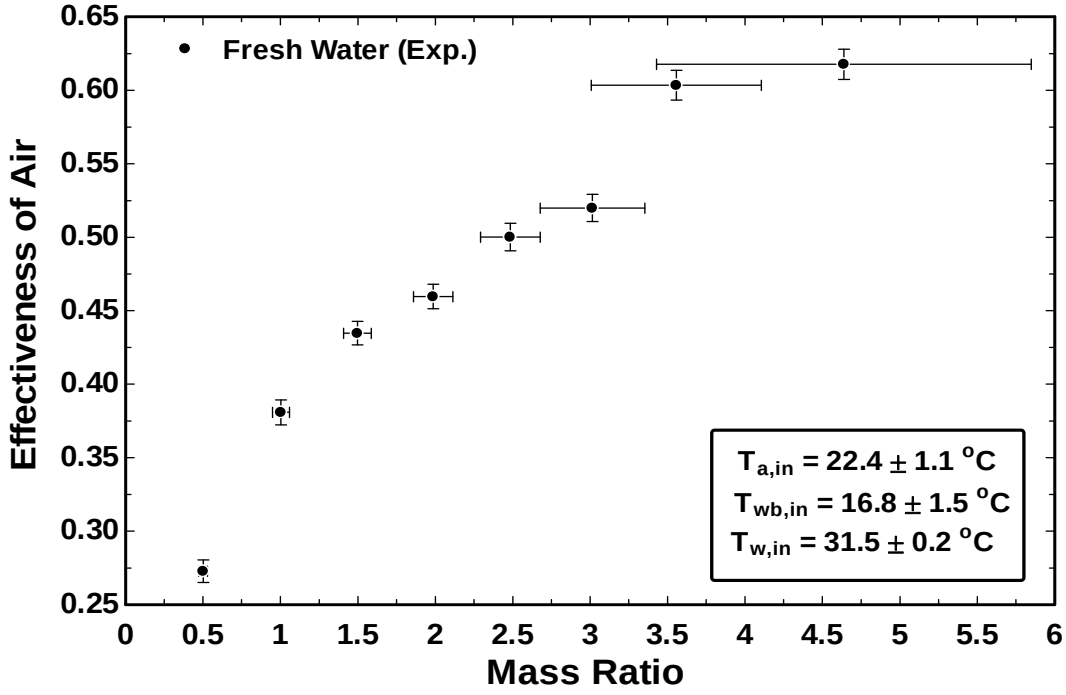

Figure B.22 Uncertainty of effectiveness of air versus mass ratio for fresh water cooling tower

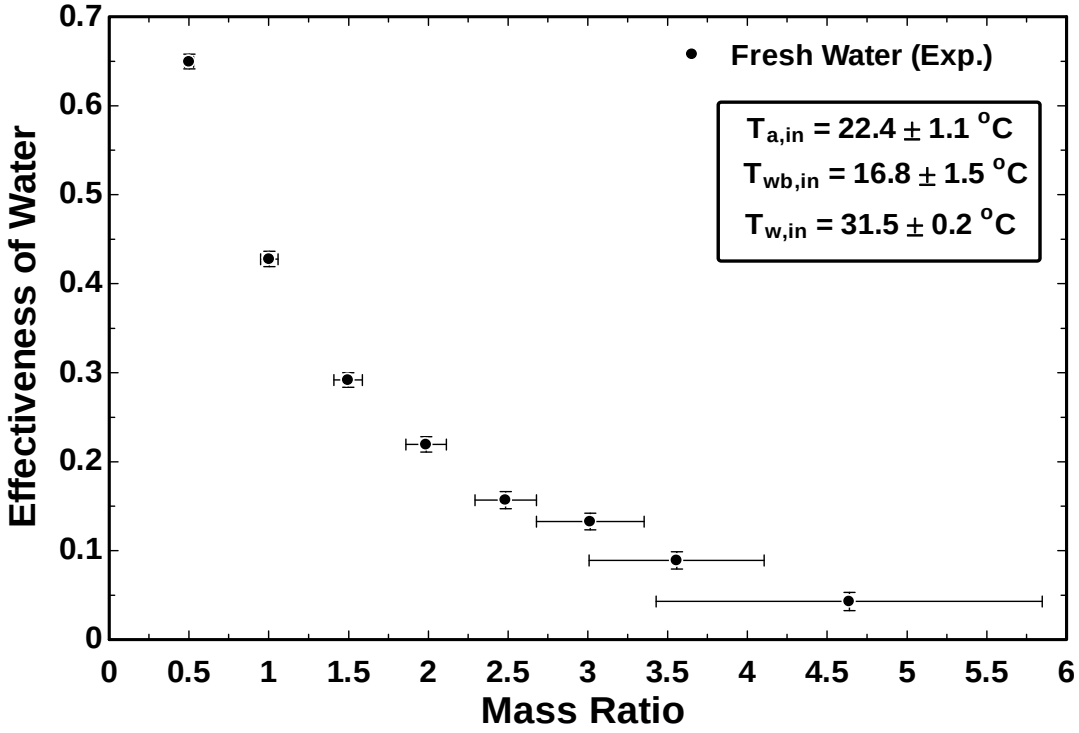

Figure B.23 Uncertainty of effectiveness of water versus mass ratio for fresh water cooling tower

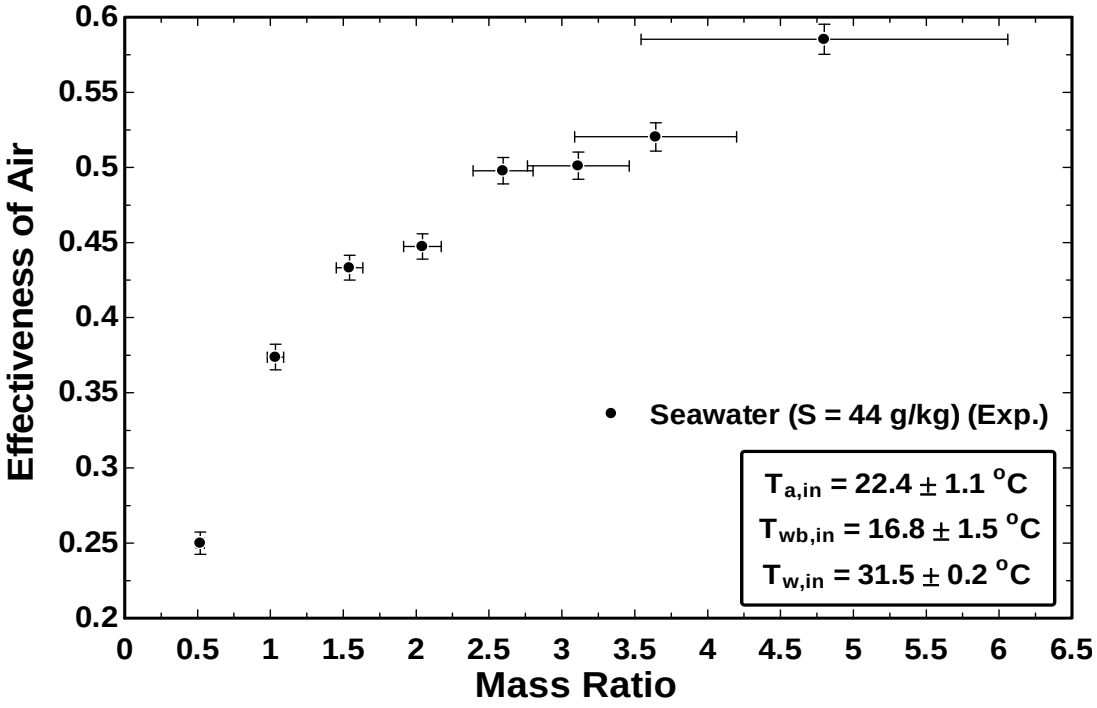

Figure B.24 Uncertainty of effectiveness of air versus mass ratio for seawater (salinity = 44 g/kg) cooling tower

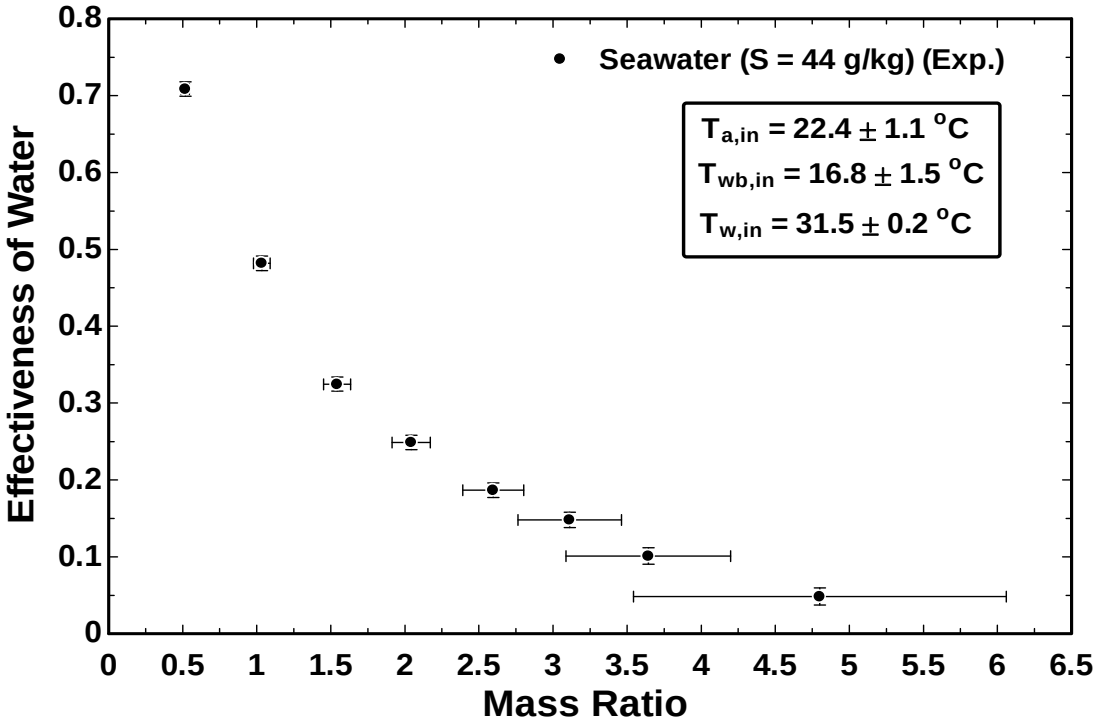

Figure B.25 Uncertainty of effectiveness of water versus mass ratio for seawater (salinity = 44 g/kg) cooling tower

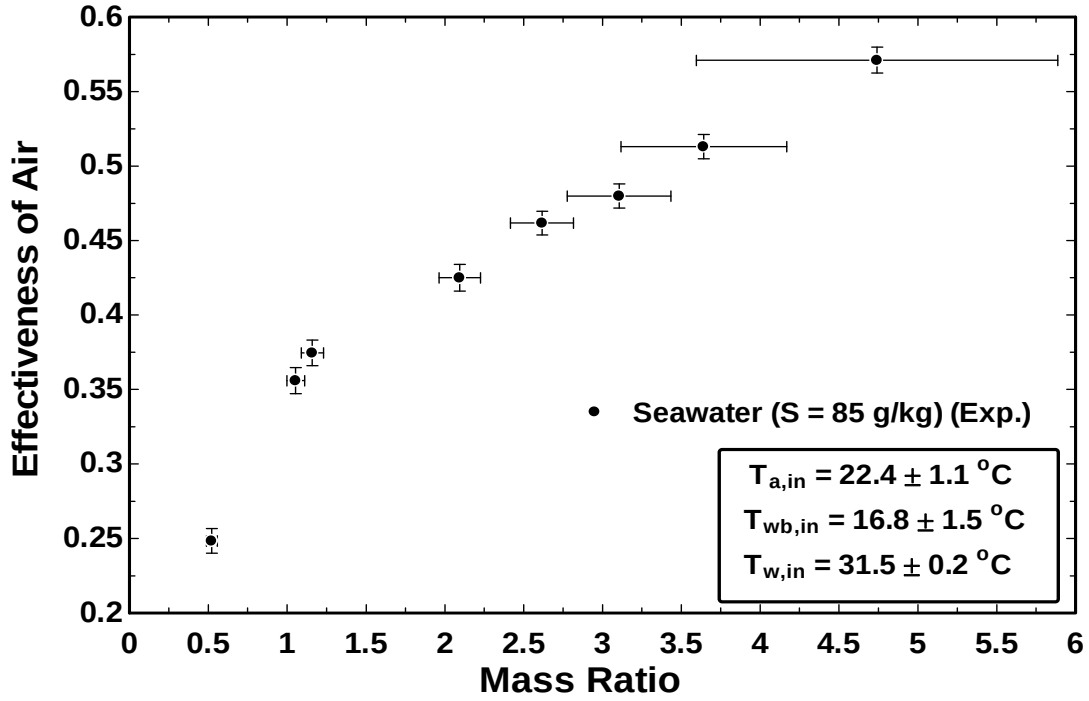

Figure B.26 Uncertainty of effectiveness of air versus mass ratio for seawater (salinity = 85 g/kg) cooling tower

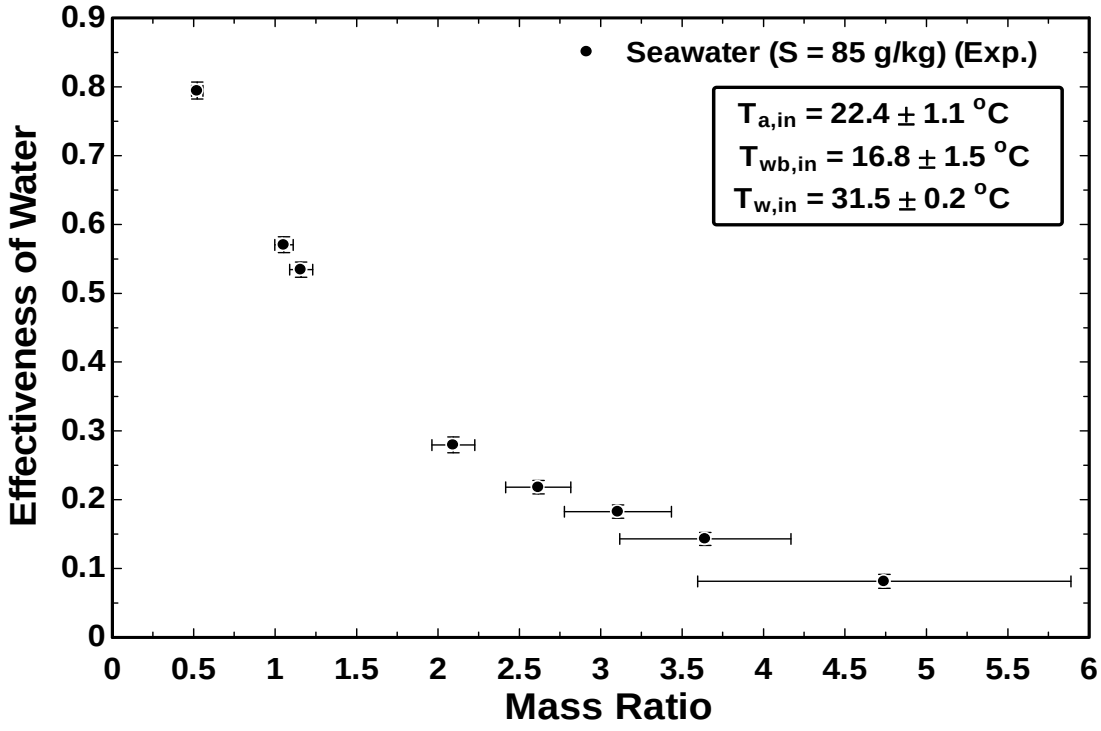

Figure B.27 Uncertainty of effectiveness of water versus mass ratio for seawater (salinity = 85 g/kg) cooling tower

APPENDIX C: SHOWER COOLING TOWER

Table C.1 Experimental data for fresh water and seawater for shower cooling tower

Run	Mass Ratio	ma (kg/s)	mw_{in} (kg/s)	$Salinity_{in}$ (g/kg)	Ta_{in} (^oC)	Twb_{in} (^oC)	Tw_{in} (^oC)	Ta_o (^oC)	Twb_o (^oC)	Tw_o (^oC)
(1)	**0.5**	0.077	0.041	0.0	21.8	15.0	31.4	22.2	17.9	27.9
(2)	**0.5**	0.075	0.041	44.0	22.0	15.5	31.3	22.6	18.2	26.5
(3)	**1.0**	0.050	0.050	0.0	22.2	15.4	31.4	22.9	18.8	29.4
(4)	**1.0**	0.050	0.051	44.0	22.0	15.7	31.4	23.1	18.9	29.1
(5)	**1.5**	0.039	0.058	0.0	21.8	15.3	31.4	23.4	19.2	30.1
(6)	**1.5**	0.039	0.060	44.0	22.2	15.7	31.4	23.9	19.9	29.9
(7)	**2.0**	0.033	0.066	0.0	21.3	15.7	31.5	24.3	20.1	30.9
(8)	**2.0**	0.032	0.065	44.0	21.6	15.5	31.4	24.2	20.5	30.2

Table C.2 Calculated results of the experimental data for fresh water and seawater for shower cooling tower

Run	ha_{in} (kJ/kg)	ha_o (kJ/kg)	hw_i (kJ/kg)	hw_o (kJ/kg)	$Energyl_{oss}$ (kW)	$Energyl_{oss}$ (%)	ε_{air}	ε_{water}	Xa_{in} (kW)	Xa_o (kW)	Xw_{in} (kW)	Xw_o (kW)	$Exergy_{loss}$ (kW)
(1)	41.9	50.3	131.5	117.0	-0.019	-0.35	0.1296	0.2204	0.00	0.01	4.27	4.23	0.035
(2)	43.2	51.3	123.3	104.2	0.201	3.95	0.1275	0.3353	0.00	0.00	3.85	3.81	0.033
(3)	42.9	53.2	131.5	123.3	-0.086	-1.32	0.1607	0.1279	0.00	0.01	5.06	5.03	0.025
(4)	43.8	53.6	123.5	114.8	-0.017	-0.26	0.1552	0.1579	0.00	0.00	4.67	4.64	0.023
(5)	42.6	54.6	131.7	126.4	-0.134	-1.76	0.1856	0.0838	0.00	0.00	5.68	5.66	0.019
(6)	43.8	57.1	123.8	117.5	-0.123	-1.65	0.2091	0.1138	0.00	0.01	5.56	5.53	0.020
(7)	43.8	57.7	132.0	129.3	-0.262	-2.99	0.2176	0.0441	0.00	0.00	5.46	5.44	0.011
(8)	43.3	59.0	123.8	118.9	-0.171	-2.12	0.2451	0.0877	0.00	0.01	5.67	5.64	0.017

The temperature variation versus time plots of the all the Experimental Data (Table C.1) of Fresh water and Seawater for Shower Cooling Tower at different mass ratios

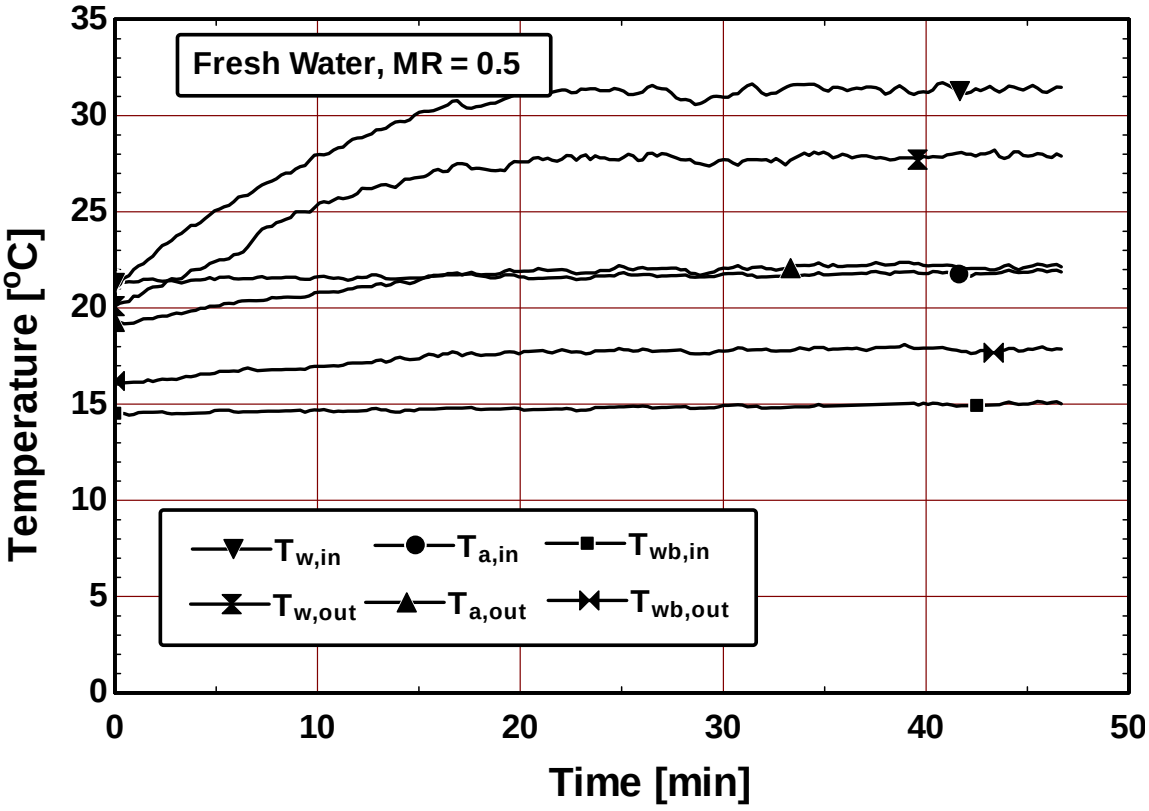

Figure C.1 Temperature variation versus time for fresh water at mass ratio of 0.5 for shower cooling tower

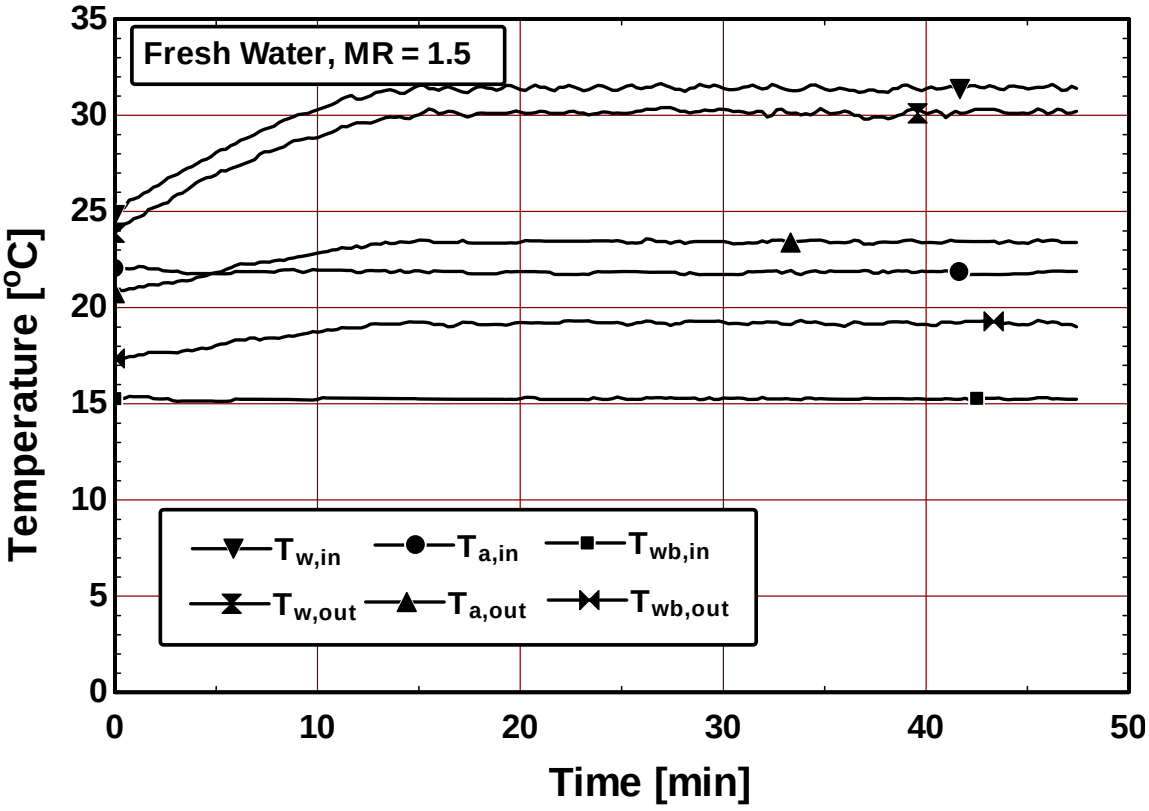

Figure C.2 Temperature variation versus time for fresh water at mass ratio of 1.5 for shower cooling tower

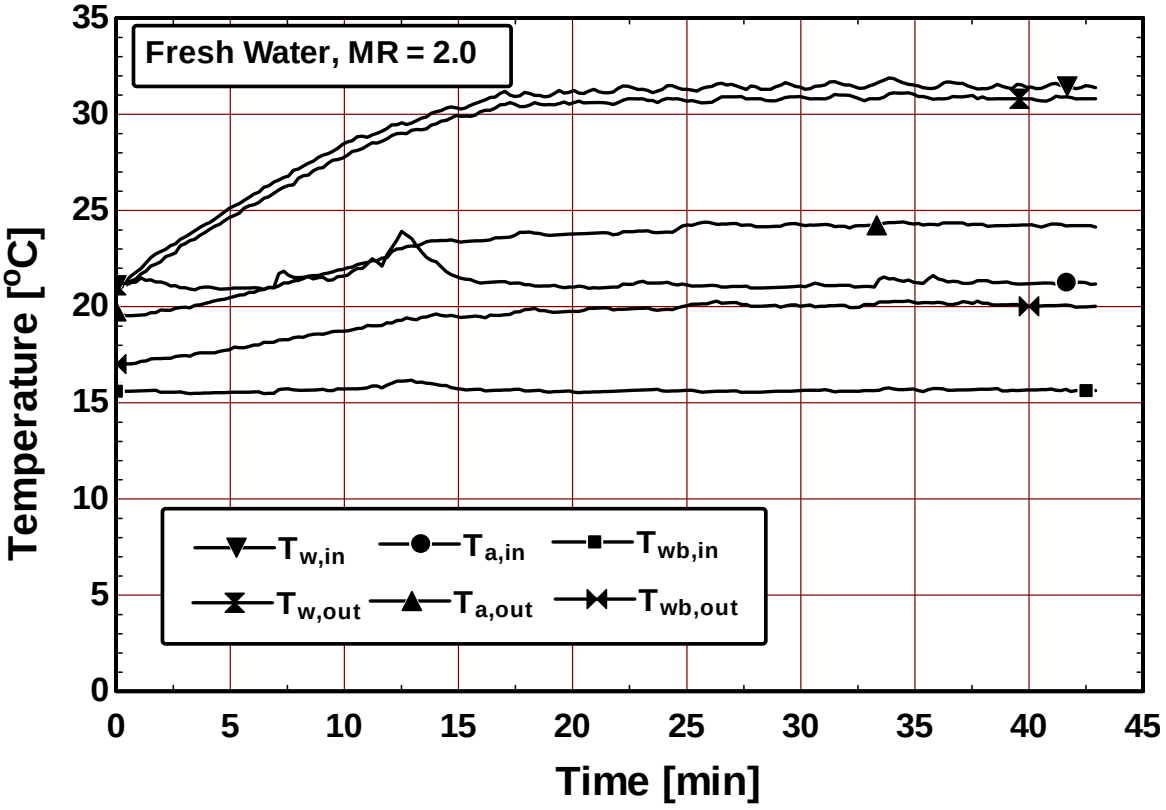

Figure C.3 Temperature variation versus time for fresh water at mass ratio of 2.0 for shower cooling tower

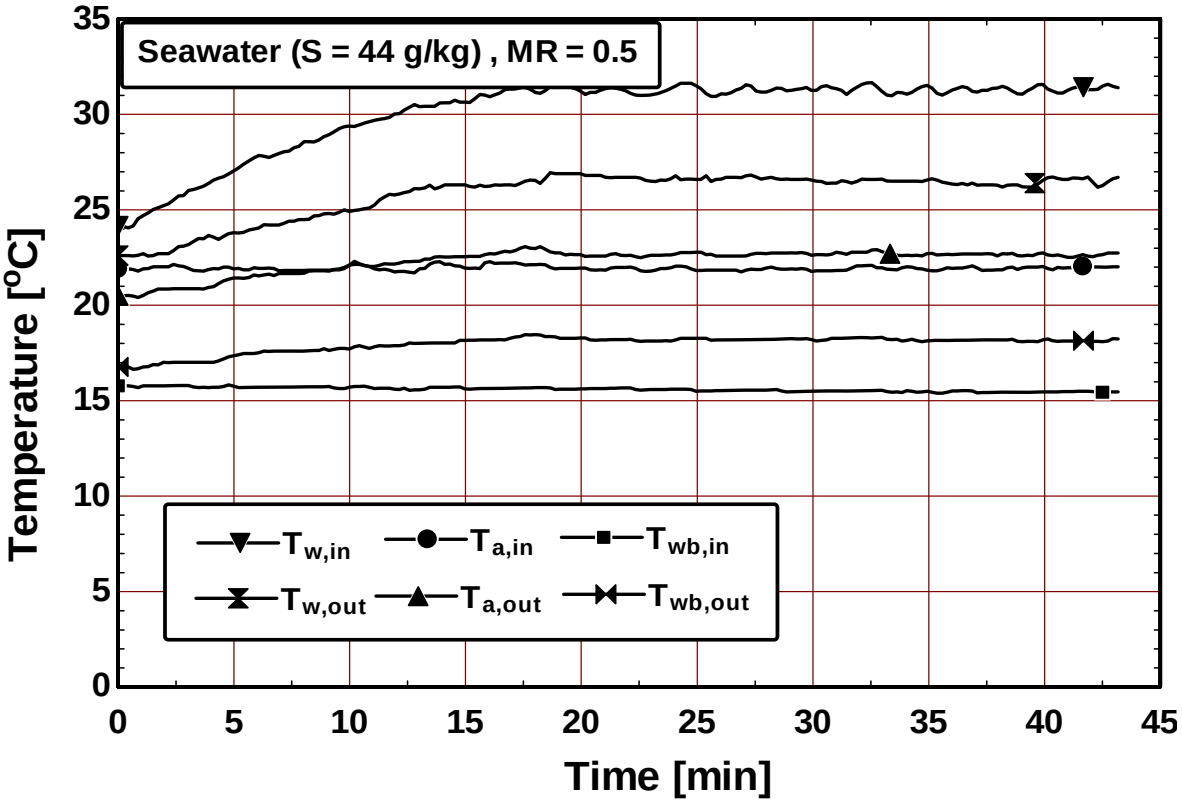

Figure C.4 Temperature variation versus time for seawater (Salinity = 44 g/kg) at mass ratio of 0.5 for shower cooling tower

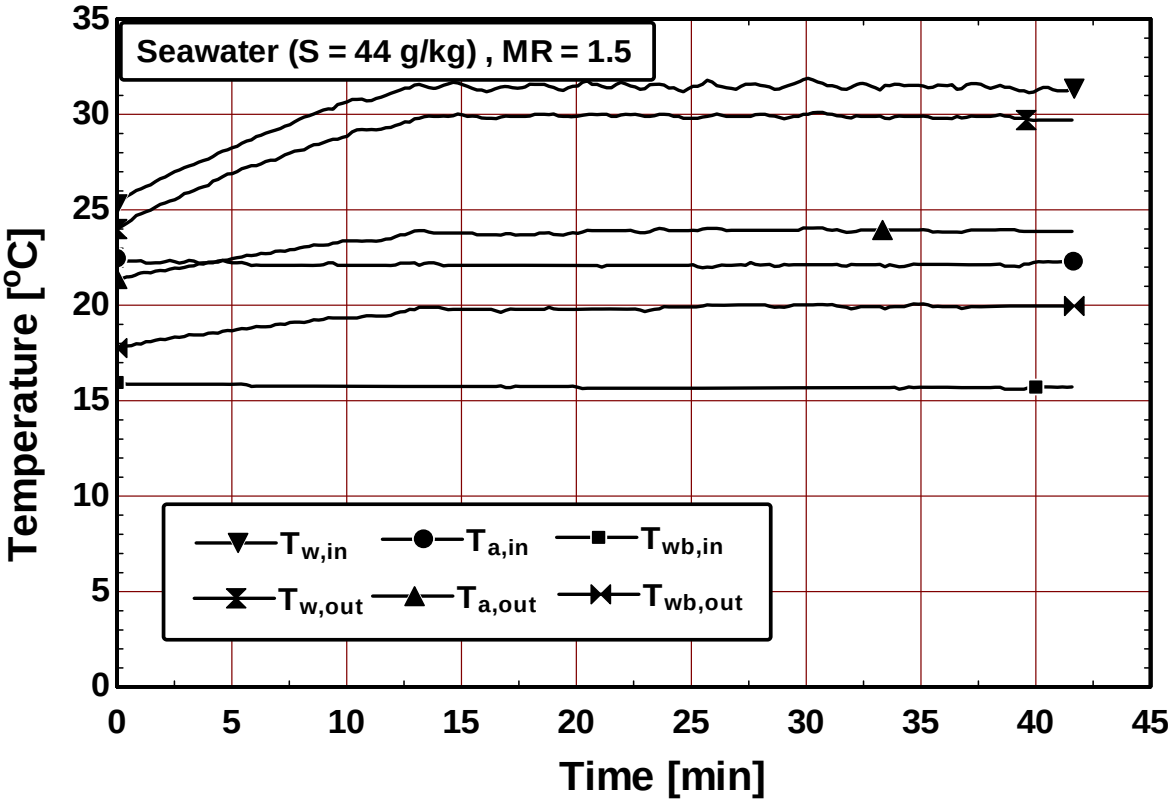

Figure C.5 Temperature variation versus time for seawater (salinity = 44 g/kg) at mass ratio of 1.5 for shower cooling tower

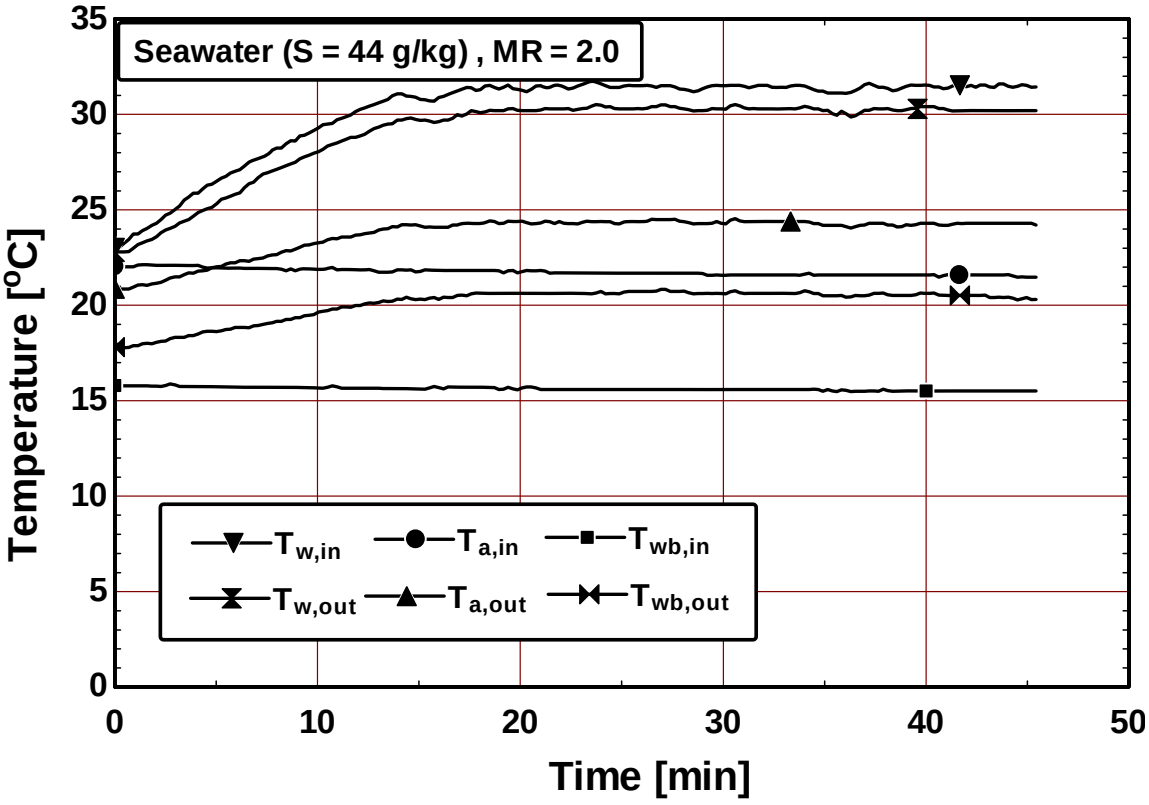

Figure C.6 Temperature variation versus time for seawater (salinity = 44 g/kg) at mass ratio of 2.0 for shower cooling tower

APPENDIX D: SEAWATER SOURCE AND SALINITY MEASUREMENT

The seawater used in the experiment of cooling tower and shower cooling tower is collected from the Arabian Gulf (26^o 16' N and 50^o 13' E) in Al-Khobar in Kingdom of Saudi Arabia. The salinity of seawater is measured by the SALINITY REFRACTOMETER S/Mill-E of ATAGO product. The value of salinity measured was 44 g/kg. The higher salinity value 85 g/kg of seawater is obtained by evaporating the seawater of salinity 44 g/kg. The seawater was evaporated by running the cooling tower system for 4 hrs to 5 hrs to achieve the desired salinity of 85 g/kg.

DESCRIPTION OF THE S/Mill-E SALINITY REFRACTOMETER

The S/Mill-E salinity meter measures the salinity and the specific gravity of sea water. The salinity of sea water is displayed in parts per mille (‰) unit that is approximately equal to grams of salt per kg of solution. This model is designed with the automatic temperature compensation feature which automatically provides the measurement values at the compensated temperature of 20 ^oC. Its range to measure salinity is 0 to 100 ‰. The accuracy of the device to measure salinity is ± 1‰.

The picture of the salinity meter is shown in Fig. D.1

Figure D.1 S/Mill-E Salinity Refractometer

APPENDIX E: EES PROGRAM CODE FOR COOLING TOWER ANALYSIS

```
$integraltable V:
0.000108,Hi,t,t_wb,t_SW,S,m_SW,h,w,h_s_SW,w_s_SW,slope,D,h_cA_V,h_fw,h_gw,c
_SW,cp_a,Le,Le_f,s_a,S_SW,S_dot_gen,X_dot_air_conv,X_dot_air_conv_kW,X_dot_ai
r_evap,X_dot_air_evap_kW,X_dot_air,X_dot_air_kW,X_dot_SW,X_dot_SW_KW,X_d
ot_D,X_dot_D_s,
Q_conv,Q_evap,Q_total,Q_conv_inst,Q_evap_inst,Q_total_inst,PT_conv,PT_evap

"conditions at dead state"
T_o = t_1                                   "[C] dead state temperature"
P_o = 101.325                               "[kPa] dead state pressure"
w_o = w_1                                   "[kgw/kga] dead state humidity
ratio"
S_o =  35 [g/kg]                            "salinity of seawater at dead state"
theta_o = RelHum(AirH2O,T=T_o,w=w_o,P=P_o) "dead state relative humidity "

h_fo=SW_Enthalpy(T_o,S_o)                   "[J/kg] enthalpy of seawater at dead
state"
s_fo = SW_Entropy(T_o,S_o)                  "[J/kg·K] entropy of seawater at dead
state"

"constants for water vapor and air"
R_v = 0.461*10^3                            "[J/(kg.K)]"
cp_v = 1.872*10^3                           "[J/(kg.K)]"
R_a = 0.287*10^3                            "[J/(kg.K)]"

" The dry bulb temperature of air is t & wet bulb temperature is t_wb , mass of seawater
is m_SW and mass of air is ( m_a ) in cooling tower ."
"1 shows for bottom and 2 shows for top of cooling tower"
```

m_a = 0.06628 [kg/s] "mass of air assumed to be constant in cooling tower"
m_SW_1 = 0.03391 [kg/s] "mass of seawater at bottom of cooling tower"
S_1 = 44.48 [g/kg] "salinity of seawater at the bottom of tower"
t_1 = 22.28 [C] "dry bulb temperature of air at the bottom of tower "
t_wb_1 = 16.68 [C] "wet bulb temperature of air at the bottom of tower"
P_ct = 101.325 [kPa]

"t_SW_1 is the temperature of seawater at the bottom of cooling tower"
t_SW_1 = 23.28 [C]

"Volume of tower is V = V_2 = 0.0108 [m^3]"
V_1 = 0
V_2 = 0.0108 [m^3]
deltaV = 0.000108 [m^3]

"tower cross-sectional area A = 0.0225 [m^2] and height is Hi "
A= 0.0225 [m^2]
Hi_1 =0
Hi = integral((1/A),V,V_1,V_2) "[m] height of tower"
Hi_2 = Hi

"h_DA_V is the average mass transfer coefficient of cooling tower"
h_DA_V = 3.6 [kg/s-m^3]

```
h_1 = Enthalpy(AirH2O,T=t_1,B=t_wb_1,P=P_ct)
h_2 = Enthalpy(AirH2O,T=t_2,B=t_wb_2,P=P_ct)

s_a_1 = Entropy(AirH2O,T=t_1,B=t_wb_1,P=P_ct)
s_a = Entropy(AirH2O,T=t,B=t_wb,P=P_ct)
s_a_2 = s_a

s_SW_1 = SW_Entropy(t_SW_1,S_1)
w_1 = HumRat(AirH2O,T=t_1,B=t_wb_1,P=P_ct)
w_2 = HumRat(AirH2O,T=t_2,B=t_wb_2,P=P_ct)

t = Temperature(AirH2O,h=h,w=w,P=P_ct)
t_wb = WetBulb(AirH2O,h=h,w=w,P=P_ct)

"relative humidity of saturated water"
RH_sw = 1

"h_s_SW is the enthalpy and w_s_SW is the humidity ratio of saturated air at temperature t_SW"
h_s_SW_1 = Enthalpy(AirH2O,T=t_SW_1,r=RH_sw,P=P_ct)
h_s_SW = Enthalpy(AirH2O,T=t_SW,r=RH_sw,P=P_ct)
h_s_SW_2 = h_s_SW

w_s_SW = (18.015/28.97)*(Pv_SW/(P_ct - Pv_SW))
Pv_SW = 0.001*SW_Psat(t_SW,S)

slope = (h_s_SW - h)/(w_s_SW - w)

"thermal conductivity of air is k_a [W/m-K] , density is rho_a [kg/m^3] and heat capacity is cp_a [kJ/kg-K]"
```

k_a = Conductivity(AirH2O,T=t,B=t_wb,P=P_ct)

rho_a = Density(AirH2O,T=t,B=t_wb,P=P_ct)

cp_a = Cp(AirH2O,T=t,B=t_wb,P=P_ct)

"heat capacity of swater is c_SW [kJ/kg-K]"

c_SW = SW_SpcHeat(t_SW,S)

"mass diffusivity of water in air D[m^2/s]"

T_film = (((t + t_wb)/2) + 273.16)

D=-2.775e-6 [m^2/s]+4.479e-8 [m^2/s-K]*T_film+1.656e-10[m^2/s-K^2]*T_film^2

"d_r=molecular weight ratio of water and air"

d_r = 0.622

"lewis number is Le and lewis factor is Le_f"

Le = (k_a)/(rho_a*cp_a*D)

Le_f = (h_cA_V/(cp_a*h_DA_V))

"Relation between Lewis factor and Lewis number is as below"

Le_f = Le^(2/3)*((w_s_SW + d_r)/(w + d_r) - 1)/(ln((w_s_SW + d_r)/(w + d_r)))

"h_fw & h_gw are the enthalpies of seawater and vapor respectively at temperature t_SW
"

h_fw_1 = SW_Enthalpy(t_SW_1,S_1) "[J/kg]"

h_fw =SW_Enthalpy(t_SW,S) "[J/kg]"

h_fw_2 = h_fw

h_gw = Enthalpy(Steam_IAPWS,T=t_SW,x=1)

"h_g_o = specific enthalpy of saturated water vapor at 0 degree C"

h_g_o = Enthalpy(Steam_IAPWS,T=0,x=1)

"dh\dw is the condition line on psychometric chart"

dh\dV = ((Le_f*slope) + (h_gw - (h_g_o*Le_f)))*dw\dV - (loss\dV)*(1/m_a)

h = h_1 + integral((dh\dV),V,V_1,V_2)

h_2 = h

(dw\dV) = (1/h_fw)*((dh\dV) - ((m_SW/m_a)*c_SW*(dt_SW\dV))) + (1/(m_a*h_fw))*(loss\dV)

loss = integral((loss\dV),V,V_1,V_2)

loss\dV = 29.24074074

{loss = 0.3158}

w = w_1 + integral((dw\dV),V,V_1,V_2)

w_2 = w

m_SW*c_SW*(dt_SW\dV) = (h_cA_V*(t_SW-t)) + (h_DA_V*(w_s_SW - w)*(h_gw - h_fw))

t_SW = t_SW_1 + integral((dt_SW\dV),V,V_1,V_2)

t_SW = t_SW_2

"differential equation of salinity of seawater"

dS\dV = -S*(m_a/m_SW)*dw\dV

S = S_1+ integral((dS\dV),V,V_1,V_2)

S_2 = S "salinity of seawater at the inlet"

"m_SW [kg/s] is variable for the mass of seawater in cooling tower"

m_SW - m_SW_1 = m_a*integral((dw\dV),V,V_1,V_2)
m_SW_2 = m_SW

"entropy change of seawater, delta_S_SW [W/K]"

S_SW = m_SW*SW_Entropy(t_SW,S)
S_SW_2 = S_SW

delta_S_SW = (m_SW_1*s_SW_1) - S_SW

"entropy change of air,delta_S [W/K]"
delta_S_a = m_a*(s_a - s_a_1)

"rate of entropy generation"
S_dot_gen = delta_S_a + delta_S_SW "[W/K]"

"exergy of air by convective heat transfer X_dot_air_conv [W]"

X_dot_air_conv_1 =
m_a*cp_a*(T_o+273.16)*(1+1.852*w_1)*(((t_1+273.16)/(T_o+273.16))-1-ln((t_1 +
273.16)/(T_o+273.16)))
X_dot_air_conv = m_a*cp_a*(T_o+273.16)*(1+1.852*w)*(((t+273.16)/(T_o+273.16))-
1-ln((t + 273.16)/(T_o+273.16)))
X_dot_air_conv_2 = X_dot_air_conv

"exergy of air by evaporation heat transfer X_dot_air_evap [W]"

```
X_dot_air_evap_1=
m_a*cp_a*(T_o+273.16)*0.2857*ln(((1+1.6078*w_o)/(1+1.6078*w_1))^(1+1.6078*w_
1)*(w_1/w_o)^(1.6078*w_1))
X_dot_air_evap=
m_a*cp_a*(T_o+273.16)*0.2857*ln(((1+1.6078*w_o)/(1+1.6078*w))^(1+1.6078*w)*(
w/w_o)^(1.6078*w))    "[W]"
X_dot_air_evap_2 = X_dot_air_evap

"total exergy of air  X_dot_air [kW]"
X_dot_air_1 = (X_dot_air_conv_1 + X_dot_air_evap_1)        "[W]"
X_dot_air = (X_dot_air_conv + X_dot_air_evap)              "[W]"
X_dot_air_2 = (X_dot_air_conv_2 + X_dot_air_evap_2)        "[W]"

X_dot_air_kW = X_dot_air/1000

"exergy of seawater X_dot_SW  [W]"
X_dot_SW_1 = m_SW_1*(SW_Exergy(t_SW_1,S_1,T_o,S_o) -
(R_v*(T_o+273.15)*ln(theta_o)))
X_dot_SW =  m_SW*(SW_Exergy(t_SW,S,T_o,S_o) -(R_v*(T_o+273.15)*ln(theta_o)))
X_dot_SW_2  =  X_dot_SW



"exergy destruction "

X_dot_D_SW = (X_dot_SW- X_dot_SW_1)
X_dot_D_air = (X_dot_air_1-X_dot_air)
X_dot_D = (X_dot_SW- X_dot_SW_1) + (X_dot_air_1-X_dot_air) + loss*(1-(0.5*(t_1
+ t)+273.16)/(t_1+273.16))                    "[W]"
X_dot_D_s = (T_o + 273.15)*S_dot_gen
```

X_dot_D_total = (X_dot_SW_2- X_dot_SW_1) + (X_dot_air_1-X_dot_air_2)

"convection heat transfer is Q_conv "

Q_conv=h_cA_V*(t_SW - t)

Q_conv_inst=Q_conv*deltaV

"evaporative heat transfer is Q_evap "

Q_evap=h_DA_V*(w_s_SW - w)*(h_gw - h_fw)

Q_evap_inst=Q_evap*deltaV

"total heat transfer is Q_total"

Q_total=Q_conv+Q_evap

Q_total_inst=Q_conv_inst+Q_evap_inst

"potential for convection is PT_conv"

PT_conv=(t_SW - t)

"potential for evaporation is PT_evap"

PT_evap=(w_s_SW - w)

"Number of transfer units of tower "

NTU=h_DA_V*V/m_a

"Range of cooling tower"

range=(t_SW-t_SW_1)

"approach of cooling tower"

approach=(t_SW_1-t_wb_1)

"air effectiveness"

epsilon_a = (h_2 - h_1)/(h_s_SW_2 - h_1)

"water effectiveness"

hw_ideal = SW_Enthalpy(t_wb_1,S_1)

epsilon_water = (m_SW_2*h_fw_2 - m_SW_1*h_fw_1)/(m_SW_2*h_fw_2 - m_SW_1*hw_ideal)

"Mass Ratio"

MR = m_SW_2/m_a

NOMENCLATURE

A_V	contact surface area of water droplets per unit volume of fill, m^2/m^3
$c_{p,a}$	specific heat at constant pressure of moist air, kJ/kg K
$c_{p,SW}$	specific heat of seawater, kJ/kg K
$c_{p,w}$	specific heat of water, kJ/kg K
$c_{p,v}$	specific heat of water vapor, kJ/kg K
D	mass diffusivity of water in air, m^2/s
d_r	molecular weight ratio of water and air
G	Gibbs energy, kJ
g	specific Gibbs energy, kJ/kg
h	enthalpy of moist air, kJ/kg
h_c	convective heat transfer coefficient of air, kW/m^2 K
h_D	convective mass transfer coefficient, (kg/m^2 s)
h_{SW}	specific enthalpy of seawater evaluated at t_{SW}, kJ/kg
$h_{SW,0}$	specific enthalpy of seawater evaluated at dead state, kJ/kg
$h_{g,SW}$	specific enthalpy of saturated water vapor, kJ/kg
$h_{s,SW}$	enthalpy of saturated moist air evaluated at t_{SW}, kJ/kg
k_a	thermal conductivity of air, kW/m K
Le	Lewis Number

Le_f	Lewis Factor
$\dot{m}_a$	mass flow rate of dry air, kg/s
$\dot{m}_S$	mass flow rate of salt, kg/s
$\dot{m}_{SW}$	mass flow rate of seawater, kg/s
$\dot{m}_w$	mass flow rate of water, kg/s
Me	Merkel Number
NTU	number of transfer units
$\dot{Q}$	heat transfer rate, kW
R_a	specific gas constant for dry air, kJ/kg K
R_v	specific gas constant for water vapor, kJ/kg K
S	salinity of seawater (g/kg)
$s_{SW,0}$	specific entropy of seawater at dead state, kJ/kg K
S_{SW}	entropy of seawater, kW/K
t	dry- bulb temperature of moist air, ^{o}C
t_w	water temperature, ^{o}C
t_{SW}	seawater temperature, ^{o}C
T	dry- bulb temperature of moist air, K
$T_{a,in}$	temperature of dry- bulb of air in, ^{o}C
$T_{a,out}$	temperature of dry- bulb of air out, ^{o}C
$T_{wb,in}$	temperature of wet-bulb of air in, ^{o}C
$T_{wb,out}$	temperature of wet-bulb of air out, ^{o}C

$T_{w,in}$ temperature of water in, ^oC

$T_{w,out}$ temperature of water out, ^oC

$T_{sw,in}$ temperature of seawater in, ^oC

$T_{sw,out}$ temperature of seawater out, ^oC

V volume of fill packing, m^3

$\dot{X}$ flow exergy, kW

$\dot{X}_D$ exergy destruction, kW

Greek Symbols

α thermal diffusivity oof air, m^2/s

μ chemical potential J/kg

θ_o dead state relative humidity

ρ density, kg/m^3

ω humidity ratio of moist air

$\omega_{s,SW}$ humidity ratio of saturated moist air evaluated at t_{SW}

Subscripts

a moist air

db dry bulb

in inlet

out outlet

s salt

SW seawater

s,SW saturated moist air at seawater temperature t_{SW}

SW, in seawater inlet

SW, out seawater outlet

air, in air inlet

air, out air outlet

w water

wb wet bulb

REFERENCES

[1] Walker WH, Lewis WK, McAdams WH, Gilliland ER. Principles of chemical engineering. 3rd ed. New York: McGraw-Hill Inc; 1923.

[2] Merkel F. Verdunstungshuhlung. Zeitschrift des Vereines Deutscher Ingenieure (VDI) 1925; 70: 123–8.

[3] London, A. L. Mason, W. E. and Boelter, L. K., "Performance Characteristics of a Mechanically Induced Draft, Counter flow, Packed Cooling Tower," Trans. ASME; 1940; 62 : 41-50.

[4] Simpson W. M., Sherwood T. K., “Performance of small mechanical draft cooling towers”. Refrig Eng 1946; 52(6): 525–43, 574–6.

[5] Sutherland JW., “Analysis of mechanical draught counter flow air/water cooling towers”. ASME J Heat Transfer 1983; 105(3): 576–83.

[6] Webb R. L., "A Unified Theoretical Treatment for Thermal Analysis of Cooling Towers, Evaporative Condensers, and Fluid Coolers," ASHRAE Tran. 1984; 90 (2): 398-415.

[7] Webb RL, Villacres A., “Algorithms for performance simulation of cooling towers, evaporative condensers, and fluid coolers”. ASHRAE Trans. 1984; 90 (2): 416–58.

[8] Jaber H, Webb RL., "Design of cooling towers by the effectiveness-NTU method". ASME J Heat Transf. 1989; 111 (4): 837–43.

[9] Braun JE, Klein SA, Mitchell JW., "Effectiveness models for cooling towers and cooling coils". ASHRAE Trans. 1989; 95 (2): 164–74.

[10] Mohiuddin AKM, Kant K., "Knowledge base for the systematic design of wet cooling towers". PartI: selection and tower characteristics. Int J Refrig 1996; 19(1): 43–51.

[11] Mohiuddin AKM, Kant K., "Knowledge base for the systematic design of wet cooling towers". PartII: fill and other design parameters. Int J Refrig 1996; 19 (1): 52–60.

[12] El-Dessouky HTA, Al-Haddad A, Al-Juwayhel F., "A modified analysis of counter flow cooling towers". ASME J Heat Transf. 1997; 119 (3): 617–26.

[13] Jorge F, Armando CO., "Thermal behavior of closed wet cooling towers for use with chilled ceilings". Appl Therm Eng 2000; 20: 1225–36.

[14] Bernier MA, "Cooling tower performance: theory and experiments". ASHRAE Trans 1994; 100 (2): 114–21.

[15] Bernier MA, "Thermal performance of cooling towers". ASHRAE J 1995; 37 (4): 56–61.

[16] Nimr MA., "Modeling the dynamic thermal behavior of cooling towers containing packing materials". Heat Transf. Eng1999; 20 (1): 91–6.

[17] Khan JR, Zubair SM., "An improved design and rating analyses of counter flow wet cooling towers". ASME J Heat Transf. 2001; 123: 770–8.

[18] Jose AS., "The use of thermo fluid dynamic efficiency in cooling towers". Heat Transf. Eng 2002; 23: 22–30.

[19] Khan JR, Yaqub M, Zubair SM, "Performance characteristics of counter flow wet cooling towers". Energy Conversion and Management 2003; 44(13): 2073–2091.

[20] Kloppers JC, Kröger DG, "A critical investigation into the heat and mass transfer analysis of counter flow wet-cooling towers". Internat. J. Heat Mass Transfer 2005; 48 (3–4): 765–777.

[21] Kloppers JC, Kröger DG, "Influence of temperature inversions on wet cooling tower Performance". Applied Thermal Engineering, 2005; 25: 1325-36.

[22] Kloppers JC, Kröger DG, "The Lewis factor and its influence on the performance prediction of wet cooling towers". International Journal of Thermal Science, 2005; 25: 879-884.

[23] Kaiser AS, Lucas M, Viedma A and Zamora B, "Numerical model of evaporative cooling processes in a new type of cooling tower". International Journal of Heat and Mass Transfer, 2005; 48: 986–999.

[24] Papaefthimiou VD, Zannis TC and Rogdakis ED, "Thermodynamic study of wet cooling tower performance". International Journal of Energy Research, 2006; 30: 411–426.

[25] Muangnoi T, Asvapoositkul W and Wongwises S, "An exergy analysis on the performance of a counter flow wet cooling tower". Applied Thermal Engineering, 2007; 27: 910-917.

[26] Nunez MP, Gasca CN, and Fuantes MA, "Simplified model for the determination of the steady state response of cooling systems". Applied Thermal Engineering, 2007; 27: 1173–1181.

[27] Gharagheizi F, Hayati R and Fatemi S, "Experimental study on the performance of mechanical cooling tower with two types of film packing". Energy Conversion and Management, 2007; 48: 277–280.

[28] Ataei A, Panjeshahi MH and Gharaie M, "Performance evaluation of counter flow wet cooling towers using exergetic analysis". Canadian Society for Mechanical Engineering, 2008; 32 (3): 499-511.

[29] Lemouari M, Boumaza M and Kaabi A, "Experimental analysis of heat and mass transfer phenomena in a direct contact evaporative cooling tower". Energy Conversion and Management, 2009; 50: 1610–1617.

[30] Lemouari M, Boumaza M, "Experimental investigation of the performance characteristics of a counter flow wet cooling tower". International Journal of Thermal Sciences, 2010; 49: 2049-2056.

[31] Sharqawy M.H., Lienhard V, J.H., Zubair, S.M., "On thermal Performance of Seawater Cooling Towers", ASME J. of Engineering for Gas Turbines and Power 133(4),43001 – 43007, DOI 10.1115/1.4002159, 2011.

[32] Sharqawy M.H., Lienhard V J.H. and Zubair S.M., "Thermophysical properties of seawater: A review of existing correlations and data". Desalination and Water Treatment, 2010; 16, 354-380.

[33] Walston K. R., "Materials Problems in salt water cooling towers". Exxon Res. & Eng. Co., Mater Performance, 1975; 14(6), 22-26.

[34] Ting B.Y. and David S., "The use of cooling towers for salt water heat rejection". The Marley Cooling Tower Co. Overland Park, KS; 1991.

[35] Kuehn TH, Ramsey JW, Threlkeld JL. Thermal environmental engineering. 3rd ed. New Jersey: Prentice-Hall Inc; 1998.

[36] Khan JR, Zubair SM. An improved design and rating analyses of counter flow wet cooling towers. ASMEJ Heat Transf 2001; 123:770–8.

[37] Wepfer WJ, Gaggioli RA, Obert EF. 1979. Proper evaluation of available energy for HVAC. ASHRAE Transactions 85(I): 214–230.

[38] Moran MJ, Shapiro HN. 1995. Fundamentals of Engineering Thermodynamics (3rd edn). Wiley: New York.

[39] Bejan A. 1997. Advanced Engineering Thermodynamics. (2nd edn). Wiley: New York.

[40] Gulf Coast Chemical Commercial Inc. Cooling Systems, 1995 www.gc3.com/techdb/manual/coolfs.htm

[41] SPX Cooling Technologies, Inc. 2006. Overland Park, Kansas USA.

[42] Experimental Operating and Maintenance Manual, Bench Top Cooling Tower H892, P. A. Hilton LTD.

VITA

Name: IQBAL HUSAIN

Place of Birth: Hamirpur, India.

Nationality: Indian

Permanent Address: Mumtaz Gate,

Qazipura, Mahoba, U.P,

India.

Telephone: +91-9795807978, +91-5281254736

Email Address: iqbalgcet@gmail.com

Educational Qualification:

M.S (Mechanical Engineering)

May2011

King Fahd University of Petroleum and Minerals

Dhahran, Saudi Arabia.

B. Tech. (Mechanical Engineering)

June 2007

Galgotias College of Engineering and Technology, Greater Noida.

Uttar Pradesh Technical University, India.